博士論文

Study of replication timing control by internally located telomeric repeats and the telomere-binding protein Taz1 in fission yeast

(分裂酵母染色体内部に存在するテロメア配列とテロメア結合蛋白質 Taz1 による複製タイミング制御の研究)

田積　充年

大阪大学大学院理学研究科　生物科学専攻

２０１２年１１月

Doctoral Thesis

Study of replication timing control by internally located telomeric repeats and the telomere-binding protein Taz1 in fission yeast

Atsutoshi Tazumi

Department of Biology

Graduate School of Science

Osaka University

November 2012

Abstract

In eukaryotes, replication of chromosome DNA is coordinated by a replication-timing program that temporally regulates the firing of individual replication origins. However, the molecular mechanism underlying the program remains elusive. Here, I report that the telomere-binding protein, Taz1, plays a crucial role in the control of replication timing in fission yeast. A DNA element located proximal to a late origin in the chromosome arm represses initiation from the origin in early S phase. Systematic deletion and substitution experiments demonstrated that two tandem telomeric repeats are essential for this repression. The telomeric repeats recruit Taz1, a counterpart of human TRF1 and TRF2, to the locus. Genome-wide analysis revealed that Taz1 regulates about half of chromosomal late origins, including those in sub-telomeres. The Taz1-mediated mechanism prevents DDK-dependent Sld3 loading onto the origins. These results demonstrate that the replication-timing program in fission yeast utilizes the internal telomeric repeats and binding of Taz1. Furthermore, many of shelterin components and Rif1 are required to repress a wide range of late origins in arm regions and sub-telomeric regions, suggesting that telomere binding proteins other than Taz1 also involved in regulation of genome-wide control of replication timing. These results place telomere binding proteins at the interface between replication timing control including the site specific regulation by internally located telomeric repeats and telomere functions probably including metabolism and sub-nuclear localization.

General Introduction

Replication of eukaryotic chromosomes

DNA replication is fundamental and essential for inheritance of the genetic information through generations. For complete duplication of large eukaryotic chromosomes within the limited period of S phase, DNA replication initiates at a large number of chromosome loci known as replication origins. Cell biological studies show that DNA replication of large chromosome domain occurs in specific times during S phase in replication foci which occupy defined nuclear regions (Leonhardt et al., 2000). Replication timing control is important for the maintenance of proper cell cycle progression and genome stability, ensuring the efficient and complete duplication of chromosomes (Loipart et al., 2000; Pflumm and Botchan, 2001). Eukaryotic chromosomes are composed of chromatin structures, largely divided in euchromatin, where gene expression is active, and heterochromatin, where genes are silenced. In general, euchromatic regions tend to replicate in early S phase and heterochromatic regions replicate in late S phase (Fig.1A) (MacAlpine and Bell, 2005). Moreover, chromatin is organized within the nucleus in early G1 phase directing the localization of chromosomal domains to defined sub-nuclear positions. For example, heterochromatic domains, such as sub-telomere, which localize to the nuclear periphery or nucleoli, replicate in late S phase. In mammalian cells, the spatio-temporal program is established during a discrete time window in early G1 phase, the timing decision point (TDP) (Dimitrova and Gilbert, 1999). The fact that replication timings are changed coupled with alterations in histone modifications and gene expression during metazoan development suggest the importance of replication timing control (RTC) (hiratani et al., 2004, 2008; Lande-Diner et al., 2009).

Structure of chromosomes

Eukaryotic chromosomes consists arm region and several chromosomal loci with specialized chromatin structures, such as centromeres and telomeres. Telomere is the DNA-protein complex formed at the ends of eukaryotic chromosomes. Telomere

DNA consists of an array of short sequence repeats ending with a 3'-overhangs of single-stranded DNA. In mammal, the shelterin complex (TRF1, TRF2, POT1, RAP1, TIN2 and TPP1) binds to the telomere DNA in a sequence dependent manner. Telomere has two essential functions: the protection of the chromosome ends from degradation or fusion and maintenance of its length. To avoid cell-cycle arrest, telomere proteins, such as mammalian TRF1, TRF2 and POT1, are involved in attenuating checkpoint signaling regulated by ATM and ATR kinases at telomeres. To maintain telomere length, telomerase, telomere-specific reverse transcriptase, replenish telomere repeats since telomere becomes shorter at each round of replication. Thus, the Shelterin complex plays an important role in control of the telomere length. In general, centromere and telomere proximal regions (sub-telomere) form constitutive heterochromatin structures and are transcriptionally silenced. A core characteristic of heterochromatin is binding of heterochromatin protein 1 (HP1), a highly conserved family of chromosomal proteins. HP1 proteins (in fission yeast, *Schizosaccharomyces pombe* Swi6 and Chp2) specifically bind to di- and trimethylated H3K9 with its chromo-domain (CD) and recruit H3K9 metyltransferase, KMT1 (Clr4 in fission yeast, Su[var]3-9 in Drosophila, and Suv39H in mammals) to chromatin (Stewart et al., 2005). H3K9 methylation and HP1 proteins promote heterochromatic gene silencing by mechanisms that Chp2 recruits SHREC complex, containing Clr3 histone deacetylase, which mediates the deacetylation of H3K14 and transcriptional gene silencing (Sugiyama et al., 2007). The fission yeast chromosome contains three major heterochromatic loci: pericentromere, the silent mating-type locus and sub-telomeric region. In sub-telomeres, heterochromatin is maintained at least by two pathways. One is the RNAi (RNA interference) dependent pathway, which is commonly used at the heterochromatic loci including cenetromere and silent mating-type (MAT) locus (Hall et al., 2002; Volpe et al., 2002). The other is the Taz1, an ortholog of human TRF1 and TRF2, dependent pathway (Kanoh et al., 2005). Therefore, function and components of heterochromatin may differ between functional chromosomal loci since Taz1 is believed to localize specifically to telomere.

Structure of replication origins

The nucleotide sequences of replication origins greatly differ among organisms mainly due to the differences in DNA binding properties of ORC. In budding yeast, *Schizosaccharomyces cerevisiae*, replication origins are confined in less than 200 bp chromosome fragments that allow autonomous replication on plasmid (ARS activity). All the origins contain an 11-bp ARS consensus sequence (ACS) that is essential for initiation of replication. On the other hand, other eukaryotic cells have no such a consensus sequence in replication origins. In fission yeast, ARSs, comprising 500 bp-2 kb fragments, are located in intergenic regions. Since fission yeast ORC prefers AT rich sequence for its binding site, genome-wide locations of replication origins have been predicted by AT content and its length (Chuang and Kelly, 1999; Segurado et al., 2003; Takahashi et al., 2003). In multicellular organisms, no specific sequence or regions required for origin activity have been determined, although several chromosomal origins such as b-globin.

Cell cycle regulation of DNA replication

The initiation of replication in eukaryotes consists of several distinct steps that are regulated by cell cycle. Replication origins are recognized and bound by origin recognition complex (ORC), which is composed of six subunits Orc1-6. In G1 phase, ORC together with Cdc6 (Cdc18 in fission yeast) and Cdt1 promotes loading of a mini-chromosome maintenance (MCM) complex, composed of heterohexameric Mcm2-7, onto replication origins, resulting in a pre-replicative complex (pre-RC) (Bell and Dutta 2002). The activity of cyclin-dependent kinase (CDK), which inhibits this process, is low in late M and G1 phase, allowing the pre-RC formation in this period. At the beginning of S phase, activation of two conserved kinases, CDK and Dbf4-dependent kinase (DDK), promotes assembly of several other replication factors, including Sld3, Cdc45 and GINS, leading to unwinding of origin DNA and initiation of DNA synthesis (Fig. 1B)(Remus and Diffley 2009; Labib 2010; Tanaka and Araki 2010). The replisome including DNA polymerases and single-stranded DNA binding protein complex, Replication protein A (RPA), proceeds and synthesizes DNA

bidirectionally from replication origins. Replication origins do not fire simultaneously at the onset of S phase but do so at distinct time points during S phase. In budding yeast and fission yeast, pre-RCs are formed at all the origins, whereas specific origins are activated in early S phase (Raghuraman et al. 2001; Wyrick et al. 2001; Hayashi et al. 2007). Recent studies have suggested that DDK-dependent origin loading of Sld3 and Cdc45 is a key step determining the timing of initiation (Tanaka et al. 2011). These findings suggest that replication-timing program regulates activation of pre-RCs in these yeasts.

Regulation of replication origins

It is generally agreed that the status of chromatin has an impact on the timing of origin activation. Replication origins in euchromatin domains, where genes are actively transcribed, initiate early, while those in heterochromatin, where genes are repressed, replicate in late S phase (MacAlpine et al. 2004; Hiratani and Gilbert 2009). However, genome-wide identification of replication origins in fission yeast indicates that a subset of euchromatic origins do not fire in early S phase (Hayashi et al. 2007). Moreover, centromeric heterochromatin and the silent mating-type (*mat*) locus replicate in early S phase (Kim et al. 2003; Hayashi et al. 2009), and interestingly, Swi6 stimulates their early replication (Hayashi et al. 2009). On the other hands, sub-telomeric heterochromatin replicates very late in S phase in the presence or absence of Swi6 (Hayashi et al. 2009), suggesting that certain mechanism independent from the heterochromatin regulates replication timing. Although the checkpoint pathway represses late origins under depletion of nucleotides by hydroxyurea (HU) in budding yeast and fission yeast, it does not affect replication timing of the origins (Santocanale and Diffley 1998; Santocanale et al. 1999; Hayashi et al. 2007). Previous studies proposed that the replication program is related with the pattern of histone modifications, nucleosome organization and the nuclear positioning of chromosomal loci. For example, deletion of histone deacetylase (HDAC), Rpd3, causes early activation of nontelomeric late origins in budding yeast (Aparicio et al., 2004). Moreover, tethering of histone acetyltransferase (HAT) to a late origin advances its time

of activation (Knott et al., 2009; Vogelauer et al., 2002). Similarly, histone hyperacetylation has been implicated to stimulate origin activation in *Drosophila* and human cells, suggesting that a similar mechanism may play a role in the regulation of origin activation in higher eukaryotes (Aggarwal and Calvi, 2004; Goren et al., 2008). In addition to a general correlation between these features of chromosome and origin activation, there exist other factors that affect replication timing of origins (See ***Part II***).

Although lots of efforts have been concentrated on the dissection of trans factors whose deletion affect the genome-wide replication timing, the knowledge about the molecular mechanism which enables the specific regions to be recognized by the factors is limited. To understand this issue, it is necessary to identify the relation between cis-acting sequences regulating the replication timing of nearby origins involved in chromosome domains replicated at specific timing and trans factors associating to the sequences.

Introduction

It is well accepted that the time at which replication origin located in the eukaryotic chromosome initiates replication within S phase is a characteristic of each origin. However, what determines the activation timing of each origin is not well understood. Due to difficulties in analyzing pre-RC sites in metazoans, it is difficult to clarify the relation between individual pre-RC site and what determines its activation timing. I speculated that replication timing of origins may be an inherent property of the origin or affected by surrounding contents. Fission yeast is a suitable model organism to study the cis-acting sequences regulating the replication origin, since several hundreds loci distributed throughout the chromosomes have been identified as pre-RC sites or actual DNA synthesis sites in fission yeast (Feng et al., 2006; Hayashi et al., 2007; Heichinger et al., 2006). In common with other eukaryotes, initiation timing of fission yeast replication origins varies during S phase. Moreover, studying the regulation of replication origins in fission yeast may provide findings of general importance since structures of fission yeast chromosome and replication origin have similarities with those in higher eukaryotes. Although previous studies in yeasts have identified several chromosomal stretches and short cis-acting sequences that can force replication origins to fire later in S phase (Friedman et al., 1996; Sharma et al., 2001; Yompakdee and Huberman, 2004), little is currently known about the cis-acting sequences origins and trans factors associating to the sequences.

In this study, I investigated a representative fission yeast late origin *AT2088* in comparison with an early origin *ars2004*. To examine whether early/efficient and late/inefficient initiation of origins at chromosomal loci is owing to an inherent property of the origin or affected by surrounding contents, replication origin fragments that posses the ARS activity were translocated to other loci on chromosome. Effects on replication timing were examined by replication kinetics analysis using BrdU incorporation. Insertion of the late origin fragment, *AT2088*, to the vicinity of the early origin *ars2004* repressed the early activation of *ars2004*. Using systematic deletion and substitution experiments for the *AT2088* fragment, I identified the 17-bp

sequence containing two tandem copies of a telomeric repeat that is essential for the repression of replication origin. Mapping of telomeric repeats in the fission yeast genome allowed to identify 13 loci where the repeats exist within the same intergenic spaces with late origins in the chromosome arm. Disruption of the one neaby a late origin *AT2035* caused early replication of the origin, suggesting that telomeric repeats are general determinant of late origins.

A recent discovery of fission yeast telomere binding proteins uncovered evolutionarily conserved elements of telomere functions between fission yeast and mammals. In fission yeast, Taz1 that binds directly to double stranded telomere DNA interacts with Rap1 and Rif1. Rap1 is a component of a Shelterin-like complex, in which Rap1 is linked with single-stranded telomere DNA binding protein, Pot1, via Poz1 (Miyoshi et al., 2008). Taz1, Rap1 and Poz1, components of the Shelterin-like complex, have inhibitory roles in recruitment or activation of telomerase (Chikashige and Hiraoka, 2001; Cooper et al., 1997; Miyoshi et al., 2008). Ccq1, another component of the Shelterin-like complex, is required for recruitment of telomerase and has a positive role in telomere elongation (Flory et al., 2004; Tomita and Cooper, 2008). On the other hand, Rif1 that associates with telomere by the interaction with Taz1 has a minor role in negative regulation of telomere length control (Kanoh and Ishikawa, 2001). In fission yeast, telomeric repeats in chromosome arm regions are essential for the repression of late origins. This finding raises the possibility that telomere binding proteins, which have been considered to act only at the chromosome ends, may function for regulation of replication in the internal chromosome regions.

In budding yeast, proximity to the telomeres confers late replication of some origins (Ferguson and Fangman, 1992). Telomeric DNA becomes shorter as a result of lagging strand synthesis, and shortened telomeres are elongated by telomerase. Interestingly, long telomeres cause a delay in the replication timing of telomere-proximal origins (Bianchi and Shore, 2007), suggesting the involvement of telomeric DNA and probably the telomere binding proteins. A recent study in fission yeast indicates that loss of rif1 rescues the growth of a null mutant of hsk1, the fission

yeast homologue of Cdc7 kinase, and changes the replication timing program (Hayano et al., 2012). In mammalian cells including human and mouse, Rif1 is also a key factor that regulates replication timing program (Daniela Cornacchi et al., 2012; Satoshi Yamazaki et al., 2012). However, what enables the specific regions to be recognized by telomere binding proteins or other trans factors has not been elucidated.

Here, I demonstrate that Taz1 binding to the internal telomeric repeats plays an essential role in the control of replication timing in fission yeast. The telomeric repeats proximal to *AT2088* and another late origin *AT2035* recruit Taz1 to the loci and the recruitment of Taz1 was essential for timing control of these late origins. In the *taz1*Δ strain, about half of previously identified late origins, including those in sub-telomeres, fire in early S phase. Remarkably, all of 13 origins associating internal telomeric repeats are regulated in a Taz1-dependent manner. These results indicate that Taz1, a well-defined telomere-binding protein, plays an essential role in replication timing control through binding to the telomeric repeats in the vicinity of internal late origins in fission yeast. Additionally, deletions of Rap1 and Poz1, which are components of the Shelterin-like complex, cause early replication of a number of late origins in chromosomal arm regions. Other telomere binding factor Rif1 causes early replication of almost all late origins in chromosomal arm regions and sub-telomeres including all the late origins that fire in *taz1*Δ. These results suggest that there are some pathways overlapping among telomere binding proteins for negative control of genome-wide replication origins.

Results

Identification of the DNA element that controls replication timing

To elucidate the mechanism that regulates timing of firing at individual replication origins, I compared two replication origins, *ars2004* and *AT2088/ARS745*, which share properties of strong replication origins but differ in replication timing. *Ars2004*, located in the left arm of chromosome II (Fig. 2A), is a well characterized early origin (Okuno et al. 1999; Takahashi et al. 2003), where initiation factors assemble efficiently at the onset of S phase (Yamada et al. 2004; Yabuuchi et al. 2006). *AT2088/ARS745* (Maundrell et al. 1988; Segurado et al. 2003) is a late/dormant origin located in the right arm of chromosome II (Fig. 2A). Despite the efficient formation of pre-RC at *AT2088*, 5-bromo-2'-deoxyuridine (BrdU), a heavy-density analogue of thymidine, was not incorporated in hydroxyurea (HU)-treated early S phase cells (Hayashi et al. 2007). Both origins are located in large intergenic regions flanked by divergent promoters, and contain long AT-rich regions that are essential for the replication origin activity. Moreover, they exhibit efficient ARS activity when the respective fragment is cloned on a plasmid (Fig. 2B). Since the previous study of early and late origins was carried out using HU-treated cells, where replication checkpoint was activated (Hayashi et al., 2007), I examined the replication timing of *ars2004* and *AT2088* in unperturbed S phase. Cells synchronously released from G2/M block by a temperature-sensitive *cdc25-22* mutation were labeled for indicated periods with BrdU. The amounts of the heavy-light and light-light DNA, separated by CsCl density-gradient centrifugation, were determined by real-time PCR (qPCR) using primers amplifying *ars2004* and *AT2088*, together with *AT2024* (internal early origin control), *AT2035* (late origin control), and *TAS59*, which is about 20 kb distant from the right end of chromosome II (Fig. 2A). Replication kinetics showed that *ars2004* and *AT2024* replicated about 10 min earlier than *AT2035* and *AT2088*, while *TAS59* replicated much later than the others (Fig. 2C). These results demonstrated that the replication timings of *ars2004* and *AT2088* differ in unperturbed S phase.

To investigate whether the replication timings of *ars2004* and *AT2088* are intrinsic to the origins, the intergenic fragment containing each origin was translocated into an ectopic chromosomal context. The 3.2-kb fragment containing *ars2004* inserted at the *AT2088* locus (*ars2004*/*AT2088*Δ) replicated as early as the control early origin *AT2024* (Fig. 3A). In contrast, the 3.6-kb fragment containing *AT2088* inserted at the *ars2004* locus (*AT2088*/*ars2004*Δ) replicated late, as the control late origin *AT2035* (Fig. 3B). Although the absolute times of replication vary between experiments, probably due to difference in period required for re-entry into the cell cycle from the G2/M block, I confirmed that the difference in $T_{1/2}$, time required for replication in half of cell population for an origin relative to that of the early origin control, *AT2024,* was maintained (Fig. 3C). The results of two-dimensional (2D) gel electrophoresis analysis indicated that replication initiated efficiently from the *ars2004* placed at the *AT2088* locus, as shown by the bubble arc (Fig. 3A), and that replication was rarely initiated from the *AT2088* fragment at the *ars2004* locus in early S phase (Fig. 3B). Moreover, the plasmids pARS2004 and pAT2088, carrying the corresponding fragments, replicated early and late in S phase, respectively (Fig. 4A, B). These results demonstrate that the replication timings are intrinsic to the *ars2004* and *AT2088* fragments.

If an element located in the *AT2088* fragment forces the origin not to fire in early S phase, it might also repress another origin placed closely to the fragment. To test this possibility, the *AT2088* fragment was inserted in the vicinity of *ars2004* on the chromosome (Fig. 5A), and the amounts of BrdU-incorporated DNA in HU-treated early S phase cells were analyzed for *ars2004* locus and other origins. In HU-treated wild-type cells without insertion, both *ars2004* and *AT2024* showed robust replication, while *AT2035* did not replicate efficiently (Fig. 5B). Although insertion of the *ura4*+ fragment alone did not cause significant change (Fig. 5B), insertion of *AT2088* markedly decreased replication of *ars2004*, indicating that the *AT2088* fragment repressed the neighboring *ars2004* (Fig. 5B). This was due to decrease in initiation from *ars2004*, as shown by reduced amount of bubble arc in 2D-gel analysis (Fig. 5C). Furthermore, the *AT2088* fragment, when inserted at a site close to another early origin

ORI12 on chromosome I (Segurado et al. 2003), also repressed early replication of the origin (Fig. 6). These results showed that the *AT2088* fragment has the ability to control the replication timing of proximal origins. Accordingly, I named the activity as *r*eplication *t*iming *c*ontrol (RTC) activity.

Identification of the essential sequence for replication timing control

To determine the minimum region of *AT2088* that is required for RTC activity, *AT2088* fragments lacking various regions were inserted next to *ars2004* (Fig. 7A). The results presented in Fig. 7B show that a 634-bp fragment (L2312) of *AT2088* is sufficient for repression of *ars2004*. Experiments using series of internal deletions in the 634-bp fragment revealed that a 32-bp fragment (2617-2648, N2617) is required for the RTC, and that the surrounding regions contribute to some extent (Fig. 7B). Base-substitutions of every 8 bp in the 32-bp region identified the 17-bp RTC essential sequence (from position 2624 to 2640) and 8-bp important sequence (from position 2641 to 2648) (Fig. 7D). Because RTC alters the replication timing of ectopically adjoined replication origins, its function is distinct from the replication origin activity of *AT2088*. The 3.6-kb intergenic fragment of *AT2088* consists of two ARS fragments, each containing a highly AT-rich region (Fig. 7C; Fig. 8A). Disruption of the RTC essential sequence, located several hundred bp distant from the closer AT-rich region, did not affect the ARS activity (Fig. 8A), confirming that RTC is distinct from the origin activity.

I here examined whether the RTC controls replication timing at the original *AT2088* locus. A 210-bp fragment containing the RTC essential sequence was deleted from the *AT2088* locus (*AT2088Δ210*), and replication initiation was analyzed by 2D-gel electrophoresis. In contrast to a faint Y-arc from the *AT2088* locus in HU-treated wild-type cells, a bubble arc, indicative of the initiation, was generated along with a strong transition Y-arc resulting from initiation from an asymmetrical position within the restriction fragment in *AT2088Δ210* (Fig. 8B). These results indicate that the RTC is required for the control of replication timing at the native *AT2088* locus.

Telomeric repeats are essential for repression of internal late replication origins

In fission yeast, telomeric repeats consist of GGTTAC followed by $A_{0-1}C_{0-1}G_{0-6}$ variations (Sugawara 1989; Cooper et al. 1997; Hiraoka et al. 1998). I found that the RTC essential sequence contains two tandem copies of a telomeric repeat, with a substitution of T for the last C (Fig. 9B). I examined whether the telomeric repeats are essential for control of replication timing at the native *AT2088* locus. Base-substitution of the essential sequence (*AT2088-S2632*) promoted early replication specifically at *AT2088* (Fig. 9B). Because the telomeric repeats in the RTC essential sequence contain an incomplete match to the consensus, I confirmed that two copies of telomere consensus sequence, GGGTTACAGGTTACAGGG, replaced functionally the incomplete sequence (Fig. 9B, *AT2088-telF*). Insertion of the consensus in the opposite direction also restored the RTC (Fig. 9B, *AT2088-telR*), suggesting that the telomeric repeats act as a discrete element, such as the protein-binding site. To explore the general role of telomeric repeats in the control of replication timing in fission yeast, I searched the fission yeast genome for two tandem telomeric sequences, GGTT A Y -$N_{(1-3)}$-GGTT A Y, where Y represents pyrimidine, using the "fuzznuc" program (Experimental Procedures). Such telomeric repeats are located at 26 loci, exclusively in the intergenic regions (Tables 1 and 2). Interestingly, 13 of them exist within the same intergenic spaces with late origins, which were identified in previous genome-wide study (Hayashi et al. 2007). To investigate whether the telomeric repeats have a general role in replication timing control, I disrupted the one located near *AT2035* on chromosome II (Fig. 9C). Base-substitutions in the telomeric repeats caused robust early replication specifically at *AT2035* (Fig. 9C, *AT2035-S1959*). These results strongly suggest that the telomeric repeats present near internal late origins play a general role in replication timing control.

Taz1 binds to the telomeric repeats near the internal late origins

At the ends of chromosomes, Taz1, a fission yeast orthologue of human TRF1 and TRF2, binds to two tandem copies of the telomeric repeat (Cooper et al. 1997; Spink et al. 2000). To elucidate the role of telomeric repeats located near the internal late

origins in the control of replication timing, I analyzed localization of 6Flag-tagged Taz1 at the internal chromosome regions using a chromatin immunoprecipitation (ChIP) assay. The experiments were accomplished by the support of Dr. Fukuura and Ami Kishimoto. ChIP recovery of DNA for *ade6*, *AT2035*, *AT2088* and the telomere-proximal fragment (*Tel-0.3*) was determined by qPCR (Fig. 10). In wild-type cells, the recovery of *Tel-0.3* was about 50-fold higher than that of *ade6* (Fig. 10, left), indicating accumulation of Taz1 at the telomeres. Taz1 was also localized at the telomeric repeats near *AT2035* and *AT2088,* as shown by recovery 3 and 4-fold higher than that of *ade6*, respectively (Fig. 10, right). Localization of Taz1 at *AT2035* was impaired by *AT2035-S1959* base-substitution, while the localization at *AT2088* was not affected (Fig. 10, right). Moreover, *AT2088-S2632* substitution abolished the Taz1 localization specifically at the *AT2088* locus (Fig. 10, right). These results demonstrate that the telomeric repeats near *AT2035* and *AT2088* recruit Taz1 to the corresponding loci.

Taz1 plays an important role in global control of replication timing

I then asked whether Taz1 is required for replication timing control at late replication origins. BrdU incorporation was determined in the wild-type and *taz1*Δ strains for *AT2035* and *AT2088*, which are associated with telomeric repeats, as well as late origins *AT2080* and *ARS727*, which are not associated with telomeric repeats, and the sub-telomeric *TAS59*. In HU-treated wild-type cells, none of the late origins but the early origin *ars2004* replicated significantly (Fig. 11). In contrast, in HU-treated *taz1*Δ cells, *AT2035* and *AT2088* showed robust replication, to a level comparable with *ars2004*, whereas *AT2080* or *ARS727* did not replicate significantly (Fig. 11). *TAS59*, which is located about 20-kb distant from the telomere, replicated more efficiently than *ars2004* (Fig. 11). These results indicate that Taz1 is required for replication timing control of a subset of late origins that are associated with telomeric repeats.

To investigate the role of Taz1 in global control of replication timing, I and other members of Prof. Masukata's laboratory analyzed the replication profile of all

chromosomes. The experiments were accomplished by the support of Dr. Fukuura and Dr. Ogawa. The BrdU-labeled DNA prepared from HU-treated wild-type and *taz1*Δ cells was subjected to sequencing by oligonucleotide ligation and detection (SOLiD) (Fig. 12; Supplemental Fig. S1). Comparison of the replication profiles in wild-type and *taz1* Δ cells revealed that 26 and 46, in chromosome arm regions and sub-telomeres, respectively, among 156 late/dormant origins fired in the HU-treated *taz1* Δ cells (Fig. 16; Supplemental Fig. S1; Supplemental Table S1). Genome-wide analysis of Taz1-localization showed that Taz1 was localized at 16 of 26 internally located late origins that fired in *taz1* Δ (Fig. 16; Supplemental Fig. S1; Supplemental Tables S1, S2). Notably, the entire sub-telomeric regions spanning 50-100 kb from the ends of chromosomes I and II, including 46 previously identified late origins, replicated robustly in *taz1* Δ cells, although Taz1 was localized only in the vicinity of the telomere (Fig. 12; Supplemental Fig. S1). These results suggest that Taz1 plays an important role in the control of global replication timing in fission yeast.

Shelterin-like components and Rif1 contribute global control of replication timing

To elucidate the roles of Taz1 in regulation of DNA replication, I investigated involvement of other telomere binding proteins. I examined the replication efficiencies of early and late origins in HU-treated strains lacking each of *rap1*$^+$, *rif1*$^+$, *poz1*$^+$ or *ccq1*$^+$.

In *rap1*Δ strain, the replication efficiencies at late origins, *AT2088* and *AT2035* increased to a similar level with *ars2004*, whereas the non-ARS locus or *TAS59* did not replicate significantly (Fig. 11). In addition, *AT2080*, which was not activated in *taz1*Δ strain, showed robust replication. The results in *poz1*Δ are similar to *rap1*Δ (Fig. 11). In contrast, in *ccq1*Δ strain, *AT2088* and *AT2035* did not significantly replicate, as observed in wild type. However, the replication efficiency of the sub-telomeric origin *TAS59* increased to a higher level than other late origins in this mutant. In case of *rif1*Δ, not only the late origins *AT2088* and *AT2035* but *TAS59* replicated efficiently, as observed in *taz*1Δ (Fig. 11). In addition to the late origins activated in *taz*1Δ, two late origins *AT2080* and *ARS727* replicated more efficiently than *ars2004* in *rif1*Δ strain.

In summary, Rif1 represses a broader range of internal late origins than Taz1 regulates, while both of which are required for repression of the sub-telomeric origin *TAS59*. Rap1 and Poz1 are required for repression of the same set of internal late origins, but both of which do not repress *TAS59*. In contrast, Ccq1 may exclusively contribute repression for sub-telomeric origins.

Heterochromatin is not formed at internal late origins nearby telomere repeat

Taz1 interacts with various partners and participates in the functions such as telomere maintenance (Kanoh and Ishikawa, 2001; Miyoshi et al., 2008), establishment of telomere heterochromatin (Kanoh et al., 2005), localization of telomere at the nuclear periphery (Chikashige et al., 2009) and replication fork passage along telomere repeats (Miller et al., 2006). It has been shown that insertion of about 300 copies of telomere repeat at an internal chromosome locus promotes localization of Taz1 as well as K9-methylated histone H3 and Swi6 (Kanoh et al., 2005; Miyoshi et al., 2003). Because the highly condensed chromatin structure may prevent access of replication factors and delay activation of replication origin, I therefore tested whether heterochromatin is locally formed at late origins controlled by Taz1. To this end, I analyzed localization of Swi6 and K9-methylated histone H3 at the internal chromosome regions using a chromatin immunoprecipitation (ChIP) assay. ChIP recovery of DNA for *TAS59*, *ars2004, AT2035* and *AT2088* was determined by qPCR (Fig. 13). The Swi6-ChIP analysis revealed that the *ars2004*, *AT2035* and *AT2088* fragments were 3-fold less than *TAS59* locus (Fig. 13A). Similarly, the localization of K9-methylated histone H3 was not detected at the internal late origins and *ars2004* (Fig. 13B). Consistently, the late replicating property of *AT2035* and *AT2088* did not change in *swi6*Δ or *clr4*Δ, (Hayashi, unpublished), suggesting that heterochromatin does not play an important role in repression of the internal late origins that are controlled by Taz1.

The acetylation status of H3K9, K14 and H4K16 at AT2088 did not change when the RTC essential sequence was deleted

As describe above, previous studies suggest that histone acetylation and deacetylation can affect the activation timing of replication origins. The late origin *AT2088* is located in the promoter region of the stress-inducible gene *SPBC19C7.04c,* which is repressed in normal S phase. Deletion of Clr6, the fission yeast homologue of Rpd3, causes derepression of this gene (Wiren et al., 2005). Moreover, several sites in histone H3 and H4 (H4 K12, K16 and H3 K9 and K14) in the promoter of this gene are deacetylated in the Clr6 dependent manner (Wiren et al., 2005). I examined whether the RTC controls histone acetylation at the original *AT2088* locus. A 210-bp fragment containing the RTC essential sequence was deleted from the *AT2088* locus (*AT2088Δ210*), and a map of H3K9, K14 and H4K16 acetylation at the late origin *AT2088* was created by ChIP assay (Fig. 14A). To compare WT and *AT2088Δ210*, I also analyzed telomere and the early origin *ars2004*. I could not detect significant difference in recovery of DNA with these three types acetylated histone between *AT2088* and *AT2088Δ210* (Fig. 14B, C and D). Then acetylation states of these sites may not be involved in origin regulation.

Taz1-mediated replication timing control prevents loading of Sld3 to late origins

Because pre-RCs are formed at both early and late replication origins, I assumed the process of pre-RC activation to be regulated by the Taz1-mediated mechanism. To elucidate the step that is regulated, I analyzed the localizations of a pre-RC component Mcm6, and Sld3, which is recruited to pre-RC in the most upstream step of origin activation process in S phase (Yabuuchi et al. 2006). Because Sld3 localization occurs only transiently under wild-type conditions, I employed the cold-sensitive *nda4-108/mcm5* mutation that allows Sld3 loading but prevents initiation of replication (Yamada et al. 2004). In *cdc25-22 nda4-108 sld3-flag* cells carrying the native *AT2088* (WT) released synchronously into S phase from G2/M, Mcm6 was efficiently localized at all the origins, but not in the non-origin (nonARS) region (Fig. 15A, left). Sld3 was preferentially enriched at the *ars2004* but not at late origins or non-ARS (Fig. 15B, left). In *AT2088-S2632* cells lacking the telomeric repeat near *AT2088*, localization of Sld3 increased specifically at *AT2088* (Fig. 15B, middle), whereas Mcm6 localizations

were not significantly different from those in the wild-type (Fig. 15A, middle). These results show that the telomeric repeat-dependent RTC activity represses Sld3 loading. I then examined whether Taz1 impacted localization of Mcm6 or Sld3. In *taz1*Δ strain, localization of Sld3 increased specifically at *AT2035*, *AT2088* and *TAS59*, but not at *AT2080* or *ARS727* (Fig. 15B, right), while Mcm6 was localized at the origins, similarly to those in wild-type (Fig. 15A, right). These results show that Taz1-mediated control of replication timing does not affect Mcm6 localization, but prevents Sld3 loading at specific late origins.

Discussion

A replication-timing program that regulates individual replication origins to fire at a pre-fixed time during S phase exists in all eukaryotes. In this study, I demonstrate that replication timing of replication origin is intrinsically determined by a proximal segment in fission yeast. The segment has the activity to repress initiation from nearby origins, even at ectopic sites, in early S phase, and two copies of the telomeric repeat are essential for this repression. This result provides novel insights into the mechanism of replication timing control, especially how chromosome regions are distinctly regulated.

The results presented here also shed light on the involvement of telomere binding proteins in the regulation of replication timing. A conserved telomere-binding protein, Taz1, binds to the internal telomeric repeats and plays an essential role in replication timing control. Genome-wide analysis revealed that about half of late origins are regulated by the Taz1-mediated mechanism. Remarkably, almost all origins in sub-telomeric regions about 100 kb long were found to be regulated by Taz1. Other shelterin components and Rif1 also affect a wide range of late origins in arm regions and sub-telomeric regions.

Replication timing control element consists of telomeric repeats

The results of replication kinetics analysis showed that late origins including *AT2088* on chromosome arm regions replicated about 10 min later than early origins such as *ars2004* (Fig. 2C). The delay is due to the absence of initiation from late origins in early S phase, as shown by 2D gel electrophoresis (Fig. 8B). However, this is not due to the absence of a strong origin activity, because *AT2088* fragment that contains previously identified *ARS745* showed robust ARS activity when cloned on a plasmid (Fig. 2B). Interestingly, the pAT2088 plasmid replicated in late S phase (Fig. 4B), suggesting that the *AT2088* fragment retains the replication timing control. It should be noted that insertion of the *AT2088* fragment in proximal to early origins, *ars2004* and *ORI12*, on the chromosome caused repression of initiation from the origins in early

S phase (Fig. 5, 6). These results imply that the timing control activity present in *AT2088* fragment is not specific to *AT2088* but rather general to other origins. A 634 bp fragment that is sufficient for repression of *ars2004* contains a 25 bp essential region and about 60 bp important region for origin repression (Fig. 7B). The essential sequence consists of two tandem copies of telomere repeat-like sequence and AG/TC motif. The results of linker substitution experiments show that both copies of telomere repeat are required. Although the telomere-like sequence differs from the telomere repeat consensus, $GGTTACA_{0-1}C_{0-1}G_{0-6}$, the RTC is restored by replacement of the consensus sequence (Fig. 9B, *AT2088-telF*). In addition, insertion of the consensus sequence in the opposite direction relative to the surrounding sequence is functional, suggesting the sequence has a distinct function such as the binding site for telomere binding protein (Fig. 9B, *AT2088-telR*). Since Taz1, an orthologue of human TRF1 and TRF2, has been reported to bind to two tandem copies of telomere repeat in vitro and in yeast one hybrid system, Taz1 and other telomere binding proteins may play an important role in regulating replication origin (Spink et al., 2000) (Cooper et al., 1997).

In addition to telomeric repeats, a flanking AAGAGAGA sequence has some importance for the RTC activity (Fig. 7D, and data not shown). A similar purine cluster is found flanking to the telomeric sequence near *AT2035* (Fig. 9C). A purine-rich sequence may either stimulate Taz1 binding or recruit a factor involved in repression of replication initiation. In addition, a region of about 60-bp (2557-2617) adjacent to the essential sequence contributes to origin repression to some extent (Fig. 7B). Since the region is included in the scaffold/matrix associating regions (SAR/MAR) (Amati and Gasser 1990), association with the nuclear scaffold may restrict the access of replication factors or increase local concentration of inhibitory factors.

Distribution and regulation of telomeric repeats in chromosome arm regions

Our results demonstrate that two tandem copies of a telomeric repeat located in the vicinity of two late origins, *AT2088* and *AT2035*, are essential for control of replication timing at these origins. Moreover, 13 telomeric repeats are associated with late origins,

suggesting that telomeric repeats are general determinant of replication timing. About half of the telomeric-repeat associated late origins (9 among 13), including *ori2081, ori2100 and AT2088/ori2114*, are flanked by the genes that are silenced in normal growth conditions and induced under various stresses or during meiosis (Table S2).

Since gene-expression at these loci might be regulated by the mechanisms involving specific transcription factors and histone modifications, control of replication timing may contribute to maintenance or alteration of histone modifications. Although the acetylation status of H3K9, K14 and H4K16 at *AT2088* did not change when the RTC essential sequence was deleted (Fig. 14), it is possible that replication timing influences other sites of histone acetylation status or other histone modifications. Therefore, further investigations of relations between replication timing and gene expression will be needed. In metazoan, histone acetylation status is distinctly regulated during replication in the early and late S phases, suggesting that change in replication timing can play a role in alteration of gene expression during development (Lande-Diner et al. 2009).

Roles of Taz1 in the control of replication timing

In this study, I demonstrated that two tandem copies of a telomeric repeat located in the vicinity of two late origins, *AT2088* and *AT2035*, are essential for control of replication timing at these origins. The results of ChIP analysis demonstrated that the telomeric repeats, which are the binding sites for a homo-dimeric Taz1 (Cooper et al. 1997; Spink et al. 2000), indeed recruit Taz1 to the internal chromosome loci (Fig. 10). Moreover, Taz1 is required for timing control of about half of late origins (72 among 156), including all the sub-telomeric origins (46 origins). Genome-wide analysis of Taz1 localization showed Taz1 binds to the vicinity of 16 among 26 internal late origins that are regulated in a Taz1-dependent manner (Fig. 12A, Fig. 16 and Table S1). Because 13 of 16 origins are associated with telomeric repeats (including 3 that are manually found), Taz1 plays a role in the control of replication timing through binding to telomeric repeats near these origins (Fig. 17A). On the other hand, Taz1-localization was not detected at 10 internal late origins that are activated in *taz1*Δ

cells, leaving the possibility that Taz1 can participate in the control from a distance through certain mechanism. It is also remarkable that control of all the sub-telomeric late origins are dependent on Taz1, despite the absence of Taz1-localization at individual origins except for the vicinity of the telomeres (Fig. 12B; Supplemental Fig. S1; Supplemental Table S1) (Kanoh et al. 2005). It is likely that Taz1 that binds to the telomere may play a role in control of sub-telomeric origins. Because the number of telomere-bound Taz1 varies depending on the length of individual telomere, Taz1 monitors the telomere length and impacts the timing of sub-telomeric replication. This is consistent with the observations that shortened telomeres induce early firing of sub-telomeric replication origins in budding yeast, in which Rap1 plays a role of Taz1 (Bianchi and Shore 2007; Shore and Bianchi 2009; Lian et al. 2011). Timing of replication fork passage through the telomere is important for stable association of the telomerase and elongation of the telomere (Dionne and Wellinger 1998; Marcand et al. 2000; Gallardo et al. 2011). Thus, Taz1 is likely to play crucial roles in the feedback loop of replication mediated maintenance of telomere length, in addition to its role in passage of the replication forks through the telomeres (Miller et al. 2006).

Roles of shelterin components and Rif1 in the control of replication timing

This study also revealed the unexpected function of other shelterin components and Rif1 in genome-wide regulation of DNA replication. Recently, the observation that Rif1, another telomere binding protein in fission yeast, is involved in global control of replication timing has been reported (Hayano et al. 2012). Genome-wide analysis of replication in *taz1* Δ as well as *rif1* Δ revealed that all the 72 late origins that fire in *taz1* Δ are also activated in *rif1* Δ (Fig. 16; Supplemental Fig. S1; Supplemental Table S1). Moreover, 47 late origins that do not fire in *taz1* Δ , including *AT2080* and *ARS727/AT2013,* are activated in *rif1* Δ (Fig. 16; Supplemental Fig. S1; Supplemental Table S1). These observations suggest that there are at least Taz1-dependent and Taz1-independent pathways for timing control and both require Rif1. It is likely that Rif1 acts downstream of Taz1. It has been reported that the *ARS727* fragment cloned on a plasmid forces late replication of a concurrently cloned early origin, and that

several copies of the late consensus sequence (LCS), A/G-G/T-G/T-GGGGGA-A/T, are required for the repression (Yompakdee and Huberman 2004). The LCS might be involved in Taz1-independent Rif1-dependent pathway (Hayano et al. 2012).

Recent studies revealed that mammlian Rif1 also affects spatio-temporal program of DNA replication (Yamazaki et al., 2012; Cornaccia et al., 2012). Interestingly, Human rif1 associates with the nuclear scaffold structures at late M to early G1 phase and colocalizes with the mid-S replication foci. Mouse Rif1 accumulates at sites and is cleared from chromatin prior to its replication in mid S phase. These results suggest the hypothesis that Rif1 may be a crucial factor for generating chromatin architecture and establish accessibility of different origin clusters for limiting replication factors. I speculate that Taz1 recruits Rif1 to Taz1-dependent late origins and tethers the sites at the nuclear scaffold to form proper chromatin structures and/or recruit some factors enriched at the nuclear scaffold for limiting access of replication factors (Fig. 17B). Supporting this hypothesis, the Scaffold/matrix associating region (SAR/MAR) adjacent to the telomeric repeats at *AT2088* contributes to repress the activation of *AT2088*. The telomeric repeats and other cis-elements on chromosome arm regions may enable the specific regions to be replicated at the specific time in S phase.

In contrast to Taz1 and Rif1 which repress late origins located in both chromosome arm regions and sub-telomeric regions, Rap1 and Poz1 are not required for repression of sub-telomeric origins. Since Rap1 is directly connected to Poz1 and binds to Taz1 independently of Rif1, Rap1 and Poz1 may posses same or similar functions in the control of replication timing (Baumann and Cech, 2001; Miyoshi et al., 2008). In *rap1*Δ or *poz1*Δ mutant, terminal telomere repeats extensively elongates as long as 3-5 kb and 1-2 kb (Kanoh and Ishikawa, 2001; Miller et al., 2005), respectively, compared with 300 bp in wild type cells, resulting in accumulation of Taz1 as well as the associating Rif1 to the elongated telomeres. This may cause decrease in Taz1 and Rif1 bound to internal chromosomes, leading to de-repression of late origins specifically in arm regions (Fig. 18A). On the other hand, deletion of the telomerase recruiter, Ccq1, leads telomere shortening (Flory et al., 2004; Tomita and Cooper,

2008). Then, the amount of Rif1 at telomere ends may be reduced in *ccq1*Δ cells, leading to partial de-repression of sub-telomeric origins (Fig. 18A). Alternatively, it is also possible that Rif1 anchored to telomeres represses replication origins, and Shelterin-like complex acts as a mediator for Rif1 and exists at both telomeres and internal late origins. The telomeres of mitotically dividing fission yeast are localized at the nuclear periphery in two to four clusters (Alfredsson-Timmins et al., 2007; Funabiki et al., 1993). In this model, Shelterin-like complex bound to chromosome arm regions may localize late origins into telomere clusters, and Rif1 repress the origins (Fig. 18B).

Taz1-dependent pathway regulates DDK-dependent Sld3 loading in initiation of replication

In Taz1-dependent control of replication timing described here, Taz1 that binds in the vicinity of late origin impacts the process of initiation. The effects diminish by distance, because an early origin 20 kb from the Taz1 binding site is not inhibited (Supplemental Fig. S1; Supplemental Table S1). These characteristics suggest that a catalytic reaction or a semi-diffusible factor may be involved in the interference with the process of replication initiation. The heterochromatin formation does not play a significant role, because Swi6 and H3K9 methylation are not detected around the late origin *AT2088* (Fig. 13). Checkpoint pathways, which are proficient in *taz1*Δ (Miller and Cooper 2003), may not play a major role in the Taz1-dependent timing control. Therefore, the Taz1-dependent regulation seems to involve a novel mechanism that affects the initiation process.

In this study, I showed that loading of Sld3 onto pre-RC is prevented at late origins by a Taz1-mediated control of replication timing. In fission yeast, loading of Sld3 onto replication origins is dependent on pre-RC and DDK, and prerequisite for CDK-dependent assembly of other replication factors (Yabuuchi et al. 2006; Fukuura et al. 2011). A recent *in vitro* study in budding yeast has shown that origin association of Sld3 is dependent on DDK and distinct from those require CDK (Heller et al. 2011). Moreover, in vivo study in budding yeast suggest that origin association of

low-abundance Sld3, Sld7 and Cdc45, which is dependent on DDK, is crucial for temporal order of origin firing (Tanaka et al. 2011). The following evidence in fission yeast further emphasizes the importance of DDK recruitment in replication timing control; Swi6/HP1-dependent recruitment of Dfp1, a regulatory subunit of DDK, stimulates early activation of origins in peri-centromeric heterochromatin and the silent *mat* locus (Hayashi et al. 2009). Furthermore, tethering of Dfp1 to the late origin *ARS727*, which is Taz1-independent and Rif1-dependent, causes early firing of the origin (Patel et al. 2008). Because DDK preferentially phosphorylates subunits of chromatin-bound Mcm2-7 complex (Francis et al. 2009), both Taz1-dependent and independent regulation may interfere with the access of DDK, or phosphorylation of chromatin-bound Mcm2-7 complex by DDK (Francis et al. 2009). Although recruitment of DDK and loading of Sld3 occur in S phase, a process that occurs in G1 phase may impact the reactions. Correlation of the origin association timing of ORC and MCM in G1 phase with initiation timing has been reported in fission yeast (Wu and Nurse 2009). In mammalian cells, it has been proposed that a replication timing program is established during a discrete window of time in G1 phase, the timing decision point (TDP) (Dimitrova and Gilbert 1999). It is possible that an early event such as chromatin modifications around individual replication origins could affect the recruitment of DDK and subsequent loading of replication factors at the origins in S phase.

Our results show that fission yeast utilizes a set of telomeric sequences and telomere binding proteins for regulation of replication timing. Recent studies revealed novel genome-wide functions of telomere binding proteins in mammals. Mouse Rap1 binds to two tandem copies of the telomere repeat outside telomeric regions and regulates expression of the genes located in vicinity of the repeats (Martinez et al. 2010). In addition, mammalian Rap1 has also been identified as a regulator of the NF-κB signaling pathway that mediates the transcriptional responses to various stresses (Teo et al. 2010). Since telomeric sequences and telomere binding proteins are highly conserved among eukaryotes, it would be interesting to investigate whether they could be involved in regulation of DNA replication in other organisms.

Materials and Methods

Strains and Media

Strains and media used in this study are described in Supplementary Information and listed in Supplemental Table S3. Media used for fission yeast cultivation were YE medium as a complete medium and EMM medium as a selection medium (Moreno et al, 1991). All solid media contained 2.0% agar. Transformation of *S. pombe* was performed by the lithium acetate method (Forsburg, 2003), and geneticin (G418) was used for selection of transformants at a final concentration of 100 μg/ml. *E. coli* DH10B was used for plasmid construction. The medium used for *E. coli* cultivation was L-medium (1% Bacto Peptone, 0.5% Bacto Yeast Extract, 1% NaCl), and ampicillin and methicillin were added at a final concentration of 30 μg/ml for plasmid selection.

Construction of fission yeast strains

The origin-exchanged strains were constructed as described below. To construct a strain carrying the *ars2004* fragment at the *AT2088* locus, two segments, d1 and d2, near the ends of the intergenic region between *SPBC19C7.04c* and *SPBC19C7.05* were PCR-amplified using pair-wise primers, AT-3 with AT-4, and AT-5 with AT-6, and cloned into modified pBluescript II (pBS-EHB), where the *Hin*dIII-*Not*I fragment was replaced with *Eco*RI-*Hin*dIII-*Bam*HI recognition sequences, resulting in pTZ1. The 1.8-kb *ura4*$^+$ fragment was inserted at the *Hin*dIII site between the d1 and d2 inserts of pTZ1 to make pTZ2. The *Bam*HI fragment of pTZ2 carrying the *ura4*$^+$ gene flanked by the d1 and d2 fragments was used for transformation of HM83 (*h*$^+$ *ura4-D18*). HM1172 carrying *ura4*$^+$ at the *AT2088* locus was selected by PCR among the Ura$^+$ transformants. A 3.2-kb *Not*I-*Xba*I fragment of pARS2004 lacking an internal *Bam*HI site (Okuno et al., 1999) was inserted into the *Not*I-*Xba*I sites between d1 and d2 of pTZ1 to form pTZ3, and the *Bam*HI fragment carrying d1, *ars2004* and d2 was co-transformed with pREP1 into HM1178. Among transformants grown on EMM plates (EMM containing 150 μg/ml uracil) and 5'FOA plates (EMM containing 500

μg/ml 2'-deoxy-5'-fluorouridine and 150 μg/ml uracil), HM1281 carrying *ars2004* in place of *ura4*$^+$ at the *AT2088* locus was selected by PCR. HM1285 carrying *cdc25-22 Pnmt1-TK* was constructed by standard genetic crossing.

To construct a strain carrying the *AT2088* fragment in place of *ars2004*, a 232-bp e1 fragment and a 235-bp e2 fragment located at each end of the *ars2004* fragment were amplified using pair-wise primers AT-7 with AT-8, and AT-9 with AT-10 and cloned at the *Eco*RI-*Hin*dIII and *Hin*dIII-*Bam*HI sites, respectively, of modified pBluescript II to form pTZ4. A 3.6-kb *AT2088* fragment amplified using primers AT-1 and AT-2 was inserted at the *Hin*dIII site between e1 and e2 of pTZ4, to form pTZ4. The *Bam*HI fragment carrying e1-*AT2088*-e2 was used for transformation of HM198, in which the essential region at the *ars2004* locus was replaced by *ura4*$^+$ (Takahashi et al, 2001). Ura$^-$ transformants were selected on 5'FOA plates, and HM1346 carrying *AT2088* integration in place of *ura4*$^+$ at the *ars2004* locus was identified by PCR. HM1389 carrying *cdc25-22 Pnmt1-TK A2088::ura4* was obtained by standard genetic crosses.

For construction of a strain carrying the *AT2088* fragment inserted next to *ars2004*, two fragments, f1 and f2, left of *ars2004* were amplified using pair-wise primers, AT-11 with AT-12, and AT-13 with AT-14, respectively. The f1 and f2 fragments digested by *Eco*RI-*Not*I and *Not*I-*Bam*HI, respectively, were cloned into modified pBluescript II forming pTZ5. The *ura4*$^+$ fragment was inserted at the *Hin*dIII site between the f1 and f2 segments of pTZ5, making pTZ6. A 3.6-kb *AT2088* fragment amplified using primers AT-15 and AT16 was inserted into the *Not*I site setoff pTZ6, resulting in pTZ7. An *Eco*RI fragment of pTZ7 carrying f1-*ura4*$^+$-*AT2088*-f2 was used for transformation of the EOY15 strain, and a transformant carrying the insertion of *AT2088* next to *ars2004* was identified by PCR. HM1800, a derivative carrying *cdc25-22 Pnmt1-TK*, was obtained by standard genetic crossing.

For construction of a strain carrying the *AT2088* fragment inserted next to the *ORI12* locus, the *ura4-AT2088* fragment was amplified by two-step PCR amplification. The first PCR amplified two fragments containing the left regions of *ORI12* with part

of the *ura4* gene and *AT2088*, using the primer sets AT-33 with AT-34, and AT-35 with AT-36. The second PCR amplified the *ura4-AT2088* fragment from pTZ7 using the first PCR products and AT-33 with AT-36 as primers. The second PCR products were used for transformation of HM2836, which has *cdc25-22*, *nmt1-TK*, *ade6::ade6*$^{+}$*-Padh1-hENT* and auxotrophy for uracil. The transformants were selected on EMM plates.

To construct a series of deletion derivatives of *AT2088* that were inserted next to *ars2004* on the chromosome, fragments were PCR-amplified using the primers listed in Table 2, and the products digested by *Not*I alone or by *Not*I and *Pst*I, were cloned into pTZ6. The plasmids carrying the truncated *AT2088* fragments were digested by *Eco*RI and used for transformation of HM2836.

For introduction of a deletion *AT2088Δ210* into the chromosomal *AT2088* locus, the *AT2088Δ210* fragment amplified using the pair-wise primers AT-1 with M2527-R and M2637-F with AT-2 was inserted into the *Hin*dIII site in pBS-EHB. For introduction of base substitutions *AT2088-telF* and *AT2088-telR* into the *AT2088* locus, the *AT2088-telF/R* fragments amplified using the pair-wise primers AT-45 with S2617-R and telF/R with AT-46 were inserted into the *Eco*RI-*Bam*HI site in pBS-EHB. The altered *AT2088* fragments were excised by digestion with *Hin*dIII or *Eco*RI and used for transformation of HM4035, which has *AT2088::ura4*, *cdc25-22*, *nmt1-TK*, *ade6::ade6*$^{+}$*-Padh1-hENT*. For introduction of a base substitution *AT2088-S2632* into the *AT2088* locus, a *Not*I fragment of the plasmid carrying f1-*ura4*$^{+}$*-AT2088-S2632*-f2 was used for transformation of HM4035. The transformants were selected on EMM plates containing 500 μg/ml 2'-deoxy-5'-fluorouridine (5'FOA) and 150 μg/ml uracil.

For construction of strains carrying base substitutions in the *AT2035* locus, two segments near the right end of the intergenic region flanked by *sds23* were amplified using the primer sets AT-37 with AT-38 and AT-39 with AT-40. The products were used as primers together with the primers AT-37 with AT-40 for PCR amplification of the *ura4*$^{+}$ gene from pTZ7, and the products were used for transformation of HM2836 to obtain *AT2035-ura* (HM4159) carrying *ura4*$^{+}$ inserted at the *AT2035* locus.

Fragments carrying base substitutions *AT2035-S1956* and *AT2035-S1985* were amplified using the primer sets AT-41 with AT-42 and AT-41 with AT-43, respectively, from strain HM4159 used as the template. The respective products were used as primers for the second PCR reactions in the presence of primers AT-41 and AT-44 from HM4159, and the PCR products were used for transformation of HM2836.

Epitope tagging of Taz1

For epitope tagging of Taz1, the upstream part of *taz1*$^+$ was amplified by PCR using the primers Taz1upF and Taz1upR, and the product was digested by *Hin*dIII and *Eco*RI, and then cloned into the *Hin*dIII-*Eco*RI sites of pBluescript II KS(+) to generate pJS1. The *Eco*RI-*Bam*HI fragment containing *kanMX6* was introduced into the *Eco*RI-*Bam*HI site of pJS1 to create pJS2. The promoter region of *taz1*$^+$ was amplified by PCR using the primers Taz1proF and Taz1proR, and the product was digested by *Bam*HI and *Spe*I and cloned into the *Bam*HI and *Spe*I sites of pBluescript II KS+ to generate pJS3. The fragment, which was generated by digestion of pJS3 with *Bam*HI and *Spe*I, was cloned into the *Bam*HI-*Spe*I site of pJS2 to generate pJS4. The N-terminal fragment of *taz1*$^+$ amplified by PCR using the primers Taz1NF and Taz1NR was digested by *Bam*HI and *Spe*I and cloned into the *Hin*dIII-*Eco*RI sites of pBluescript II KS+ to generate pJS5. pJS5 was then digested by *Nde*I and *Spe*I, and the product containing the N-terminal fragment of *taz1*$^+$ was introduced into the *Nde*I-*Spe*I site of pJS4 to create pJS6. The *Nde*I fragment containing six tandem copies of FLAG-epitopes (6Flag) was cloned into the *Nde*I site of pJS6, resulting in pJS7, and the sequences were confirmed. The *Sal*I-*Spe*I fragment of pJS7 was used for transformation of HM4045 (*h*$^-$ *972E*). Transformants were selected on YE-geneticin (100 μg/ml) plates, and insertion of the 6flag-tag at the N-terminal of *taz1*$^+$ was confirmed by genomic sequencing. The resulting strain showed normal replication profiles, and the telomere lengths were maintained as those in wild-type strain, suggesting that the Flag-tagged Taz1 was functional.

Construction of ARS plasmids and ARS assay

A 3.2-kb fragment containing *ars2004* had been cloned into pYC11, a derivative of pBluescriptII SK(-) carrying the *LEU2* marker gene (pXN289) (Okuno et al, 1997). A 3.6-kb intergenic fragment between *SPBC19C7.04c* and *SPBC19C7.05* containing *AT2088* was PCR-amplified using the primers AT-1 with AT-2 and cloned at the *Hin*dIII site of pYC11, resulting in pAT2088. To analyze the ARS activity, derivatives of pYC11 plasmids were introduced into HM123 (h^- *leu1-32*) by the electroporation method, and Leu^+ transformants were selected on EMM plates for 4 days at 30 °C.

Construction of ARS plasmids and ARS assay

To obtain the deletion mutants of telomere binding proteins $taz1^+$ (JK702), $rap1^+$ (JK774), $rif1^+$ (JK690), $poz1^+$ (TM2374) and $ccq1^+$ (TM2370) were gifted from Dr. J. Kanoh (JK702, JK774 and JK690) and Dr. F. Ishikawa (TM2374 and TM2370). The deletion mutants carrying *cdc25-22 Pnmt1-TK* were obtained by standard genetic crosses.

***S. pombe* strains used in this study. (Supplemental Table S3)**

Strain	Genotype
EOY15	*h- ura4-D18*
HM83	*h$^+$ ura4-D18*
HM198	*h$^+$ ura4-D18 leu1-32 ars2004::ura4$^+$*
HM668	*h- cdc25-22 ura4-D18:: ura4$^+$nmt1-TK$^+$*
HM1172	*h$^+$ ura4-D18 ura4-D18:: ura4$^+$nmt1-TK$^+$*
HM1235	*h- cdc25-22 ura4-DS/E:nmt1-TK$^+$*
HM1281	*h- ura4-D18 leu1-32 AT2088::ars2004 pREP1*
HM1285	*h$^+$ cdc25-22 ura4-D18:: ura4$^+$nmt1-TK$^+$ ars2004::ura4$^+$ AT2088::ars2004*
HM1346	*h$^+$ ura4-D18 leu1-32 ars2004::AT2088*
HM1389	*h? cdc25-22 ura4-D18:: ura4$^+$nmt1-TK$^+$ ars2004::AT2088 AT2088:: ura4$^+$*
HM1415	*h? cdc25-22 ura4-D18:: ura4$^+$nmt1-TK$^+$ ars2004::ura4$^+$ AT2088::AT2088-ars2004-ura4$^+$*
HM1800	*h? cdc25-22 ura4-D18:: ura4$^+$nmt1-TK$^+$ ars2004::ura4$^+$AT2088-ars2004 AT2088::ura4$^+$*
HM1847	*h? cdc25-22 ura4-D18:: ura4$^+$nmt1-TK$^+$ ars2004::ura4$^+$ars2004 AT2088::ura4$^+$*
HM1864	*h- cdc25-22 ura4-D18:: ura4$^+$nmt1-TK$^+$ ade6::ade6$^+$adh1-hENT$^+$*
HM1921	*h- cdc25-22 ura4-DS/E:nmt1-TK$^+$ ars2004::ura4$^+$AT2088R1630-ars2004*
HM1922	*h- cdc25-22 ura4-DS/E:nmt1-TK$^+$ ars2004::ura4$^+$AT2088R2017-ars2004*
HM1923	*h- cdc25-22 ura4-DS/E:nmt1-TK$^+$ ars2004::ura4$^+$AT2088R2527-ars2004*
HM1924	*h- cdc25-22 ura4-DS/E:nmt1-TK$^+$ ars2004::ura4$^+$AT2088R2947-ars2004*
HM1926	*h- cdc25-22 ura4-DS/E:nmt1-TK$^+$ ars2004::ura4$^+$AT2088L476-ars2004*
HM1930	*h- cdc25-22 ura4-DS/E:nmt1-TK$^+$ ars2004::ura4$^+$AT2088L1519-ars2004*
HM2418	*h- cdc25-22 ura4-DS/E:nmt1-TK$^+$ ars2004::ura4$^+$AT2088L1519R2947-ars2004*
HM2484	*h- cdc25-22 ura4-DS/E:nmt1-TK$^+$ ars2004::ura4$^+$AT2088L1707R2947-ars2004*
HM2485	*h- cdc25-22 ura4-DS/E:nmt1-TK$^+$ ars2004::ura4$^+$AT2088L2107R2947-ars2004*
HM2487	*h- cdc25-22 ura4-DS/E:nmt1-TK$^+$ ars2004::ura4$^+$AT2088L2312R2947-ars2004*
HM2419	*h- cdc25-22 ura4-DS/E:nmt1-TK$^+$ ars2004::ura4$^+$AT2088L2508R2947-ars2004*
HM2488	*h- cdc25-22 ura4-DS/E:nmt1-TK$^+$ ars2004::ura4$^+$AT2088L2681R2947-ars2004*
HM2595	*h- cdc25-22 ura4-D18:: ura4$^+$nmt1-TK$^+$ ade6::ade6$^+$adh1-hENT$^+$ taz1:: kanMX6*
HM2637	*h- cdc25-22 ura4-D18:: ura4$^+$nmt1-TK$^+$ nda4-108 sld3-5Flag::kanMX6*
HM2836	*h- cdc25-22 ura4-DS/E:nmt1-TK$^+$ ade6::ade6$^+$adh1-hENT$^+$*
HM2853	*h- cdc25-22 ura4-DS/E:nmt1-TK$^+$ ars2004::ura4$^+$AT2088-ars2004 ade6::ade6$^+$adh1-hENT$^+$*
HM2854	*h- cdc25-22 ura4-DS/E:nmt1-TK$^+$ ars2004::ura4$^+$AT2088L2312R2947-ars2004 ade6::ade6$^+$adh1-hENT$^+$*
HM2857	*h- cdc25-22 ura4-DS/E:nmt1-TK$^+$ ars2004::ura4$^+$AT2088M2433-ars2004 ade6::ade6$^+$adh1-hENT$^+$*
HM2875	*h- cdc25-22 ura4-DS/E:nmt1-TK$^+$ ars2004::ura4$^+$AT2088L2412R2947-ars2004 ade6::ade6$^+$adh1-hENT$^+$*
HM2877	*h- cdc25-22 ura4-DS/E:nmt1-TK$^+$ ars2004::ura4$^+$AT2088M2527-ars2004 ade6::ade6$^+$adh1-hENT$^+$*
HM2878	*h- cdc25-22 ura4-DS/E:nmt1-TK$^+$ ars2004::ura4$^+$AT2088M2637-ars2004 ade6::ade6$^+$adh1-hENT$^+$*
HM2881	*h- cdc25-22 ura4-DS/E:nmt1-TK$^+$ ars2004::ura4$^+$AT2088M2737-ars2004 ade6::ade6$^+$adh1-hENT$^+$*
HM2882	*h- cdc25-22 ura4-DS/E:nmt1-TK$^+$ ars2004::ura4$^+$AT2088R2849-ars2004 ade6::ade6$^+$adh1-hENT$^+$*
HM2895	*h- cdc25-22 ura4-D18:: ura4$^+$nmt1-TK$^+$ ade6::ade6$^+$adh1-hENT$^+$ rif1:: ura4*
HM2901	*h- cdc25-22 ura4-D18:: ura4$^+$nmt1-TK$^+$ ade6::ade6$^+$adh1-hENT$^+$ rap1:: ura4*
HM2926	*h- cdc25-22 ura4-DS/E:nmt1-TK$^+$ ars2004::ura4$^+$AT2088N2527-ars2004 ade6::ade6$^+$adh1-hENT$^+$*
HM2927	*h- cdc25-22 ura4-DS/E:nmt1-TK$^+$ ars2004::ura4$^+$AT2088N2557-ars2004 ade6::ade6$^+$adh1-hENT$^+$*

HM2930	*h- cdc25-22 ura4-DS/E:nmt1-TK$^+$ ars2004::ura4$^+$AT2088N2587-ars2004 ade6::ade6$^+$adh1-hENT$^+$*
HM2932	*h- cdc25-22 ura4-DS/E:nmt1-TK$^+$ ars2004::ura4$^+$AT2088N2617-ars2004 ade6::ade6$^+$adh1-hENT$^+$*
HM2933	*h- cdc25-22 ura4-DS/E:nmt1-TK$^+$ ars2004::ura4$^+$AT2088N2649-ars2004 ade6::ade6$^+$adh1-hENT$^+$*
HM2936	*h- cdc25-22 ura4-DS/E:nmt1-TK$^+$ ars2004::ura4$^+$AT2088N2677-ars2004 ade6::ade6$^+$adh1-hENT$^+$*
HM2939	*h- cdc25-22 ura4-DS/E:nmt1-TK$^+$ ars2004::ura4$^+$AT2088N2707-ars2004 ade6::ade6$^+$adh1-hENT$^+$*
HM3085	*h- cdc25-22 ura4-DS/E:nmt1-TK$^+$ ars2004::ura4$^+$AT2088X2617-ars2004 ade6::ade6$^+$adh1-hENT$^+$*
HM3190	*h- cdc25-22 ura4-DS/E:nmt1-TK$^+$ ars2004::ura4$^+$AT2088S2617-ars2004 ade6::ade6$^+$adh1-hENT$^+$*
HM3191	*h- cdc25-22 ura4-DS/E:nmt1-TK$^+$ ars2004::ura4$^+$AT2088S2624-ars2004 ade6::ade6$^+$adh1-hENT$^+$*
HM3192	*h- cdc25-22 ura4-DS/E:nmt1-TK$^+$ ars2004::ura4$^+$AT2088S2632-ars2004 ade6::ade6$^+$adh1-hENT$^+$*
HM3429	*h- cdc25-22 ura4-D18:: ura4$^+$nmt1-TK$^+$ ade6::ade6$^+$adh1-hENT$^+$ taz1-3Flag::kanMX6*
HM3663	*h$^+$ cdc25-22 ura4-D18:: ura4$^+$nmt1-TK$^+$ poz1:: hyg$^+$*
HM3667	*h$^+$ cdc25-22 ura4-D18:: ura4$^+$nmt1-TK$^+$ ade6::ade6$^+$adh1-hENT$^+$ ccq1:: hyg$^+$*
HM3707	*h- cdc25-22 ura4-D18:: ura4$^+$nmt1-TK$^+$ AT2088::AT2088S2632 ade6::ade6$^+$adh1-hENT$^+$ taz1-3Flag::kanMX6*
HM3887	*h- cdc25-22 ura4-DS/E:nmt1-TK$^+$ ars2004::ura4$^+$ AT2088::ura4$^+$ ade6::ade6$^+$adh1-hENT$^+$ pXN289*
HM3888	*h- cdc25-22 ura4-DS/E:nmt1-TK$^+$ ars2004::ura4$^+$ AT2088::ura4$^+$ ade6::ade6$^+$adh1-hENT$^+$ pYC11+AT2088*
HM4034	*h- cdc25-22 ura4-DS/E:nmt1-TK$^+$ ars2004::ura4$^+$AT2088S2641-ars2004 ade6::ade6$^+$adh1-hENT$^+$*
HM4035	*h- cdc25-22 ura4-DS/E:nmt1-TK$^+$ AT2088::ura4$^+$ ade6::ade6$^+$adh1-hENT$^+$*
HM4037	*h- cdc25-22 ura4-DS/E:nmt1-TK$^+$ AT2088::AT2088-telF ade6::ade6$^+$adh1-hENT$^+$*
HM4040	*h- cdc25-22 ura4-DS/E:nmt1-TK$^+$ AT2088::AT2088-telR ade6::ade6$^+$adh1-hENT$^+$*
HM4041	*h- cdc25-22 ura4-D18:: ura4$^+$nmt1-TK$^+$ AT2088::AT2088S2632 ade6::ade6$^+$adh1-hENT$^+$*
HM4155	*h- cdc25-22 ura4-D18:: ura4$^+$nmt1-TK$^+$ nda4-108 sld3-5Flag::kanMX6 AT2088::AT2088S2632*
HM4159	*h- cdc25-22 ura4-DS/E:nmt1-TK$^+$ ade6::ade6$^+$adh1-hENT$^+$ AT2035::AT2035-ura4 control*
HM4211	*h- cdc25-22 ura4-DS/E:nmt1-TK$^+$ ade6::ade6$^+$adh1-hENT$^+$ AT2035::AT2035-S1956-ura4*
HM4212	*h- cdc25-22 ura4-DS/E:nmt1-TK$^+$ ade6::ade6$^+$adh1-hENT$^+$ AT2035::AT2035-S1985-ura4*
HM4265	*h- cdc25-22 ura4-D18:: ura4$^+$nmt1-TK$^+$ nda4-108 sld3-5Flag::kanMX6 taz1::natMX6*
JK690	*h- ura4-D18 leu1-32 rif1:: ura4*
JK702	*h- ura4-D18 leu1-32 taz1:: ura4*
JK774	*h- ura4-D18 leu1-32 rap1:: ura4*
TM2370	*h- ura4-D18 leu1-32 ccq1:: Hyg*
TM2374	*h- ura4-D18 leu1-32 poz1:: Hyg*

Oligonucleotide sequences of primers (Supplemental table S4)

Primers for construction of strains and plasmids

AT-1: 5'- AAAAAGCTTGAGAAGGAGTTGTTTG-3'
AT-2: 5'- AAAAAGCTTCTGATGCAAATATAGGC-3'
AT-3: 5'- AAAGAATTCGGATCCTTGAGAAGGAGTTGTTTG-3'
AT-4: 5'- AAAAAGCTTGCGGCCGCGTTGTGTCAGATTTGATAC -3'
AT-5: 5'- AAAAAGCTTCTAGATTATCTTCATCAACCTGC-3'
AT-6: 5'- AAAGGATCCACTGATGCAAATATAGGC-3'
AT-7: 5'- AAAGAATTCGGATCCGAAGATTCGCGAGGCACC -3'
AT-8: 5'- AAAAAGCTTCTGGCGAGCTATCTGTG-3'
AT-9: 5'- AAAAAGCTTCCAAATCAACACACCCTAAC-3'
AT-10: 5'- AAAGGATCCGAATTCGTTAGATGTCTGTACAGG-3'
AT-11: 5'-AAAGAATTCGATGAATGCAGTGACC-3'
AT-12: 5'-AAAGCGGCCGCAAGCTTGCCTTCTTTTCCCAGTCC-3'
AT-13: 5'-AAAGCGGCCGCGAAGATTCGCGAGGCACC-3'
AT-14: 5'-AAAGGATCCGAATTCTGGCGAGCTATCTGTG-3'
AT-15: 5'-AAAGCGGCCGCTTGAGAAGGAGTTGTTTG-3'
AT-16: 5'-AAAGCGGCCGCACTGATGCAAATATAGGC-3'
AT-17: 5'-GAAGAGGAGAATGAGCTTTACG-3'
AT-18:
5'-CCGTGATGATGATGGTGGTGAGATTGATAATTAACAAGCTCTTCC-3'
AT-19: 5'-CGCCTCGACATCATCTGCCCCTCCGGATAGAGTTTGTTCA-3'
AT-20: 5'-GGACAATTAACGCTTGAC-3'
AT-21: 5'-CCGGTCCGACTATAATCAT-3'
AT-22:
5'-CCGTGATGATGATGGTGGTGAGAAGTTTGTTTTGAAAGTAGTTTAGC-3'
AT-23: 5'-CGCCTCGACATCATCTGCCCGCATCTCTGCCCAAATTC-3'
AT-24: 5'-GTTGATTTACTCTGCTACATCAAAG-3'
AT-25: 5'-CAATCAATGACGGAAGCCA-3'
AT-26:
5'- CCGTGATGATGATGGTGGTGAGCAATTCTAGATAAAATAGCTCTCTG-3'
AT-27: 5'-CGCCTCGACATCATCTGCCCTTATTCAACTCATGGGTACAGG-3'
AT-28: 5'-GATTTTGGACGCCAAACT-3'
AT-29:
5'-AAACTGCAGGAAGGGTTACAGGTTACAGGGTCTCTCTTTAGACAAAGCTA
AAAATC -3'
AT-30: 5'- AAGGATCCGAATTCACTGATGCAAATATAGGCAAA -3'
AT-31:
5'-AAACTGCAGGAACCCTGTAACCTGTAACCCTCTCTCTTTAGACAAAGCTA
AAAATC -3'
AT-32: 5'-AAGAATTCTTGAGAAGGAGTTGTTTGTTTAC -3'
AT-33: 5'-CACTTGAATAGATTAGCATTGTCC-3'
AT-34: 5'-TGCCTTCTTTTCCCAGTCCCTATTCACTTGCCGCGTAAAC-3'
AT-35:
5'-GCCTATATTTGCATCAGTGCTAGAATAACCTATGGTCTGTTTAAATCG-3'
AT-36: 5'-AAAGCCTTCATAGCAAAGT-3'
AT-37: 5'-GCAATGGTAATGATGATCATCTG-3'
AT-38: 5'-CAAATGCATACATATAGCCAGCATCTACCCAATCTTGA-3'
AT-39: 5'-AGCCAATGAAAGATGTATGTAGATCGCAACGTTGAATTATGTAT-3'

AT-40: 5'-TTGTAGATGCAGTGTAGGTC-3'
AT-41: 5'-CTAGATGAGCGTCTATTTGTGTC-3'
AT-42:
5'- TCACTCCGGGGAAGAGGTTCCTGCAGGACGTAAAAAGACTCATGTGC-3'
AT-43:
5'-GTTTCAATATTGAGTAAATGGTCCGCCTGCAGGCACTCCGGGGAAGAGG-3'
AT-44: 5'-CATAAAGTGGGAAAGTGGGGCAG -3'
AT-45: 5'- AAGAATTCTTGAGAAGGAGTTGTTTGTTTAC-3'
AT-46: 5'- AAGGATCCGAATTCACTGATGCAAATATAGGCAAA-3'

Primers for construction of AT2088 truncated fragments
L476-F: 5'-GGAATTCGCGGCCGCGTCTCATTTGAACTGATCC-3'
L1519-F: 5'-GGAATTCGCGGCCGCATTCATGTTGTTCCACTACG-3'
R2947-R: 5'-AGGAATTCGCGGCCGCGAATGTATGGACGACACAC-3'
R2527-R: 5'-AGGAATTCGCGGCCGCTATCCCTTGTTATGGAGAG-3'
R2017-R: 5'-GGAATTCGCGGCCGCTGTGTGTGCCTCCTTTGAAC-3'
R1630-R: 5'-AGGAATTCGCGGCCGCTACACGCATGAGACAGTCG-3'
L1707-F: 5'-AAGGAATTCGCGGCCGCAAGGTTGCTATAGAGTC-3'
L2107-F: 5'-AGGAATTCGCGGCCGCGACGATGTTGTTTCACGCA-3'
L2312-F: 5'-AGGAATTCGCGGCCGCGTGTGCGCCATGAAAGTGG-3'
L2508-F: 5'-AGGAATTCGCGGCCGCTCTACGTTTTAGTTGTAATATCTG-3'
L2681-F: 5'-AGGAATTCGCGGCCGCTCTCCATAACAAGGGATA-3'
L2432-F: 5'-GAATTCGCGGCCGCATTCGCACATGTATCTC-3'
M2433-R: 5'-AACTGCAGGAAAAATACAATACAGCTCAAG-3'
M2433-F: 5'-AACTGCAGAAATATATTGAAACATCTTTGTATC-3'
M2527-R: 5'-AACTGCAGTATCCCTTGTTATGGAGAG-3'
M2527-F: 5'-AACTGCAGAACCTCTCTCTTTAGACAAAG-3'
M2637-R: 5'-AACTGCAGACGAGGTTATATTTGAAATGTAC-3'
M2637-F: 5'-AACTGCAGTGAATTACAAAAGTTTTTTGGTT-3'
M2737-R: 5'-AACTGCAGAAAGAAGAAAATATGAAAGGAGTA-3'
M2737-F: 5'-AACTGCAGTTCGTCCGCCTTTTCC-3'
N2527-R: M2627-R
N2527-F: 5'-AACTGCAGTTAATATTCAATTCTGTACG-3'
N2557-R: 5'-AACTGCAGTTTAAGATACAAAGATGTTTC-3'
N2557-F: 5'-AACTGCAGATAACAAAAACTATGACT-3'
N2587-R: 5'-AACTGCAGCTTGAAACGTACAGAATTG-3'
N2587-F: 5'-AACTGCAGTTTCAAATATAACCTCGT-3'
N2617-R: 5'-AACTGCAGTACATTTTAAAGTCATAGTT-3'
N2617-F: 5'-AACTGCAGTAGACAAAGCTAAAAATC-3'
N2649-R: 5'-AACTGCAGAGAGAGGTTACGAGGTT-3'
N2649-F: 5'-AACTGCAGTACACAGCGTGGAATTTGG-3'
N2677-R: 5'-AACTGCAGAGCGTAAATAGATTTTTAGC-3'
N2677-F: 5'-AACTGCAGATAAAATACTCCTTTCATAT-3'
N2707-R: 5'-AACTGCAGAAGTTTAAGACCCAAATTCC-3'
N2707-F: F9.1
S2617-R: N2617-R
S2617-F: 5'-ACCTGCAGGAATATAACCTCGTAACCTCT-3'
S2624-R: 5'-ACCTGCAGGTGAAATGTACATTTTAAAGT-3'
S2624-F: 5'-ACCTGCAGGCTCGTAACCTCTCTCTTTAG-3'

S2632-R: 5'-ACCTGCAGGGTTATATTTGAAATGTACATTTT-3'
S2632-F: 5'-ACCTGCAGGCTCTCTCTTTAGACAAAGCT-3'
S2641-R: 5'- AAACCTGCAGGGGTTACGAGGTTATATTTGAAATG-3'
S2641-F: 5'- AAACCTGCAGGTAGACAAAGCTAAAAATCTATTTACGC-3'
Tel-F:
5'-AAACTGCAGGAACCCTGTAACCTGTAACCCTCTCTCTTTAGACAAAGCTA
AAAATC-3'
Tel-R:
5'-AAACTGCAGGAAGGGTTACAGGTTACAGGGTCTCTCTTTAGACAAAGCT
AAAAATC-3'

Primers for Southern hybridization probes
AT2046-F: 5'-GGATATGATACTGCGGTTGG-3'
AT2046-R: 5'-CCACTCTGTTGGGGTATC-3'
AT2047-F: 5'-GCACTGCTGGCACCAAC-3'
AT2047-R: 5'-GAGACAAGAAGCCTGG-3'

Primers for detection of replication efficiencies
AT2024-F: 5'-GATGATTCGAGCTCTGCT-3'
AT2024-R: 5'-GCTCTTTAATCTCTCACTCC-3'
RT-*AT2024*-F: 5'-GCGACGGAGATGTCCAGAAA-3'
RT-*AT2024*-R: 5'-TGCACATGCACAATACACACCTT-3'
RT-*AT2035*-F: 5'-TGGTACGTCGAGTGAGACACAAT-3'
RT-*AT2035*-R: 5'-AAAGACTCATGTGCTGTGGGAAT-3'
RT-*ars2004*-F: 5'-AAAATGCCAACCCGTATTGAC-3'
RT-*ars2004*-R: 5'-ATAACATACCAACCCTTACAAC-3'
RT-*AT2088*(-1.2 kb)-F: 5'-TCCTCACTTCCTTAAAAACAGATTAAGAAATA-3'
RT-*AT2088*(-1.2 kb)-R: 5'-CGCAAAATAACATCGTAGTGGAAC-3'
RT-*TAS59*-F: 5'-CAGAAGAGACTACAGAGGCGGTTT-3'
RT-*TAS59*-R: 5'-GGATGCCTTATCTGCGACCA-3'
RT-*AT2080*-F: 5'-CGAACAACAGGCTTGGTTAGAA -3'
RT-*AT2080*-R: 5'- GAAGTACGGACTTGTTTCGATTCC -3'
RT-*ARS727*-F: 5'-TTGCTTTACCCATGATACCCTTT-3'
RT-*ARS727*-R: 5'-CCGCGCATACCGAATGTA-3'

Primers for Taz1-ChIP analysis
RT-tel0.3kb-F: 5'-TATTTCTTTATTCAACTTACCGCACTTC-3'
RT-tel0.3kb-R: 5'-CAGTAGTGCAGTGTATTATGATAATTAAATGG-3'
RT-*AT2035*-F: 5'-TGGTACGTCGAGTGAGACACAAT-3'
RT-*AT2035*-R: 5'-AAAGACTCATGTGCTGTGGGAAT-3'
RT-*AT2088*-core element-F: 5'-TCAATTCTGTACGTTTCAAGCAAAT-3'
RT-*AT2088*-core element-R: 5'-CCCAAATTCCACGCTGTGTA-3'
RT-*ade6*-F: 5'- TGATGGAGGACGTGAGCACATTGA-3'
RT-*ade6*-R: 5'- TTGAATGCATCGCAGAGTTGCAGG-3'

Primers for Swi6 and H3K9Me-ChIP analysis
RT-*AT2035*-F: 5'-TGGTACGTCGAGTGAGACACAAT-3'
RT-*AT2035*-R: 5'-AAAGACTCATGTGCTGTGGGAAT-3'
RT-*AT2088*-core element-F: 5'-TCAATTCTGTACGTTTCAAGCAAAT-3'
RT-*AT2088*-core element-R: 5'-CCCAAATTCCACGCTGTGTA-3'

RT-*ars2004*-F: 5'-AAAATGCCAACCCGTATTGAC-3'
RT-*ars2004*-R: 5'-ATAACATACCAACCCTTACAAC-3'
RT-*TAS59*-F: 5'-CAGAAGAGACTACAGAGGCGGTTT-3'
RT-*TAS59*-R: 5'-GGATGCCTTATCTGCGACCA-3

Primers for H3K9Ac, K14Ac and H4K16Ac-ChIP analysis
RT-tel0.3kb-F: 5'-TATTTCTTTATTCAACTTACCGCACTTC-3'
RT-tel0.3kb-R: 5'-CAGTAGTGCAGTGTATTATGATAATTAAATGG-3'
RT-*ars2004*-F: 5'-AAAATGCCAACCCGTATTGAC-3'
RT-*ars2004*-R: 5'-ATAACATACCAACCCTTACAAC-3'
RT-*AT2088 0.7kb*-F: 5'-GGAGTAAGGATGGAAATGTGGAA -3'
RT-*AT2088 0.7kb*-R: 5'-CATGATCGACGACCTATAAGTTGCT-3
RT-*AT2088 1.1kb*-F: 5'-GAGAAGTTTTGTAATTCCAATGCCA -3'
RT-*AT2088 1.1kb*-R: 5'-ATAACCGCACCAAAATACCCATATC -3
RT-*AT2088 1.5kb*-F: 5'-TCCTCACTTCCTTAAAAACAGATTAAGAAATA -3'
RT-*AT2088 1.5kb*-R: 5'-CGCAAAATAACATCGTAGTGGAAC -3
RT-*AT2088 1.7kb*-F: 5'-TGCTGTCAGAGGCTTACACTAAC -3'
RT-*AT2088 1.7kb*-R: 5'-GAAAATATCCAAGTCATGTTCATTGC -3
RT-*AT2088 2.1kb*-F: 5'-TCTTAACGTTACTTGGAAGCCATATGTAAA -3'
RT-*AT2088 2.1kb*-R: 5'-CCACTTTCATGGCGCACA -3
RT-*AT2088 3.0kb*-F: 5'-AGCAGCTAGTTCATTCGTATATCAATTT -3'
RT-*AT2088 3.0kb*-R: 5'-GAATGTATGGACGACACACATGTTCGAAA -3

Primers for Mcm6 and Sld3-ChIP analyses
RT-*ars2004*-F: 5'-AAAATGCCAACCCGTATTGAC-3'
RT-*ars2004*-R: 5'-ATAACATACCAACCCTTACAAC-3'
RT-*AT2035*-1F: 5'-CACTAAGCTACTGGCAGTTTGTACG-3'
RT-*AT2035*-1R: 5'-GGTAAAACACCCACGTGCG-3'
RT-*AT2088*(-1.2 kb)-F: 5'-TCCTCACTTCCTTAAAAACAGATTAAGAAATA-3'
RT-*AT2088*(-1.2 kb)-R: 5'-CGCAAAATAACATCGTAGTGGAAC-3'

BrdU incorporation and replication timing analysis

Fission yeast strains carrying P_{nmt1}-*TK cdc25-22* were cultured in EMM medium lacking thiamine to induce transcription of the TK gene at 25°C for 18 h to 5 x 10_6 cells/ml. Cells arrested at the G2/M boundary by *cdc25-22* mutation at 36°C for 3 h were released at 25°C and cultured for indicated periods in the presence of 200 ⌈M 5-bromo-2'-deoxyuridine (BrdU). Preparation of cellular DNA and separation of BrdU-labeled DNA by CsCl density gradient centrifugation were carried out as described previously (Hayashi et al., 2007). For replication kinetics analysis, the amount of DNA in the HL and LL densities was determined by real-time PCR using the primer sets listed in Supplemental Table S4. Replication (%) at each time point was

calculated with the equation 100 x (1/2HL)/(1/2HL+LL). To determine replication (%) of specific loci in early S phase, 10 mM hydroxyurea (HU) was added upon release from G2/M block.

Chromatin immunoprecipitation

ChIP assay was performed essentially as described previously (Hayashi et al., 2009), except for the following modifications. For Taz1-ChIP, approximately 2.5 x 10_8 *flag-taz1* cells grown at 30°C were disrupted with glass beads in 0.4 ml of lysis buffer (50 mM Tris-HCl [pH 8.0], 280 mM NaCl, 1 mM EDTA, 1% Triton X-100, 0.1% sodium deoxycholate, 1 mM phenylmethylsulfonyl fluoride, supplemented with proteinase inhibitor cocktail [Sigma-Aldrich]). The soluble extracts diluted with lysis buffer to adjust the TritonX-100 to 0.3% were used for immunoprecipitation with magnetic beads (Dynal) conjugated with mouse monoclonal anti-FLAG M2 (1:400; Sigma-Aldrich). For Mcm6- and Sld3-ChIP, *cdc25-22 sld3-flag nda4-108/mcm5* cells grown at 28°C were synchronized at the G2/M boundary at 36°C for 3 h and released at 20°C, which is the restrictive temperature for the *nda4-108* (Yamada et al. 2004). Cell extracts were used for ChIP assays with mouse anti-Flag and rabbit anti-Mcm6 antibodies. For Sld3- and H3K9diMe, H3K9Ac, H3K14Ac and H4K16Ac-ChIP, *cdc25-22* cells grown at 25°C were synchronized at the G2/M boundary at 36°C for 3 h and released at 25°C and cultured for 40 min. Cell extracts were used for ChIP assays with rabbit anti-Swi6 (Living Colors Full-length A.v. Polyclonal Antibody, Clontech) and anti-H3K9diMe, H3K9Ac, H3K14Ac and H4K16Ac (a gift from Dr. H Kimura) antibodies. DNA prepared from whole-cell extracts or immunoprecipitated fractions was quantified by qPCR using SYBR green I in the 7300 PCR system (Applied Biosystems).

Two-dimensional gel electrophoresis

Neutral-neutral 2D gel electrophoresis was carried out as described (Hayashi et al., 2007). For Southern blotting probes, relevant origin fragments, as described below, were used after random prime labeling with ^{32}P-dCTP using the Megaprime DNA

labeling system (GE Healthcare). For detection of *ars2004*, a 940-bp *Not*I- *Hin*dIII fragment from p940 was labeled for probe to prevent cross-hybridization between the translocated *ars2004* and *ars2004* partially substituted with *ura4*$^+$ at the native locus. The *ars2004* probe was used to detect a 6.5-kb *Eco*T22I fragment and a 6-kb *Fba*1-*Nco*1 fragment (for re-hybridization after *AT2088* detection) in HM668 and a 5.1-kb *Fba*I-*Nco*I fragment in HM1285 and a 7.4-kb *Sty*I fragment in HM1800. The 3.6-kb *Hin*dIII fragment from pAT2088 was used to detect a 5.5-kb *Fba*I-*Nco*I fragment in HM668 and a 7.4-kb *Eco*T22I fragment in HM1389 both containing *AT2088*. Fragments of 1.7 kb and 2 kb amplified by PCR using primers *AT2046*-F with *AT2046*-R, and *AT2047*-F with *AT2047*-R, were labeled to detect a 5.5-kb *Eco*T22I fragment containing *AT2046* in HM1389 (for re-hybridization after detection of the translocated *AT2088*) and a 7.4-kb *Sty*I fragment containing *AT2047* in HM668 and HM1800, respectively. Radioactive signals were detected with a BAS2500 system (Fuji Film) and measured using Image Gauge software.

Nucleotide pattern search

For search of two copies of telomere-like sequence, the pattern of GGTTAYN(1,3)GGTTAY was searched using the EMBOS "fuzznuc" program, which was obtained at http://emboss.sourceforge.net/apps/release/6.3/emboss/apps/fuzznuc.html.

SOLiD analysis

BrdU-labeled DNA prepared at 120 min after G2/M release from HU-treated wild-type, *taz1*Δ and *rif1*Δ strains and separated by CsCl density gradient centrifugation, and those obtained by FLAG-Taz1-IP were used for SOLiD deep sequencing analysis, which was performed according to the manufacturer's standard protocol (Applied Biosystems).

Accession numbers

Sequecne data have been deposited to the Sequence Read Archive

(http://www.ncbi.nlm.nih.gov/Traces/sra/) with the accession number SRP011412.

Supplementary References

Forsburg, S.L. (2003). Introduction of DNA into *S. pombe* cells. Curr Protoc Mol Biol *Chapter 13*, Unit 13 17.

Maundrell, K., Hutchison, A., and Shall, S. (1988). Sequence analysis of ARS elements in fission yeast. EMBO J *7*, 2203-2209.

ACKNOWLEDGEMENTS

This study would not have been possible without the support of many people.
I am deeply grateful to Professor Hisao Masukata whose guidance, support and encouragement from the initial to the final phase enables me to develop an understanding of this study. I am also indebted to Drs. Takuro Nakagawa and Tatsuro Takahashi for valuable and constructive suggestions during the planning and development of this study. I also deeply appreciate to Drs. Katsuhiko Shirahige and Ryuichiro Nakato for great contribution to the tiling chip analysis. I thank Drs. Junko Kanoh and Fuyuki Ishikawa for providing plasmids and strains, Dr. Hiroshi Kimura for providing antibodies for histone modifications, Dr. Teruo Yasunaga for searching nucleotide sequence pattern, Dr. Makoto Hayashi for critical reading of the manuscript and providing materials. I would also like to thank all of the members of Prof. Masukata's laboratory for the supports. I received generous support from Drs. Masayoshi Fukuura and Shiho Ogawa. I have greatly benefited from Ami Kishimoto, Tomokazu Takenaka and Ji-hoon Song for providing materials and helpful discussions. This study was supported by a Grant-in-Aid for JSPS fellows.

References

Aggarwal B D, Calvi B R. 2004. Chromatin regulates origin activity in Drosophila follicle cells. *Nature* **430**(6997): 372-376.

Alfredsson-Timmins J, Henningson F, Bjerling P. 2007. The Clr4 methyltransferase determines the subnuclear localization of the mating-type region in fission yeast. *J Cell Sci* **120**: 1935-1943.

Amati B, Gasser SM. 1990. Drosophila scaffold-attached regions bind nuclear scaffolds and can function as ARS elements in both budding and fission yeasts. *Mol Cell Biol* **10**(10): 5442-5454.

Aparicio, J. G., Viggiani, C. J., Gibson, D. G., and Aparicio, O. M. (2004). The Rpd3-Sin3 histone deacetylase regulates replication timing and enables intra-S origin control in Saccharomyces cerevisiae. Mol Cell Biol *24*, 4769-4780.

Baumann P, Cech T R. 2001. Pot1, the putative telomere end-binding protein in fission yeast and humans. *Sience* **292**:1171-1175

Bell SP, Dutta A. 2002. DNA replication in eukaryotic cells. *Annu Rev Biochem* **71**: 333-374.

Bianchi A, Shore D. 2007. Early replication of short telomeres in budding yeast. *Cell* **128**(6): 1051-1062.

Chikashige, Y., and Hiraoka, Y. (2001). Telomere binding of the Rap1 protein is required for meiosis in fission yeast. Curr Biol *11*, 1618-1623.

Chuang, R.Y. and Kelly, T.J. (1999) The fission yeast homologue of Orc4p binds to replication origin DNA via multiple AT-hooks. *Proc. Natl. Acad. Sci. U. S. A.*, **96**, 2656-2661.

Cooper JP, Nimmo ER, Allshire RC, Cech TR. 1997. Regulation of telomere length and function by a Myb-domain protein in fission yeast. *Nature* **385**(6618): 744-747.

Daniela Cornacchia, Vishnu Dileep, Jean-Pierre Quivy, Rossana Foti, Federico Tili, Rachel Santarella-Mellwig, Claude Antony, Genevieve Almouzni, David M Gilbert and Sara BC Buonomo. 2012. Mouse Rif1 is a key regulator of the replication-timing programme in mammalian cells. *EMBO J* **31**: 3678-3690.

Dimitrova DS, Gilbert DM. 1999. The spatial position and replication timing of chromosomal domains are both established in early G1 phase. *Mol Cell* **4**(6): 983-993.

Dionne I, Wellinger RJ. 1998. Processing of telomeric DNA ends requires the passage of a replication fork. *Nucleic Acids Res* **26**(23): 5365-5371.

Feng, W., Collingwood, D., Boeck, M.E., Fox, L.A., Alvino, G.M., Fangman, W.L., Raghuraman, M.K. and Brewer, B.J. (2006) Genomic mapping of single-stranded DNA in hydroxyurea-challenged yeasts identifies origins of replication. *Nat. Cell Biol.*, **8**, 148-155.

Ferguson BM, Fangman WL. 1992. A position effect on the time of replication origin activation in yeast. *Cell* **68**(2): 333-339.

Flory M R, Carson A R, Muller E G, Aebersold R. 2004. An SMC-domain protein in fission yeast links telomeres to the meiotic centrosome. *Mol Cell* **16**(4): 619-630.

Francis LI, Randell JC, Takara TJ, Uchima L, Bell SP. 2009. Incorporation into the prereplicative complex activates the Mcm2-7 helicase for Cdc7-Dbf4 phosphorylation. *Genes Dev* **23**(5): 643-654.

Friedman KL, Diller JD, Ferguson BM, Nyland SV, Brewer BJ, Fangman WL. 1996. Multiple determinants controlling activation of yeast replication origins late in S phase. *Genes Dev* **10**(13): 1595-1607.

Fukuura M, Nagao K, Obuse C, Takahashi TS, Nakagawa T, Masukata H. 2011. CDK promotes interactions of Sld3 and Drc1 with Cut5 for initiation of DNA replication in fission yeast. *Mol Biol Cell* **22**(14): 2620-2633.

Funabiki H, Hagan I, Uzawa S, Yanagida M. 1993. Cell cycle-dependent specific positioning and clustering of centromeres and telomeres in fission yeast. *J Cell Biol* **121**(5): 961-976

Gallardo F, Laterreur N, Cusanelli E, Ouenzar F, Querido E, Wellinger RJ, Chartrand P. 2011. Live cell imaging of telomerase RNA dynamics reveals cell cycle-dependent clustering of telomerase at elongating telomeres. *Mol Cell* **44**(5): 819-827.

Gilbert DM, Takebayashi SI, Ryba T, Lu J, Pope BD, Wilson KA, Hiratani I. 2010. Space and time in the nucleus: developmental control of replication timing and chromosome architecture. *Cold Spring Harb Symp Quant Biol* **75**: 143-153.

Goren A, Tabib A, Hecht M, Cedar H. 2008. DNA replication timing of the human beta-globin domain is controlled by histone modification at the origin. *Genes Dev* **22**: 1319-1324

Hayano M, Kanoh Y, Matsumoto S, Renard-Guillet C, Shirahige K, Masai H. 2012. Rif1 is a global regulator of timing of replication origin firing in fission yeast. *Genes Dev* **26**(2): 137-150.

Hayashi M, Katou Y, Itoh T, Tazumi A, Yamada Y, Takahashi T, Nakagawa T, Shirahige K, Masukata H. 2007. Genome-wide localization of pre-RC sites and identification of replication origins in fission yeast. *EMBO J* **26**(5): 1327-1339.

Hayashi MT, Takahashi TS, Nakagawa T, Nakayama J, Masukata H. 2009. The heterochromatin protein Swi6/HP1 activates replication origins at the pericentromeric region and silent mating-type locus. *Nat Cell Biol* **11**(3): 357-362.

Hall I M, Shankaranarayana G D, Noma K, Ayoub N, Cohen A, Grewal S I. 2002. Establishment and maintenance of a heterochromatin domain. *Science* **297**: 2232-2237.

Heichinger C, Penkett CJ, Bahler J, Nurse P. 2006. Genome-wide characterization of fission yeast DNA replication origins. *EMBO J* **25**: 5171-5179.

Heller RC, Kang S, Lam WM, Chen S, Chan CS, Bell SP. 2011. Eukaryotic origin-dependent DNA replication in vitro reveals sequential action of DDK and S-CDK kinases. *Cell* **146**(1): 80-91.

Hiraoka Y, Henderson E, Blackburn EH. 1998. Not so peculiar: fission yeast telomere repeats. *Trends Biochem Sci* **23**(4): 126. Hiratani I, Gilbert DM. 2009. Replication timing as an epigenetic mark. *Epigenetics* **4**(2): 93-97.

Hiratani I, Leskovar A, Gilbert DM. 2004. Differentiation-induced replication-timing changes are restricted to A T -rich/long interspersed nuclear element (LINE)-rich isochores. *Proc Natl Acad Sci USA* **101**(48): 16861-16866.

Hiratani I, Ryba T, Itoh M, Yokochi T, Schwaiger M, Chang CW, Lyou Y, Townes TM, Schubeler D, Gilbert DM. 2008. Global reorganization of replication domains during embryonic stem cell differentiation. *PLoS Biol* **6**(10): e245.

Kanoh J, Ishikawa F. 2001. spRap1 and spRif1, recruited to telomeres by Taz1, are essential for telomere function in fission yeast. *Curr Biol* **11**(20): 1624-1630.

Kanoh J, Sadaie M, Urano T, Ishikawa F. 2005. Telomere binding protein Taz1 establishes Swi6 heterochromatin independently of RNAi at telomeres. *Curr Biol* **15**(20): 1808-1819.

Kim SM, Dubey DD, Huberman JA. 2003. Early-replicating heterochromatin. *Genes Dev* **17**(3): 330-335.

Knott, S. R., Viggiani, C. J., Tavare, S., and Aparicio, O. M. (2009). Genome-wide replication profiles indicate an expansive role for Rpd3L in regulating replication initiation timing or efficiency, and reveal genomic loci of Rpd3 function in Saccharomyces cerevisiae. *Genes Dev 23*, 1077-1090.

Labib K. 2010. How do Cdc7 and cyclin-dependent kinases trigger the initiation of chromosome replication in eukaryotic cells? *Genes Dev* **24**(12): 1208-1219.

Lande-Diner L, Zhang J, Cedar H. 2009. Shifts in replication timing actively affect histone acetylation during nucleosome reassembly. *Mol Cell* **34**(6): 767-774.

Leonhardt, H Sporbert, A., Cardoso, M. C. 2000, Targeting regulatory factors to intranuclear replication sites. Crit Rev Eukaryot Gene Expr. **10**(2): 127-133.

Lian HY, Robertson ED, Hiraga S, Alvino GM, Collingwood D, McCune HJ, Sridhar A, Brewer BJ, Raghuraman MK, Donaldson AD. 2011. The effect of Ku on telomere replication time is mediated by telomere length but is independent of histone tail acetylation. *Mol Biol Cell* **22**(10): 1753-1765.

Loupart, M.L., Krause, S.A., and Heck, M.S. (2000). Aberrant replication timing induces defective chromosome condensation in Drosophila ORC2 mutants. Curr Biol *10*, 1547-1556.

MacAlpine DM, Bell SP. 2005. A genomic view of eukaryotic DNA replication. *Chromosome Res* **13**(3): 309-326.

MacAlpine DM, Rodriguez HK, Bell SP. 2004. Coordination of replication and transcription along a Drosophila chromosome. *Genes Dev* **18**(24): 3094-3105.

Marianna Wiren, Rebecca A Silverstein, Indranil Sinha, Julian Walfridsson, Hand-mao Lee, Patricia Laurenson, Lorraine Pillus, Daniel Robyr, Michael Grunstein and Karl Ekwall. 2005. Genome-wide analysis of nucleosome density histone acetylation and HDAC function in fission yeast. *EMBO J* **24**: 2906-2918.

Marcand S, Brevet V, Mann C, Gilson E. 2000. Cell cycle restriction of telomere elongation. *Curr Biol* **10**(8): 487-490.

Martinez P, Thanasoula M, Carlos AR, Gomez-Lopez G, Tejera AM, Schoeftner S, Dominguez O, Pisano DG, Tarsounas M, Blasco MA. 2010. Mammalian Rap1 controls telomere function and gene expression through binding to telomeric and extratelomeric sites. *Nat Cell Biol* **12**(8): 768-780.

Maundrell K, Hutchison A, Shall S. 1988. Sequence analysis of ARS elements in fission yeast. *Embo J* **7**(7): 2203-2209.

Miller KM, Cooper JP. 2003. The telomere protein Taz1 is required to prevent and repair genomic DNA breaks. *Mol Cell* **11**(2): 303-313.

Miller KM, Rog O, Cooper JP. 2006. Semi-conservative DNA replication through telomeres requires Taz1. *Nature* **440**(7085): 824-828.

Miyoshi, T., Kanoh, J., Saito, M., and Ishikawa, F. (2008). Fission yeast Pot1-Tpp1 protects telomeres and regulates telomere length. Science *320*, 1341-1344.

Miyoshi, T., Sadaie, M., Kanoh, J., and Ishikawa, F. (2003). Telomeric DNA ends are essential for the localization of Ku at telomeres in fission yeast. J Biol Chem *278*, 1924-1931.

Okuno Y, Satoh H, Sekiguchi M, Masukata H. 1999. Clustered adenine/thymine stretches are essential for function of a fission yeast replication origin. *Mol Cell Biol* **19**(10): 6699-6709.

Patel PK, Kommajosyula N, Rosebrock A, Bensimon A, Leatherwood J, Bechhoefer J,Rhind N. 2008. The Hsk1(Cdc7) replication kinase regulates origin efficiency. *Mol Biol Cell* **19**(12): 5550-5558.

Pflumm, M.F., and Botchan, M.R. (2001). Orc mutants arrest in metaphase with abnormally condensed chromosomes. Development *128*, 1697-1707.

Raghuraman MK, Winzeler EA, Collingwood D, Hunt S, Wodicka L, Conway A, Lockhart DJ, Davis RW, Brewer BJ, Fangman WL. 2001. Replication dynamics of the yeast genome. *Science* **294**(5540): 115-121.

Remus D, Diffley JF. 2009. Eukaryotic DNA replication control: lock and load, then fire. *Curr Opin Cell Biol* **21**(6): 771-777.

Santocanale C, Diffley JF. 1998. A Mec1- and Rad53-dependent checkpoint controls late-firing origins of DNA replication. *Nature* **395**(6702): 615-618.

Santocanale C, Sharma K, Diffley JF. 1999. Activation of dormant origins of DNA replication in budding yeast. *Genes Dev* **13**(18): 2360-2364.

Satoshi Yamazaki, Aii Ishii, Yutaka Kanoh, Masako Oda, Yasumasa Nishito and Hisao Masai. 2012. Rif1 regulates the replication timing domains on the human genome. *EMBO J* **31**: 3667-3677.

Segurado M, de Luis A, Antequera F. 2003. Genome-wide distribution of DNA replication origins at A+T-rich islands in *Schizosaccharomyces pombe*. *EMBO Rep* **4**(11): 1048-1053.

Sharma K, Weinberger M, Huberman JA. 2001. Roles for internal and flanking sequences in regulating the activity of mating-type-silencer-associated replication origins in Saccharomyces cerevisiae. *Genetics* **159**(1): 35-45.

Shore D, Bianchi A. 2009. Telomere length regulation: coupling DNA end processing to feedback regulation of telomerase. *Embo J* **28**(16): 2309-2322.

Spink KG, Evans RJ, Chambers A. 2000. Sequence-specific binding of Taz1p dimers to fission yeast telomeric DNA. *Nucleic Acids Res* **28**(2): 527-533.

Stewart M. F, Li J, Lee I. 2005. Relationship between histone H3 lysine 9methylation, transcription repression, and heterochromatin protein 1 recruitment. Mol Cell Biol **25**: 2525-2538

Sugawara N. 1989. *PhD thesis, Harvard Univ*.

Sugiyama T, Cam H P, Sugiyama R, Noma K, Zofall M, Kobayashi R, Grewal S I. 2007. SHREC, an effector complex for heterochromatic transcriptional silencing, Cell **128**: 491-504.

Takahashi T, Ohara E, Nishitani H, Masukata H. 2003. Multiple ORC-binding sites are required for efficient MCM loading and origin firing in fission yeast. *EMBO J* **22**(4): 964-974.

Takahashi T, Ohara E, Nishitani H, Masukata H. 2003. Multiple ORC-binding sites are required for efficient MCM loading and origin firing in fission yeast. *EMBO J* **22**(4): 964-974.

Tanaka S, Araki H. 2010. Regulation of the initiation step of DNA replication by cyclin-dependent kinases. *Chromosoma* **119**(6): 565-574.

Tanaka S, Nakato R, Katou Y, Shirahige K, Araki H. 2011. Origin association of sld3, sld7, and cdc45 proteins is a key step for determination of origin-firing timing. *Curr Biol* **21**(24): 2055-2063.

Teo H, Ghosh S, Luesch H, Ghosh A, Wong ET, Malik N, Orth A, de Jesus P, Perry AS, Oliver JD et al. 2010. Telomere-independent Rap1 is an IKK adaptor and regulates NF-kappaB-dependent gene expression. *Nat Cell Biol* **12**(8): 758-767.

Tomita K, Cooper J P. 2008. Fission yeast Ccq1 is telomerase recruiter and local checkpoint controller. *Genes Dev* **22**(24): 3461-3474.

Volpe T A, Kidner C, Hall I M, Teng G, Grewal S I, Martienssen R A. 2002. Regulation of heterochromatic silencing and histone H3 lysine-9 methylation by RNAi. *Science* **297**: 1833-1837.

Vogelauer, M., Rubbi, L., Lucas, I., Brewer, B. J., and Grunstein, M. (2002). Histone acetylation regulates the time of replication origin firing. Mol Cell *10*, 1223-1233.

Wu PY, Nurse P. 2009. Establishing the program of origin firing during S phase in fission Yeast. *Cell* **136**(5): 852-864.

Wyrick JJ, Aparicio JG, Chen T, Barnett JD, Jennings EG, Young RA, Bell SP, Aparicio OM. 2001. Genome-wide distribution of ORC and MCM proteins in *S. cerevisiae*: high-resolution mapping of replication origins. *Science* **294**(5550): 2357-2360.

Yabuuchi H, Yamada Y, Uchida T, Sunathvanichkul T, Nakagawa T, Masukata H. 2006. Ordered assembly of Sld3, GINS and Cdc45 is distinctly regulated by DDK and CDK for activation of replication origins. *EMBO J* **25**(19): 4663-4674.

Yamada Y, Nakagawa T, Masukata H. 2004. A novel intermediate in initiation complex assembly for fission yeast DNA replication**.** *Mol Biol Cell* **15**(8): 3740-3750.

Yompakdee C, Huberman JA. 2004. Enforcement of late replication origin firing by clusters of short G-rich DNA sequences. *J Biol Chem* **279**(40): 42337-42344.

Figure 1

A

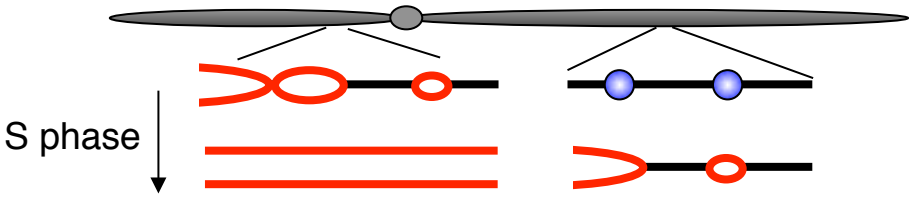

	Transcriptional regulation	Nuclear positioning	Histone modifications
Early origin	Active	Interior	Acetylation
Late origin (late / dormant)	Inactive	Peripheral	Methylation/deacetylation

B

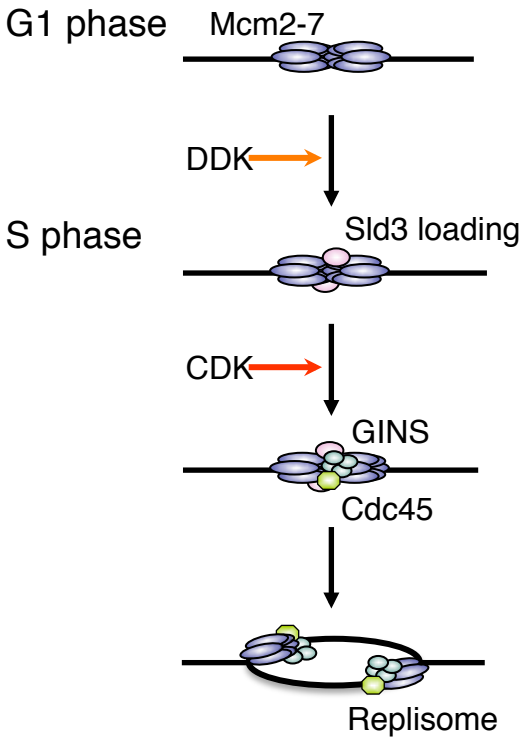

Figure 1. Introduction

(A) General correlations between features of chromosomes and activation of replication origin. (B) Activation of replication origin occurs in a step-wise manner. When cells enter S phase, Sld3 is recruited to pre-RCs in a DDK dependent manner. Then, GINS is recruited in a CDK dependent manner followed by Cdc45 loading. MCM is activated and double strand DNA is unwound. Finally, RPA assembles to single strand DNA and replication initiates.

Figure 2

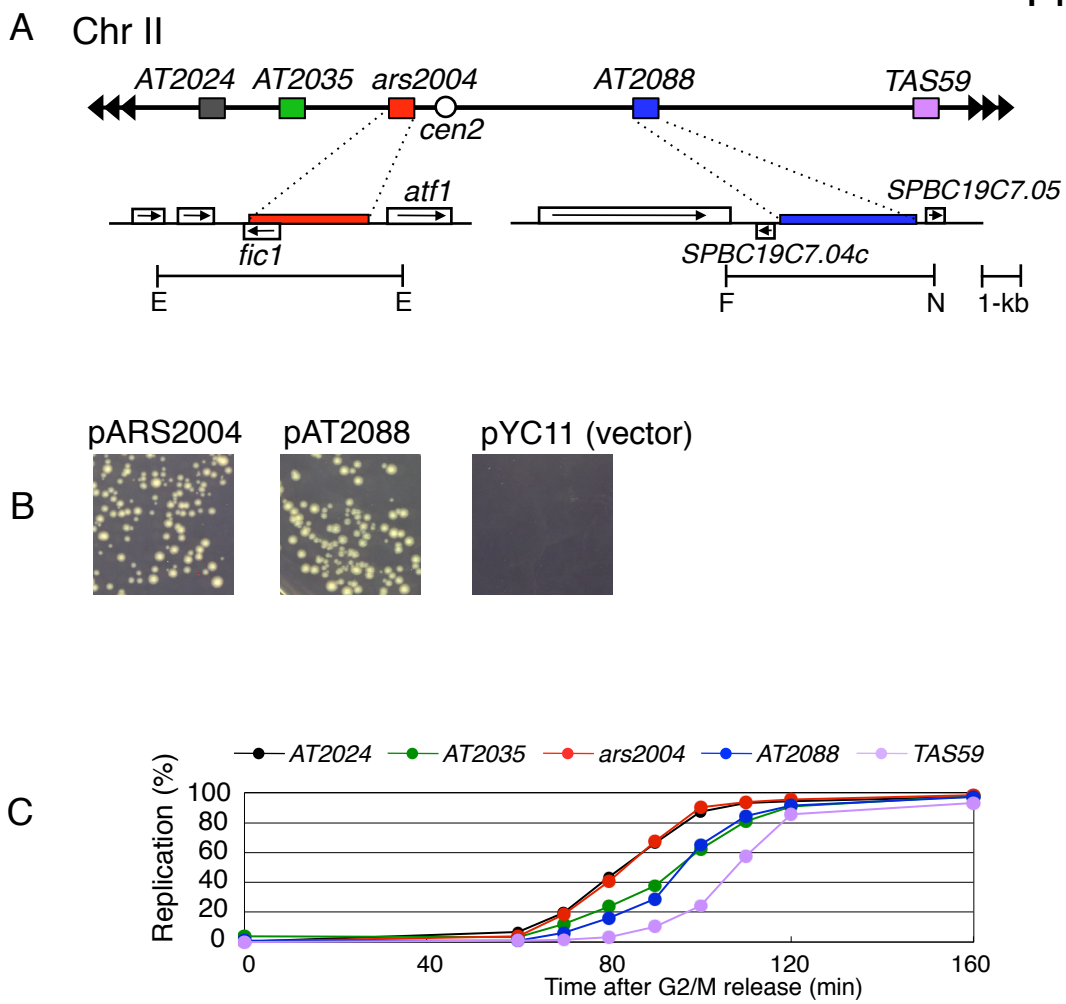

Figure 2. Replication timings of origins in fission yeast

(A) The locations of early and late replication origins on *S. pombe* chromosome II are presented schematically. Positions of early origins, *AT2024* (gray) and *ars2004* (red), *cen2*, late origins, *AT2035* (green) and *AT2088* (blue), and a sub-telomeric origin *TAS59* (purple) are shown. For the *ars2004* and *AT2088* loci, locations of the genes with the direction of transcription (arrow) and fragments (red: 3.2-kb *ars2004*, blue: 3.6-kb *AT2088*) used for translocation are presented. Relevant restriction fragments (E, *Eco*T22I; F, *Fba*I; N, *Nco*I) analyzed by two-dimensional (2D) gel electrophoresis are shown below the maps. (B) Derivatives of the pYC11 (*LEU2*) plasmid carrying a 3.2-kb *ars2004* and a 3.6-kb *AT2088* were introduced into HM123 (h^- *leu1-32*). Transformants formed on minimal media plates after 4 days at 30°C are presented. (C) Replication kinetics of early and late origins. Fission yeast *cdc25-22 nmt1-TK+* cells arrested at G2/M boundary at 36°C for 3 h were released at 25°C in the presence of BrdU (200 mM). At the indicated time points, the replicated heavy-light (HL) DNA was separated from light-light (LL) DNA using CsCl density gradient centrifugation and the amount of DNA of *AT2024* (black), *AT2035* (green), *ars2004* (red), *AT2088* (blue) and *TAS59* (purple) in the LL and HL densities were determined by qPCR. Replication kinetics of each origin are presented. The results of biologically independent experiments are shown in Supplementary Fig. S1A.

Figure 3

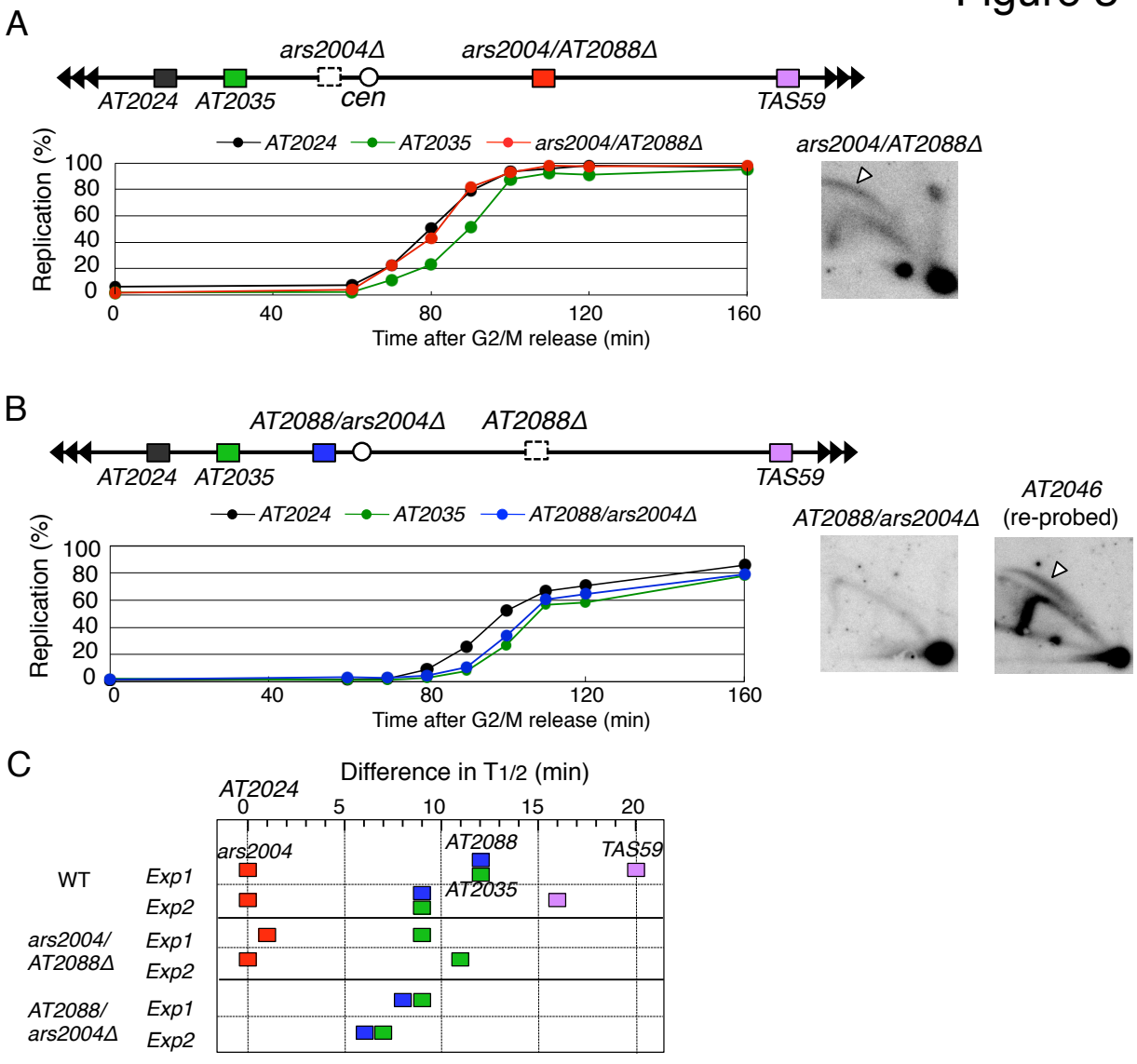

Figure 3. Replication timings of ars2004 and AT2088 origin fragments are maintained at ectopic loci.

Replication kinetics of *ars2004* (red) inserted at the *AT2088* locus (A) and *AT2088* at the *ars2004* locus (B) were obtained as described in Fig. 2C. Right panels show the results of 2D gel analysis of *ars2004* (*Fba*I-*Nco*I fragment) at the *AT2088* locus (A) and *AT2088* (*Eco*T22I fragment) at the *ars2004* locus (B) prepared at 90 min after G2/M release in the presence of HU (10 mM). The membrane was re-hybridized with the early origin *AT2046* probe (B). An arrowhead indicates the bubble arc. (C) Comparison of time required for replication in half of cell population (T1/2). T1/2 (min) for each origin was obtained from the results presented in Figs. 2C, 3A, 3B and unpublished data. The difference in T1/2 between an origin and *AT2024* (early origin control) was presented. *AT2035* and *AT2088* replicate 6-12 min later than *ars2004* and *AT2024*, regardless of their locations on the chromosome.

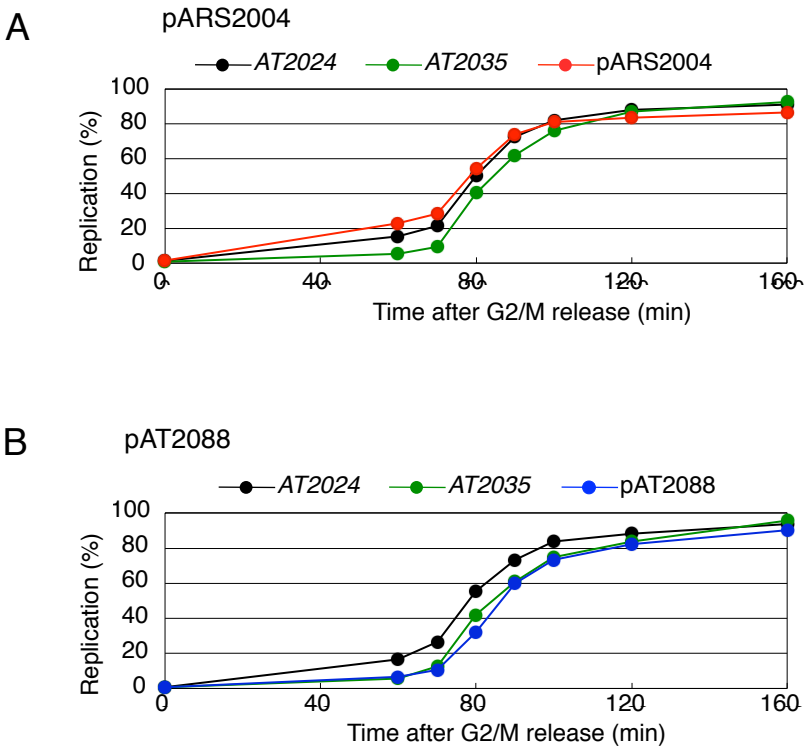

Figure 4. Replication timings of ars2004 and AT2088 origin fragments cloned on plasmids.

Replication kinetics of *ars2004* (red) cloned on a plasmid pXN289 (A; pARS2004) and *AT2088* (blue) cloned on the pXN289 (B; pAT2088) were obtained as described in Fig. 2C.

Figure 5

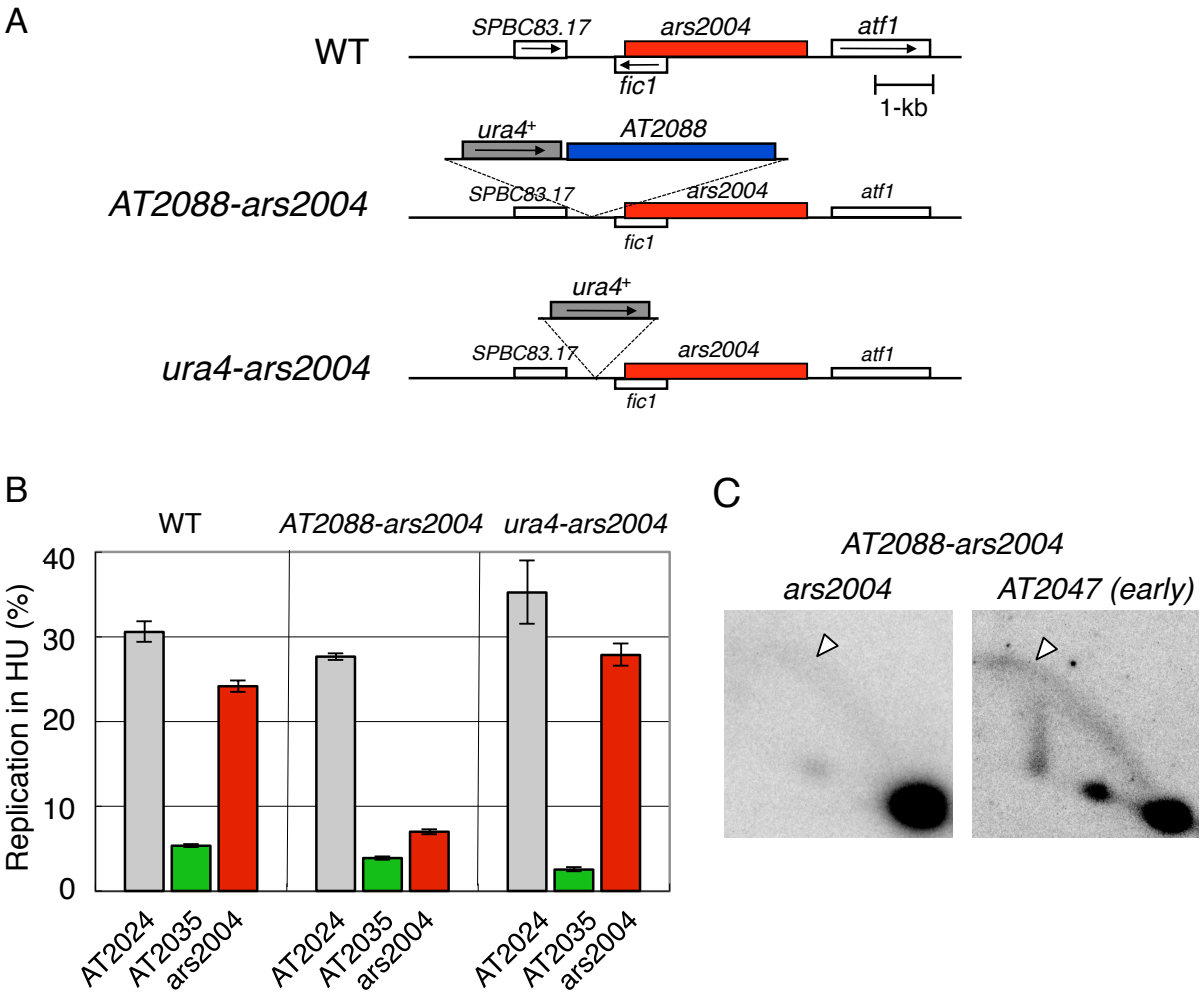

Figure 5. Repression of early initiation from ars2004 origin by the adjoining AT2088 fragment.

(A) Schematic presentation of the *ars2004* locus carrying the *ura4+-AT2088* or *ura4+* insertion. (B) *cdc25-22 nmt1-TK+* derivatives with or without insertion of *ura4+-AT2088* or *ura4+* alone next to the *ars2004* locus were released from G2/M block and labeled with BrdU for 120 min in the presence of HU (10 mM). Replication (%) in the presence of HU was determined for *ars2004* (red) as well as the control early and late origins, *AT2024* (gray) and *AT2035* (green), respectively. Mean ± s.d. obtained from multiple measurements in qPCR is presented. (C) The replication intermediates of *ars2004* (*Sty*I fragment) and a control early origin *AT2047* (*Sty*I fragment) prepared at 90 min after G2/M release of the HU-treated *AT2088-ars2004* cells were analyzed by 2D gel electrophoresis. An arrowhead shows the bubble arc.

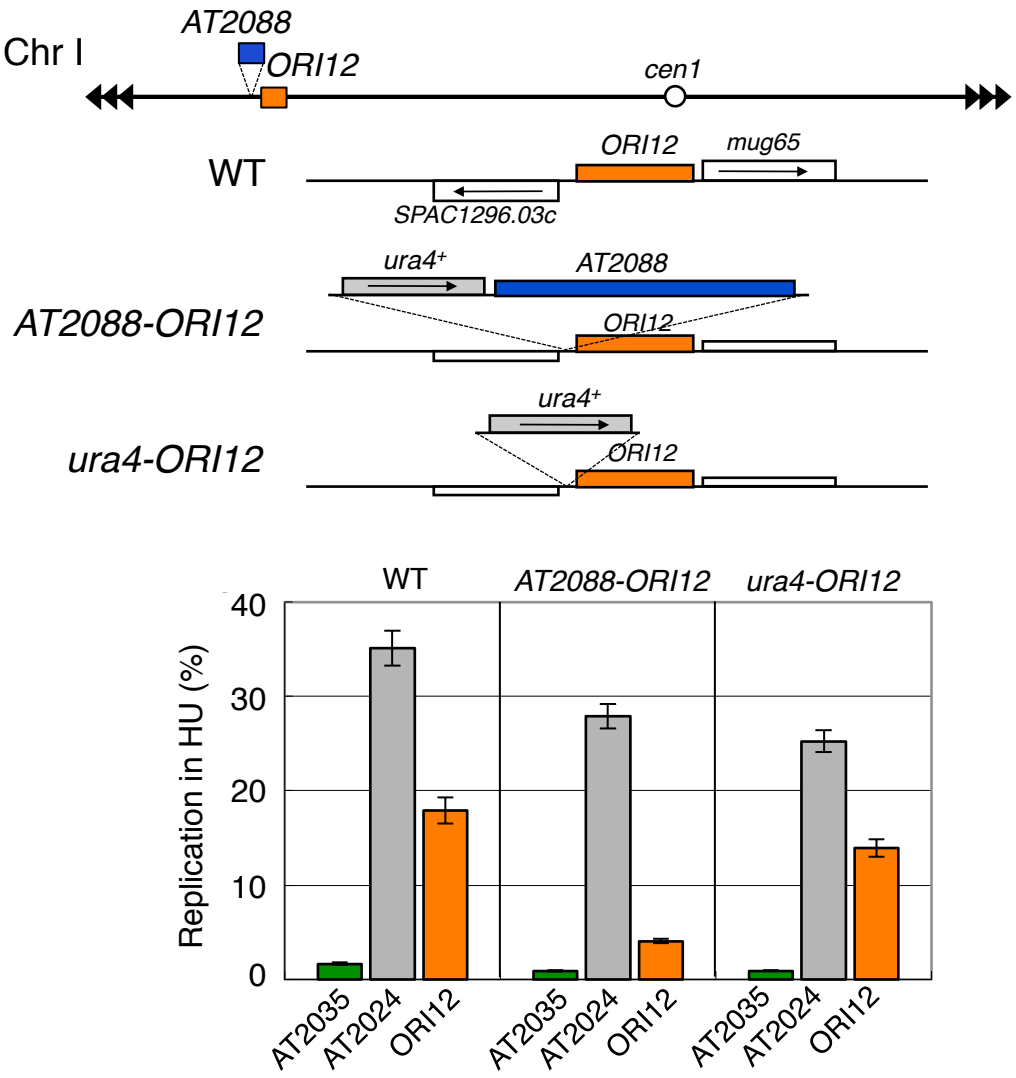

Figure 6. Repression of early replication origin ORI12 by insertion of the AT2088 fragment.

The position of *ORI12* on chromosome I and a physical map of the *ORI12* locus with insertions of *ura4*$^+$*-AT2088* and *ura4*$^+$ alone are schematically presented. For BrdU assay, cells were cultured for 120 min in the presence of HU after G2/M release. The replication efficiencies of *AT2035* (green), *ars2004* (red) and *ORI12* (orange) were determined as described in Fig 5.

Figure 7

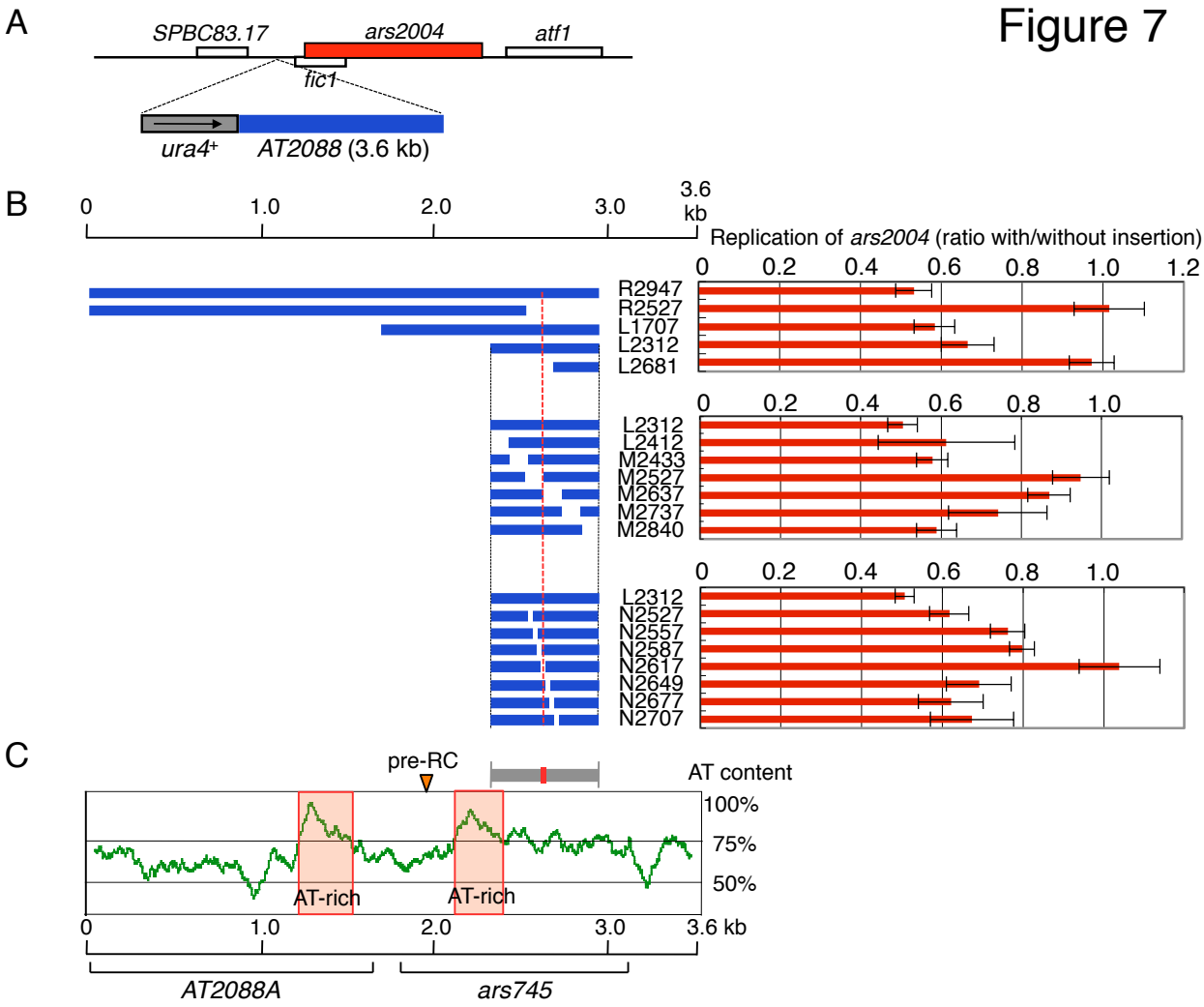
A
SPBC83.17
ars2004
atf1
fic1
ura4+
AT2088 (3.6 kb)
B
0
1.0
2.0
3.0
3.6 kb
Replication of ars2004 (ratio with/without insertion)
0 0.2 0.4 0.6 0.8 1.0 1.2
R2947
R2527
L1707
L2312
L2681
0 0.2 0.4 0.6 0.8 1.0
L2312
L2412
M2433
M2527
M2637
M2737
M2840
0 0.2 0.4 0.6 0.8 1.0
L2312
N2527
N2557
N2587
N2617
N2649
N2677
N2707
C
pre-RC
AT content
100%
75%
50%
AT-rich
AT-rich
0
1.0
2.0
3.0
3.6 kb
AT2088A
ars745
D
RTC Essential Sequence
2648
2617
AAGAGAGAGGTTACGAGGTTATATTTGAAATG
cctgcaG
ccTgcAgg
ccTgCAgg
cctgcAGg
Replication of ars2004 (ratio with base-substituted AT2088 / without AT2088)
0 0.2 0.4 0.6 0.8 1.0
AT2088
S2617
S2624
S2632
S2641

Figure 7. Identification of the essential sequence for replication timing control.
(A) The structure of *ars2004* locus with the insertion of *AT2088* fragment is presented schematically. (B) Cells carrying insertion of various portions of *AT2088* fragment (blue horizontal bars) next to the *ars2004* locus were synchronously released from G2/M and labeled with BrdU in the presence of HU (10 mM) for 120 min (top panel), 90 min (middle panel) or 80 min (bottom panel). Replication (%) of the *ars2004* and that of the internal control origin *AT2024* were determined as mean ± s.d. from multiple qPCR measurements, as described in Fig. 5. To compare the effects of insertions on early replication of *ars2004*, relative replication of *ars2004* to that of *AT2024* was obtained, and the ratio of relative replication (*ars2004*/*AT2024*) with insertion to value without insertion was determined (red horizontal bars). (C) The profile of AT content of every 100-bp window in a 3.6-kb *AT2088* region is presented together with two AT-rich regions (>75%, shaded rectangles), the pre-RC site (arrowhead) (Hayashi et al., 2007) and locations of two ARS fragments, *AT2088A* (Fig. 8) and *ars745* (Maundrell et al., 1988). The regions sufficient (gray) and essential (red) for replication timing control are shown above the AT content profile. (D) The 3.6-kb *AT2088* fragment with base substitutions in the essential region from position 2617 to 2648, as determined in (B), was inserted next to the *ars2004* and the effects of base-substitutions on repression of early replication of *ars2004* were analyzed as described in (B). The nucleotide sequence of the complementary strand of 2617-2648 is presented together with base-substitutions (lower case letter). The RTC essential sequence is indicated.

Figure 8

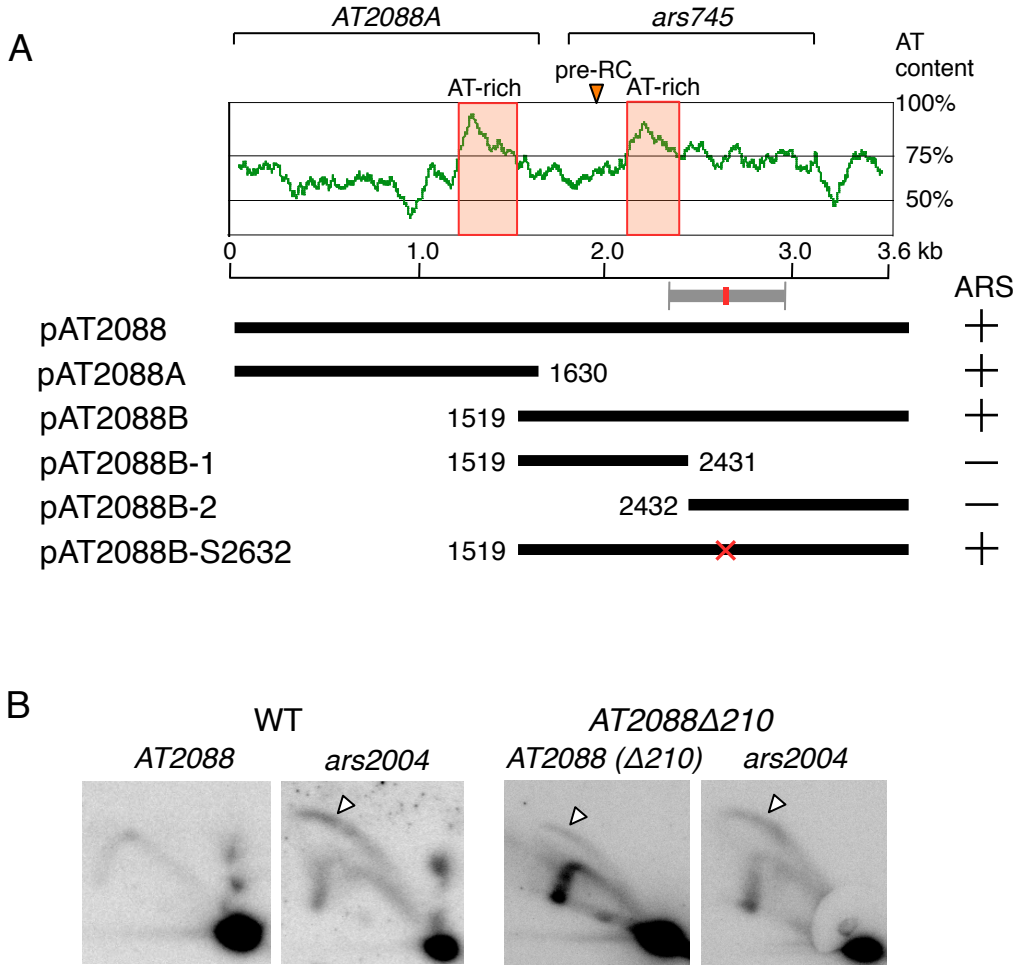

Figure 8. ARS assay for fragments of AT2088.
(A) The ARS activity of pYC11 (*LEU2*) derivatives carrying fragments of *AT2088*, shown by black bars, was examined by high-frequency transformation of HM123 (h^- *leu1-32*) as described in Fig. 2B. The locations of two ARS fragments, *AT2088A* and *ars745* (Maundrell et al., 1988), are indicated above the AT-content profile. (B) Replication intermediates in the HU-treated wild-type (left panels) and *AT2088Δ*210 cells (right panels) lacking the 210-bp (2527-2736) sequence were analyzed by 2D gel electrophoresis for *ars2004* (*Eco*T22I fragment) and *AT2088* (*Fba*I-*Nco*I fragment) at 90 min after G2/M release. Arrowheads indicate the bubble arcs.

Figure 9

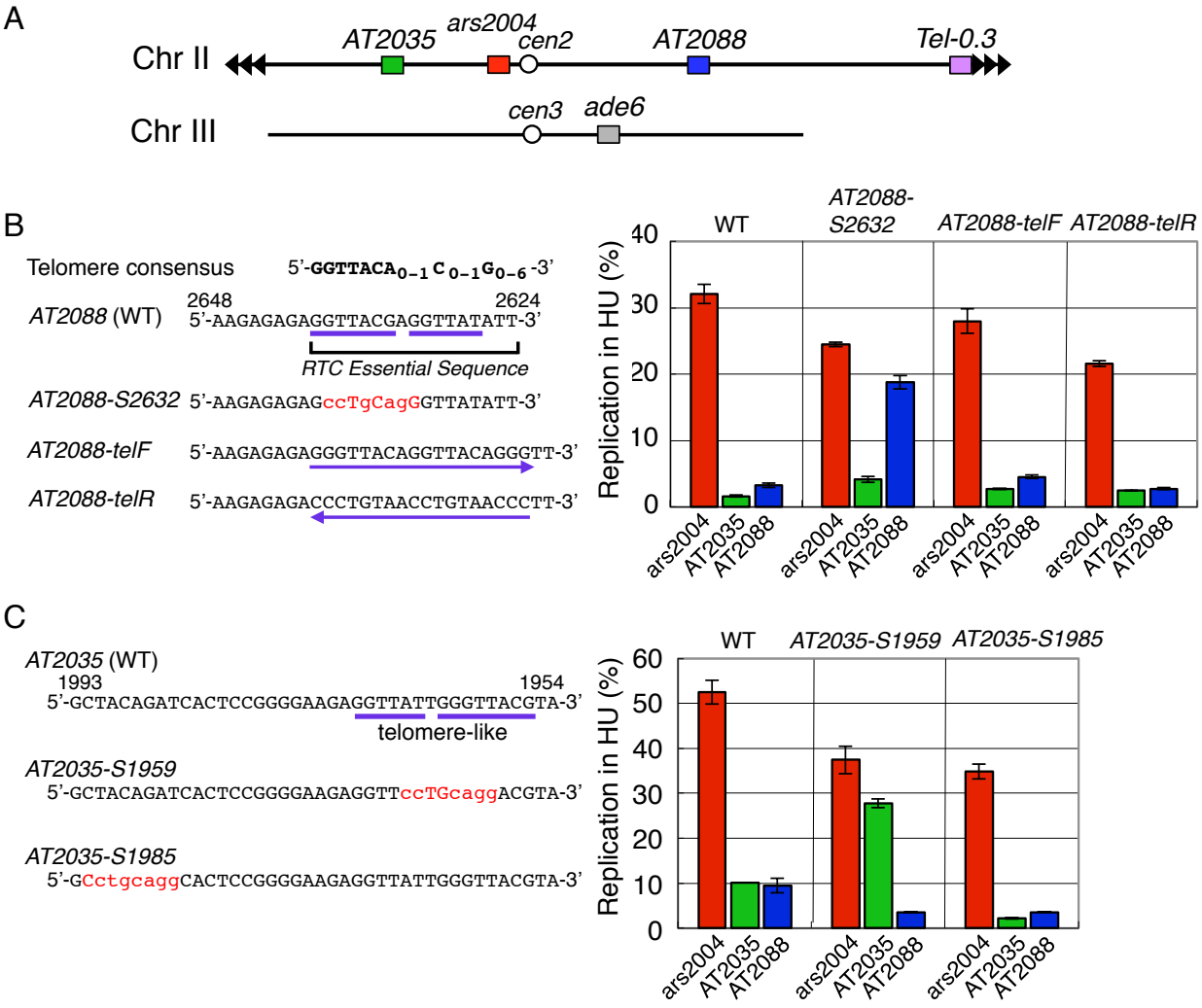

Figure 9. ***Telomeric repeats are essential for repression of late replication origins.*** (A) The positions of *AT2035* (green), *AT2088* (blue) and *Tel-0.3* (purple) on chromosome II and *ade6* (gray) on chromosome III are presented schematically. (B) (left) The nucleotide sequences of the relevant regions of *AT2088* (2624-2648, complementary strand) containing two copies of telomere-like repeats (blue underlining), *AT2088-S2632* carrying base substitutions (red), *AT2088-telF* and *-telR* with two telomeric repeats (blue underlining) in either orientation, respectively, are presented together with the consensus sequence of fission yeast telomeres (Cooper et al. 1997). (right) Replication (%) of the *AT2088* (blue), *ars2004* (red) and *AT2035* (green) were measured in the HU-treated wild-type and strains carrying base substitutions in *AT2088* at 120 min after G2/M release as described in Fig 5. Mean ± s.d. obtained from multiple measurements in qPCR is presented. **(C)** Replication of the *AT2035* was examined as described in (B). The nucleotide sequences of the region (1954-1993, complementary strand) containing telomere-like repeats (blue underlining) and base substitutions (red) in *AT2035-S1959* and *AT2035-S1985* are presented.

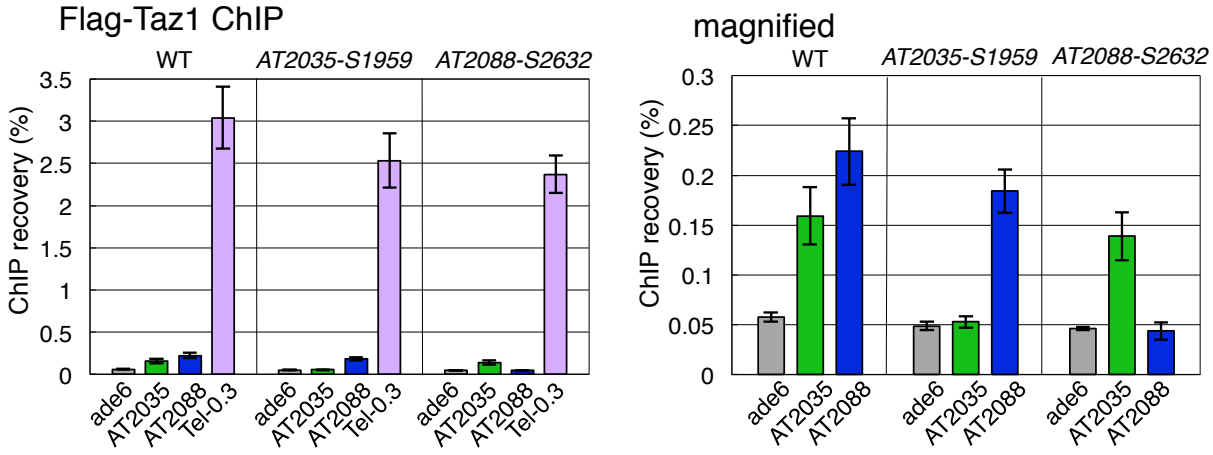

Figure 10. Telomeric repeats recruit Taz1 to the internally located late origin
Flag-Taz1 was immunoprecipitated from asynchronously cultured wild-type, *AT2035-S1959* and *AT2088-S2632* cells. IP recovery of the chromosome locus against the total cellular DNA was measured by qPCR for *ade6+* (gray), *AT2035* (green), *AT2088* (blue) and *Tel-0.3* (purple). Bars indicate the mean of IP-recovery (%) with standard error (SE) obtained from three biologically independent experiments. (right) The results except for those of *Tel-0.3* are presented for better comparison of Taz1 localization at the internal sites.

Figure 11

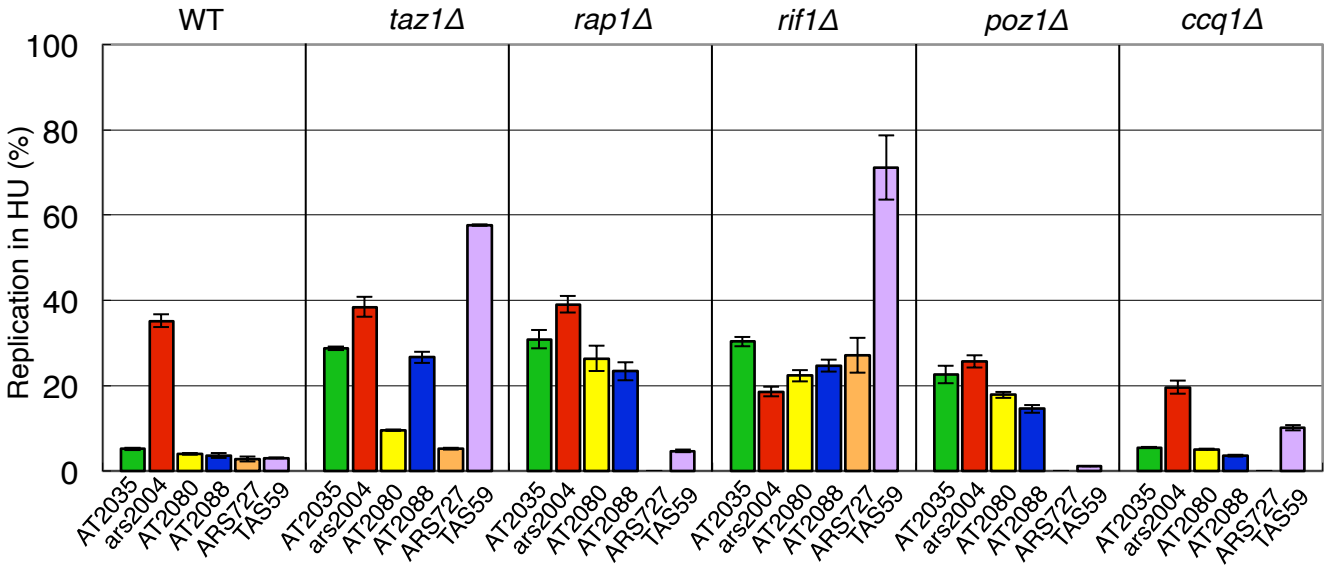

Figure 11. Taz1 and other telomere binding proteins are required for repression of a subset of late replication origins.

Replication (%) of *AT2035* (green), *ars2004* (red), *AT2088* (blue), *ARS727* (orange) and *TAS59* (purple) was determined in HU-treated wild-type and cells lacking *taz1*$^{+}$, *rap1*$^{+}$, *rif1*$^{+}$, *poz1*$^{+}$ and *ccq1*$^{+}$ at 120 min after release from G2/M. Mean ± s.d. obtained from multiple measurements in qPCR is presented. Replication (%) of ARS727 was not examined in *poz1*Δ and *ccq1*Δ cells.

Figure 12

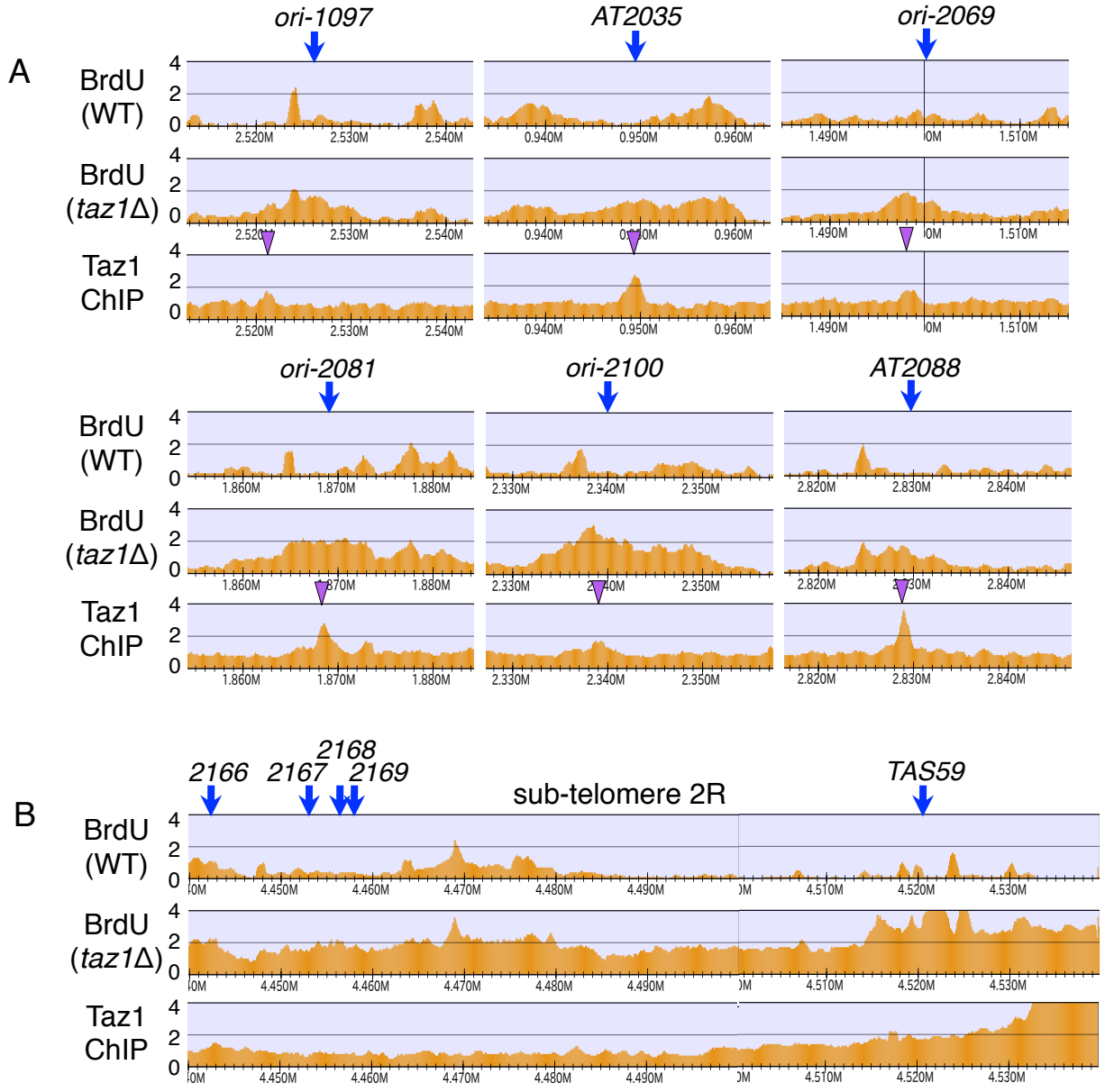
A
ori-1097
AT2035
ori-2069
BrdU (WT)
BrdU (taz1Δ)
Taz1 ChIP
ori-2081
ori-2100
AT2088
B
2166
2167
2168
2169
sub-telomere 2R
TAS59

Figure 12. Replication profiles and Taz1 binding of late origins associated with the telomeric repeats.

(A) BrdU-incorporation profiles of 6 late origins associated with the telomeric repeats in wild-type (top) and *taz1*Δ (middle) are presented together with profiles of Taz1-ChIP-seq (bottom). The sequence read from the HL density DNA prepared from 120 min sample after G2/M release in HU-treated wild-type (top) and *taz1*Δ (middle) was compared with the sequence read from the total cellular DNA of the respective cells and the relevant enrichment was plotted over the chromosome region (Supplementary Fig. S1). Flag-Taz1 was immunoprecipitated as described in Fig. II-1 and the relevant enrichment, the sequence read from ChIP in *flag-taz1* cells versus the sequence read from ChIP in non-tag strain, was plotted (bottom). The positions of late origins and telomeric repeats are shown by blue arrows and purple triangles, respectively. The results covering the entire genome are presented in Supplementary Fig. S1 and summarized in Supplementary Table S1. **(B)** Replication profile of the sub-telomere 2R is presented. Blue arrows show late origins.

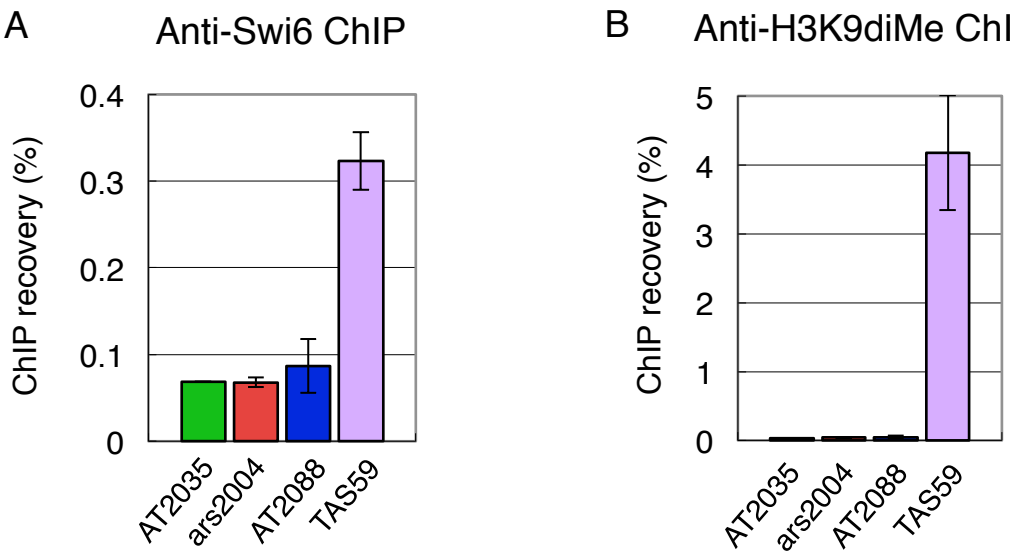

Figure 13. Heterochromatin is not formed at late origin AT2088 and AT2035
Localizations of Swi6 **(A)** and K9 di-methyled histone **(B)** at replication origins were analyzed by ChIP assay. Cells, carrying the *cdc25-22* mutation, were synchronously released from the G2/M boundary and incubated at 25°C for 40 min. DNA of the indicated loci recovered by immunoprecipitation with Swi6 **(A)** and K9 di-methyled histone was measured by qPCR for *AT2035* (green), *ars2004* (red), *AT2088* (blue) and *TAS59* (purple). Mean ± s.d. obtained from multiple measurements in qPCR is presented.

Figure 14

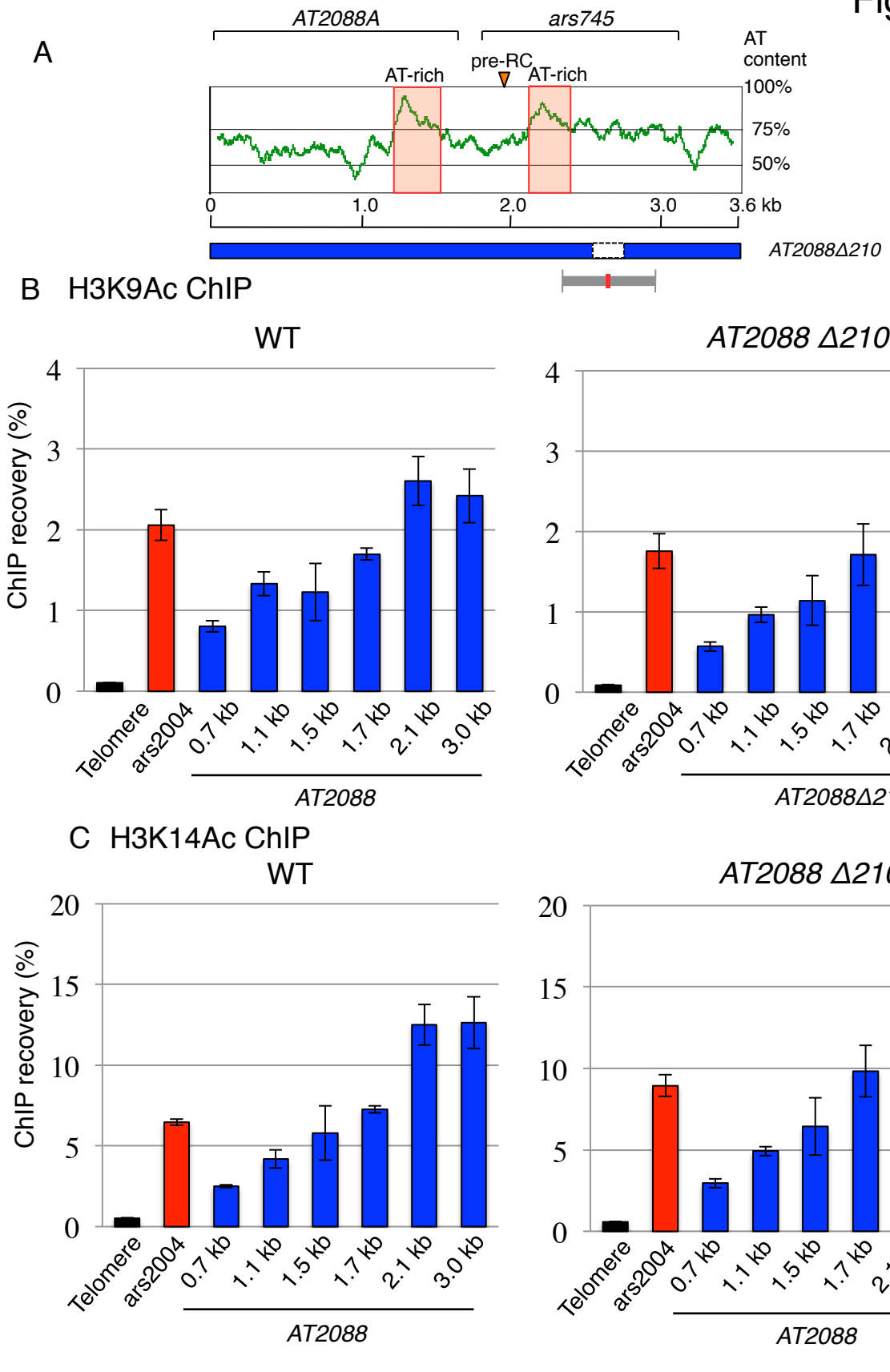
A
AT2088A
ars745
AT content
pre-RC
AT-rich
AT-rich
100%
75%
50%
0
1.0
2.0
3.0
3.6 kb
AT2088Δ210
B H3K9Ac ChIP
WT
AT2088 Δ210
ChIP recovery (%)
4
3
2
1
0
Telomere
ars2004
0.7 kb
1.1 kb
1.5 kb
1.7 kb
2.1 kb
3.0 kb
AT2088
AT2088Δ210
C H3K14Ac ChIP
WT
AT2088 Δ210
ChIP recovery (%)
20
15
10
5
0
Telomere
ars2004
0.7 kb
1.1 kb
1.5 kb
1.7 kb
2.1 kb
3.0 kb
AT2088
AT2088

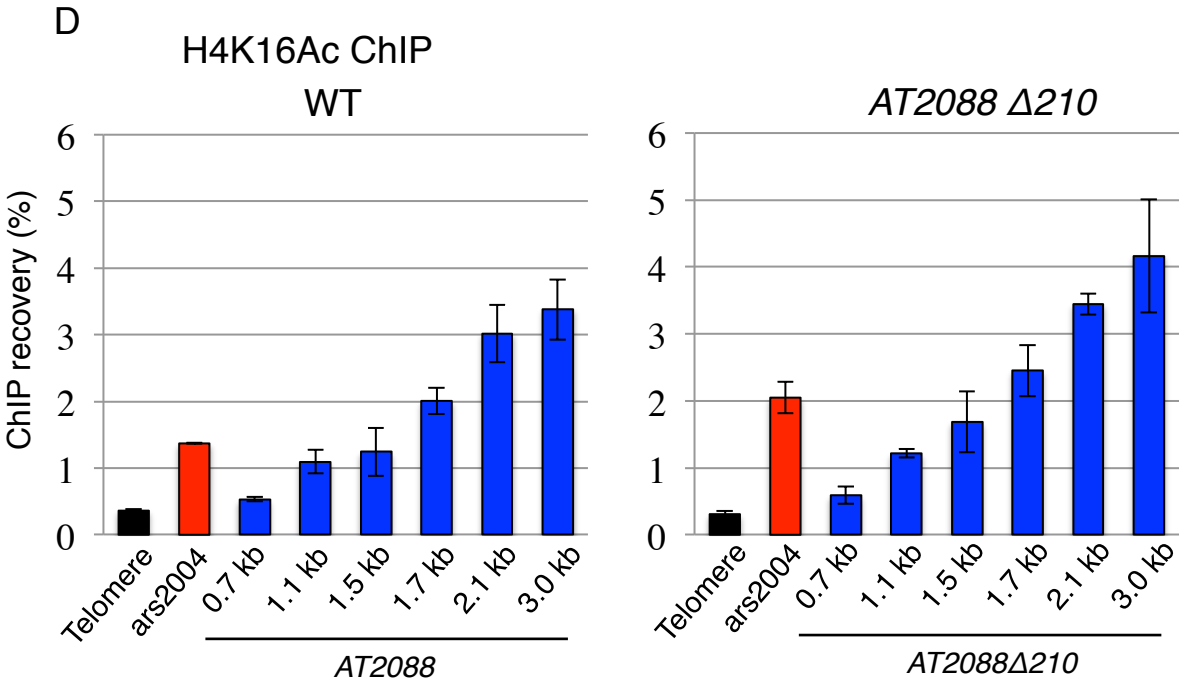

Figure 14. Change of replication timing doesn't affect the acetylation status of H3K9, H3K14 and H4K16 at the AT2088 locus.

(A) The ARS activity of pYC11 (*LEU2*) derivatives carrying fragments of *AT2088*, shown by black bars, was examined by high-frequency transformation of HM123 (*h⁻ leu1-32*) as described in Fig. 2B. The locations of two ARS fragments, *AT2088A* and *ars745* (Maundrell et al., 1988), are indicated above the AT-content profile. (B~D) Effects of early firing on histone acetylation states at L1. Fission yeast *cdc25-22* cells (WT), or *cdc25-22 AT2088Δ210* mutant cells (*AT2088Δ210*) were arrested at G2/M boundary by incubating at 36℃ for 3 hr and then incubated at 25℃ for 40 min (G1). Cells were fixed with formaldehyde and the DNA fragments cross-linked to specific sites (H3K9,14 and H4K16) acetylated histones were immunoprecipitated with anti-AcH3K9 (B), anti-AcH3K14 (C) or anti-AcH4K16 (D) antibody (Hiroshi Kimura, Osaka Univ). DNA recovered was quantified by Real-Time PCR analysis. Mean ± s.d. obtained from multiple measurements in qPCR is presented.

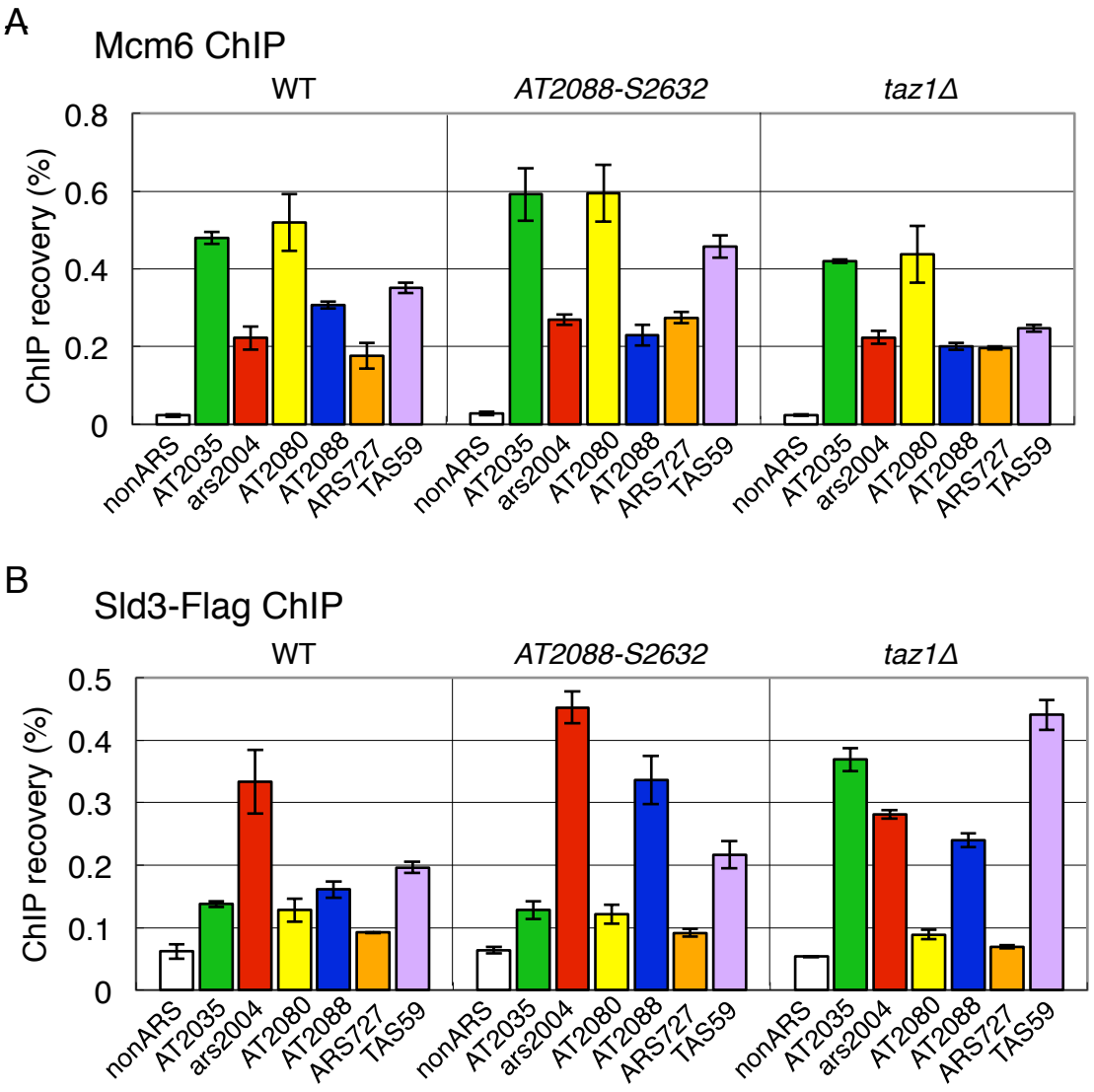

Figure 15. Recruitment of Sld3 to a subset of late origins in taz1Δ.
Localizations of Mcm6 (A) and Sld3-5Flag (B) at replication origins were analyzed by ChIP assay. Wild-type, *AT2088-S2632* and *taz1*Δ strains, carrying the *nda4-108*/*mcm5* and *cdc25-22* mutations, were synchronously released from the G2/M boundary and incubated at 20°C for 120 min, causing arrest before initiation of replication due to the *nda4-108* mutation (Yamada et al., 2004). DNA of the indicated loci recovered by immunoprecipitation with Mcm6 or Sld3-5Flag was measured by qPCR for non-ARS (white), *AT2035* (green), *ars2004* (red), *AT2080* (yellow), *AT2088* (blue), *ARS727* (orange) and *TAS59* (purple). Mean ± s.d. obtained from multiple measurements in qPCR is presented.

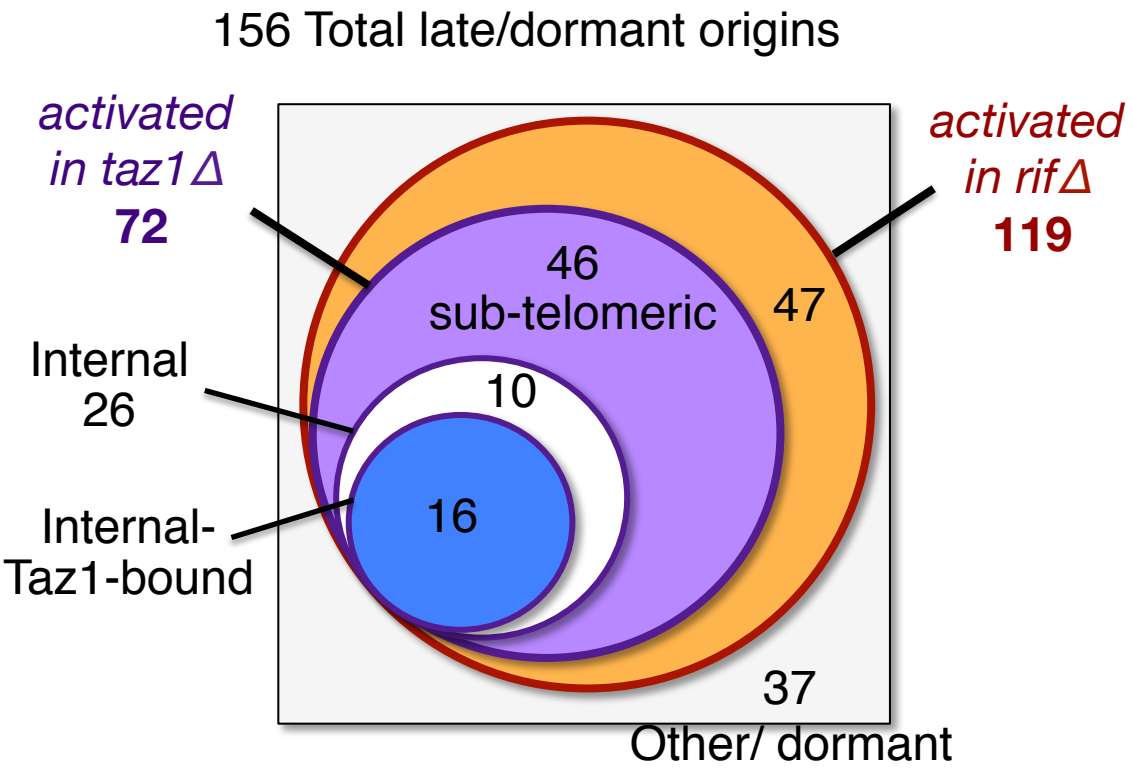

Figure 16. Comparison of late origins that are activated in taz1Δ and rif1Δ
A Venn diagram shows 72 late origins activated in *taz1*Δ (purple) that contain 46 sub-telomeric and 26 internal origins (white), including 16 internal origins where Taz1 was localized (blue). Interestingly, all of 72 late origins activated in *taz1*Δ are included in 119 late origins activated in *rif1*Δ (orange).

Figure 17

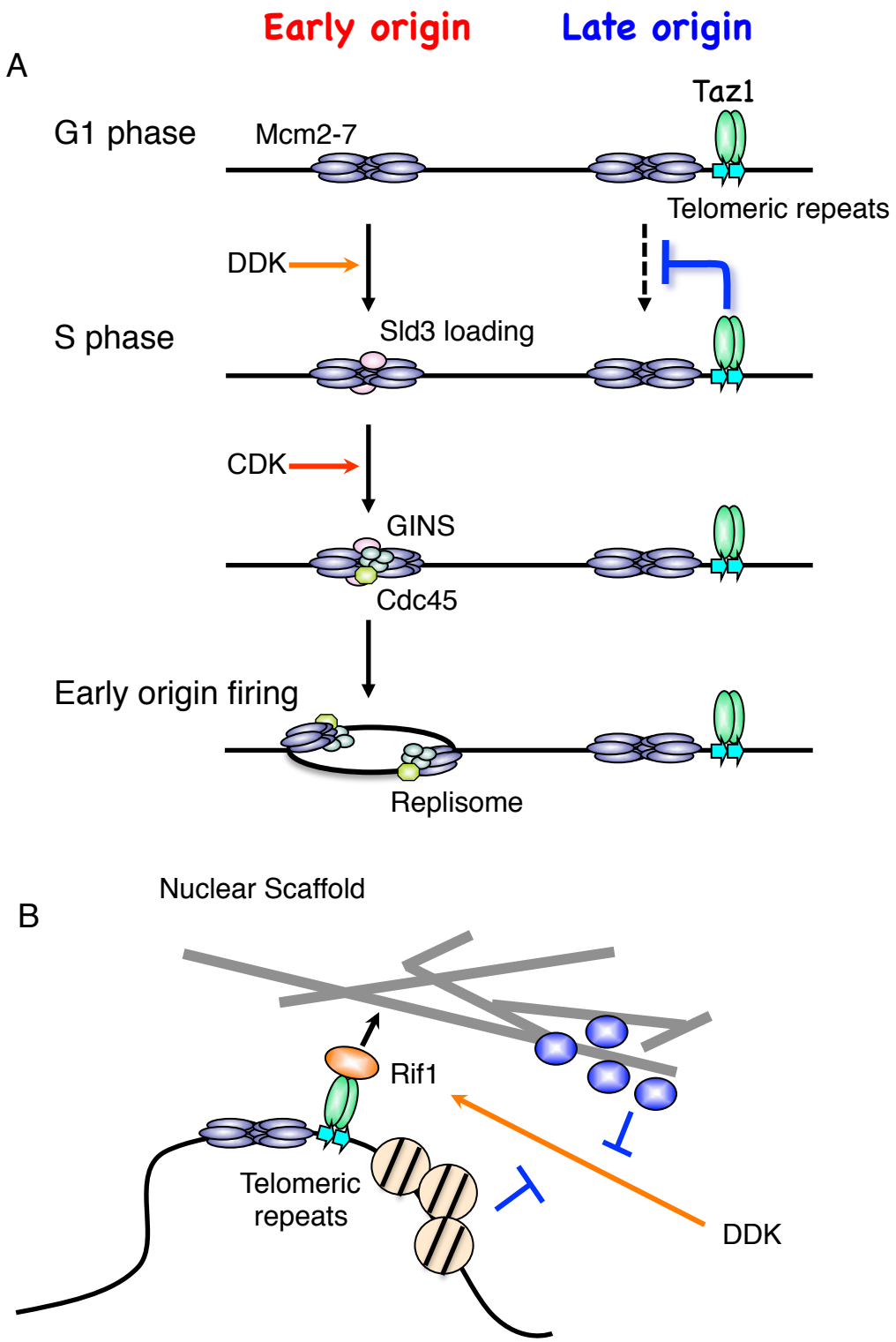

Figure 17.
(A) Summary of results. Taz1 binds to the internally located telomeric repeats near the late origins exerting a novel role in control of replication (repression of late origin firing in early S phase). Taz1 inhibits DDK-dependent Sld3 loading onto late origins. (B) A model for regulation of Taz1-dependent late origins. Taz1-Rif1 complex may tether Taz1-dependent late origins at the nuclear scaffold. The local environment of the nuclear scaffold may promote forming some specific chromatin structure and/or recruiting factors for limiting replication factors.

Figure 18

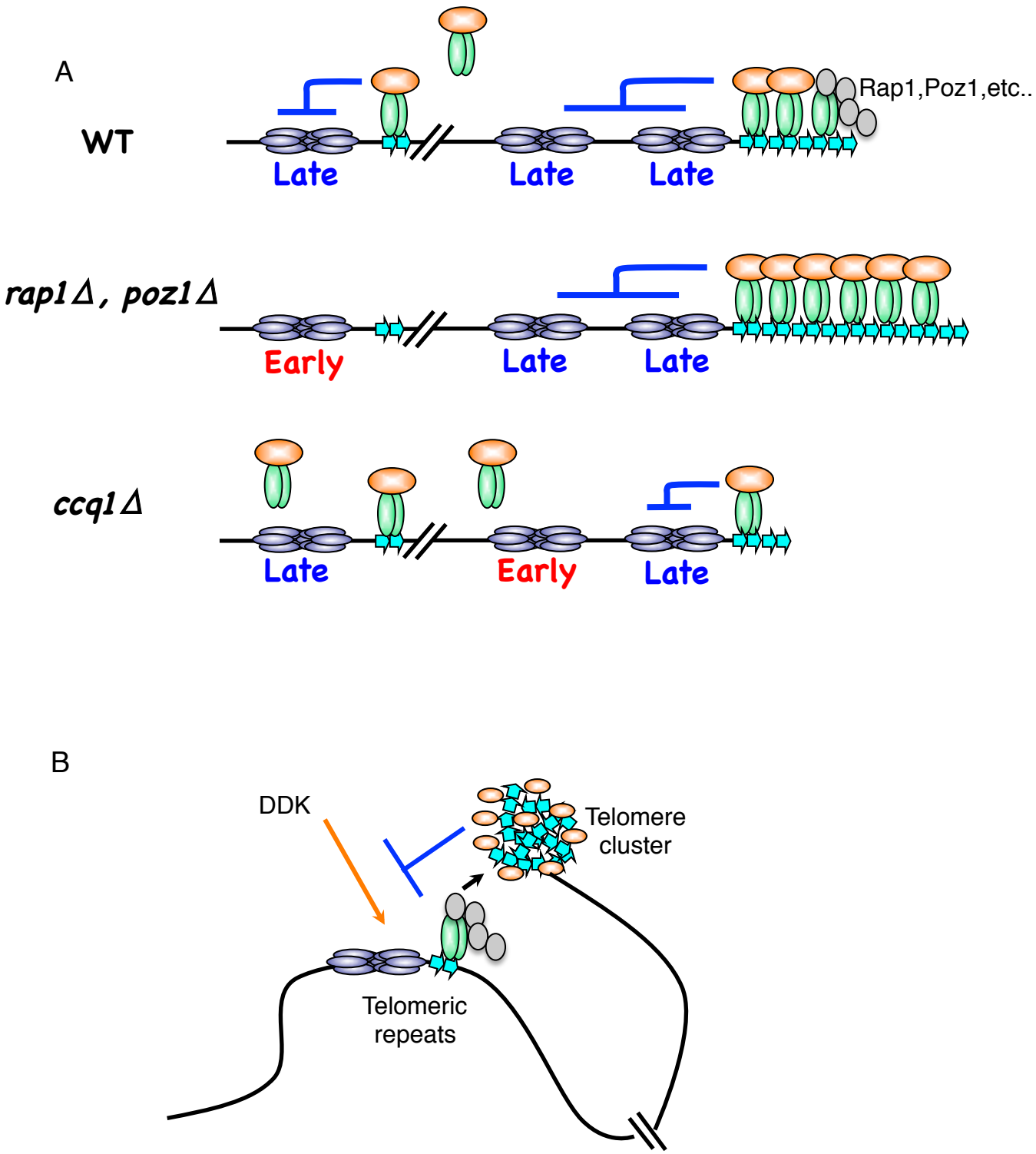
A
WT
Rap1,Poz1,etc..
Late
Late
Late
rap1Δ, poz1Δ
Early
Late
Late
ccq1Δ
Late
Early
Late
B
DDK
Telomere
cluster
Telomeric
repeats

Figure 18.
(A) A model for regulation of sub-telomeric origins by counting the terminal telomere length by Taz1-Rif1 complex. In normal condition, Rif1 connected to telomere via Taz1 inhibits activation of sub-telomeric origins. Similarly, Taz1 (and Rif1) may repress internal late origins by binding to the nearby telomeric repeats. In *rap1*Δ and *poz1*Δ, telomere length extensively elongates several times more than the length in WT. Excessive binding of Taz1-Rif1 complex to the elongated telomeres may cause depletion of these factors outside of telomeres, resulting de-repression of late origins specifically in arm regions. In *ccq1*Δ, telomere length becomes shorter due to a defect of recruitment of telomerase. Then, a number of Taz1-Rif1 complex bound to telomere is insufficient for repression of subtelomeric origins. (B) Shelterin-like complex may bind to the telomeric repeats located in chromosome arms and mediates origin silencing through Rif1 accumulated in telomere clusters. Rap1 and Poz1 play a role in mediating repression of late origins, but Ccq1 is not requires for the function.

Supplementary Table S1. Comparison of origin activity in wild-type, *taz1Δ* and *rif1Δ*

Chromosome I

Ori-number (Hayashi)	AT-islands (Segurado)	Origin name	Class	Fire in WT	Fire in taz1Δ	Fire in rif1Δ	Position of telomere seq	Telomeric sequence	Localization of Taz1	Localization of Rif1	Localization of LCS	Orc1 binding	Mcm6 binding	5' Gene/ORF	3' Gene/ORF
1001			L	-	+	+						15375.5	15375.5	SPAC212.07c	SPAC212.06c
1002			L	-	+	+						51625.5	*	SPAC977.09c	SPAC977.10
1003			L	-	+	+						54625.5	55375.5	SPAC977.10	SPAC977.11
1004	1011		L	-	+	+						63375.5	62875.5	SPAC977.14c	SPAC977.15
1005	1012		L	-	+	+						71125.5	*	SPAC977.17	SPAPJ695.01c
1006			L	-	+	+						75375.5	75375.5		
1007	1013		L	-	+	+						80125.5	*	SPAPJ695.01c	ght3/SPAC1F8.01
1008	1014		L	-	+	+						85625.5	*	ght3/SPAC1F8.01	SPAC1F8.02c
1009			L	-	+	+						89125.5	88625.5	SPAC1F8.02c	str3/SPAC1F8.03c
1010			L	-	+	+						95125.5	96375.5	SPAC1F8.04c	isp3/SPAC1F8.05
1011	1015		E	+	+	+						113875.5	113875.5	SPAC11D3.03c	SPAC11D3.04c
1012			L	-	+	+						151125.5	150875.5	SPAC5H10.02c	SPAC5H10.03
1013			L	-	+	+						167125.5	166375.5	gmh1/SPAC5H10.11	SPAC5H10.12c
1014			E	+	+	+						191125.5	191125.5	SPAC13G6.08	SPAC13G6.09
1015	1018		E	+	+	+						200125.5	200625.5	SPAC24B11.02	aps1/SPAC24B11.03
1016			L	-	+	+						239375.5	240875.5	rps2601/SPAC806.03c	SPAC806.04c
1017	1020		L	-	+	+						244875.5	245125.5	SPAC806.04c	SPAC806.05
1018	1021		L	-	-	+						295375.5	295375.5	SPAC1F5.02	SPAC18B11.11
1019	1022		L	-	-	+				+	304403	303125.5	303125.5	tup11/SPAC18B11.10	SPAC18B11.09c
1020	1025		E	+	+	+						365625.5	365625.5	SPAC630.09c	SPAC630.10
1021	1026		L	-	+	+	410504*	GGTTAGGAGGTTACC*	+			411125.5	411375.5	cuf1/SPAC31A2.11c	SPAC31A2.12
1022	1027		E	+	+	+						441625.5	441625.5	rad32/SPAC13C5.07	fep1/SPAC23E2.01
1023			L	-	-	+				+	457818	457875.5	457125.5	ste7/SPAC23E2.03c	SPAC24H6.13
1024			E	+	+	+						465125.5	465125.5	uba3/SPAC24H6.12c	SPAC24H6.11c
1025	1028		E	+	+	+						474375.5	474375.5	gef1/SPAC24H6.09	SPAC24H6.08
1026	1029		E	+	+	+						490375.5	490625.5	SPAC24H6.02c	SPAPB21F2.01
1027	1030		E	+	+	+						563625.5	563625.5	SPAC2F7.14c	rsm24/SPAC2F7.15
1028			L	-	-	-						593375.5	593125.5	SPAC3H8.03	SPAC3H8.04
1029	1031		L	-	-	+						608625.5	609125.5	SPAC3H8.09c	spo20/SPAC3H8.10
1030	1032		L	-	+	+			-			651125.5	650875.5	SPAC1D4.07c	SPAC1D4.08
1031	1033	ORI12	E	+	+	+						716125.5	715875.5	sxa2/SPAC1296.03c	SPAC1296.04
1032			L	-	-	-						741125.5	739875.5	SPAC22G7.05	ura1/SPAC22G7.06c
1033			L	-	-	-						750875.5	750125.5	SPAC22G7.07c	ppk8/SPAC22G7.08
1034	1034		L	-	+	+			+			762375.5	*	SPAC4G8.03c	SPAC4G8.15c
1035			L	-	+	+	765644*	GGTTAGTAGGTTATA*	+			766125.5	765875.5		
1036			L	-	-	-				+	784297	785625.5	784625.5	atp10/SPAC4G8.11c	SPAC4G8.12c
1037	1035		E	+	+	+						794875.5	794875.5	SPAC16C9.02c	SPAC16C9.03
1038			E	+	+	+						845375.5	*	SPAC521.02	SPAC521.03
1039			E	+	+	+						894375.5	893875.5	SPAC23G3.12c	SPAC22H12.01c
1040	1039		E	+	+	+						902875.5	903375.5	SPAC22H12.05c	rpc19/SPAC1687.01
1041			L	-	-	-						939375.5	939125.5	ssl3/SPAC1687.18c	SPAC1687.19c
1042	1040		E	+	+	+						966125.5	966875.5	byr4/SPAC222.10c	hem13/SPAC222.11
1043	1041		L	-	+	+			-			1028626	1028126	fap2/SPAC139.04c	SPAC139.05
1044	1042		E	+	+	+						1080126	1080376	plb1/SPAC1A6.04c	SPAC1A6.05c
1045			E	+	+	+						1084126	1084376	meu31/SPAC1A6.06c	SPAC1A6.07
1046	1043		E	+	+	+						1091126	1091376	lag1/SPAC1A6.09c	SPAC30D11.15c
1047	1044	ARS1	E	+	+	+						1097126	1097126	hus5/SPAC30D11.13	rpl3802/SPAC30D11.12
1048	1045		L	-	-	+				+	1151622	1148876	1148876	SPAC56F8.12	SPAC56F8.13
1049	1046		E	+	+	+						1157376	1157626	esc1/SPAC56F8.16	pso2/SPAC22A12.01c
1050			E	+	+	+						1163376	1162876	csn4/SPAC22A12.03c	rps2201/SPAC22A12.04c
1051			E	+	+	+						1191876	1192126	SPAC22A12.17c	SPAC4C5.01
1052	1047		E	+	+	+						1197376	1197126	ryh1/SPAC4C5.02c	SPAC4C5.03
1053			E	+	+	+						1226376	1226376	psm3/SPAC10F6.09c	SPAC10F6.10
1054	1048		E	+	+	+						1255876	1255876	cut6/SPAC56E4.04c	SPAC56E4.05
1055	1049		E	+	+	+						1275876	1276126	csn2/SPAPB17E12.04c	rpl3703/SPAPB17E12.05
1056	1050		L	-	-	+						1360626	1360626	fin1/SPAC19E9.02	pas1/SPAC19E9.03
1057	1052		E	+	+	+						1445126	1445126	SPAC3A12.13c	cam1/SPAC3A12.14
1058	1053		E	+	+	+						1477626	1477626	SPAC9.07c	SPAC9.08c
1059			L	-	-	-						1499876	*	SPAC5D6.09c	mes1/SPAC5D6.08c
1060	1055		E	+	+	+						1510126	1509876	SPAC5D6.04	SPAC5D6.02c
1061			E	+	+	+						1574126	1575126	SPAC23H4.19	rbx1/SPAC23H4.18c
1062			L	-	-	+				+	1601298	1600376	1600126	gln1/SPAC23H4.06	SPAC23H4.05c
1063	1056		E	+	+	+						*	*	msc1/SPAC343.11c	rds1/SPA343.12
1064			E	+	+	+						1667376	1667626		
1065	1057		E	+	+	+						1709126	1709126	SPAC664.02c	SPAC664.03
1066			E	+	+	+						1719626	1719626	SPAC664.08c	ggt1/SPAC664.09
1067	1059		L	-	-	-						1766126	1768126	ulp2/SPAC17A5.07c	SPAC17A5.08
1068			E	+	+	+	1822620	GGTTATGGTGGTTAC	+			1823876	*	psu1/SPAC1002.13c	SPAC1002.20
1069	1061		E	+	+	+						1834876	1835126	SPAC1002.18	SPAC1002.21
1070			L	-	+	+			+			1892626	*	SPAPB1A10.14	SPAPB1A10.15
1071	1062		L	-	+	+	1894950	GGTTATTAGGTTAC	+			1894876	1895626	SPAPB1A10.15	sdh2/SPAC140.01
1072			L	-	-	+				+	1952635	1947376	1947126	SPAC3H1.08c	SPAC3H1.09c
1073	1063		L	-	-	+						1954876	1954876	SPAC3H1.10	SPAC3H1.11
1074			L	-	-	+						*	1959376		
1075	1064		E	+	+	+						1975876	1975876	rpl3001/SPAC9G1.03c	oxa101/SPAC9G1.04
1076			L	-	-	+						2026126	2026126	ddb1/SPAC17H9.10c	SPAC17H9.11
1077	1065		L	-	-	+						2042876	2042876	snu13/SPAC607.03c	SPAC607.04
1078	1067		L	-	-	+						2097126	2096876	obr1/SPAC3C7.14c	SPAC25A8.03c
1079	1068		L	-	-	+						2141376	2141126	pnk1/SPAC23C11.04c	SPAC23C11.05
1080	1069		E	+	+	+	2199362	GGTTACTGGTTAT				2195376	2195126	hst4/SPAC1783.04c	hrp1/SPAC1783.05
1081	1070		E	+	+	+						2228876	2228876	SPAC18G6.05c	SPAC18G6.06
1082			L	-	-	-						2233126	2233126	mra1/SPAC18G6.07c	SPAC18G6.09c
1083	1073		E	+	+	+						2250626	2250626	byr3/SPAC13D6.02c	SPAC13D6.03c
1084			L	-	-	-						2263876	2264126	SPAC4G9.06c	B8647-3/SPAC4G9.07
1085			E	+	+	+						2274626	2274376	arg11/SPAC4G9.09c	arg3/SPAC4G9.10
1086	1074		E	+	+	+						2280876	2280876	vps26/SPAC4G9.13c	SPAC4G9.14
1087			L	-	-	+						2305126	2305626	mac1/SPAC13G7.04c	SPAC13G7.05
1088	1077		L	-	-	+						2340376	2340626	SPAC6C3.08	SPAC6C3.09
1089			L	-	-	-						2363376	2363876	SPAC17G8.11c	SPAC17G8.12
1090	1079		L	-	-	+				+	2407146	2406876	2407126	sck1/SPAC1B9.02c	SPAC1B9.03c
1091			L	-	-	+						2417126	2416626	SPAC6B12.03c	SPAC6B12.04c
1092	1080		E	+	+	+						2439376	2439376	SPAC6B12.14c	cpc2/SPAC6B12.15
1093	1081		E	+	+	+						2442876	2442876	cpc2/SPAC6B12.15	meu26/SPAC6B12.16
1094	1082		E	+	+	+						2452876	2452626	SPAC32A11.02c	phx1/SPAC32A11.03c
1095			E	+	-	+						2457126	2458126	phx1/SPAC32A11.03c	trp2/SPAC19A8.15

1096			L	-	-	-						2510126	2511126	gly1/SPAC23H3.09c	ssr2/SPAC23H3.10
1097			L	-	+	+	2521205	GGTTATACGGTTACGCGGTTAT	+			2526376	2526376	SPAC25H1.01c	jmj1/SPAC25H1.02
1098			L	-	+	+			+			2528626	2528626	jmj1/SPAC25H1.02	mug66/SPAC25H1.03
1099			E	+	+	+						2579126	2579376	prs1/SPAC4A8.14	cdc3/SPAC4A8.15c
1100			L	-	-	-						2601126	2601376	SPAC823.11	SPAC823.12
1101			E	+	+	+						2615876	2615626	SPAC7D4.13c	SPAC7D4.12c
1102	1085		E	+	+	+						2618876	2618626	SPAC7D4.12c	sec39/SPAC7D4.11c
1103	1086		L	-	-	+						2644126	2644126	itr1/SPAC4F8.15	hcs1/SPAC4F8.14c
1104	1088		L	-	-	+				+	2666263	2668626	*	hxk2/SPAC4F8.07c	SPAC4F8.06
1105	1090		E	+	+	+				+	2689933	2720626	2720626	SPAPB2B4.04c	vma5/SPAPB2B4.05
1106	1092		E	+	+	+						2762626	2762626	SPAC6F6.13c	ypt5/SPAC6F6.15
1107			E	+	+	+						2804376	2804376	SPAC1805.16c	crm1/SPAC1B2.01
1108			L	-	-	+				+	2877795	2875626	2876126	SPACUNK4.17	SPACUNK4.19
1109	1094		L	-	-	+						2883876	2883626	SPACUNK4.15	SPACUNK4.14
1110			E	+	+	+						2938876	2938626	SPAC2E1P3.05c	SPAPB2C8.01
1111	1095		E	+	+	+						2960626	2961126	SPAPB24D3.07c	SPAPB24D3.08c
1112			E	+	+	+						2978126	2978126	agl1/SPAPB24D3.10c	SPAPB1A11.01
1113			E	+	+	+						*	2980626	SPAPB1A11.01	SPAPB1A11.02
1114			E	+	+	+						2984126	2984126	SPAPB1A11.02	SPAPB1A11.03
1115	1096		E	+	+	+						3010876	3010876	maf1/SPAC31G5.12c	SPAC31G5.21
1116	1097		E	+	+	+						3023626	3022876	SPAC31G5.18c	SPAC31G5.19
1117			E	+	+	+						3032126	3034126	SPAC1786.01c	SPAC1786.04
1118			E	+	+	+						3053876	3053626	SPAC24C9.06c	bgs2/SPAC24C9.07c
1119	1098		E	+	+	+						3060876	3061126	bgs2/SPAC24C9.07c	SPAC24C9.08
1120			L	-	-	-						3071126	*	SPAC24C9.11	SPAC24C9.12c
1121	1099		E	+	+	+						3127876	3127876	srb8/SPAC688.08	SPAC688.09
1122	1100		E	+	+	+						3145376	3145376	SPAC688.14	bet5/SPAC3G9.16c
1123			L	-	-	+				+	3158966	3159376	3159376	peg1/SPAC3G9.12	SPAC3G9.11c
1124	1101		E	+	+	+						3185376	3185376	SPAC3G9.01	SPAC1486.01
1125	1104		E	+	+	+						3301626	3301626	eme1/SPAPB1E7.06c	SPAPB1E7.07
1126	1105		E	+	+	+						3321876	3321876	rps602/SPAPB1E7.12	mns1/SPAC2E1P5.01c
1127	1106		E	+	+	+						3405626	3405876	apc5/SPAC959.09c	SPAP32A8.02
1128	1107		E	+	+	+						3411376	3411376	SPAP32A8.03c	rpl501/SPAC3H5.12c
1129	1109		E	+	+	+						3499126	3499126	rps502/SPAC328.10c	SPAC16E8.01
1130	1110		E	+	+	+						3542126	3542126	SPAC1B1.02c	kap95/SPAC1B1.03c
1131	1111		E	+	+	+						3549626	3549626	SPAC1B1.04c	bsu1/SPAC17A2.01
1132	1112		E	+	+	+						3571376	3570626	SPAC17A2.15	csx1/SPAC17A2.09c
1133	1114		E	+	+	+						3577626	3577876	SPAC17A2.10c	SPAC17A2.11
1134			E	+	+	+						*	*	SPAC17A2.11	SPAC17A2.12
1135			E	+	+	-						3592876	3593376	SPAC17G6.02c	SPAC17G6.03
1136			E	+	+	+						3611376	3612626	SPAC17G6.11c	cul1/SPAC17G6.12
1137	1115		E	+	+	+						3635626	3635626	SPAC1142.04	ctr5/SPAC1142.05
1138			E	+	+	-						3646126	3647126	cgs1/SPAC8C9.03	SPAC8C9.04
1139	1116		E	+	+	+						3701376	3701626	mde6/SPAC15A10.10	ubr11/SPAC15A10.11
1140			E	+	+	+						3746876	3749876	rpl1002/SPAP7G5.05	SPAP7G5.06
1141			E	+	+	+						3753626	3753626	SPAP7G5.06	centromere
1142			E	+	+	+						3841126	3841376	SPAC4H3.07c	SPAC4H3.08
1143	1124		E	+	+	-						3853376	3853376	SPAC4H3.12c	SPAC4H3.13
1144	1125/1126		E	+	+	+						3878876	3879376	pma1/SPAC1071.10c	SPAC1071.11
1145			E	+	+	+						3882876	*		
1146	1127		E	+	+	-						3898626	3898876	SPAC926.07c	SPAC926.08c
1147	1128		E	+	+	+						3954126	3953876	SPAC2F3.14c	lsk1/SPAC2F3.15
1148			E	+	+	+						3992876	3992876	SPAPB15E9.01c	SPAPB15E9.02c
1149	1129		E	+	+	+						3995876	3995876	SPAPB15E9.02c	Tf2-5/SPAPB15E9.03c
1150			L	-	-	-						4010626	4010126	SPAC27E2.03c	SPAC27E2.11c
1151	1130		E	+	+	+						4020126	4020376	SPAC27E2.06c	pvg2/SPAC27E2.07
1152	1131		E	+	+	+						4073126	4072376	SPAC19G12.13c	its3/SPAC19G12.14
1153	1132		E	+	+	+						4089126	4089126	mnl1/SPAC23A1.04c	SPAC23A1.05
1154	1133		E	+	+	+						4137376	4137376	bgl2/SPAC26H5.08c	SPAC26H5.09c
1155			E	+	+	+						4141126	4141126	SPAC26H5.09c	tif51/SPAC26H5.10c
1156			E	+	+	+						4154626	4154626	SPAC26H5.13c	SPAC25B8.01
1157			L	-	-	+						4178126	*	SPAC25B8.11	SPAC25B8.12c
1158			L	-	-	+						4180876	4180626	SPAC25B8.12c	isp7/SPAC25B8.13c
1159	1134		E	+	+	+						4185876	4185876	isp7/SPAC25B8.13c	mal2/SPAC25B8.14
1160			E	+	+	+						4197626	4197876	SPAC683.03	SPAC683.02c
1161			E	+	+	+						4232626	4232626	SPAC1F7.06	fip1/SPAC1F7.07c
1162			E	+	+	+						4240126	4239876	fio1/SPAC1F7.08	SPAC1F7.09c
1163	1135		E	+	+	+						4255126	4255126	pcr1/SPAC21E11.03c	ppr1/SPAC21E11.04
1164	1136		E	+	+	+						4275626	4275626	SPAC2C4.07c	SPAC2C4.08
1165	1137		E	+	+	+						4326626	4326876	SPAC27F1.05c	SPAC27F1.10
1166	1138		L	-	-	+				+	4361585	4365876	4366626	SPAC23D3.12	SPAC23D3.13c
1167			L	-	-	-						4387376	*	SPAC1527.03	sec72/SPAC30.01c
1168	1139		E	+	+	+						4415626	4415876	SPAC29E6.06c	SPAC29E6.07
1169			E	+	+	+						4439626	4439876	SPAC9E9.17c	leu2/SPAC9E9.03
1170	1140		L	-	-	+						4451376	4451376	ypt2/SPAC9E9.07c	rad26/SPAC9E9.08
1171			L	-	-	+				+	4458396	4459626	4457376	SPAC9E9.09c	cbh1/SPAC9E9.10c
1172			L	-	-	-						4468876	4468376	SPAC9E9.12c	wos2/SPAC9E9.13
1173			E	+	+	+						4484626	4484626	stm1/SPAC17C9.10	tim13/SPAC17C9.09c
1174	1141		E	+	+	+						4534126	4534126	SPAC27D7.11c	but1/SPAC27D7.12
1175	1142		L	-	+	+	4604051	GGTTATTCAGGTTAT	-			4605376	4605376	SPAC12B10.16c	SPAC1093.01
1176	1143		L	-	+	+			-			4653376	4653626	SPAC144.01	SPAC144.02
1177			L	-	-	+						4674876	4675126	gwt1/SPAC144.10c	rps1102/SPAC144.11
1178	1145		E	+	+	+						4740376	4740376	SPAC458.04c	pik3/SPAC458.05
1179	1146		E	+	+	+				+	4789684	4779626	4779626	SPAC11H11.02c	SPAC11H11.03c
1180			L	-	-	-						4803876	4803876	SPAC22F8.08	rrp16/SPAC22F8.09
1181			E	+	+	+						4845626	4845126	atg13/SPAC4F10.07c	SPAC4F10.08
1182	1147		E	+	+	+						4853376	4853626	SPAC4F10.10c	spn1/SPAC4F10.11
1183	1148		E	+	+	+						4883126	4882876	SPAC19B12.02c	bgs3/SPAC19B12.03
1184			L	-	-	-						4912376	4913126	rpn502/SPAPB8E5.02c	mae1/SPAPB8E5.03
1185			E	+	+	+						4917376	4917626	SPAPB8E5.04c	mfm1/SPAPB8E5.05
1186	1149		E	+	+	+						4964126	4964126	vht1/SPAC1B3.16c	clr2/SPAC1B3.17
1187			L	-	-	-						4985626	4984876	SPAC1952.09c	SPAC1952.10c
1188	1152		E	+	+	+						5025376	5025376	SPAC22E12.03c	ccs1/SPAC22E12.04
1189	1154		L	-	+	+			-			5098126	5097376	rpl3002/SPAC1250.05	atl1/SPAC1250.04c
1190	1155		E	+	+	+						5156626	5157376	SPAC26F1.12c	SPAC26F1.11/dubious
1191			E	+	+	+						5178626	5178626	SPAC26F1.05	etr1/SPAC26F1.04c
1192			L	-	-	+						5190376	5190376	SPAPJ691.02	SPAPJ691.03
1193	1156		E	+	+	+						5234126	5234626	mek1/SPAC14C4.03	B22918-2/SPAC14C4.04
1194	1158		L	-	-	+						5272376	5272376	adg1/SPAPJ760.03c	SPAC2H10.01
1195	1159		L	-	+	+			+			5322876	5323126	hsp9/SPAP8A3.04c	SPAP8A3.05

1196	1160		E	+	+	+						5394126	5393876	SPAC3G6.07	erv1/SPAC3G6.08
1197	1162		E	+	+	+						5449126	5449626	SPAC1039.01	SPAC1039.02
1198			E	+	+	+						5470376	5470376	isp5/SPAC1039.09	mmf2/SPAC922.01
1199	1163		E	+	+	+						5477126	5476876	SPAC1039.11c	SPAC922.03
1200	1164		E	+	+	+						5483376	5482626	SPAC922.04	SPAC922.05c
1201			E	+	+	+						5487626	5487376	SPAC922.06	SPAC922.07c
1202	1166		L	-	+	+						5502626	5502876	mei1/SPAC869.07c	SPAC869.06c
1203	1167		L	-	+	+						*	5506626	SPAC869.06c	SPAC869.05c
1204			L	-	+	+						5510876	*	SPAC869.05c	SPAC869.04
1205			L	-	+	+						5517876	5516126	SPAC869.03c	SPAC869.02c
1206	1168		L	-	+	+						5521876	*	SPAC869.02c	SPAC869.01
1207	1169		L	-	+	+						5529876	*	SPAC186.01	SPAC186.02c

Chromosome II

Ori-number (Hayashi)	AT-islands (Segurado)		Class	Fire in WT	Fire in taz1Δ	Fire in rif1Δ	Position of telomeric seq	Telomeric sequence	Localization of Taz1	Localization of Rif1	Localization of LCS	Position of Orc1	Position of Mcm6	5' Gene/ORF	3' Gene/ORF
2001			L	-	+	+						*	31375.5	SPBC1348.10c	SPBC1348.11
2002			L	-	+	+						38125.5	38125.5	SPBC1348.13	SPBC1348.14c
2003			L	-	+	+						53125.5	53125.5	grt1/SPBPB8B6.04c	SPBPB8B6.05c
2004			L	-	+	+						63375.5	61875.5	SPBPB21E7.02c	SPBPB21E7.04c
2005			L	-	+	+	65194	GGTTACGTTGGTTAT	-			66875.5	*	SPBPB21E7.05	SPBPB21E7.06
2006			L	-	+	+						69875.5	*	SPBPB21E7.06	aes1/SPBPB21E7.07
2007			L	-	+	+						74375.5	74375.5	SPBPB21E7.08	SPBPB21E7.09
2008			L	-	+	+						78125.5	*	SPBPB21E7.09	SPBPB21E7.10
2009			L	-	+	+						81875.5	81375.5	SPBPB21E7.10	SPBPB10D8.01
2010	2001		L	-	+	+						86875.5	*	SPBPB10D8.02c	SPBPB10D8.03
2011	2002		L	-	+	+						90875.5	91375.5	SPBPB10D8.03	SPBPB10D8.04c
2012	2006		L	-	+	+						104625.5	*	SPBPB10D8.07c	SPBC359.01
2013	2007		L	-	+	+						112125.5	111875.5	air2/SPBC359.02	SPBC359.03c
2014	2008		L	-	+	+						*	117625.5	SPBC359.03c	SPBC359.04c
2015	2010		L	-	+	+						132375.5	132625.5	SPBC359.06	SPBC1683.01
2016	2011		L	-	+	+	147229	GGTTACGCGGTTAT	-			142375.5	142125.5	SPBC1683.03c	SPBC1683.04
2017	2012		E	+	+	+						152125.5	152125.5	SPBC1683.05	SPBC1683.06c
2018	2013		L	-	-	+				+		201875.5	202125.5	fbp1/SPBC660.04c	SPBC660.05
2019	2014		L	-	-	+						204375.5	*	SPBC660.05	SPBC660.06
2020			L	-	-	-				+	228966	228875.5	228875.5	SPBC660.15	SPBC660.16
2021	2015		E	+	+	+				+		259125.5	259125.5	clr3/SPBC800.03	rpl4301/rpl37a-1
2022	2016		E	+	+	+				+		278625.5	278625.5	SPBC800.11	SPBC800.12c
2023			E	+	+	+						282375.5	282375.5	SPBC800.13	SPBC1773.01
2024			E	+	+	+						324125.5	*	SPBC1773.17c	car1/SPBP26C9.02c
2025	2018		E	+	+	+				+		326625.5	326625.5	car1/SPBP26C9.02c	SPBP26C9.03c
2026	2019		E	+	+	+						333375.5	333375.5	SPBP26C9.03c	SPBC1271.15c
2027			E	+	+	-				+		354875.5	357375.5	SPBC1271.09	SPBC1271.08c
2028	2023		L	-	+	+	459208	GGTTATGGGTTAT	-			454625.5	454625.5	SPBC428.06c	meu6/SPBC428.07
2029			L	-	-	-						485375.5	484875.5	alp6/SPBC902.01c	ctf18/SPBC902.02c
2030			E	+	+	+						*	518625.5	rps27/SPBC1685.10	rlp1/SPBC1685.11
2031	2024		E	+	+	+						521125.5	*	rlp1/SPBC1685.11	SPBC1685.12c
2032			E	+	+	+						523625.5	523125.5		
2033			E	+	+	+						529375.5	529625.5	SPBC1685.13	SPBC1685.14c
2034	2025		E	+	+	+						571125.5	570625.5	SPBC354.09c	SPBC354.10
2035			E	+	+	+						593375.5	592875.5	tea4/wsh3	wtf2/SPBC1706.02c
2036	2026		E	+	+	+						604125.5	604125.5	rpl803/rpkD4	rps1701/SPBC839.05c
2037			E	+	+	+						670125.5	670375.5	SPBC947.05c	SPBC947.04
2038	2028		E	+	+	+						674875.5	675125.5	SPBC947.04	SPBC947.03c
2039			E	+	+	+						717875.5	717625.5	ubc4/SPBC119.02	SPBC119.03
2040			E	+	+	+						721875.5	*	mei3/SPBC119.04	csh3/SPBC119.05c
2041			E	+	+	+						724125.5	723875.5	csh3/SPBC119.05c	sco1/SPBC119.06
2042	2029		E	+	+	+						746375.5	746125.5	SPBC119.18	rti1/SPBC119.14
2043			E	+	+	+						833875.5	833875.5	SPBC530.15c	SPBC36.01c
2044			E	+	+	+						838625.5	*	SPBC36.01c	SPBC36.02c
2045	2031		E	+	+	+						*	841375.5	SPBC36.02c	SPBC36.03c
2046			E	+	+	+						844625.5	843875.5		
2047	2032		E	+	+	+						848125.5	848125.5	SPBC36.03c	cys11/SPBC36.04
2048	2033		L	-	-	+				+	892038	890875.5	892875.5	pmp1/SPBC713.11c	erg1/SPBC713.12
2049	2035		L	-	+	+	949359	GGTTATTGGGTTAC	+			949625.5	949625.5	gap1/SPBC646.12c	sds23/SPBC646.13
2050	2036		L	-	+	+			-			958125.5	958125.5	SPBC646.15c	SPBC646.16
2051			L	-	-	-						962875.5	962875.5	dic1/SPBC855.01c	SPBP35G2.02
2052			E	+	+	+						1055876	1055876	gtr1/SPBC337.13c	rpb4/SPBC337.14
2053			L	-	-	-				+	1080770	1079126	1080876	SPBC1734.10c	SPBC1734.11
2054	2038		E	+	+	+						1106376	1106626	cyp3/SPBC1709.04c	sks2/SPBC1709.05
2055	2039		E	+	+	+						1142646	1142626	skp1/SPBC409.05	uch2/SPBC409.06
2056			E	+	+	+						1148626	1148876	wis1/SPBC409.07c	SPBC409.08
2057			E	+	+	+						1244876	1245126	gyp10/SPBC651.03c	SPBC651.04
2058	2041		E	+	+	+						1255876	1255626	rpc1/SPBC651.08c	SPBC651.09c
2059	2042/2043		E	+	+	+						1267376	1266126	cwl1/SPBC31A8.01c	SPBC31A8.02
2060			E	+	+	+						1269626	*	SPBC31A8.02	but2/SPBC3D6.02
2061	2044		E	+	+	+						1278376	1278876	mad1/SPBC3D6.04c	ptp4/SPBC3D6.05
2062	2046		E	+	+	+						1313626	1313626	sol1/SPBC30B4.04c	kap109/SPBC30B4.05
2063			L	-	-	-						1352126	1351126	SPBC27B12.14	SPBC27B12.12c
2064			L	-	-	-						1366876	*	hht2/SPBC8D2.04	sfi1/SPBC8D2.05c
2065			E	+	+	+						1389876	1390126	SPBC8D2.16c	SPBC8D2.17
2066	2047		E	+	+	+						1444626	1444376	SPBP22H7.05c	SPBP22H7.06
2067	2048		E	+	+	+						1457626	1457626	nep2/SPBC32H8.02c	bem46/SPBC32H8.03
2068			E	+	-	-						1462376	1462376	SPBC32H8.05	SPBC32H8.06
2069			L	-	+	+	1497617*	GGTTAGCAGGTTATA*	+			1500876	1501126	SPBC11B10.08	cdc2/SPBC11B10.09
2070	2049	ars2004	E	+	+	+						1546626	1546376	SPBC83.18c	atf1/SPBC29B5.01
2071		ars2003	E	+	+	-						1557126	1556876	isp4/SPBC29B5.02c	rpl26/SPBC29B5.03c
2072	2051	ars2002	E	+	+	+						1589876	1590126	kap1/SPBC28F2.10c	SPBC28F2.11
2073			E	+	+	+						1656876	1656876	SPBC21B10.09	SPBC21B10.08c
2074			E	+	+	+						1667626	1668376	nrf1/SPBC21B10.04c	SPBC21B10.03c
2075			L	-	-	-						1683376	1683126	ubp11/SPBC1902.04c	ran1/SPBC19C2.05
2076			E	+	+	+						1707876	1708376	SPBC2F12.15c	gua1/SPBC2F12.14c
2077			E	+	+	+						1718876	1718376	SPBC2F12.12c	rep2/SPBC2F12.11c
2078			E	+	+	+						1752126	1750626	SPBC1D7.03	scr1/SPBC1D7.02c
2079			E	+	+	+						1780376	1780126	sce3/SPBC18H10.04c	SPBC18H10.05
2080			E	+	+	+						1807626	1806876	SPBC18H10.18c	SPBC18H10.19
2081	2062		L	-	+	+	1868344	GGTTATTGGGTTAT	+			1869876	1869876	mug142/SPBC3H7.09	SPBC3H7.08c
2082			E	+	+	+						1894626	1894626	spo14/SPBP16F5.01c	mcs2/SPBP16F5.02
2083			E	+	+	+						1943376	1943876	pab2/SPBC16E9.12c	ksp1/SPBC16E9.13
2084			E	+	+	+						1954626	1955126	SPBC16E9.16c	rem1/SPBC16E9.17c

2085			E	+	+	-						1965626	1965876	SPBC1E8.03c	Tf2-10-pseudo/SPBC1E8.04
2086	2063		E	+	+	+						2025626	2024876	SPBP23A10.11c	SPBP23A10.12
2087	2065		E	+	+	+						2053626	2053876	SPBC29A3.07c	pof4/SPBC29A3.08
2088	2066		E	+	+	+						2071876	2071626	SPBC29A3.16	gef3/SPBC29A3.17
2089	2067		L	-	-	+						2106376	2106626	nif1/SPBC23G7.04c	sui1/SPBC23G7.05
2090			L	-	-	-					+	2114000	2112626	2112376	SPBC23G7.07c	rga7/SPBC23G7.08c
2091	2068	ARS756	E	+	+	+							2119626	2119376	matmc_2/SPBC23G7.09	SPBC23G7.10c
2092	2069/2070		E	+	+	+							*	2131126	rpp202/SPBC23G7.15c	matmi_1/SPBC1711.01c
2093			E	+	+	+							2134126	2134376		
2094	2071		E	+	+	+							2139626	2139126	matmc_1/SPBC1711.02	SPBC1711.03
2095			E	+	+	+							2178876	2178876	nup85/SPBC17G9.04c	cyp6/SPBC17G9.05
2096	2072		E	+	+	+							2188626	2187626	csx2/SPBC17G9.08c	tif213/SPBC17G9.09
2097	2073		E	+	+	+							2247876	2247876	SPBC15C4.04c	SPBC15C4.05
2098			L	-	+	+			+				2267126	2267626	SPBC21H7.06c	his5/SPBC21H7.07c
2099	2074		E	+	+	+							2320626	2320876	trx2/SPBC12D12.07c	ned8/SPBC24C6.01c
2100			L	-	+	+	2339313	GGTTATGGGGTTAC	+				2340126	2341126	SPBC24C6.09c	SPBC24C6.10c
2101	2075		L	-	+	+			-				2412876	2412376	mex67/SPBC1921.03c	SPBC1921.04c
2102	2076		E	+	+	+							2445376	2445126	ucp3/SPBC21D10.05c	fnx1/SPBC12C2.13c
2103			E	+	+	+							2525376	2525376	SPBC365.14c	alp4/SPBC365.15
2104			L	-	-	-							2532876	2532876	alp4/SPBC365.15	SPBC365.16
2105	2078		E	+	+	+							2554876	2554876	SPBC29A10.07	SPBC29A10.08
2106	2080	AT2080	L	-	-	+					+	2589042	2582876	2583126	SPBC2G5.02c	SPBC2G5.03
2107	2081		E	+	+	+							2595626	2595626	rpc25/SPBC2G5.07c	SPBC25B2.01
2108			L	-	-	-							2614626	*	SPBC25B2.08	SPBC25B2.09c
2109			L	-	-	+					+	2647595	2649876	2650126	SPBC6B1.08c	SPBC6B1.12c
2110	2084		E	+	+	+							2704876	2703626	mrpl39/SPBC4F6.08c	str1/SPBC4F6.09
2111	2085		E	+	+	+							2740626	2740376	SPBC336.02	efc25/SPBC336.03
2112	2086		E	+	+	+							2793126	2792376	gpx1/SPBC32F12.03c	tug1/SPBC32F12.04
2113	2087		E	+	+	+							2801376	2801376	duo1/SPBC32F12.08c	rum1/SPBC32F12.09
2114	2088	ARS745	L	-	+	+	2828987	GGTTACGAGGTTAT	+				2829876	2830126	SPBC19C7.04c	SPBC19C7.05
2115	2089	ARS772	E	+	+	+							2903126	2902376	SPBP4H10.14c	SPBP4H10.15
2116			L	-	-	-							2911876	*	SPBP4H10.18c	SPBP4H10.19c
2117	2091		E	+	+	+							2941126	2940876	ubp9/SPBC1703.12	SPBC1703.13c
2118	2092		E	+	+	+							2988876	2988626	SPBC2D10.11c	rhp23/SPBC2D10.12
2119	2094		L	-	-	+							3054126	3053876	SPBC13E7.06	SPBC13E7.07
2120	2095		L	-	-	+							3099876	3099376	zuo1/SPBC30D10.01	rap1/SPBC1778.02
2121			L	-	-	+							3163376	3163876	SPBC609.01	ptn1/SPBC609.02
2122	2097		E	+	+	+							3177876	3177876	dis2/SPBC776.02c	SPBC776.03
2123	2100		E	+	+	+							3288876	3289126	SPBC20F10.02c	SPBC20F10.03
2124			E	+	+	+							3339126	3339626	SPBC17D1.05	dbp3/SPBC17D1.06
2125	2102		E	+	+	+							3363376	3363126	SPBC11C11.12	rpl1807/SPBC11C11.07
2126	2103	ARS727	L	-	-	+					+	3381484	3381126	3381126	SPBC3B8.08	dsd1/SPBC3B8.07c
2127	2104		L	-	-	-							3410126	3410126	ptr2/SPBC13A2.04c	SPBC4B4.01c
2128	2105		E	+	+	+							3423876	3424126	smg1/SPBC4B4.05	vps25/SPBC4B4.06
2129			E	+	+	+							3468376	3468376	SPBC2G2.16	SPBC2G2.17c
2130	2107		E	+	+	+							3489876	3489626	zfs1/SPBC1718.07c	SPBPB7E8.01
2131			E	+	+	+							3493126	3493126		
2132			L	-	+	+			-				3503876	3504126	SPBPB7E8.02	SPBC1105.01
2133			E	+	+	+							3512876	3511876	mrpl16/SPBC1105.03c	cbp1/SPBC1105.04c
2134			E	+	+	+							3515126	3515126	cbp1/SPBC1105.04c	exg1/SPBC1105.05
2135	2108		E	+	+	+							3558376	3558376	SPBC887.09c	mcs4/SPBC887.10
2136			E	+	+	+							3599126	3599126	dna2/SPBC16D10.04c	mok13/SPBC16D10.05
2137	2110		E	+	+	+							3607126	3607376	mok13/SPBC16D10.05	SPBC16D10.06
2138	2111		E	+	+	+							3636876	3636876	SPBP8B7.01c	SPBP8B7.02
2139			L	-	-	+					+	3703810	3703126	3705126	puc1/SPBC19F5.01c	SPBC19F5.02c
2140	2114		E	+	+	+							3722876	3722376	mcm7/SPBC25D12.03c	suc22/SPBC25D12.04
2141	2115		E	+	+	+							3765126	3764376	sar1/SPBC31F10.06c	SPBC31F10.07
2142			L	-	-	-	3775231	GGTTATACTGGTTAC					3779376	3779376	hip1/SPBC31F10.13c	hip3/SPBC31F10.14c
2143			L	-	-	-							3804126	3804126	SPBC21C3.02c	SPBC21C3.03
2144			E	+	+	+							3816876	3817126	SPBC21C3.10c	SPBC21C3.11
2145	2116		E	+	+	+							3840876	3840876	SPBC23E6.01c	SPBC23E6.02
2146	2119		E	+	+	+							3917876	3918126	SPBC1604.09c	imp1/SPBC1604.08c
2147			E	+	+	+							3928126	3928626	SPBC1604.04	SPBC1604.03c
2148	2120		E	+	+	+	3946958	GGTTATGCTGGTTAT	+				3940126	3940876	SPBC1677.03c	thi2/SPBC26H8.01
2149			L	-	-	+							3976126	3977376	dis3/SPBC26H8.10	SPBC26H8.11c
2150			L	-	-	+							3985876	3986876	SPBC26H8.12	ste11/SPBC32C12.02
2151	2123		E	+	+	+							4021126	4021376	nup120/SPBC3B9.16c	isa2/SPBC3B9.17
2152			E	+	+	+							4033376	4032126	git11/SPBC215.04	gpd1/SPBC215.05
2153			E	+	+	+							4035626	4035126		
2154	2125		L	-	+	+			-				4109376	4109376	SPBC56F2.06	SPBC56F2.05c
2155			L	-	+	+			+				4131126	4131126	cnp3/SPBC1861.01c	abp2/SPBC1861.02
2156	2128		E	+	+	+							4204876	4204876	alg6/SPBC342.01c	SPBC342.02
2157			E	+	+	+							4228126	4228126	SPBC16G5.07c	trp4/SPBC16G5.08
2158			E	+	+	+							4238626	4238626	top3/SPBC16G5.12c	SPBC16G5.13
2159			L	-	-	+					+	4259434	4253626	4253876	erg24/SPBC16G5.18	SPBC16G5.19
2160	2129		L	-	+	+							4294126	4294626	rsm25/SPBC16A3.04	lyn1/SPBC16A3.03c
2161			L	-	+	+							4345876	4346126	rpt1/SPBC16C6.07c	qcr6/SPBC16C6.08c
2162	2130		L	-	+	+							4361876	4362126	SPBC244.02c	sid4/SPBC244.01c
2163			L	-	+	+							4413126	4414126	SPBC1289.13c	SPBC1289.14
2164	2131		L	-	+	+							4421876	4421876	Tf2-11/SPBC1289.17	SPBC1289.15
2165			L	-	+	+							4427876	4427876	SPBC1289.15	SPBC1289.16c
2166	2132		L	-	+	+							4442376	4442126	SPBC8E4.03	SPBC8E4.02c
2167	2133		L	-	+	+							4453126	4453376	pho1/SPBP4G3.02	SPBP4G3.03
2168			L	-	+	+							4456126	*	SPBP4G3.03	SPBPB2B2.01
2169			L	-	+	+							4458876	*		

Chromosome III

Ori-number (Hayashi)	AT-islands (Segurado)		Class	Fire in WT	Fire in taz1Δ	Fire in rif1Δ	Position of telomeric seq	Telomeric sequence	Localization of Taz1	Localization of Rif1	Localization of LCS	Position (bp of Orc1	Position (bp of Mcm6	5' Gene/ORF	3' Gene/ORF
3001	3002		E	+	+	+						35375.5	35375.5	SPCP20C8.03	SPCC1884.01
3002	3003		E	+	+	+						76375.5	76625.5	SPCC757.12	SPCC757.13
3003	3005	ars3002/4	E	+	+	+						123875.5	122875.5	SPCC330.07c	alg11/SPCC330.08
3004			E	+	+	+						188125.5	189125.5	fft2/SPCC1235.05c	sif1/SPCC1235.06
3005	3006		E	+	+	+						206875.5	207875,5	ght6/SPCC1235.13	ght5/SPCC1235.14
3006	3007		E	+	+	+						232125.5	231875.5	SPCC548.06c	ght1/SPCC548.07c
3007	3009		E	+	+	+						254125.5	253875.5	SPCC794.04c	SPCC794.6
3008			E	+	+	+						279375.5	278125.5	mae2/SPCC794.12c	SPCC794.15
3009	3010		E	+	+	+						286375.5	286625.5	SPCC553.10	spb70/pol12
3010			E	+	+	+						305875.5	305875.5	SPCC553.03	SPCC553.02
3011			L	-	-	-						347625.5	347625.5	dis1/SPCC736.14	SPCC736.15

3012	3012		E	+	+	+						370125.5	370375.5	SPCC594.07c	qcr9/SPCC1682.01
3013	3013		E	+	+	+						398125.5	398125.5	ubp16/SPCC1682.12c	SPCC1682.13
3014	3015		E	+	+	+						505625.5	505625.5	SPCC970.06	rpl3601/SPCC970.05
3015	3016		E	+	+	+						518625.5	518875.5	rad16/SPCC970.01	prp11/SPCC10H11.01
3016	3017		E	+	+	+						565625.5	565625.5	sap1/SPCC1672.02c	SPCC1672.03c
3017	3018		E	+	+	+						575125.5	575125.5	asp1/SPCC1672.06c	SPCC1672.07
3018			E	+	+	+						605625.5	605375.5	ung1/SPCC1183.06	SPCC1183.07
3019	3019		E	+	+	+						643125.5	643125.5	taf72/SPCC5E4.03c	cut1/SPCC5E4.04
3020	3020		E	+	+	+						666125.5	666125.5	pin1/SPCC16C4.03	SPCC16C4.04
3021	3021		E	+	+	+						720125.5	720125.5	SPCC18B5.02c	wee1/SPCC18B5.03
3022	3022		E	+	+	+						764125.5	764125.5	oca2/SPCC1020.10	SPCC1020.09
3023	3023		E	+	+	+						826875.5	827875.5	SPCC1393.13	SPCC2H8.02
3024			E	+	+	+						847875.5	847875.5	SPCC63.06	SPCC63.07
3025	3024		E	+	+	+						853625.5	853625.5	ppk36/SPCC63.08c	SPCC63.10c
3026	3025		E	+	+	+						936375.5	936875.5	SPCC24B10.19c	SPCC24B10.20
3027	3026		L	-	-	-						966375.5	967875.5	SPCC1795.13	SPCC1795.12c
3028			E	+	+	+						971125.5	971375.5		
3029			E	+	+	+						986125.5	985875.5	SPCC1795.07	map2/SPCC1795.06
3030	3027		L	-	+	+	1039066	GGTTATGGCGGTTAT	+			1039626	1039626	SPCC1259.02c	rpa12/SPCC1259.03
3031			E	+	+	+						1066126	1065876	meu27/SPCC1259.14c	centromere
3032			E	+	+	+						1141876	1142126	centromere	SPCC4B3.18
3033	3039		E	+	+	+						1254126	1254126	snd1/SPCC645.08c	mrpl37/SPCC645.09
3034	3040		E	+	+	+						1324126	1323876	rpl3402/SPCC1322.15	SPCC1322.16
3035			E	+	+	+						1343376	1343376	SPCC338.18	rad21/SPCC338.17c
3036	3042		E	+	+	+						1371876	1371126	SPCC338.02	ags1/SPCC1281.01
3037			E	+	+	+						*	1373876		
3038			E	+	+	+						1393626	*	rsc7/SPCC1281.05	SPCC1281.06c
3039			E	+	+	+						1396876	1396876	SPCC1281.06c	SPCC1281.07c
3040	3043		E	+	+	+						1411126	1411376	SPCC622.07	hta1/SPCC622.08c
3041	3044		E	+	+	+						1417876	1417876	SPCC622.10c	SPCC622.11
3042	3045		E	+	+	+						1449126	1449126	SPCC61.04c	SPCC61.05
3043	3046		E	+	+	+						1511876	1511876	dcr1/SPCC584.10c	SPCC584.11c
3044			L	-	-	-						1524876	1524876	SPCC584.15c	SPCC584.16c
3045	3047		E	+	+	+						1532626	1532126	SPCC584.01c	cuf2/SPCC584.02
3046			E	+	+	+						1556376	1556376	SPCC162.12	SPCC162.11c
3047			E	+	+	+						1576876	1576626	ent1/SPCC162.07	SPCC162.06c
3048	3048		E	+	+	+						1595376	1595126	SPCC13B11.02c	SPCC13B11.03c
3049	3049		E	+	+	+						1609876	1609876	SPCC777.06c	SPCC777.07
3050			E	+	+	+						1672876	1672876	dad5/SPCC417.02	SPCC417.03
3051			E	+	+	+						1675876	1675626	SPCC417.04	chr2/SPCC417.05c
3052			E	+	+	+						1680626	1680626	ppk35/SPCC417.06c	mto1/SPCC417.07c
3053	3051		E	+	+	+						1687126	1685126	mto1/SPCC417.07c	tef3/SPCC417.08
3054	3052		E	+	+	+						1690126	1690626	tef3/SPCC417.08	SPCC417.09c
3055	3053		E	+	+	+						1720126	*	SPCC191.08	gst1/SPCC191.09c
3056			E	+	+	+						*	1723376	SPCC191.10	inv1/SPCC191.11
3057	3054		E	+	+	+						1728626	1728876	SPCC1450.01c	SPCC1450.02
3058			E	+	+	+						1754626	1754876	cek1/SPCC1450.11c	SPCC1450.12
3059			E	+	+	+						1815376	1814626	cgs2/SPCC285.09c	SPCC285.10c
3060	3055		E	+	+	+						1823126	1823126	SPCC285.13c	SPCC285.14
3061	3056		E	+	+	+						1838376	1838626	SPCC1223.01	nmt1/SPCC1223.02
3062	3057		E	+	+	+						1845376	1845376	gut2/SPCC1223.03c	SPCC1223.04c
3063			E	+	+	+						1861376	1860626	SPCC1223.09	SPCC1223.10c
3064	3058		E	+	+	+						1868126	1868376	ptc2/SPCC1223.11	meu10/SPCC1223.12c
3065			E	+	+	-						1878626	1879126	SPCC297.01	ssp1/SPCC297.03
3066			E	+	+	-						1922626	1923626	SPCC74.09	sly1/SPCC74.01
3067	3059		E	+	+	+						1930126	1929876	SPCC74.02c	ssp2/SPCC74.03c
3068			E	+	+	+						1937376	1936126	ssp2/SPCC74.03c	SPCC74.04
3069			E	+	+	+						1969376	1969626	SPCC18.06c	rpc53/SPCC18.07
3070	3060		E	+	+	+						2036376	2036376	SPCC1739.04c	set5/SPCC1739.05
3071			E	+	+	+						*	*	set5/SPCC1739.05	SPCC1739.06c
3072			E	+	+	+						2042626	*	SPCC1739.07	SPCC1739.08c
3073			E	+	+	+						2046376	2046626	SPCC1739.08c	cox13/SPCC1739.09c
3074			E	+	+	+						2064376	2064626	npp106/SPCC1739.14	wtf21/SPCC1739.15
3075			E	+	+	+						2068626	2068626	wtf21/SPCC1739.15	amt1/SPCPB1C11.01
3076			E	+	+	+						2072376	2072876	amt1/SPCPB1C11.01	SPCPB1C11.02
3077			L	-	-	-						2076376	2076626	SPCPB1C11.02	SPCPB1C11.03
3078	3062	ARS744	E	+	+	+						2108376	2108376	ksg1/SPCC576.15c	wtf22/SPCC576.16c
3079	3064		E	+	+	+						2201876	2201876	SPCC830.09c	SPCC830.10
3080			E	+	+	+						2258376	2258626	bgs4/SPCC1840.02c	sal3/SPCC1840.03
3081	3065		E	+	+	+						2277126	2277126	SPCC1840.09	lsm8/SPCC1840.10
3082			L	-	-	+						2300876	2301376	alr1/SPCC965.08c	SPCC965.09
3083	3066		L	-	-	+				+	2310626	2309626	SPCC965.12	SPCC965.13
3084	3068		E	+	+	+						2383626	2383376	SPCC1827.03c	SPCC1827.04

Ori number (Hayashi): Number of origins identified in Hayashi etal (2007); first digit indicates chromosome number (1-3).
Late origins that are activated in HU-treated *taz1Δ* and *rif1Δ*, in *rif1Δ* only and those not activated are highlited in purple, brown and gray, respectively.

AT-islands (Segurado): Origins predicted by Bioinformatics (Segurado et al., 2003).

Class: Activity of origins defined by BrdU incorporation in HU-treated wild-type cells (Hayashi et al, 2007). E; Early origin, L; Late or dormant origin (highlighted in light blue).
E (in red); Early origins that had been previously classified as late origins, L (in red); Late/dormant origins that had been previously classified as early origins.

Firing in *taz1*Δ or *rif1Δ*: "+" denotes a late origin that incorporates BrdU in HU-treated *taz1Δ* and *rif1Δ* (highlighted in purple) or *rif1Δ* (highlighted in brown), respectively, in Supplementary Figure S4.

Positions of telomere seq: Positions (bp) of GGTTAY-N(1-3)-GGTTAY sequence found within 10 kb from the Orc1 binding site using "fuzznuc" program. Telomeric sequences near *ori1021*, *ori1034* and *ori2069* (with a

Telomeric sequence: The telomeric sequence found in the internal arm regions.

Localization of Taz1; "+" and "-" denotes Taz1-dependnet late origins where Taz1 was localized and not localized, respectively, in 10 kb distance in ChIP-seq analysis (Supplementary Figure S4).

Localization of Rif1; "+" denotes origins where Rif1 was localized in 5 kb distance (Hayao et al, 2012).

Localization of LCS: Positions (bp) where LCS-like sequence was identified (Hayano et al, 2012, Supplemental Table S3)

Positions of Orc1: The peak position (bp) of Orc1 (Hayashi et al, 2007).

Positions (bp) of Mcm6: The peak position of Mcm6 (Hayashi et al, 2007).

5' Gene/ORF, 3' Gene/ORF: The name of the 5' gene/ORF or 3' gene/ORF flanking the region containing theOrc1-Mcm6 binding sites.

Supplementary Table S2. Characteristics of replication origins and genes near the internal telomeric repeats.

Chr	Proximal origin	Class	Early firing in *taz1*Δ	Localization of Taz1	Start	End	St	Sequence	Left ORF	Response to stress	Response to meiosis	Response to pheromone	Remarks (gene)	Right ORF	Response to stress	Response to meiosis	Response to pheromone	Remarks (gene)
Chr1	1068	E	NA	+	1822620	1822634	-	GGTTATGGTGGTTAC	SPAC1002.13c		+			itt1	+	+		ubiquitin-protein ligase E3
	1071/AT1062	L	+	+	1894950	1894963	+	GGTTATTAGGTTAC	SPAPB1A10.15		+		Arv1-like family protein	SPAC140.01				ubiquinone iron-sulfur protei n
	1080/AT1069	E	NA	-	2199362	2199374	-	GGTTACTGGTTAT	SPAC1783.05									
	1097	L	+	+	2521205	2521226	-	GGTTATACGGTTACG CGGTTAT	SPAC23H3.13c				G protein alpha-2, Gpa2	SPAC23H3.14				LAlv9 family protein
		NA	NA	-	2859912	2859926	+	GGTTACTCGGGTTAT	SPAC8F11.04					SPAC8F.06		+		nuclear envelope protein Brr6/Brl1
		NA	NA	-	3982509	3982521	-	GGTTATCGGTTAT						SPAPB18E9.04c				
		NA	NA	-	4547725	4547739	-	GGTTATCCTGGTTAT						SPAC637.05c				
	1175/AT1142	L	+	-	4604051	4604065	-	GGTTATTCAGGTTAT	SPAC12B10.16c		+		conserved protein Mug157	SPAC1093.01				PPR repeat protein Ppr5
		NA	NA	-	5250680	5250692	+	GGTTATCGGTTAT	SPAC14C4.11				polyphosphate synthetase	SPAC14C4.12c				Clr6 L associated factor 1 Laf1
Chr2	2005	L	+	-	65194	65208	-	GGTTACGTTGGTTAT	SPBPB21E7.05					SPBPB21E7.05				
	2016/AT2011	L	+	-	147229	147242	+	GGTTACGCGGTTAT	SPBC1683.04	+			glycosyl hydrolase family	SPBC1683.05		+	+	
	2028/AT2023	L	+	-	459208	459220	-	GGTTATGGGTTAT	SPBC428.08c		+		histone H3 methylase Clr4	SPBC428.10			+	
	2049/AT2035	L	+	+	949359	949372	-	GGTTATTGGGTTAC	SPBC646.12c				GTPase activating Gap1	SPBC646.13	+			PP2A inhibitor Sds23/Moc1
		NA	NA	-	1626423	1626436	-	GGTTACAGGGTTAC	cnt									
	2081/AT2062	L	+	+	1868344	1868357	-	GGTTATTGGGTTAT	SPBC3H7.09		+		palmitoyltransferase Erf2	SPBC3H7.08c	+		+	conserved fungal protein
	2100	L	+	+	2339313	2339326	+	GGTTATGGGGTTAC	SPBC24C6.09c	+	+	+	phosphoketolase family	SPBC24C6.10c				cytoskeletal protein
	2114/AT2088	L	+	+	2828987	2829000	-	GGTTACGAGGTTAT	SPBC19C7.04c	+	+		conserved fungal protein	SPBC19C7.05				cell wall organization
		NA	NA	-	3011366	3011378	+	GGTTACTGGTTAT	SPBC15D4.01c	+	+		kinesin-like protein Klp9	SPBC15D4.02		+		transcription factor
	2142	L	-	-	3775231	3775245	-	GGTTATACTGGTTAC	SPBC31F10.13c				histone chaperone Hip1	SPBC31F10.14c		+		HIRA interacting protein Hip3
		NA	NA	+	3861682	3861694	-	GGTTATCGGTTAC	SPBC23E6.08					SPBC23E6.09				transcriptional corepressor Ssn6
	2148/AT2120	E	NA	-	3946958	3946972	+	GGTTATGCTGGTTAT	SPBC26H8.03					SPBC26H8.04c		+		DEP domain protein
	sub-telomeric	L	+	+	4535529	4535542	+	GGTTACATGGTTAT	tlh2									
Chr3		NA	NA	+	4815	4828	-	GGTTACATGGTTAC						SPRRNA.47				
		NA	NA	+	15685	15698	-	GGTTACATGGTTAC	SPRRNA.43					SPRRNA.48				
	3030/AT3027	L	+	+	1039066	1039080	+	GGTTATGGCGGTTAT	SPCC1259.02c				ER metallopeptidase 1	SPCC1259.03				RNA polymerase I subunit Rpa12
		NA	NA	+	2448448	2448461	+	GGTTACATGGTTAC	SPRRNA.49					SPNCRNA.1299				

Proximal origin : the name of ealry and late origins idnetified by Hayashi et al. (2007)/AT-island identified by Segurado et al. (2003), located within 10-kb from the telomeric sequence.
Class : "E" and "L" indicate early and late/dormant origins, respectively. NA show no origin is located.
Early firing in *taz1*Δ : "+" denotes BrdU-incorporation at late origin in Supplementary Fig. S5.
Localization of Taz1 : "+" shows enrichment of Taz1 localization in Supplementary Fig. S5.
Start/end : positions of start and end of telomeric sequence.
St : strandness is shown either "+" or "-".
Response to stress, meiosis and pheromone: a plas sign indicates increase in mRNA level (>2) of mRNA in the stress (high temperature, ionic and oxidative stresses), during meiosis and sporulation, and to the phoromone, according to Gene Data Base at Sanger Center.

Figure S1.
BrdU-labeled DNA prepared at 120 min after G2/M release from HU-treated wild-type, *taz1*Δ and *rif1*Δ strains and separated by CsCl density gradient centrifugation, and those obtained by FLAG-Taz1-IP were used for SOLiD deep sequencing analysis, which was performed according to the manufacturer's standard protocol (Applied Biosystems).

chrI_1

genes

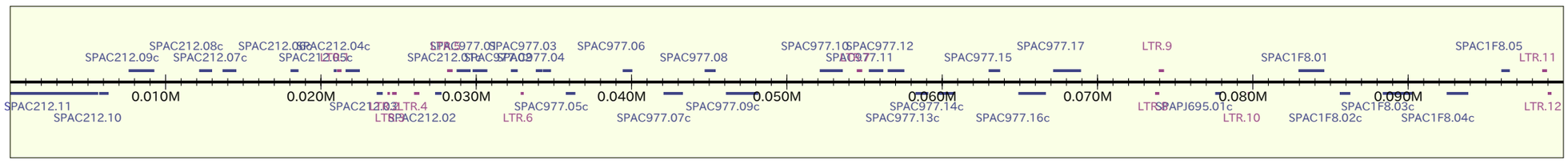

WT

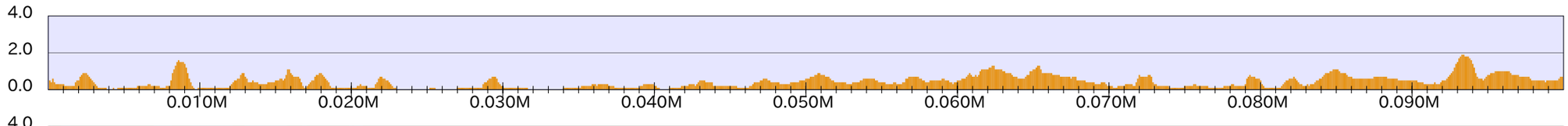

taz1

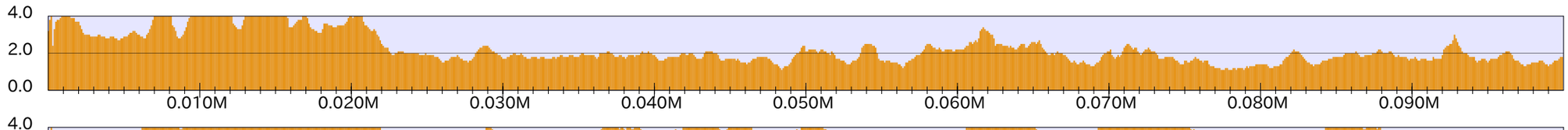

rif1

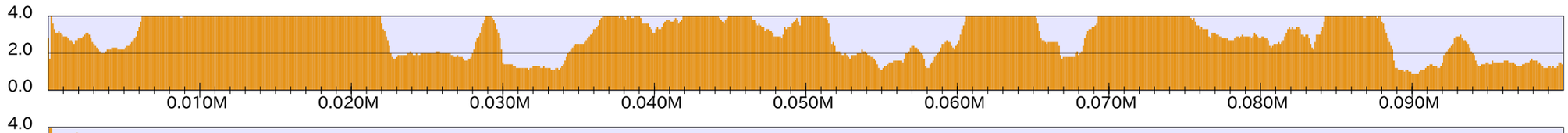

Taz1/notag

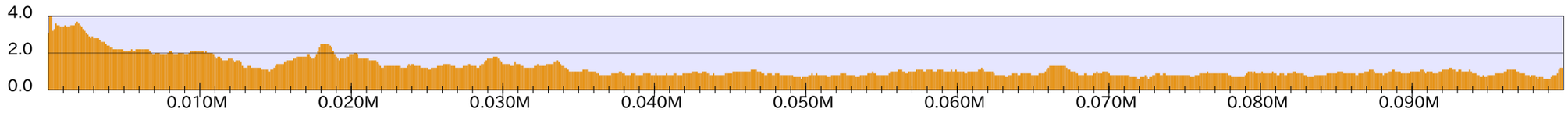

genes

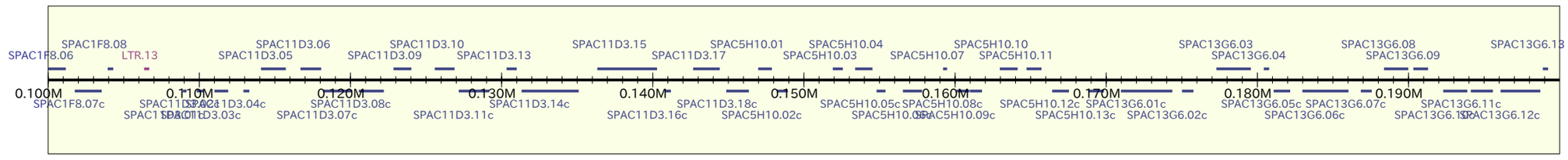

WT

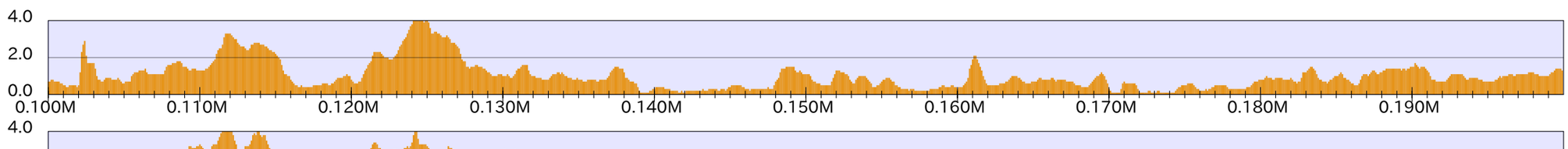

taz1

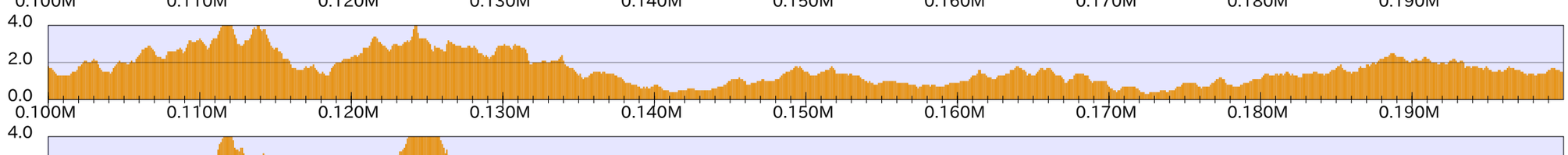

rif1

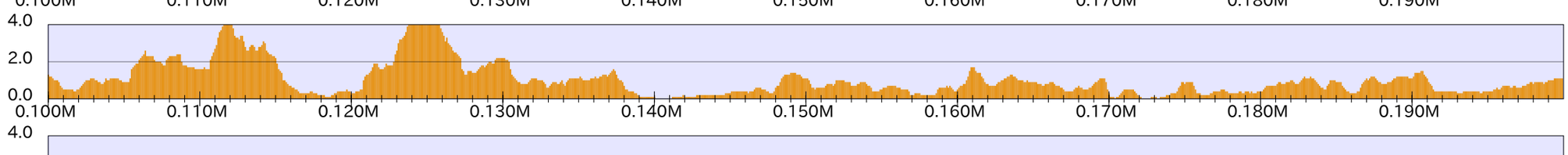

Taz1/notag

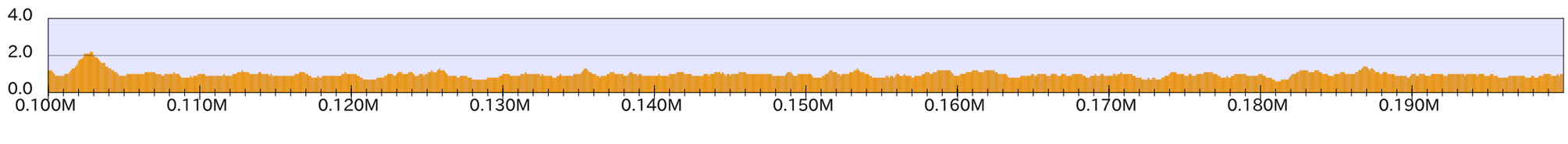

genes

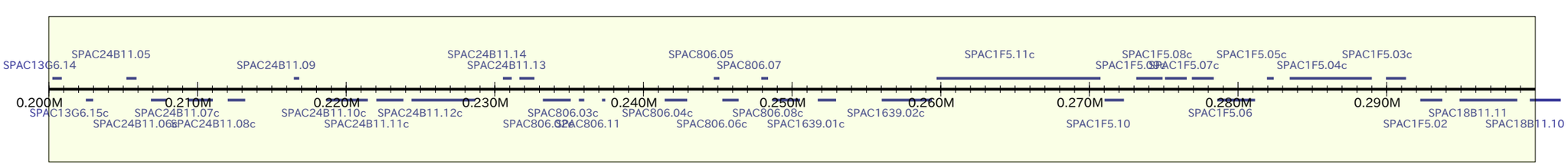

WT

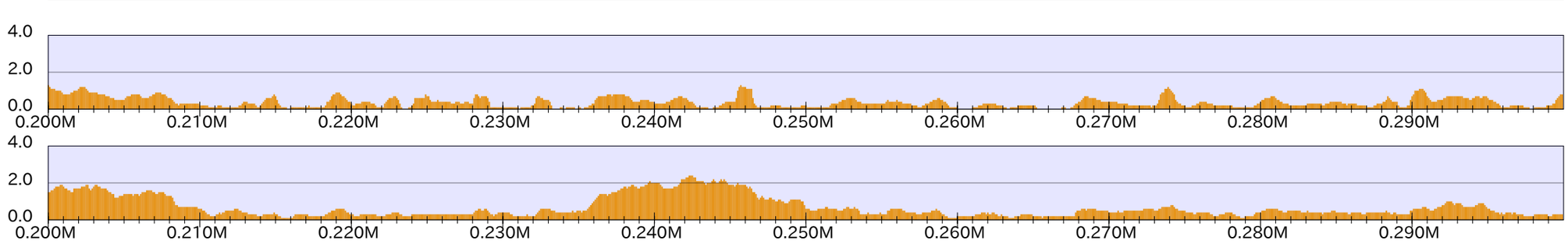

taz1

rif1

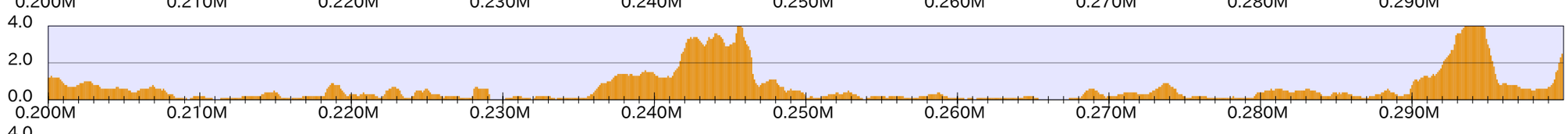

Taz1/notag

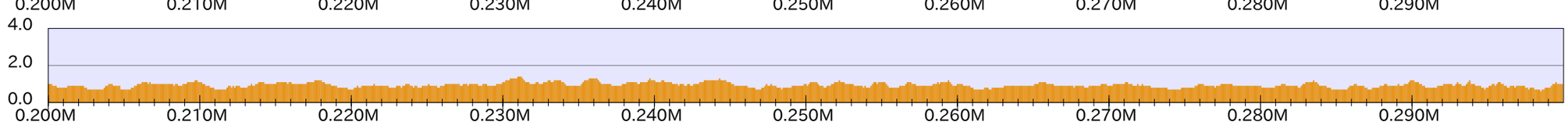

chrI_2

genes

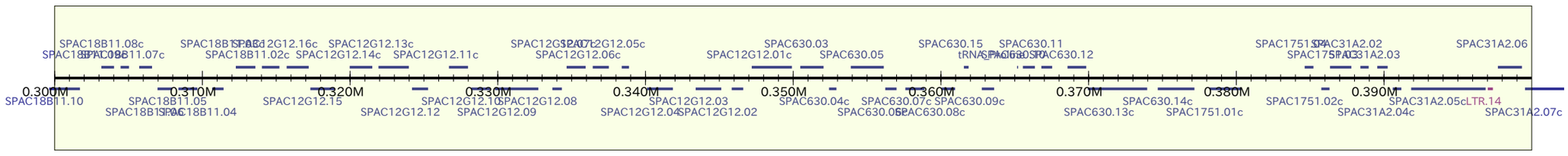

WT

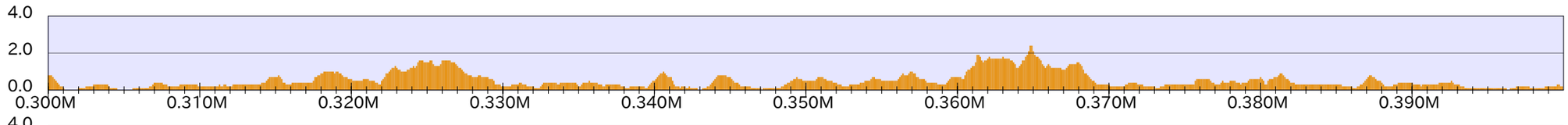

taz1

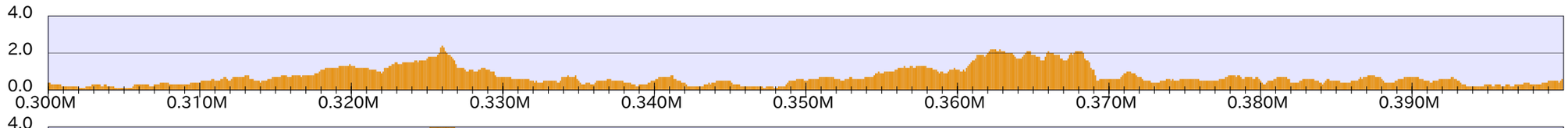

rif1

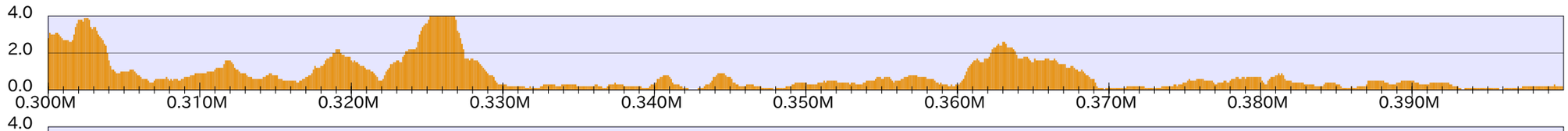

Taz1/notag

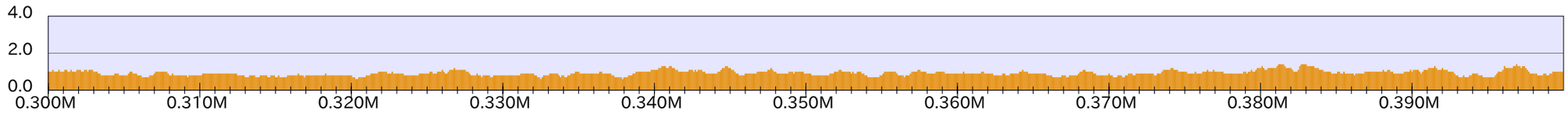

genes

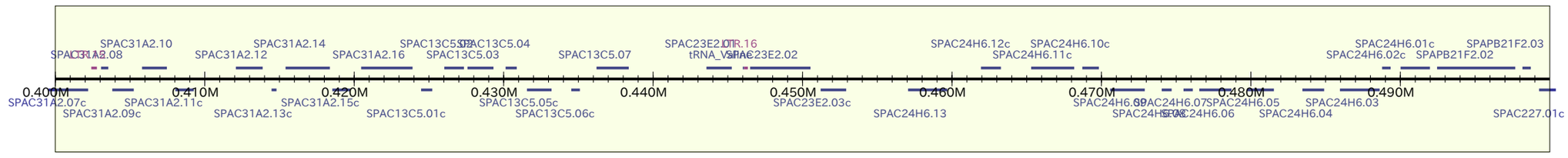

WT

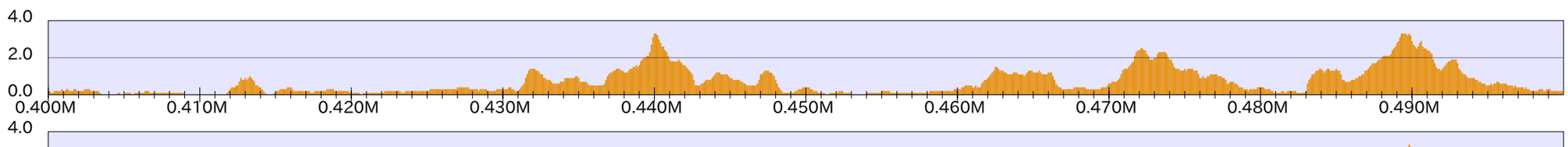

taz1

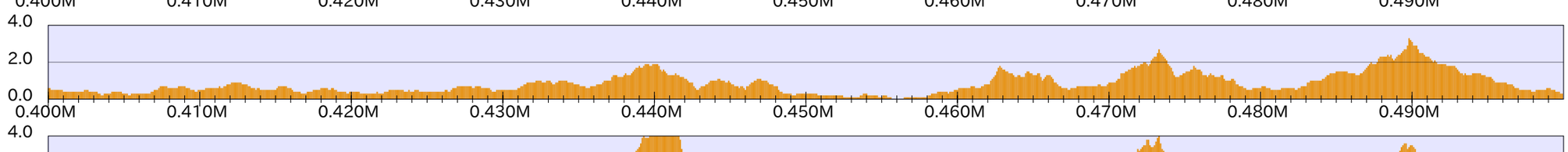

rif1

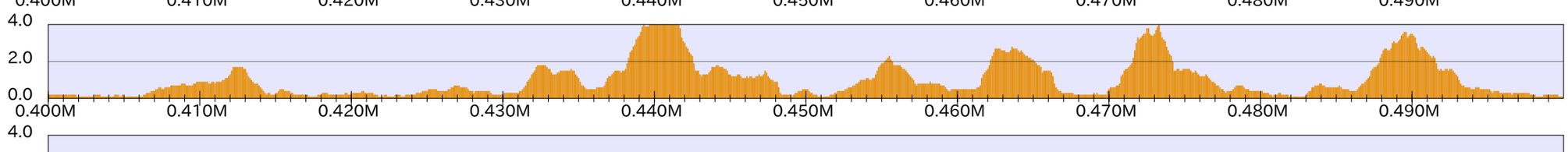

Taz1/notag

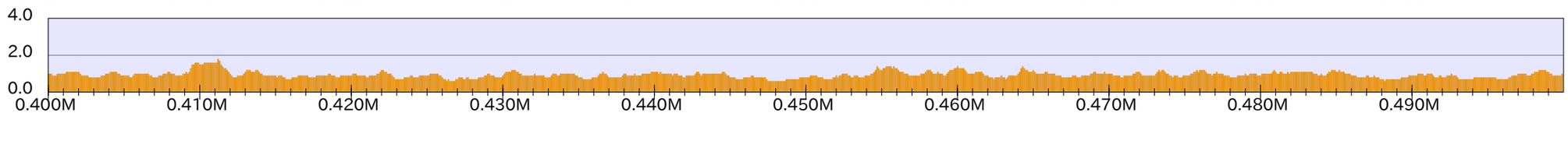

genes

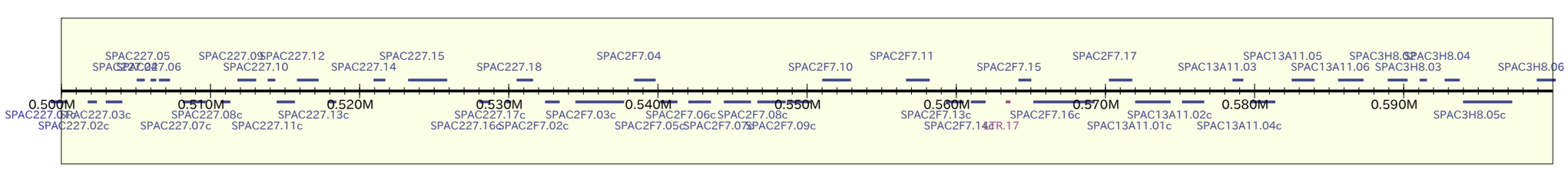

WT

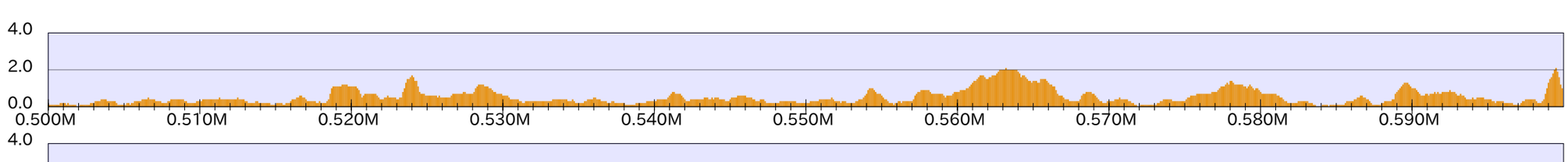

taz1

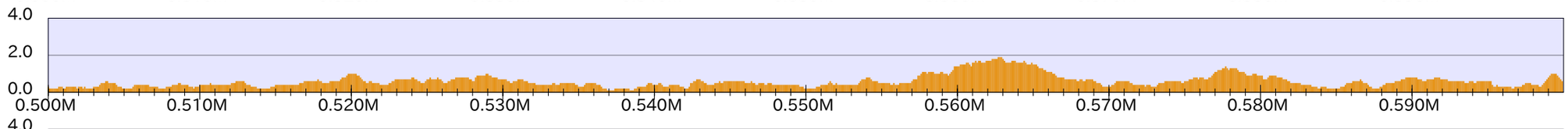

rif1

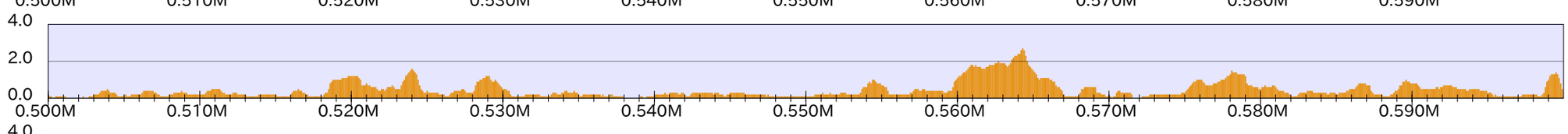

Taz1/notag

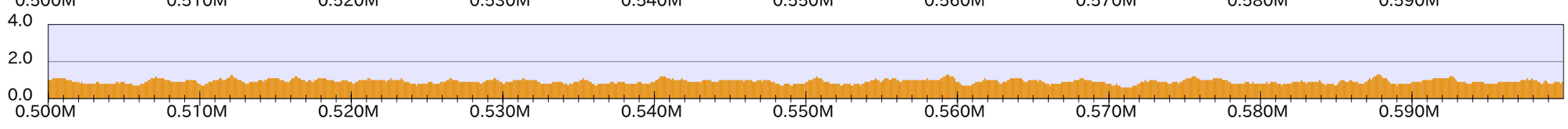

chrI_3

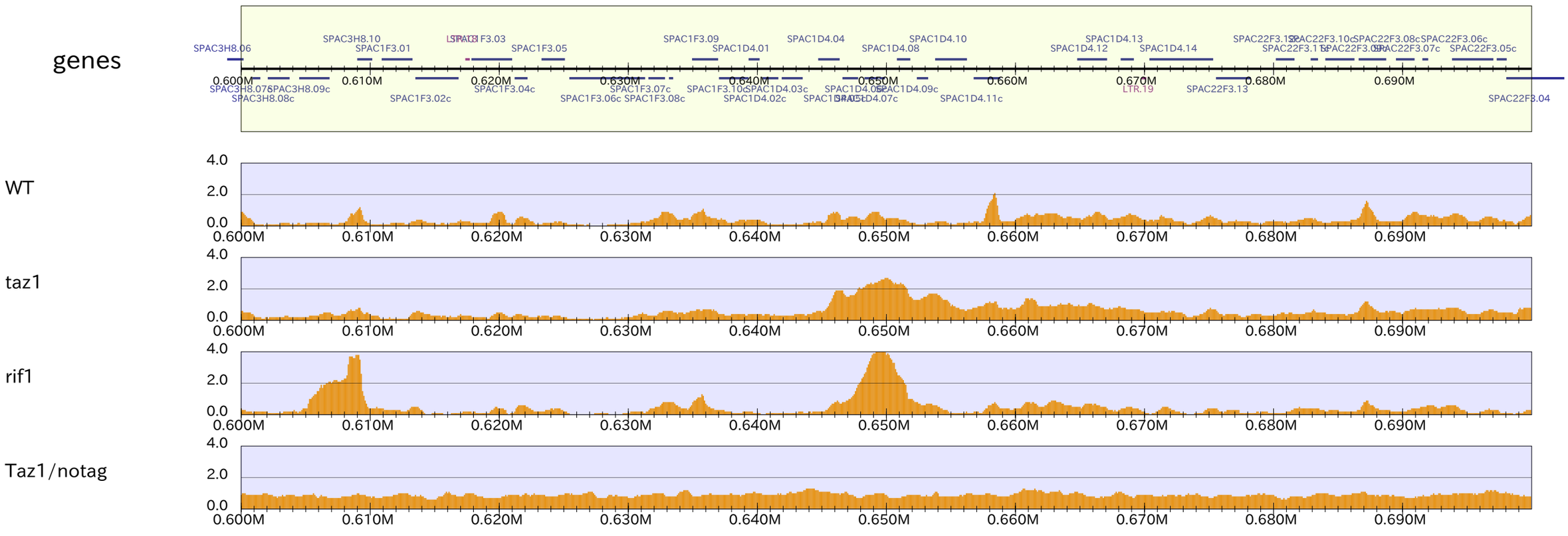
genes
SPAC3H8.06
SPAC3H8.10
SPAC1F3.01
SPAC1F3.03
SPAC1F3.05
SPAC1F3.09
SPAC1D4.01
SPAC1D4.04
SPAC1D4.08
SPAC1D4.10
SPAC1D4.12
SPAC1D4.13
SPAC1D4.14
SPAC22F3.12
SPAC22F3.10c
SPAC22F3.08c
SPAC22F3.06c
SPAC22F3.11
SPAC22F3.09
SPAC22F3.07c
SPAC22F3.05c
0.600M
0.610M
0.620M
0.630M
0.640M
0.650M
0.660M
0.670M
0.680M
0.690M
SPAC3H8.07
SPAC3H8.09c
SPAC3H8.08c
SPAC1F3.02c
SPAC1F3.04c
SPAC1F3.06c
SPAC1F3.07c
SPAC1F3.08c
SPAC1F3.10c
SPAC1D4.02c
SPAC1D4.03c
SPAC1D4.05
SPAC1D4.07c
SPAC1D4.09c
SPAC1D4.11c
LTR.19
SPAC22F3.13
SPAC22F3.04
WT
taz1
rif1
Taz1/notag
4.0
2.0
0.0

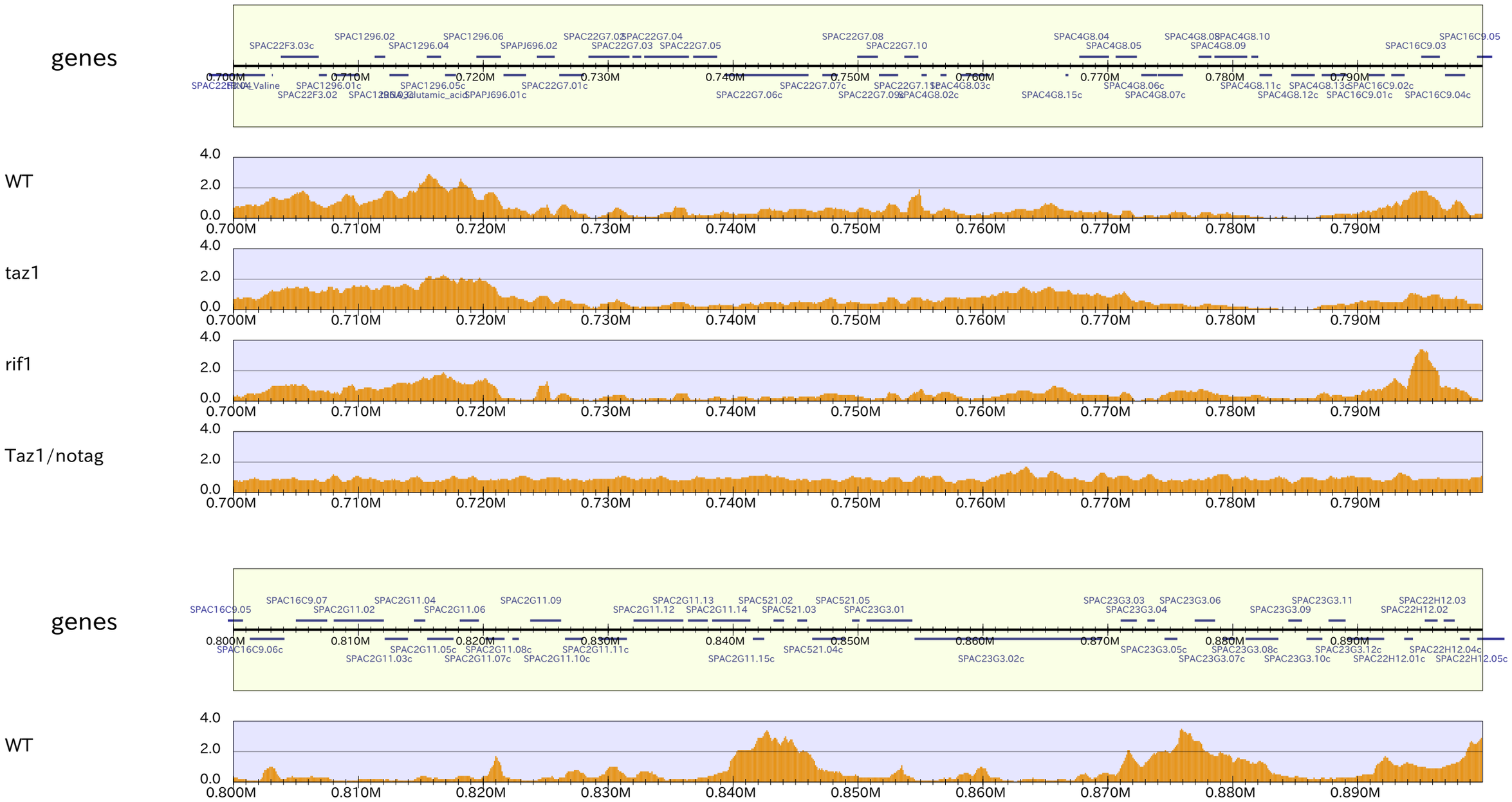
genes
SPAC22F3.03c
SPAC1296.02
SPAC1296.04
SPAC1296.06
SPAPJ696.02
SPAC22G7.02
SPAC22G7.03
SPAC22G7.04
SPAC22G7.05
SPAC22G7.08
SPAC22G7.10
SPAC4G8.04
SPAC4G8.05
SPAC4G8.08
SPAC4G8.09
SPAC4G8.10
SPAC16C9.03
SPAC16C9.05
0.700M
0.710M
0.720M
0.730M
0.740M
0.750M
0.760M
0.770M
0.780M
0.790M
SPAC1296.01c
SPAC1296.05c
SPAC22F3.02
SPAPJ696.01c
SPAC22G7.01c
SPAC22G7.06c
SPAC22G7.07c
SPAC4G8.02c
SPAC4G8.03c
SPAC4G8.06c
SPAC4G8.07c
SPAC4G8.11c
SPAC4G8.12c
SPAC4G8.13c
SPAC16C9.01c
SPAC16C9.02c
SPAC16C9.04c
WT
taz1
rif1
Taz1/notag
4.0
2.0
0.0

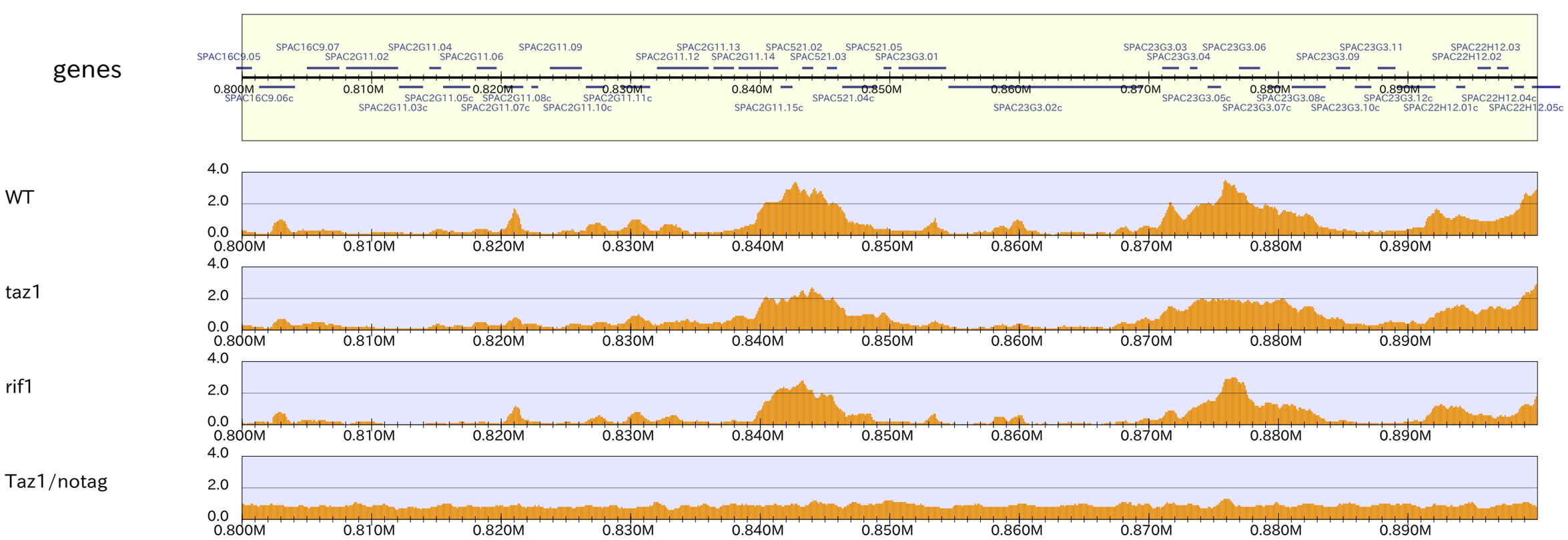
genes
SPAC16C9.05
SPAC16C9.07
SPAC2G11.02
SPAC2G11.04
SPAC2G11.06
SPAC2G11.09
SPAC2G11.12
SPAC2G11.13
SPAC2G11.14
SPAC521.02
SPAC521.03
SPAC521.05
SPAC23G3.01
SPAC23G3.03
SPAC23G3.04
SPAC23G3.06
SPAC23G3.09
SPAC23G3.11
SPAC22H12.02
SPAC22H12.03
0.800M
0.810M
0.820M
0.830M
0.840M
0.850M
0.860M
0.870M
0.880M
0.890M
SPAC16C9.06c
SPAC2G11.03c
SPAC2G11.05c
SPAC2G11.07c
SPAC2G11.08c
SPAC2G11.10c
SPAC2G11.11c
SPAC2G11.15c
SPAC521.04c
SPAC23G3.02c
SPAC23G3.05c
SPAC23G3.07c
SPAC23G3.08c
SPAC23G3.10c
SPAC23G3.12c
SPAC22H12.01c
SPAC22H12.04c
SPAC22H12.05c
WT
taz1
rif1
Taz1/notag
4.0
2.0
0.0

chrI_4

genes

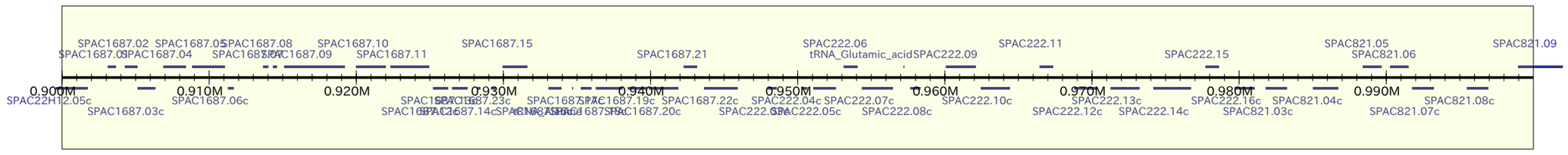

WT

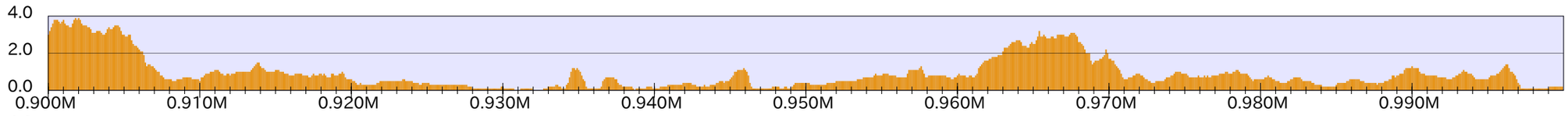

taz1

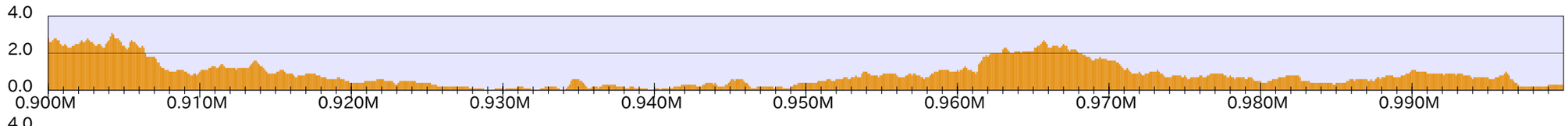

rif1

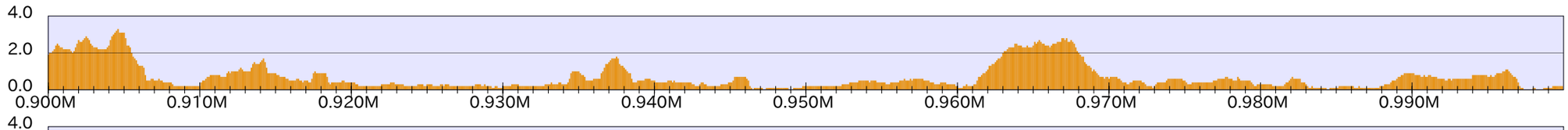

Taz1/notag

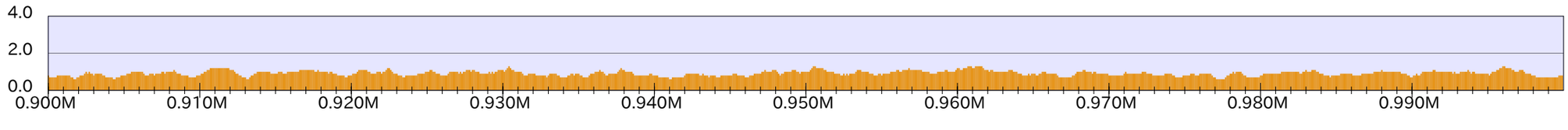

genes

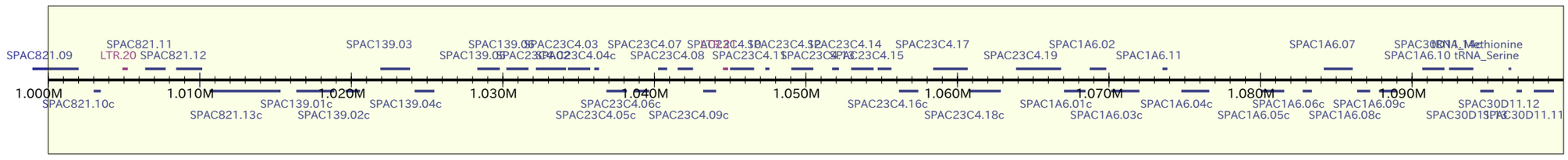

WT

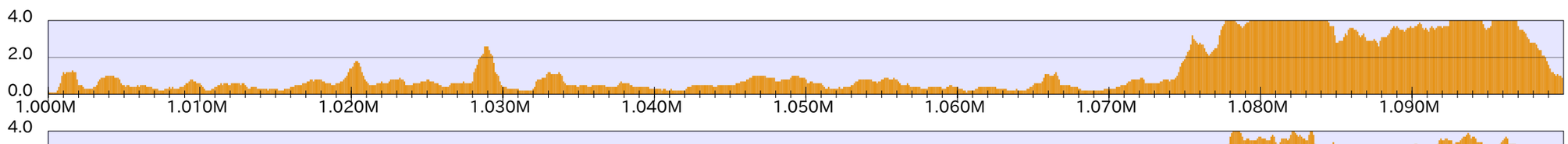

taz1

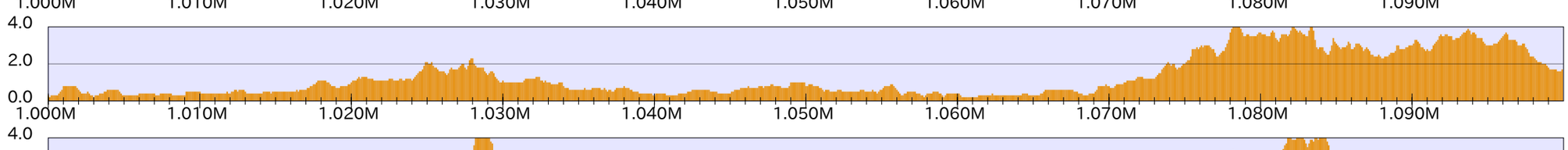

rif1

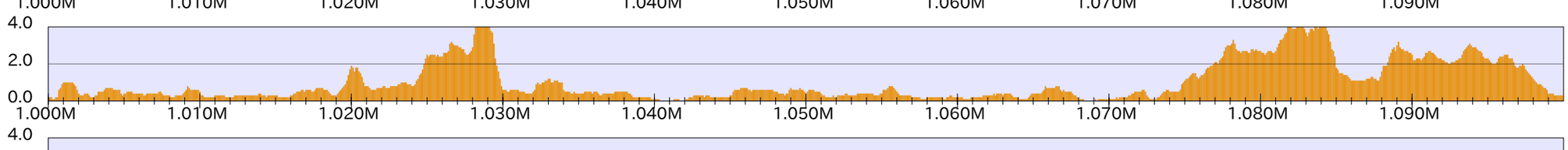

Taz1/notag

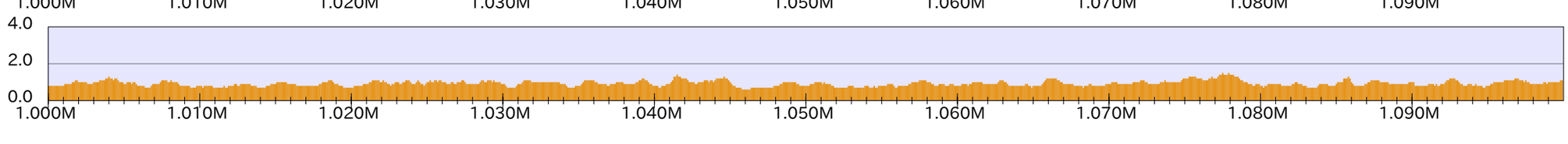

genes

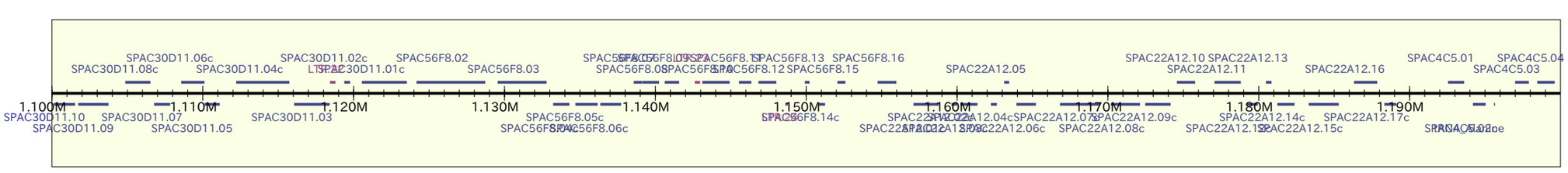

WT

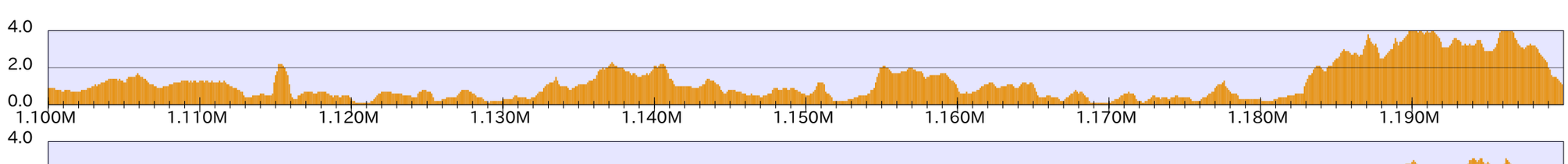

taz1

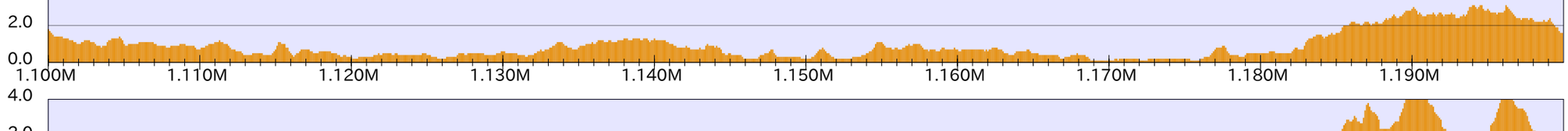

rif1

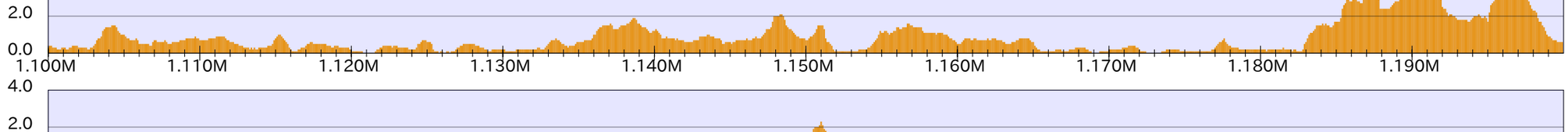

Taz1/notag

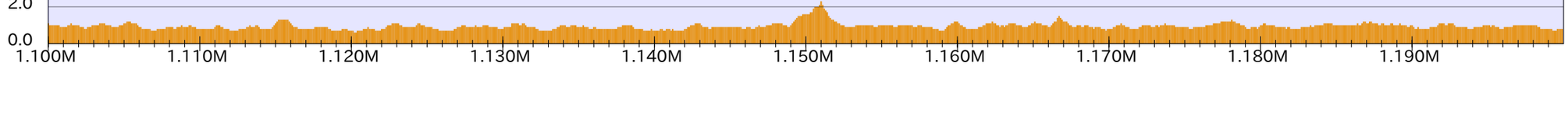

chrI_5

genes

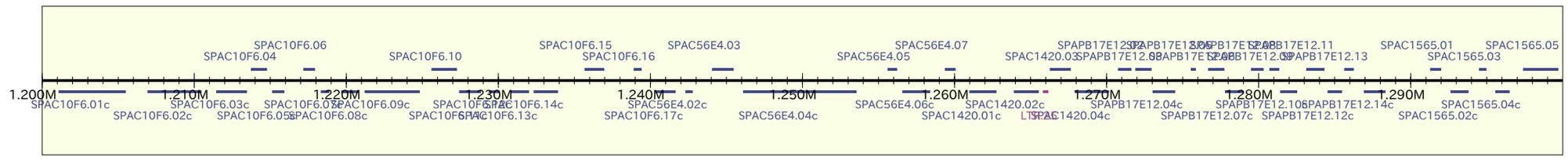

WT

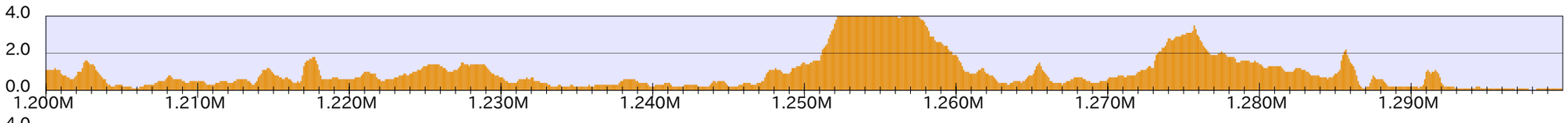

taz1

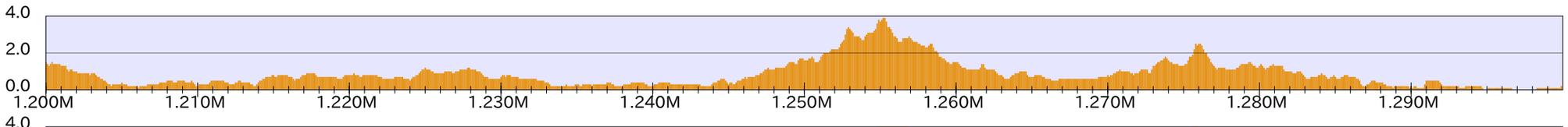

rif1

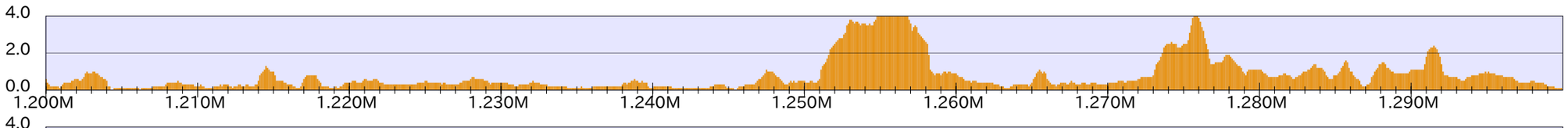

Taz1/notag

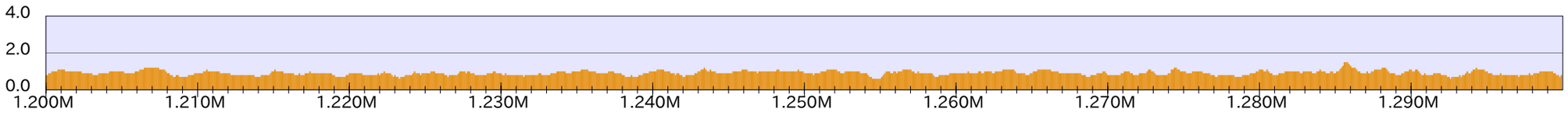

genes

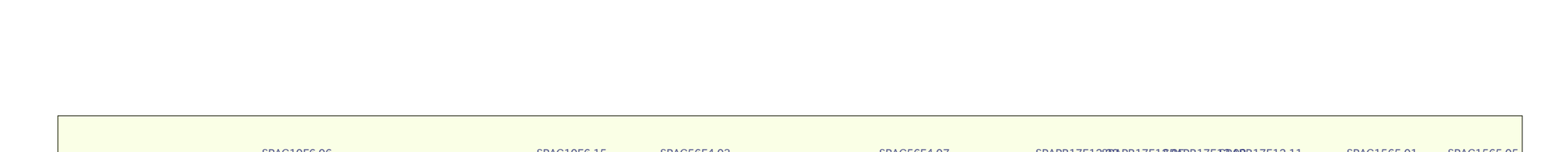

WT

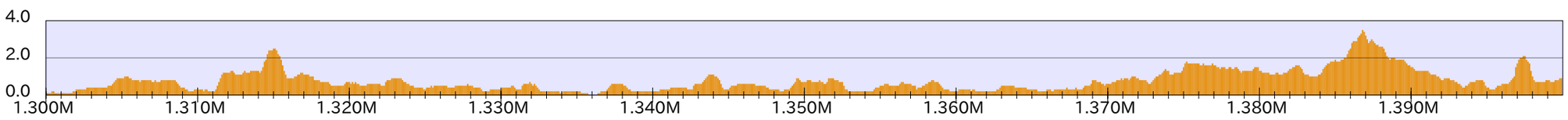

taz1

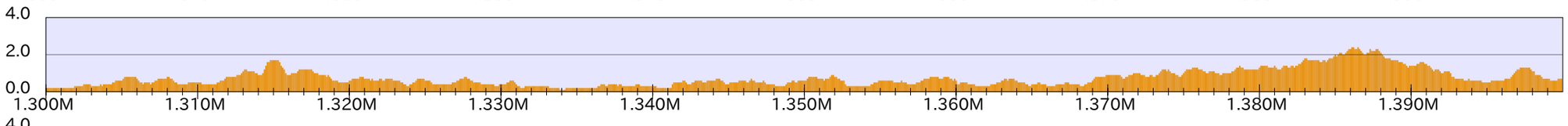

rif1

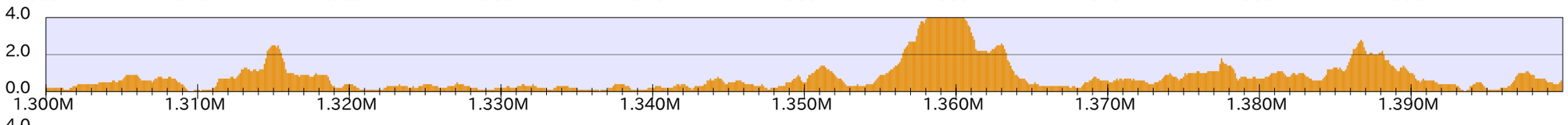

Taz1/notag

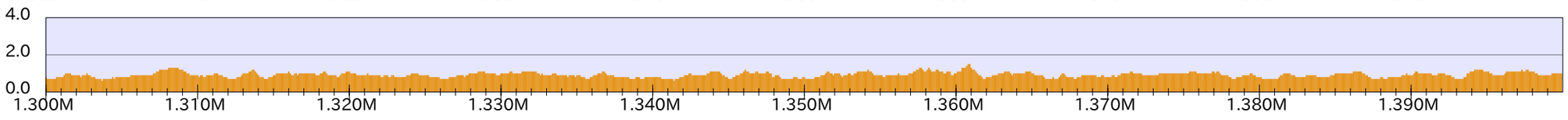

genes

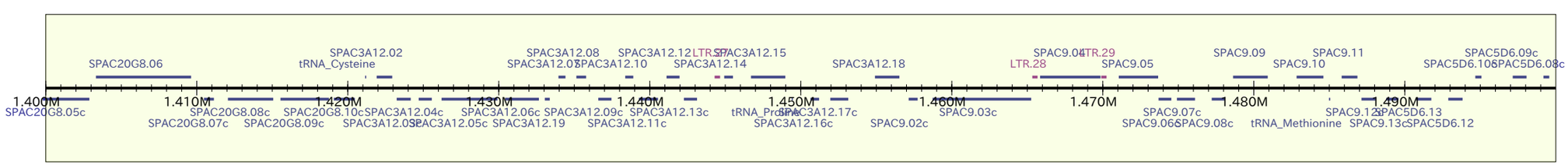

WT

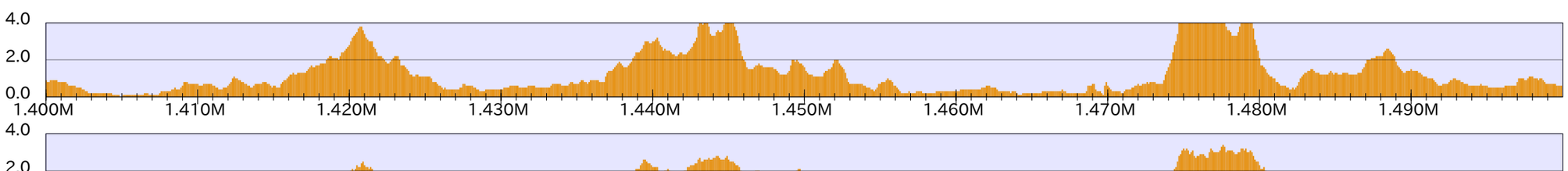

taz1

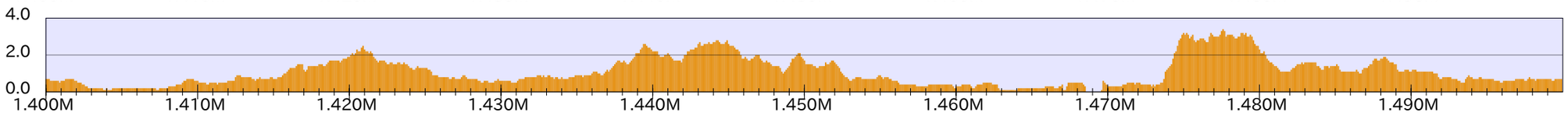

rif1

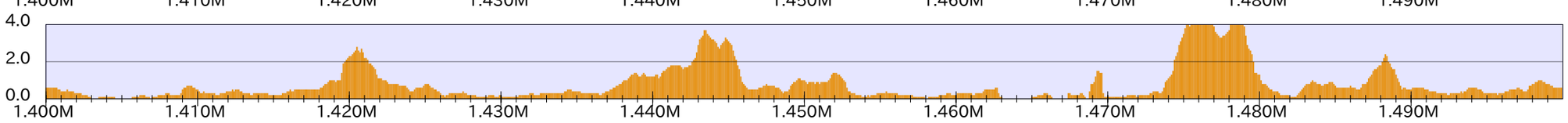

Taz1/notag

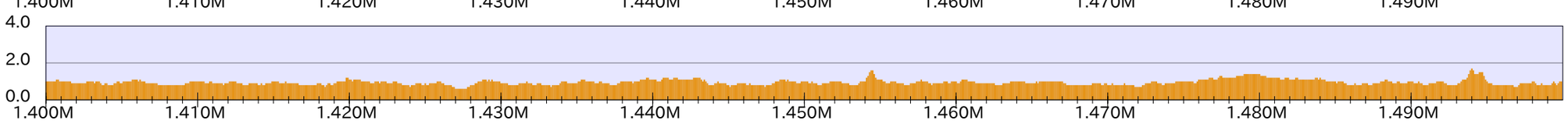

chrI_6

genes

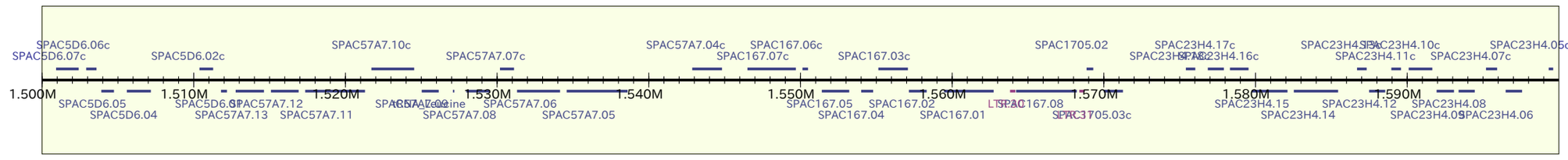

WT

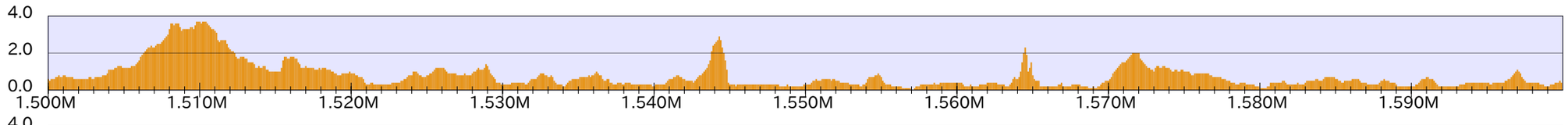

taz1

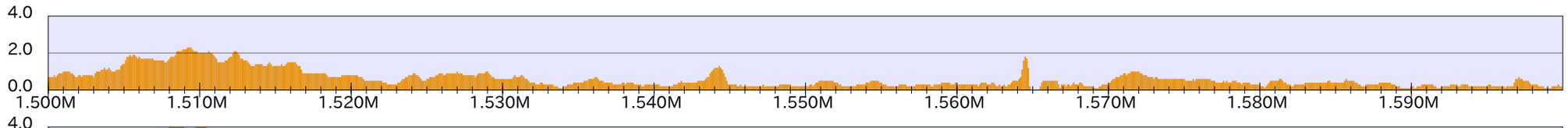

rif1

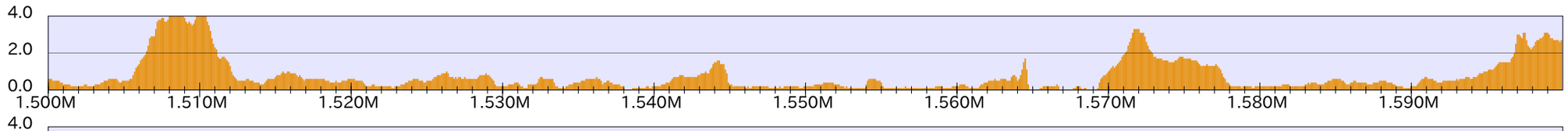

Taz1/notag

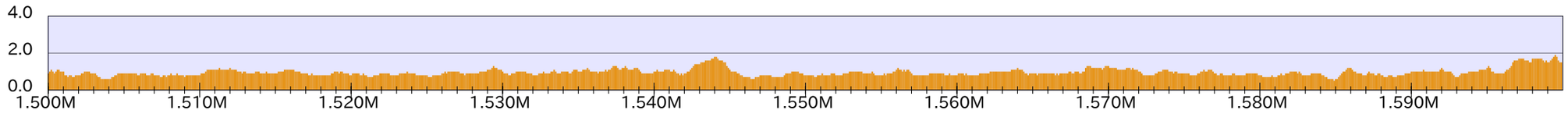

genes

WT

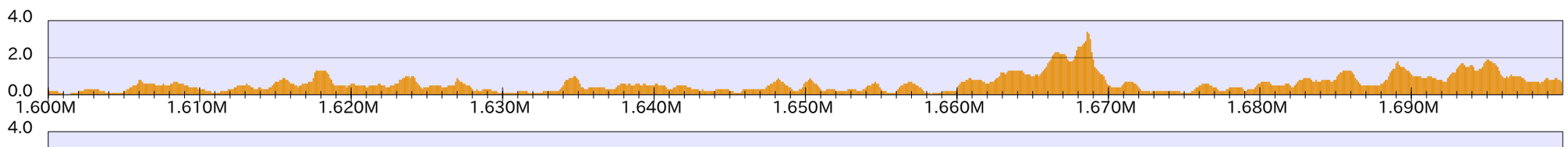

taz1

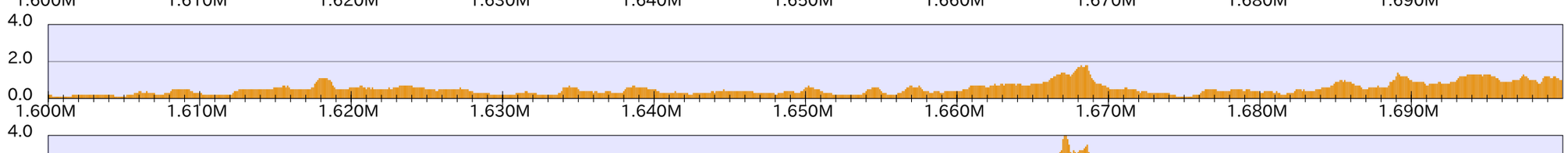

rif1

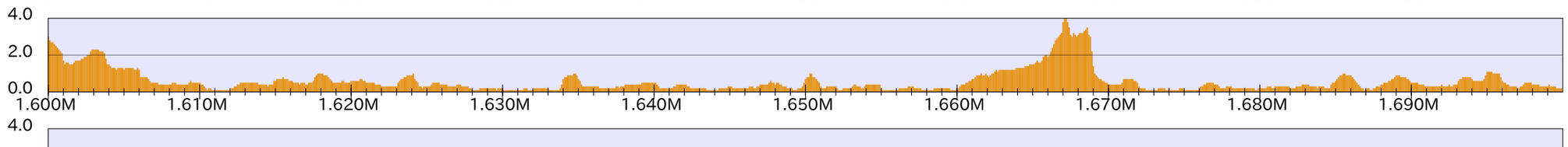

Taz1/notag

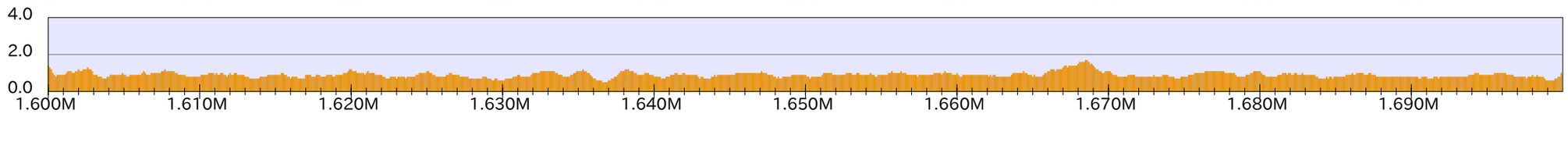

genes

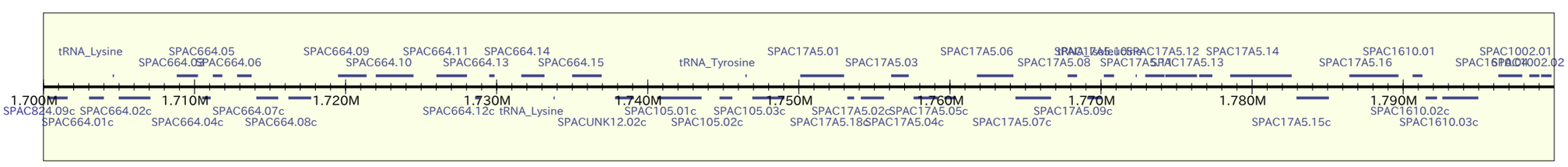

WT

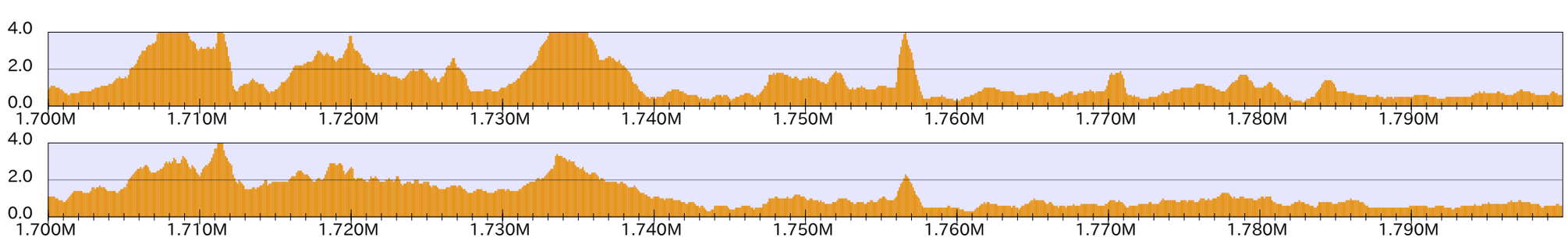

taz1

rif1

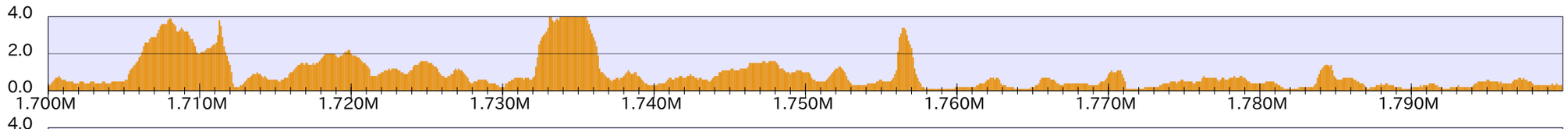

Taz1/notag

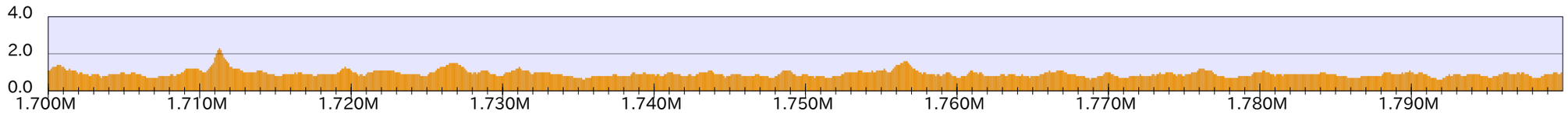

chrI_7

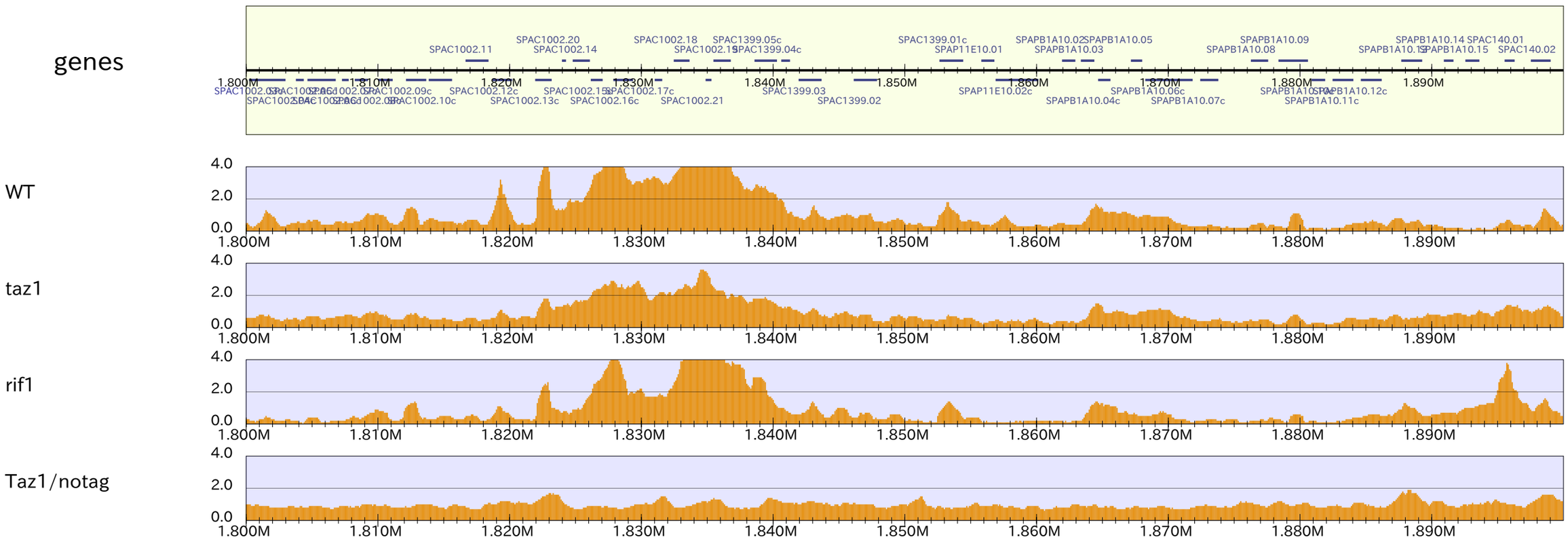
genes
WT
taz1
rif1
Taz1/notag
1.800M
1.810M
1.820M
1.830M
1.840M
1.850M
1.860M
1.870M
1.880M
1.890M
4.0
2.0
0.0

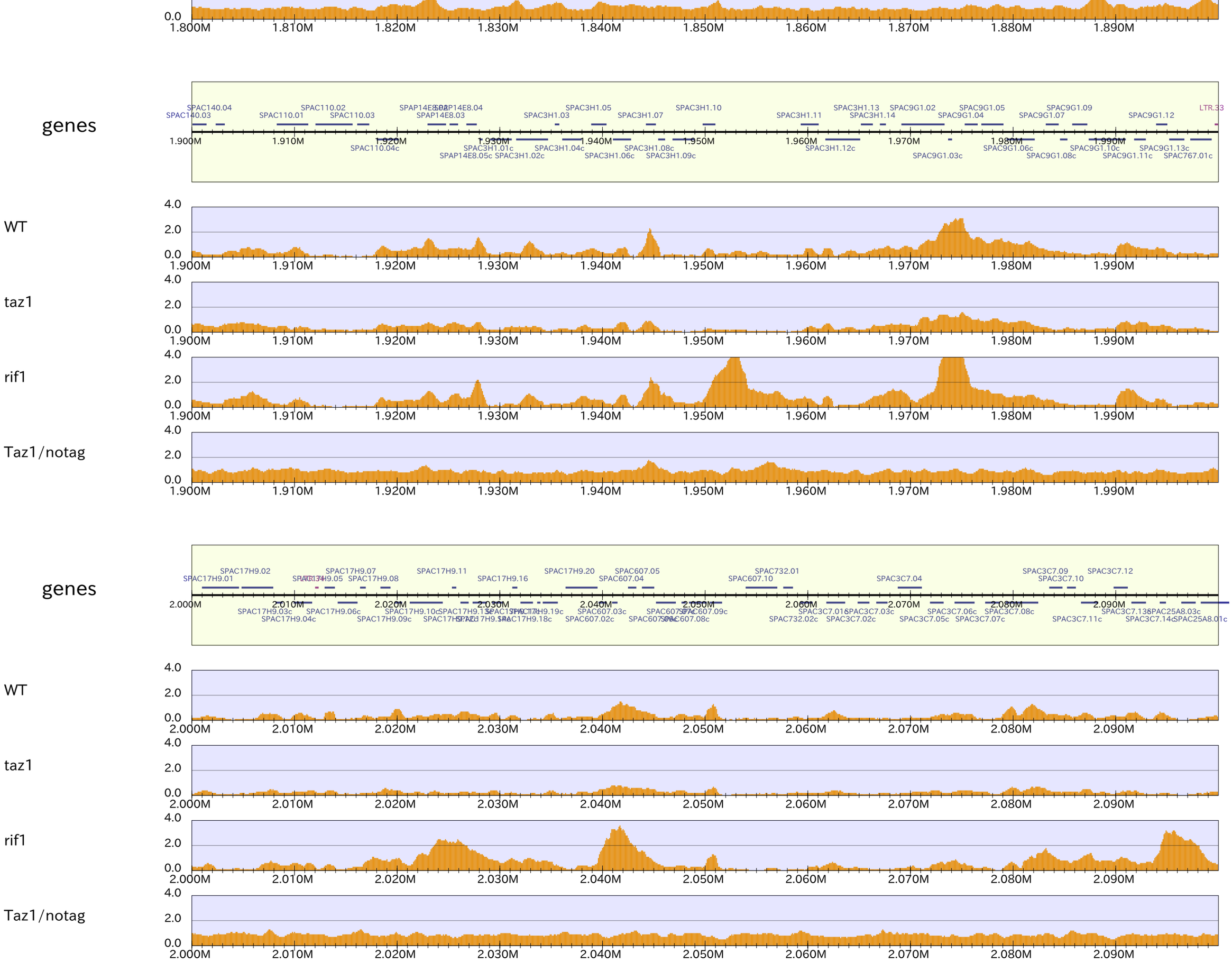
genes
WT
taz1
rif1
Taz1/notag
1.900M
1.910M
1.920M
1.930M
1.940M
1.950M
1.960M
1.970M
1.980M
1.990M
2.000M
2.010M
2.020M
2.030M
2.040M
2.050M
2.060M
2.070M
2.080M
2.090M
4.0
2.0
0.0

chrI_8

genes

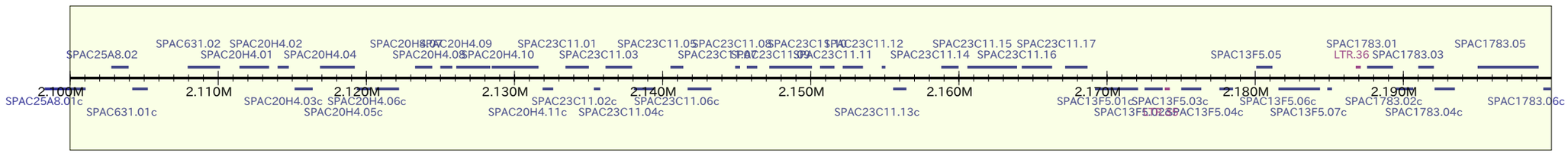

WT

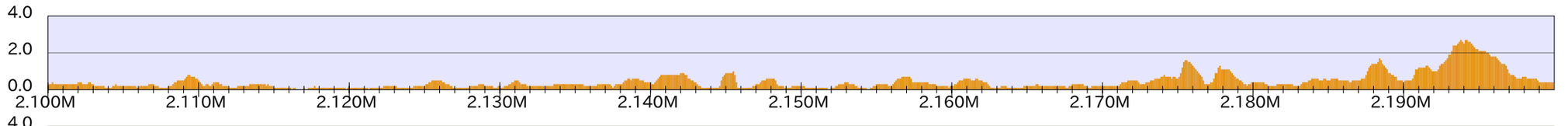

taz1

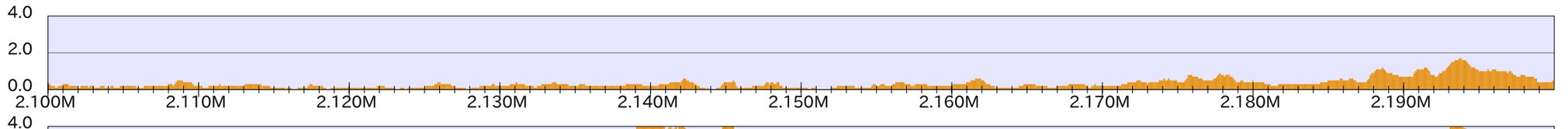

rif1

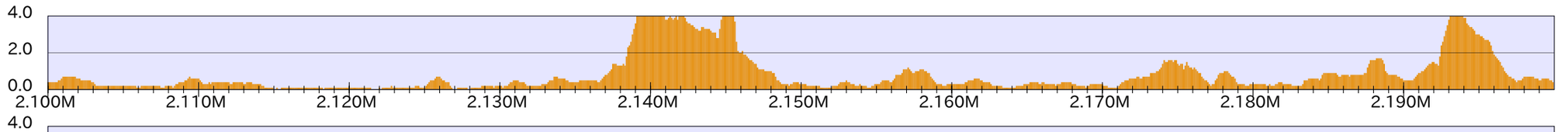

Taz1/notag

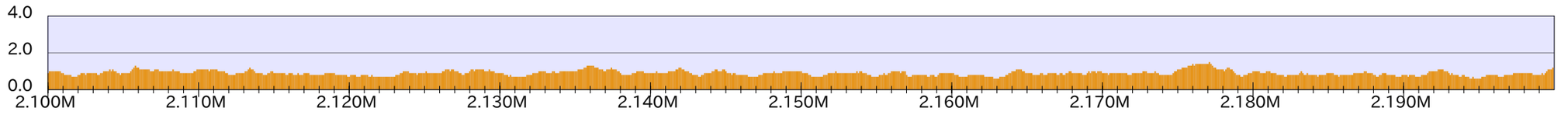

genes

WT

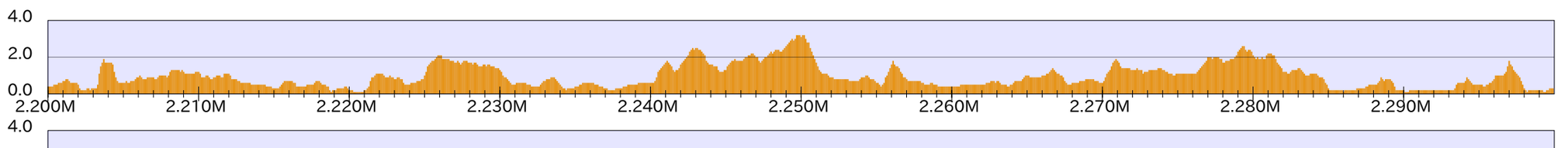

taz1

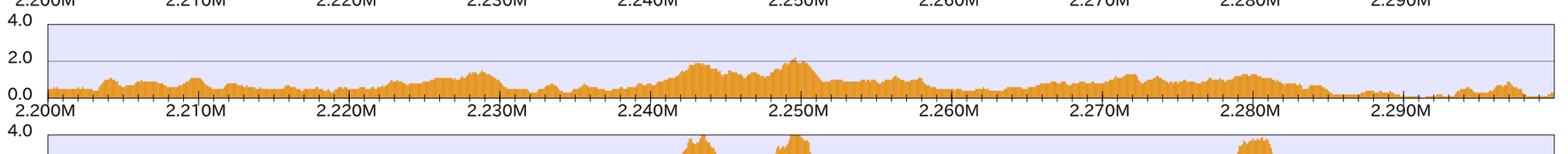

rif1

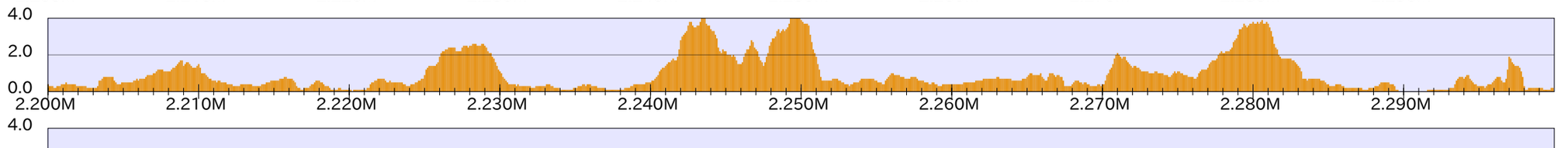

Taz1/notag

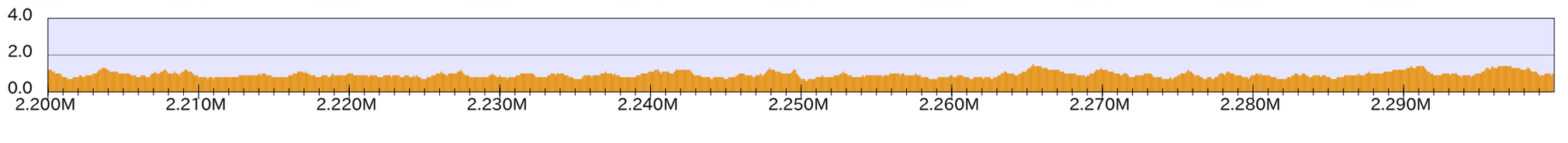

genes

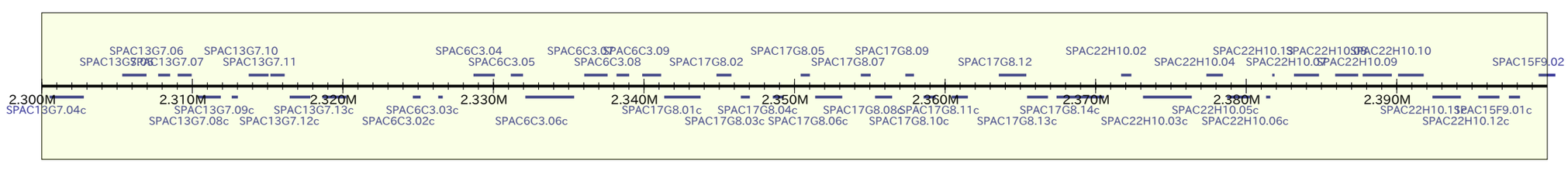

WT

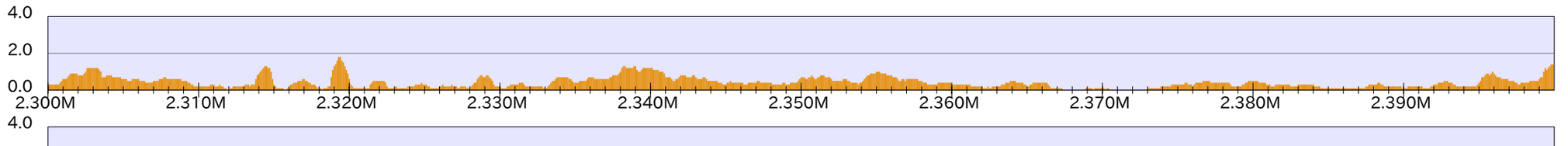

taz1

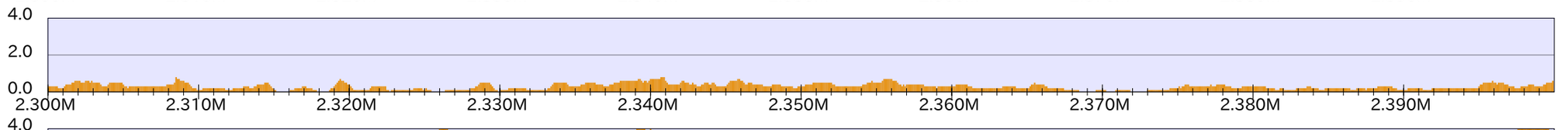

rif1

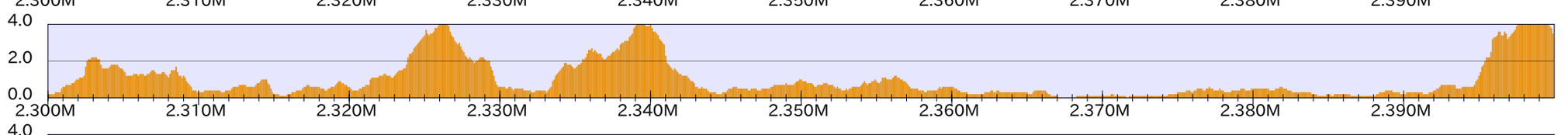

Taz1/notag

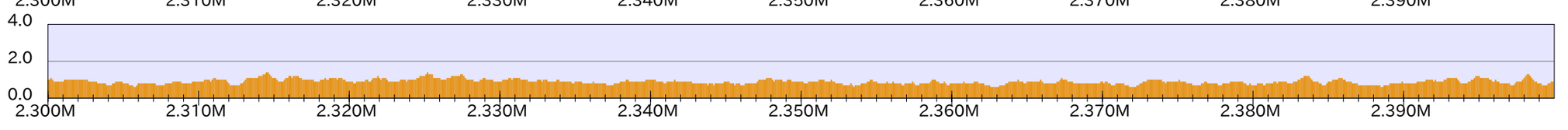

chrI_9

genes

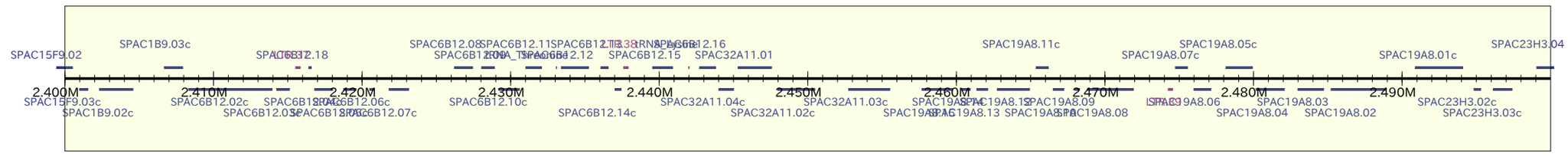

WT

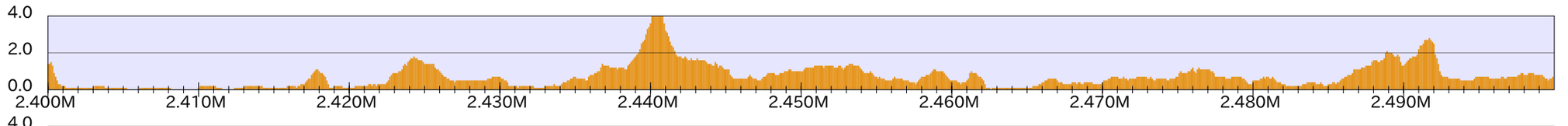

taz1

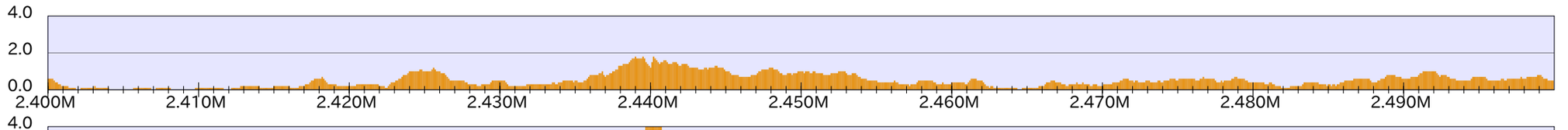

rif1

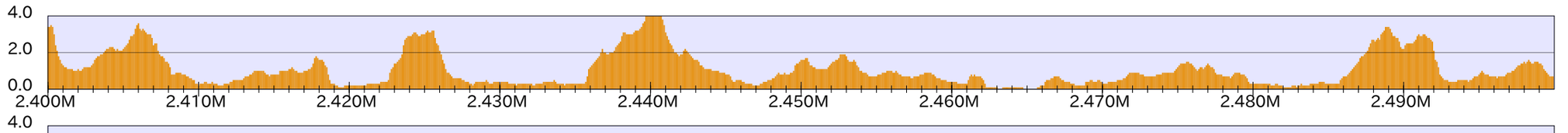

Taz1/notag

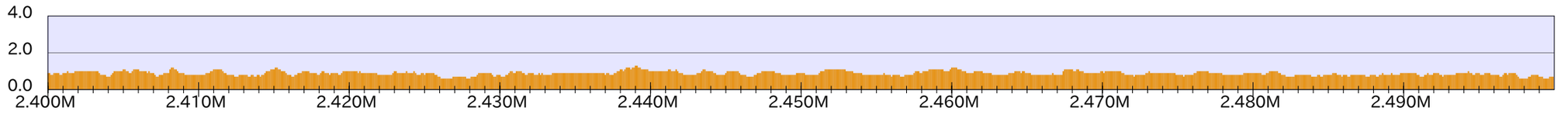

genes

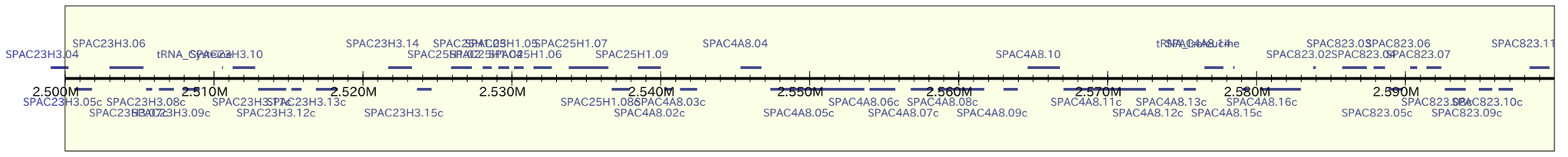

WT

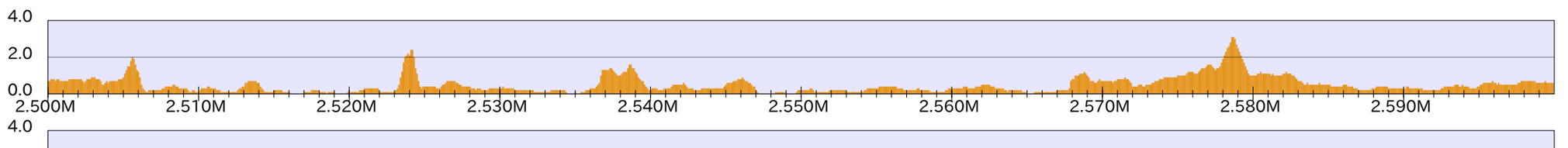

taz1

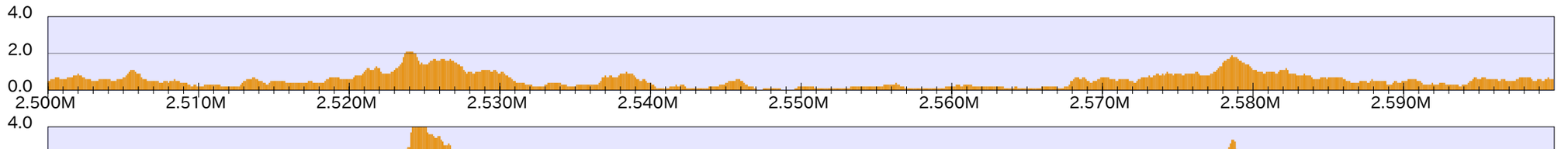

rif1

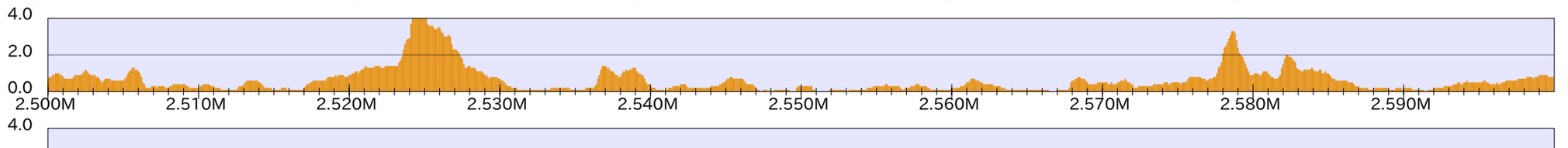

Taz1/notag

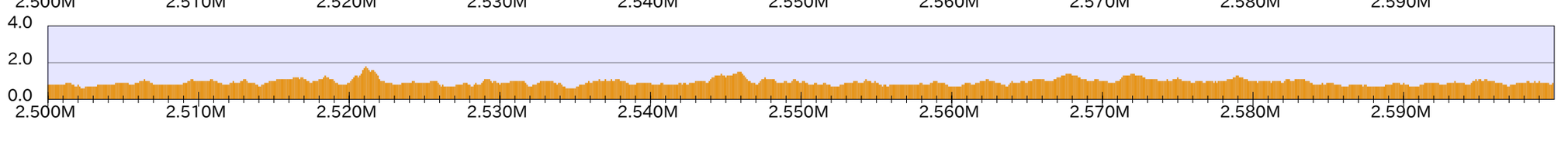

genes

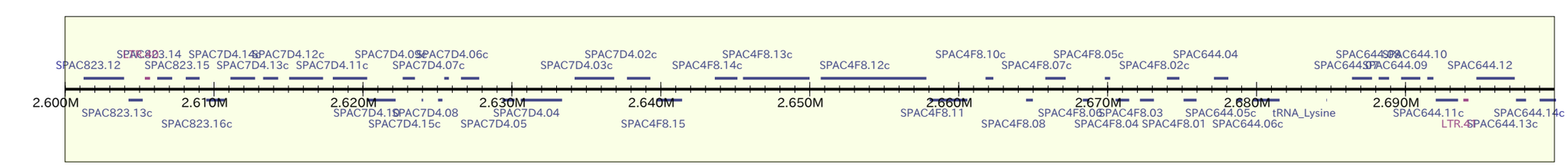

WT

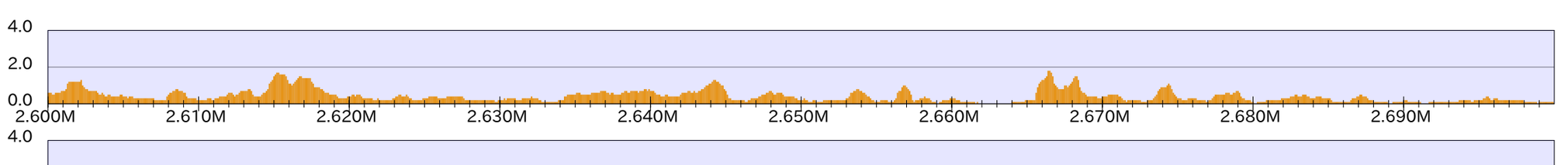

taz1

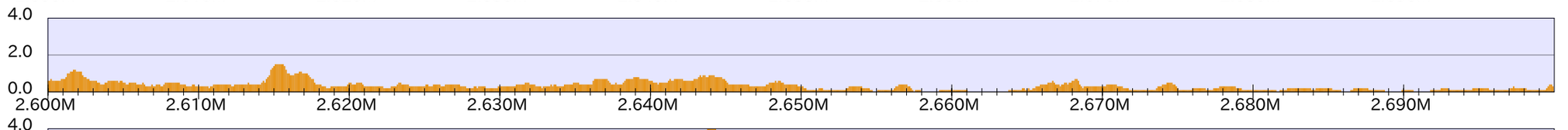

rif1

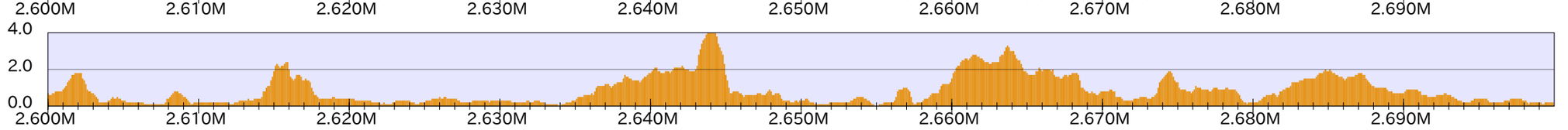

Taz1/notag

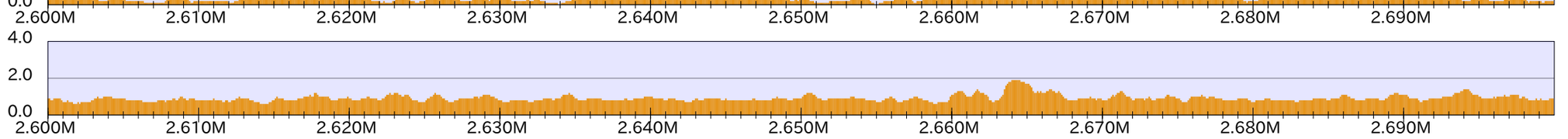

chrI_10

genes

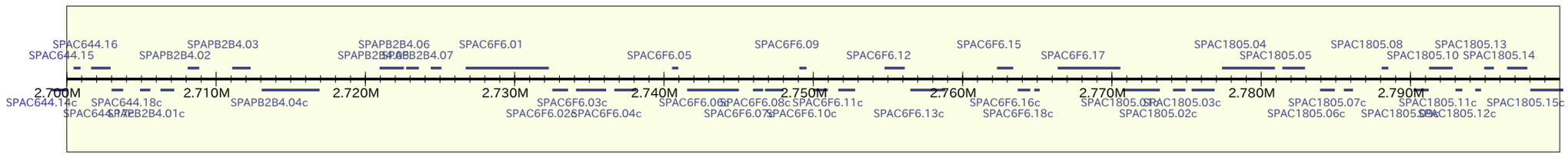

WT

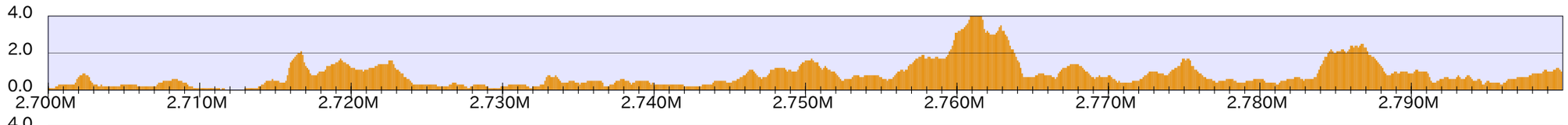

taz1

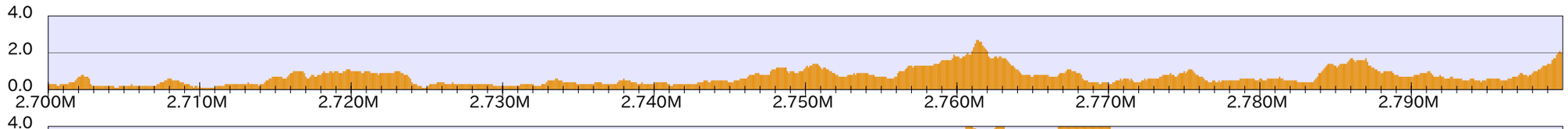

rif1

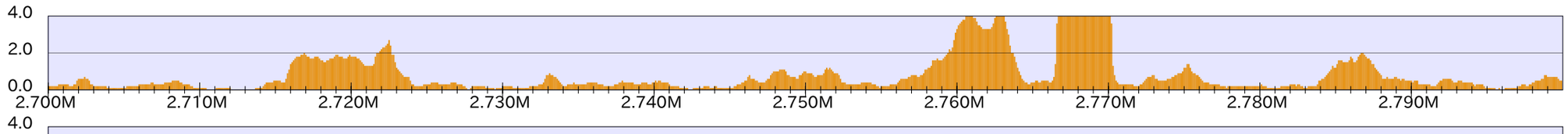

Taz1/notag

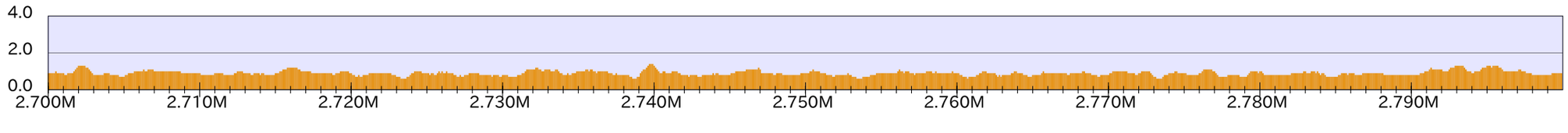

genes

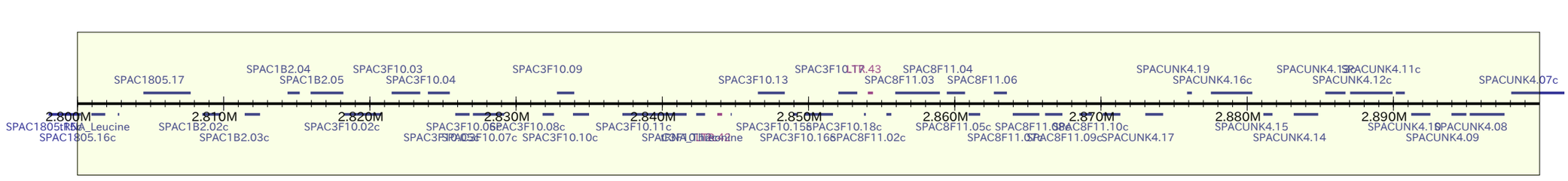

WT

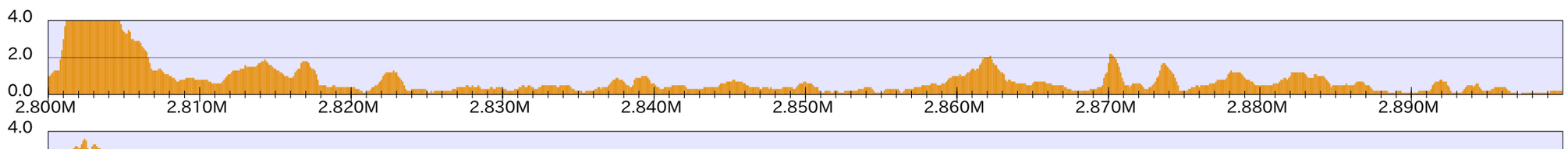

taz1

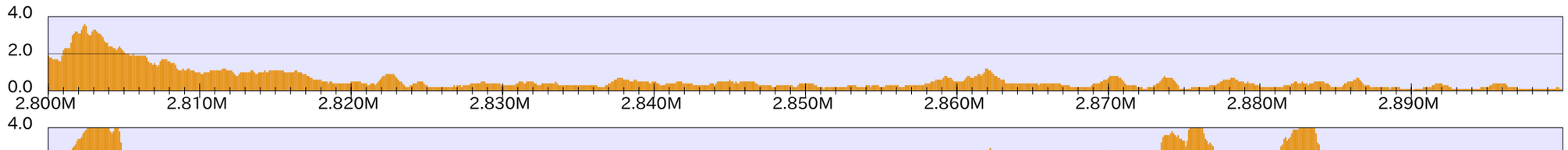

rif1

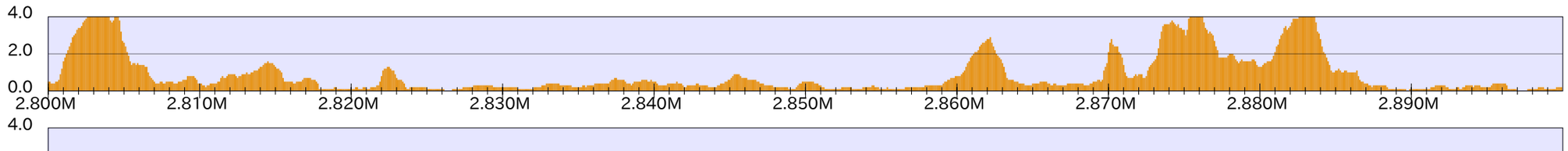

Taz1/notag

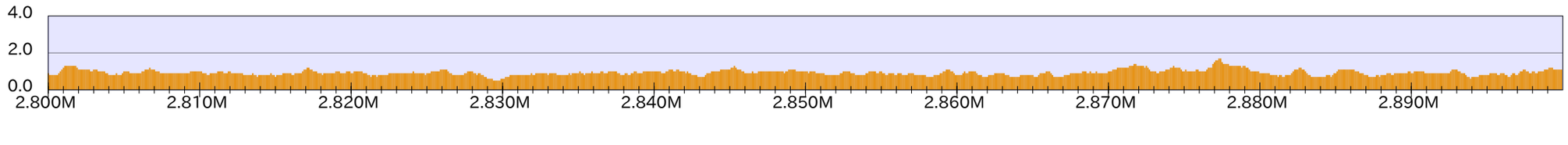

genes

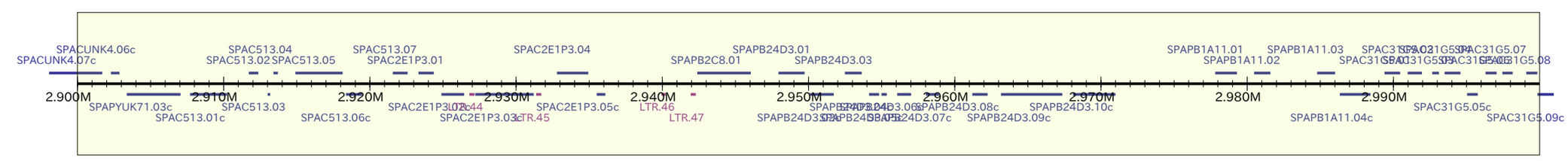

WT

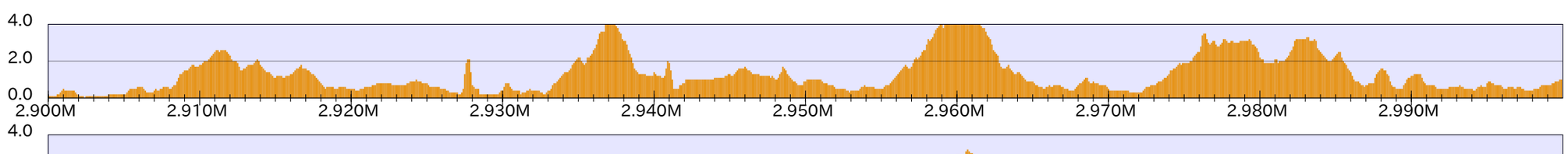

taz1

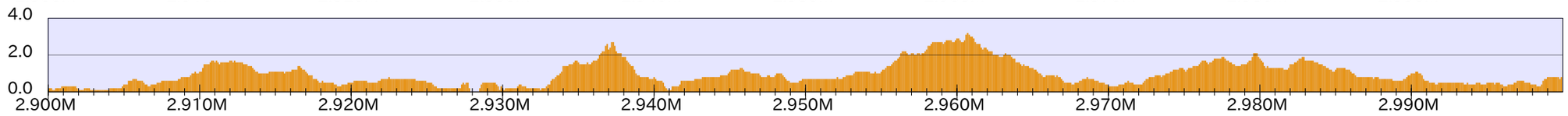

rif1

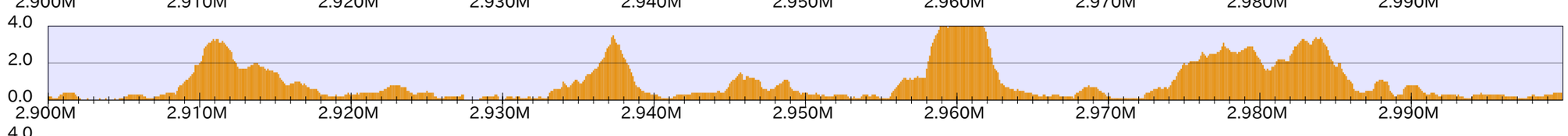

Taz1/notag

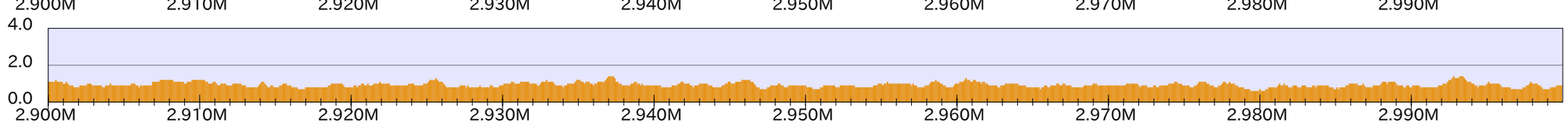

chrI_11

genes

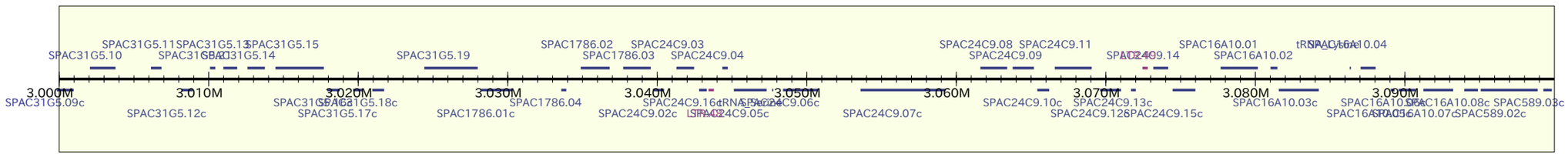

WT

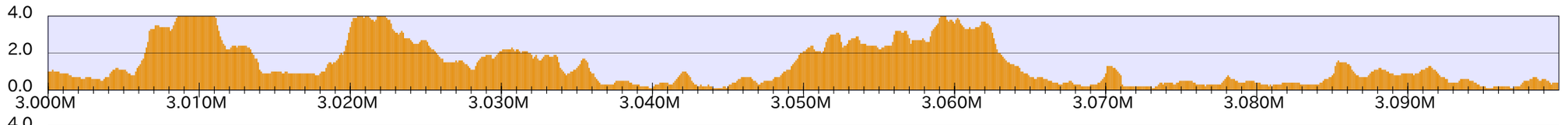

taz1

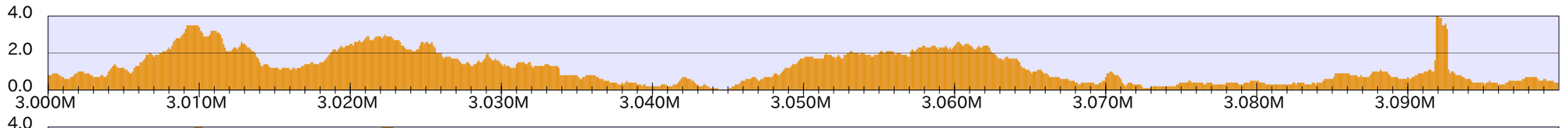

rif1

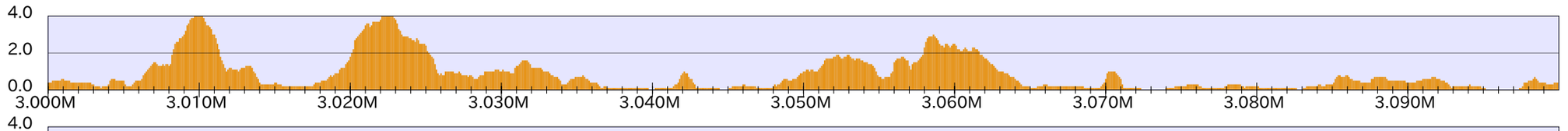

Taz1/notag

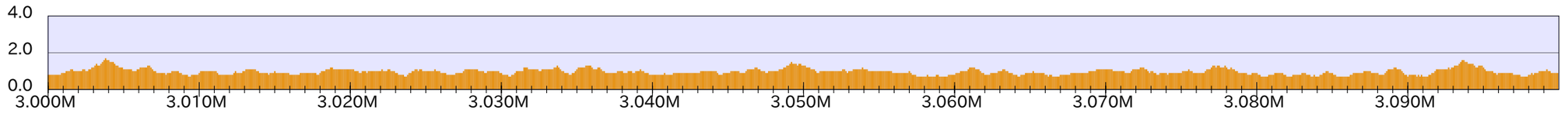

genes

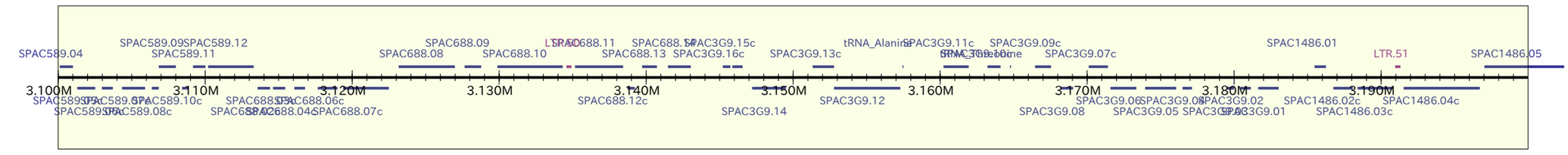

WT

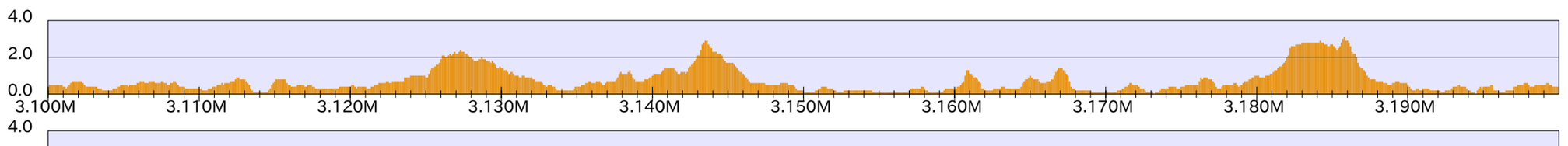

taz1

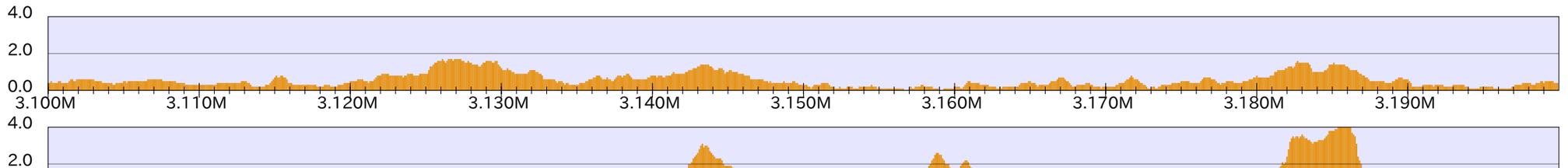

rif1

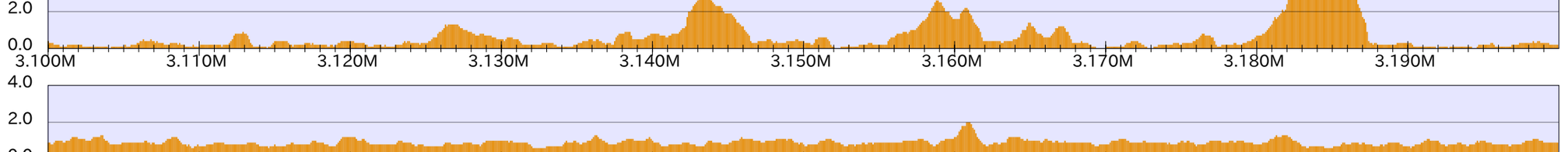

Taz1/notag

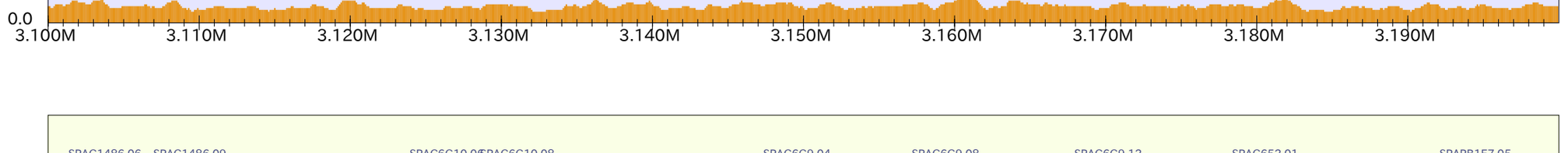

genes

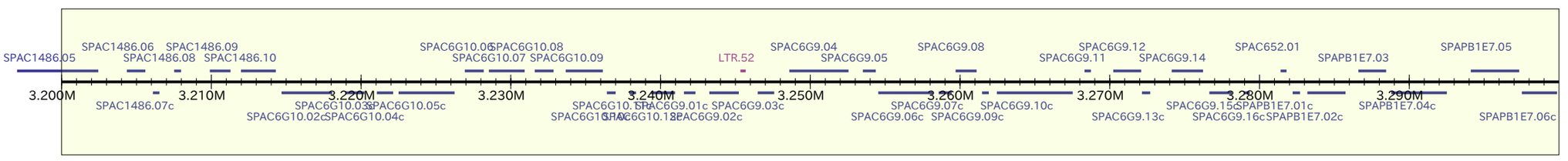

WT

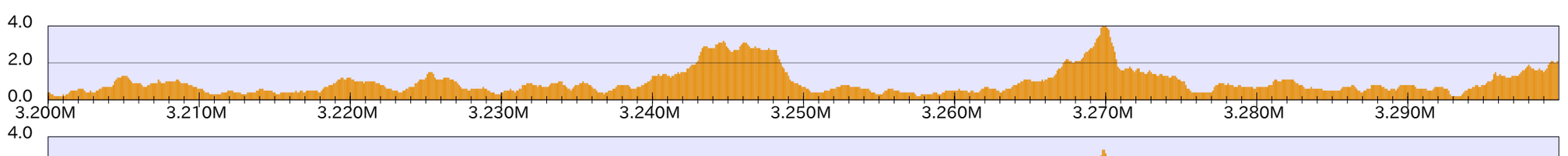

taz1

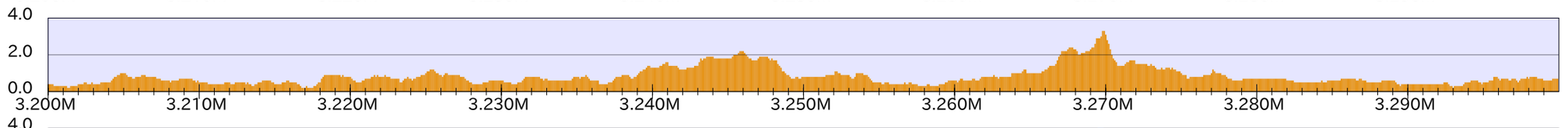

rif1

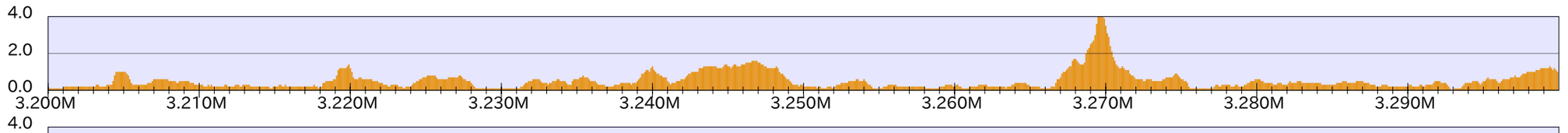

Taz1/notag

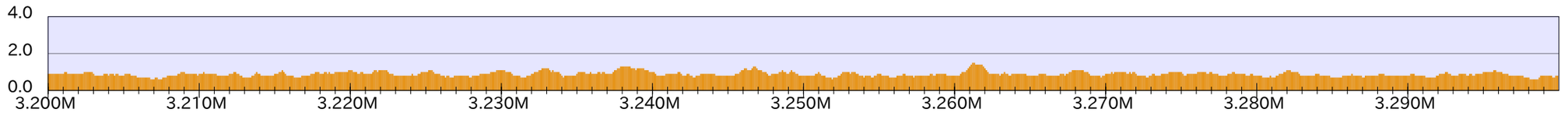

chrI_12

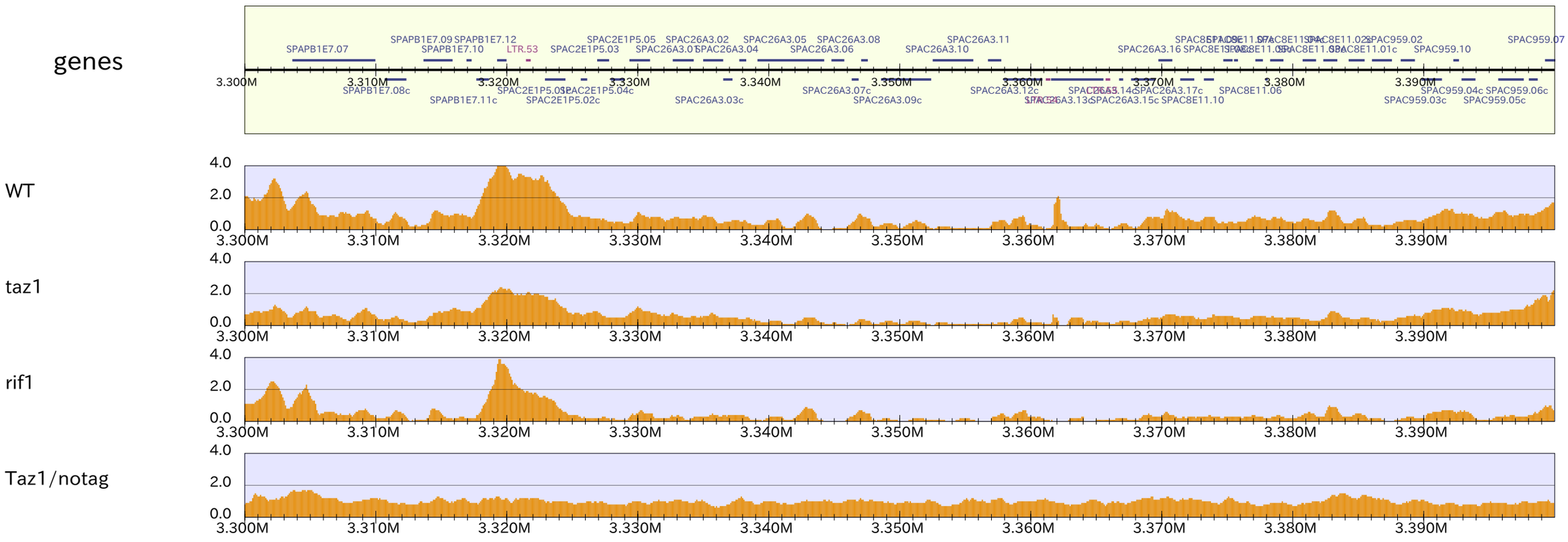
genes
WT
taz1
rif1
Taz1/notag
4.0
2.0
0.0
3.300M
3.310M
3.320M
3.330M
3.340M
3.350M
3.360M
3.370M
3.380M
3.390M

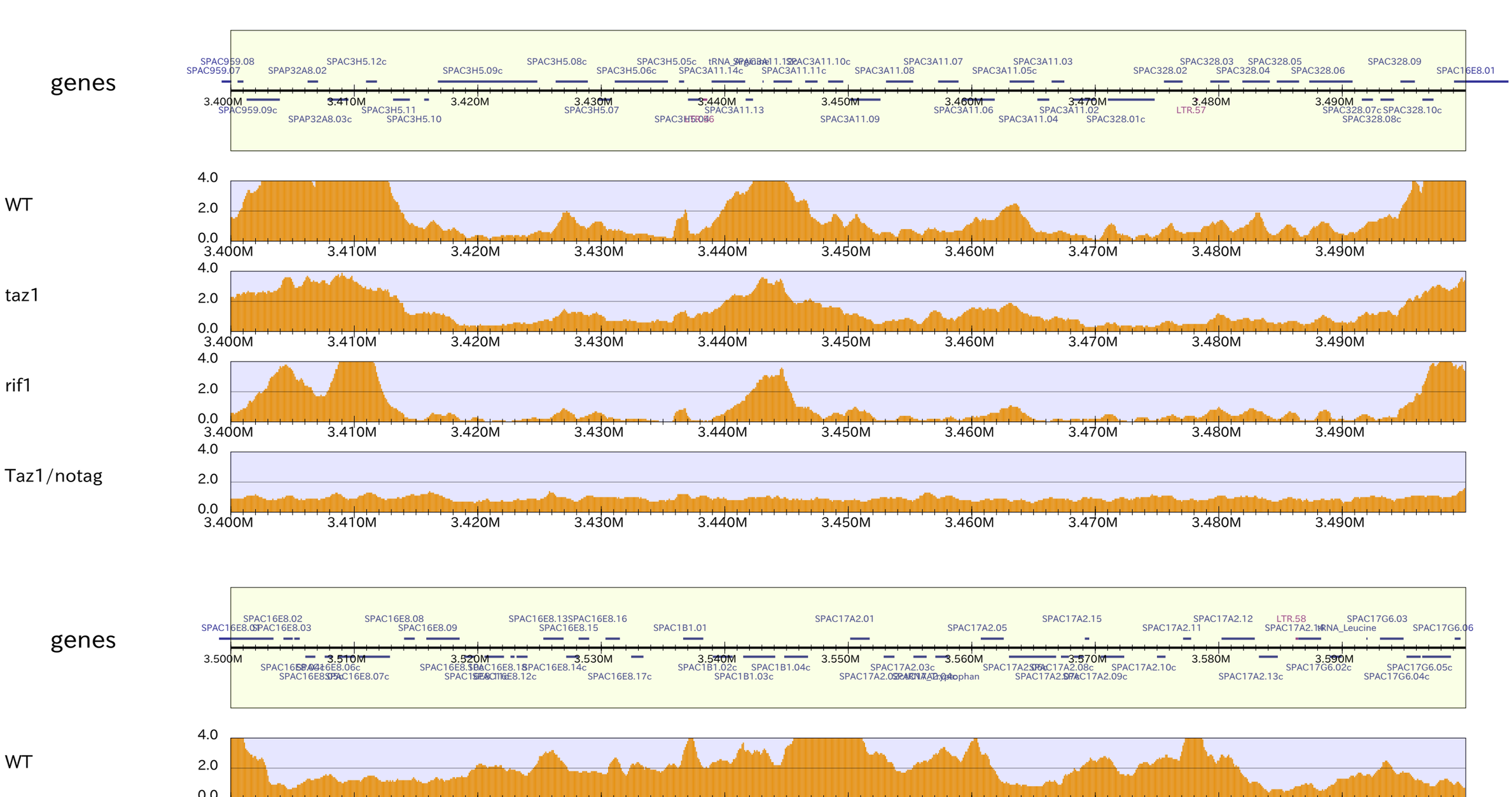
genes
WT
taz1
rif1
Taz1/notag
4.0
2.0
0.0
3.400M
3.410M
3.420M
3.430M
3.440M
3.450M
3.460M
3.470M
3.480M
3.490M

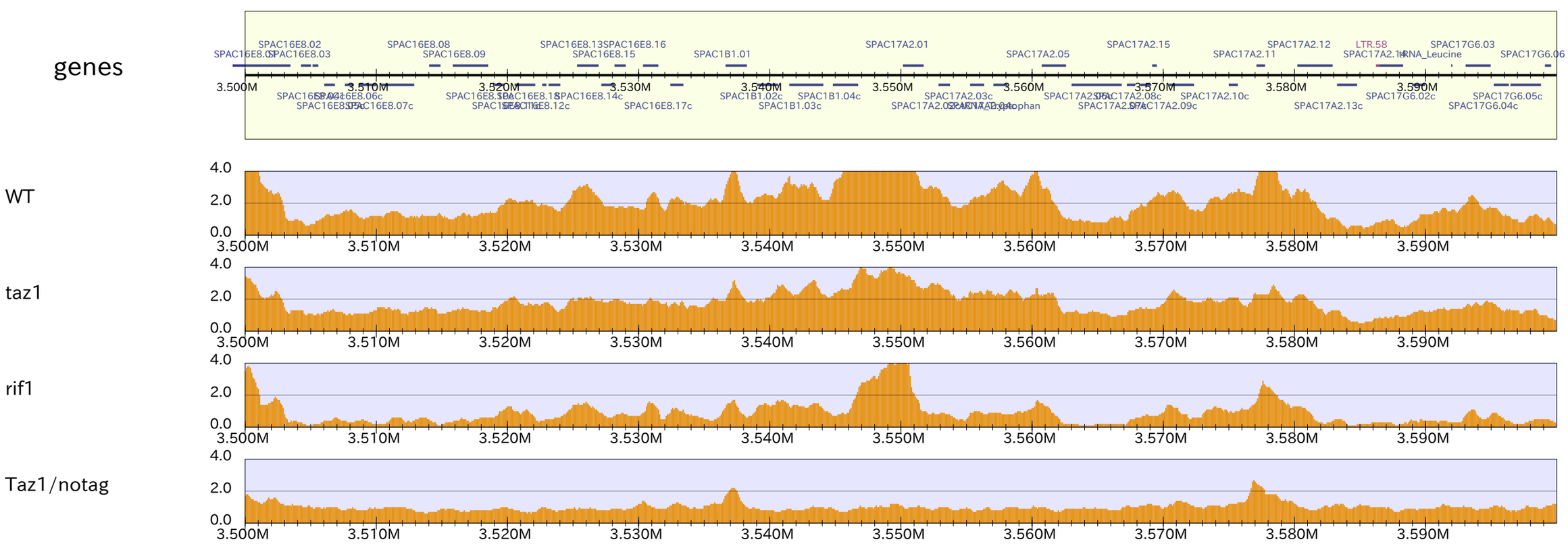
genes
WT
taz1
rif1
Taz1/notag
4.0
2.0
0.0
3.500M
3.510M
3.520M
3.530M
3.540M
3.550M
3.560M
3.570M
3.580M
3.590M

chrI_13

genes

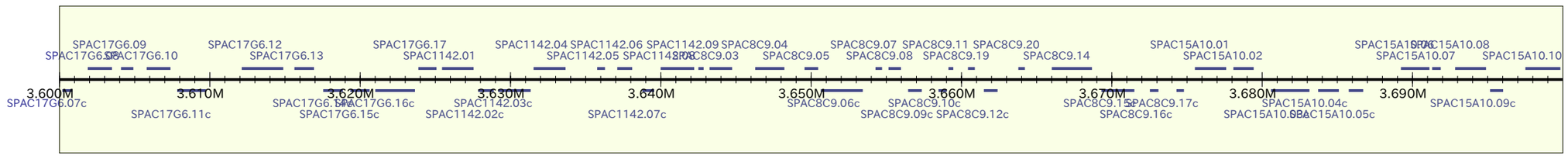

WT

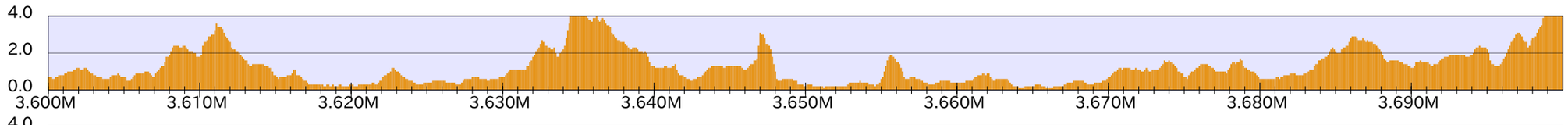

taz1

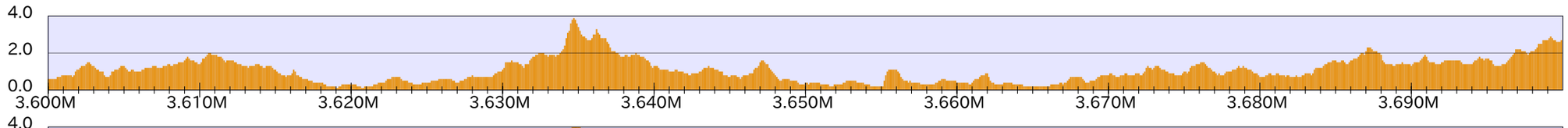

rif1

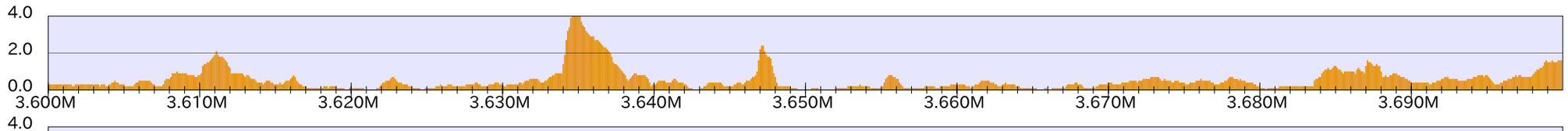

Taz1/notag

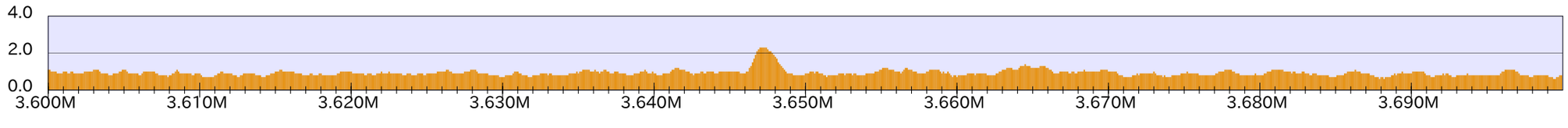

genes

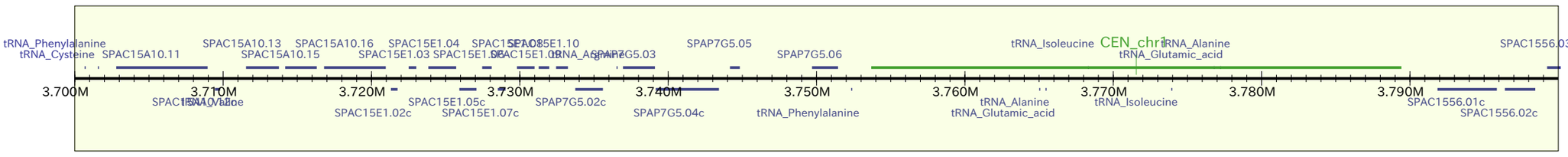

WT

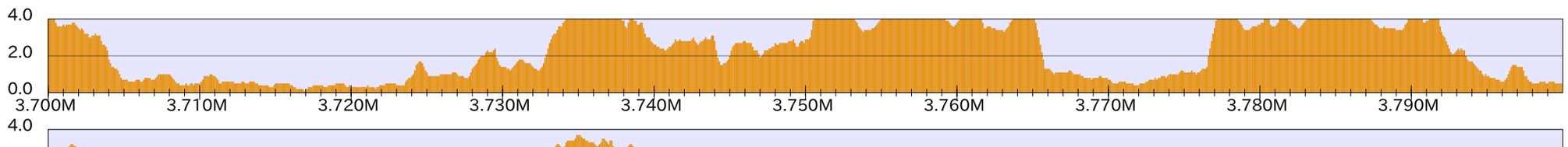

taz1

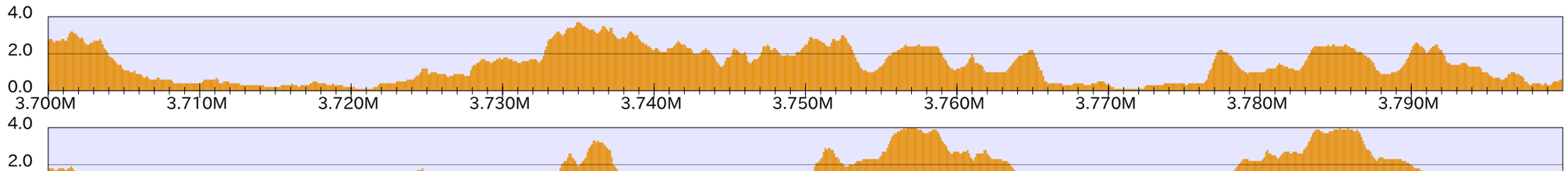

rif1

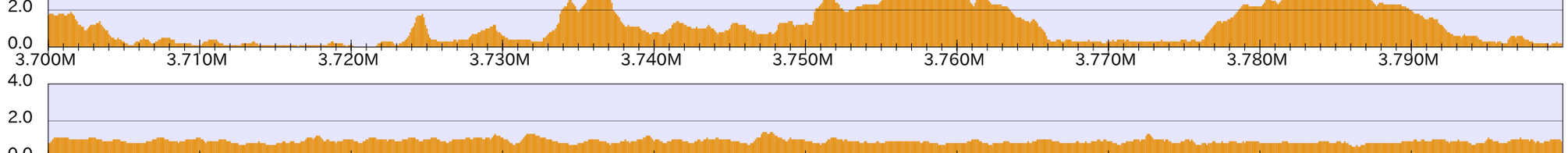

Taz1/notag

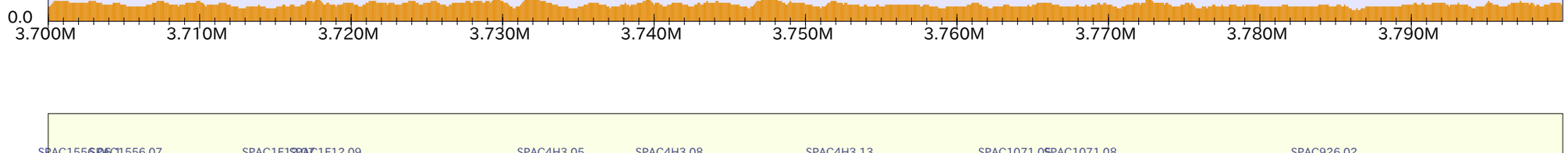

genes

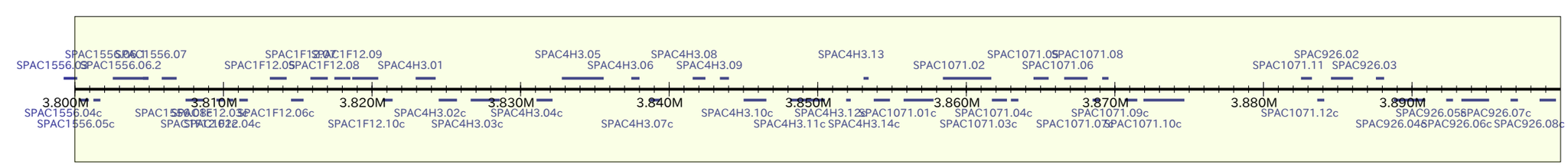

WT

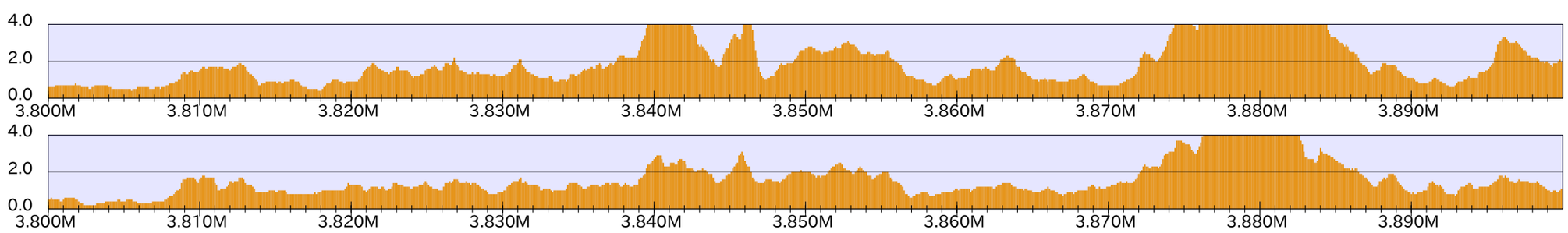

taz1

rif1

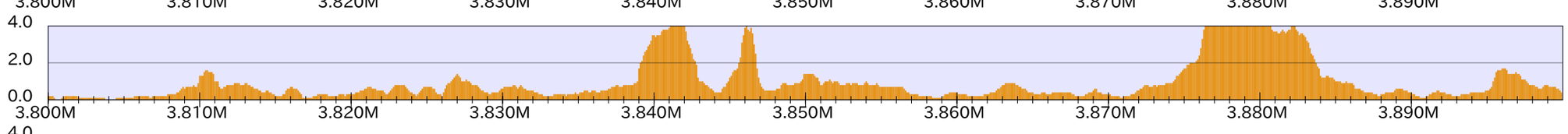

Taz1/notag

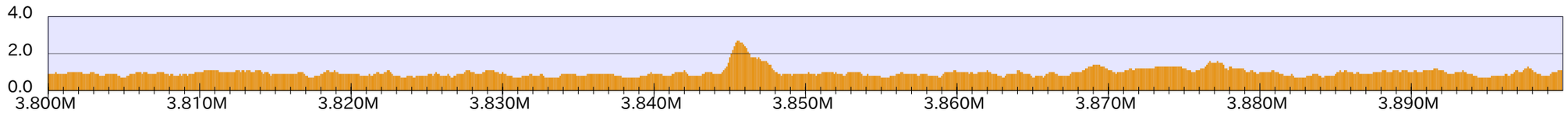

chrI_14

genes

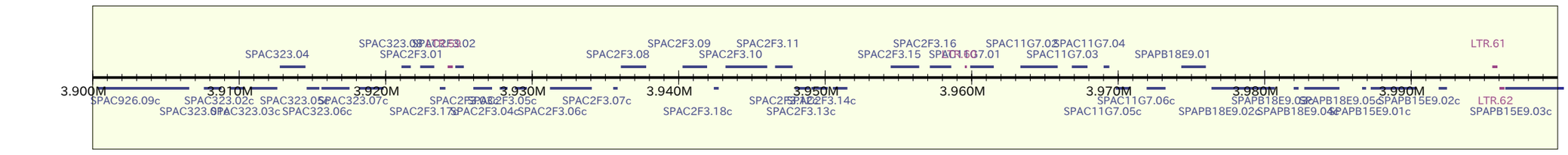

WT

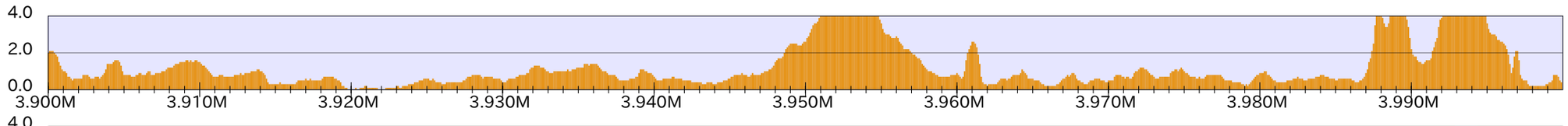

taz1

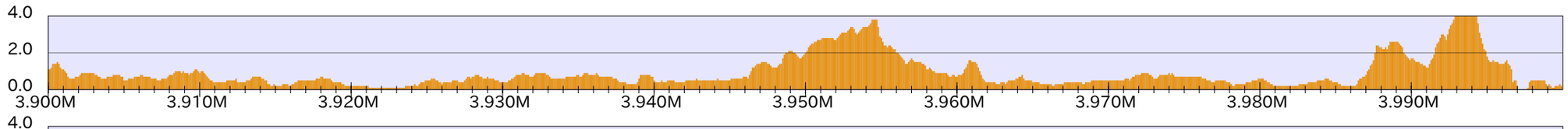

rif1

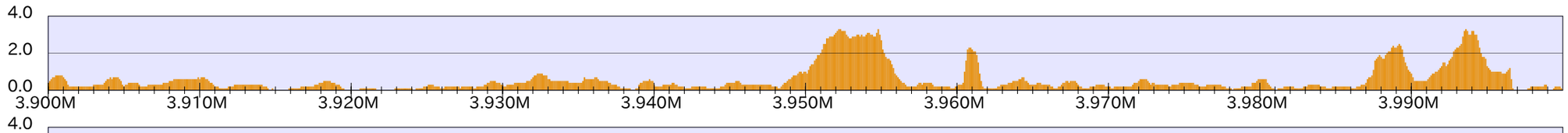

Taz1/notag

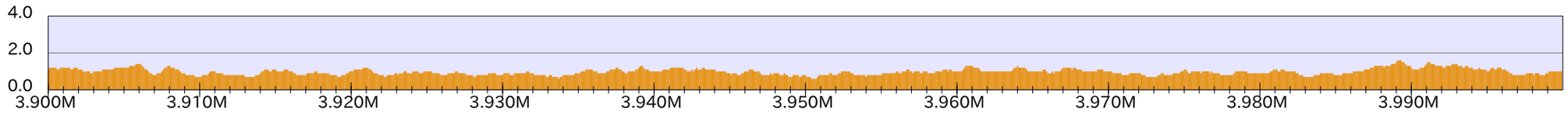

genes

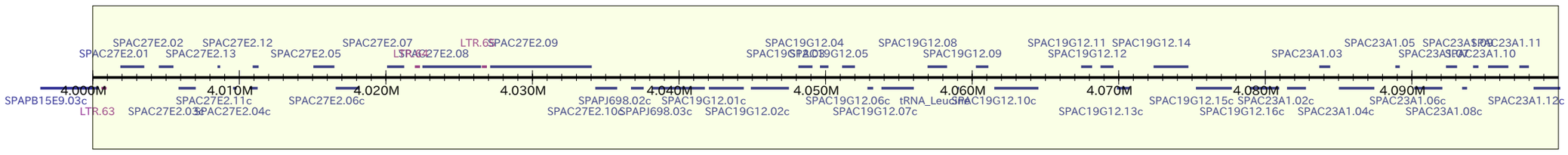

WT

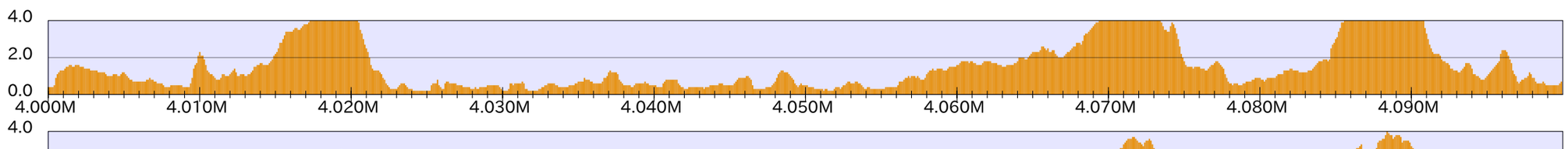

taz1

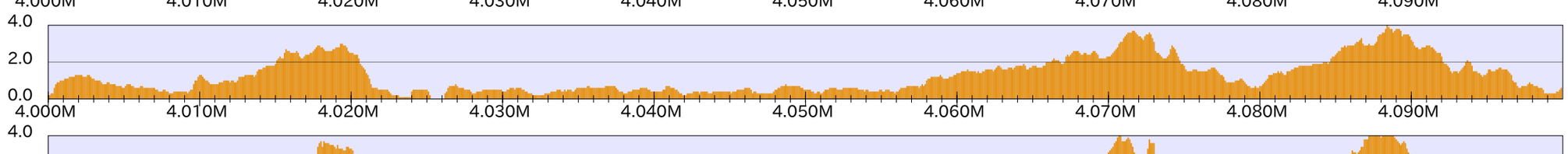

rif1

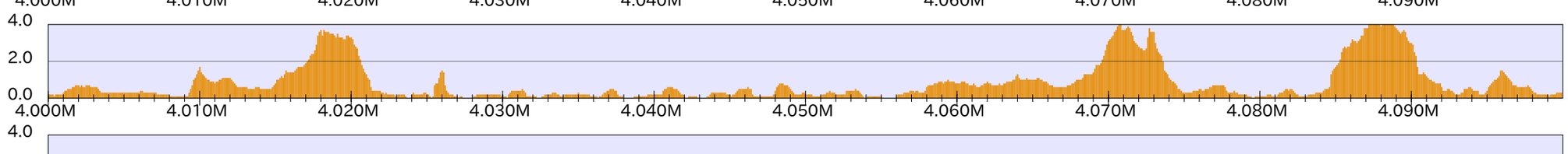

Taz1/notag

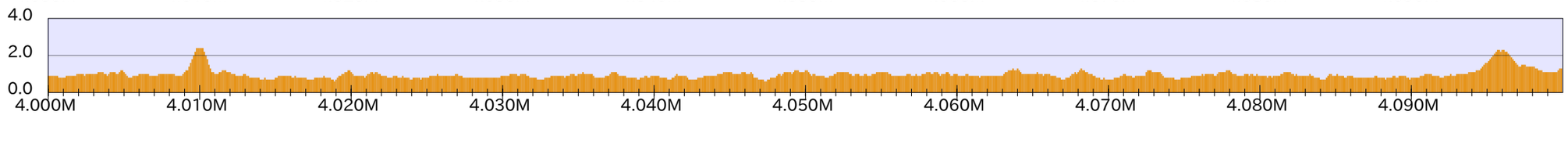

genes

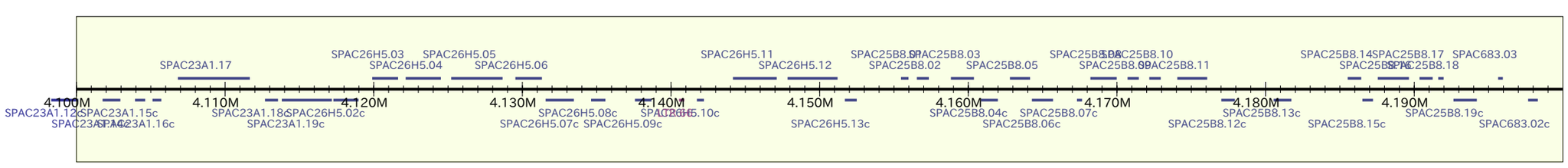

WT

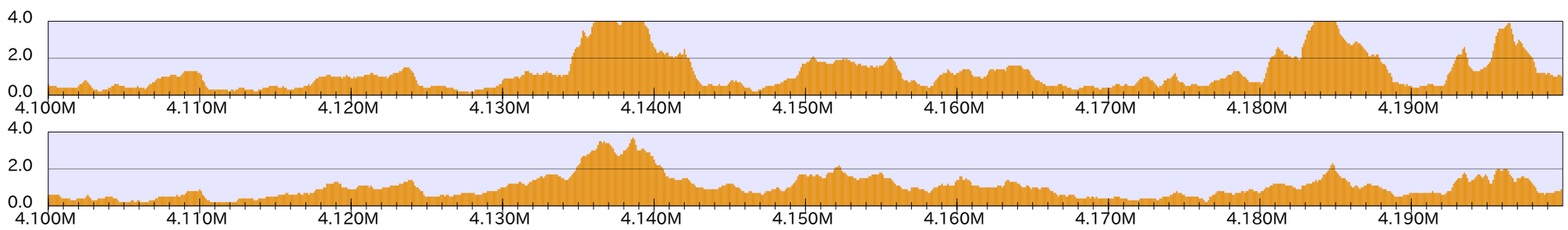

taz1

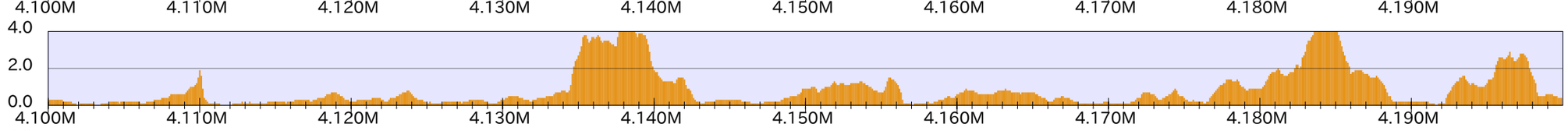

rif1

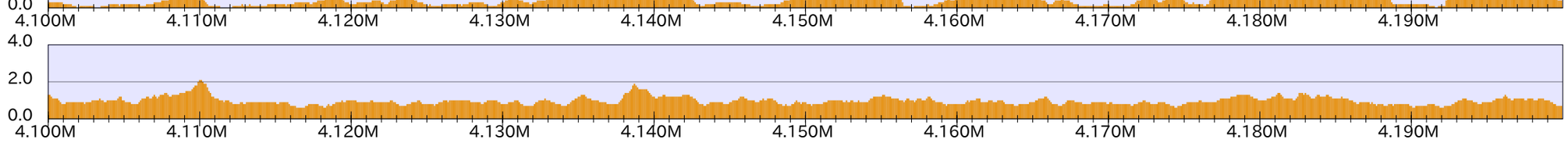

Taz1/notag

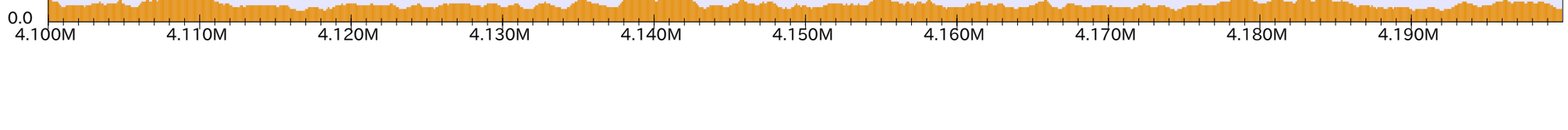

chrI_15

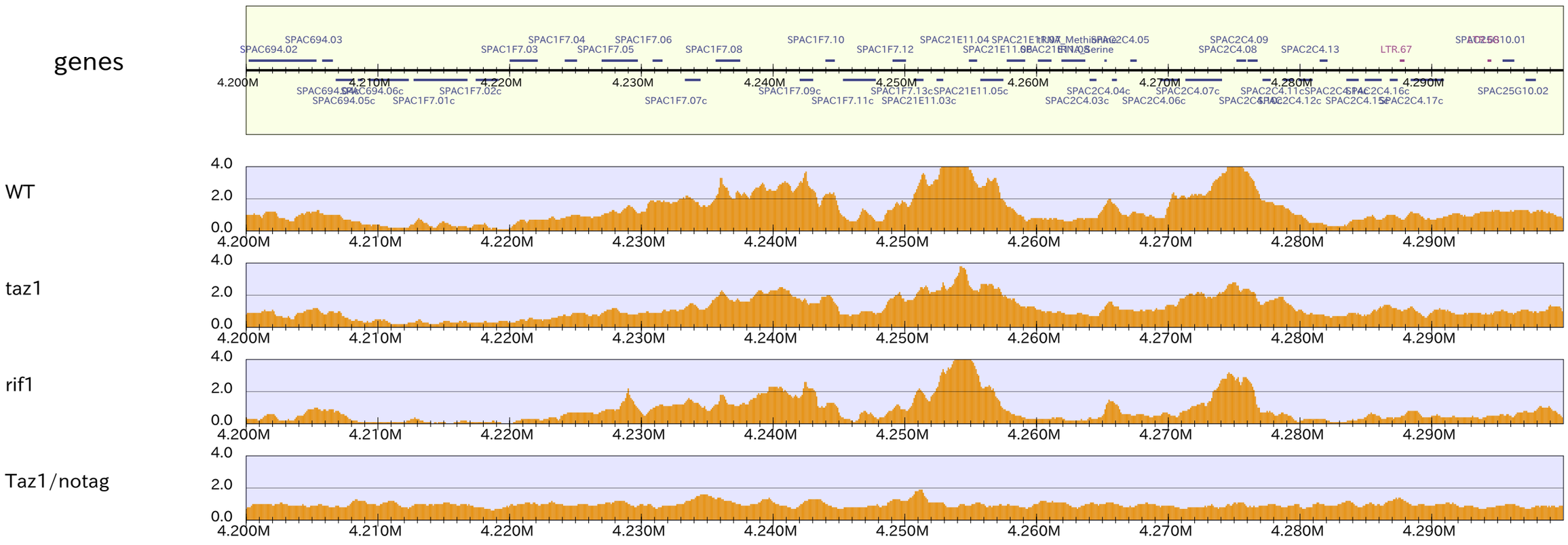
genes
WT
taz1
rif1
Taz1/notag
4.200M
4.210M
4.220M
4.230M
4.240M
4.250M
4.260M
4.270M
4.280M
4.290M
4.0
2.0
0.0

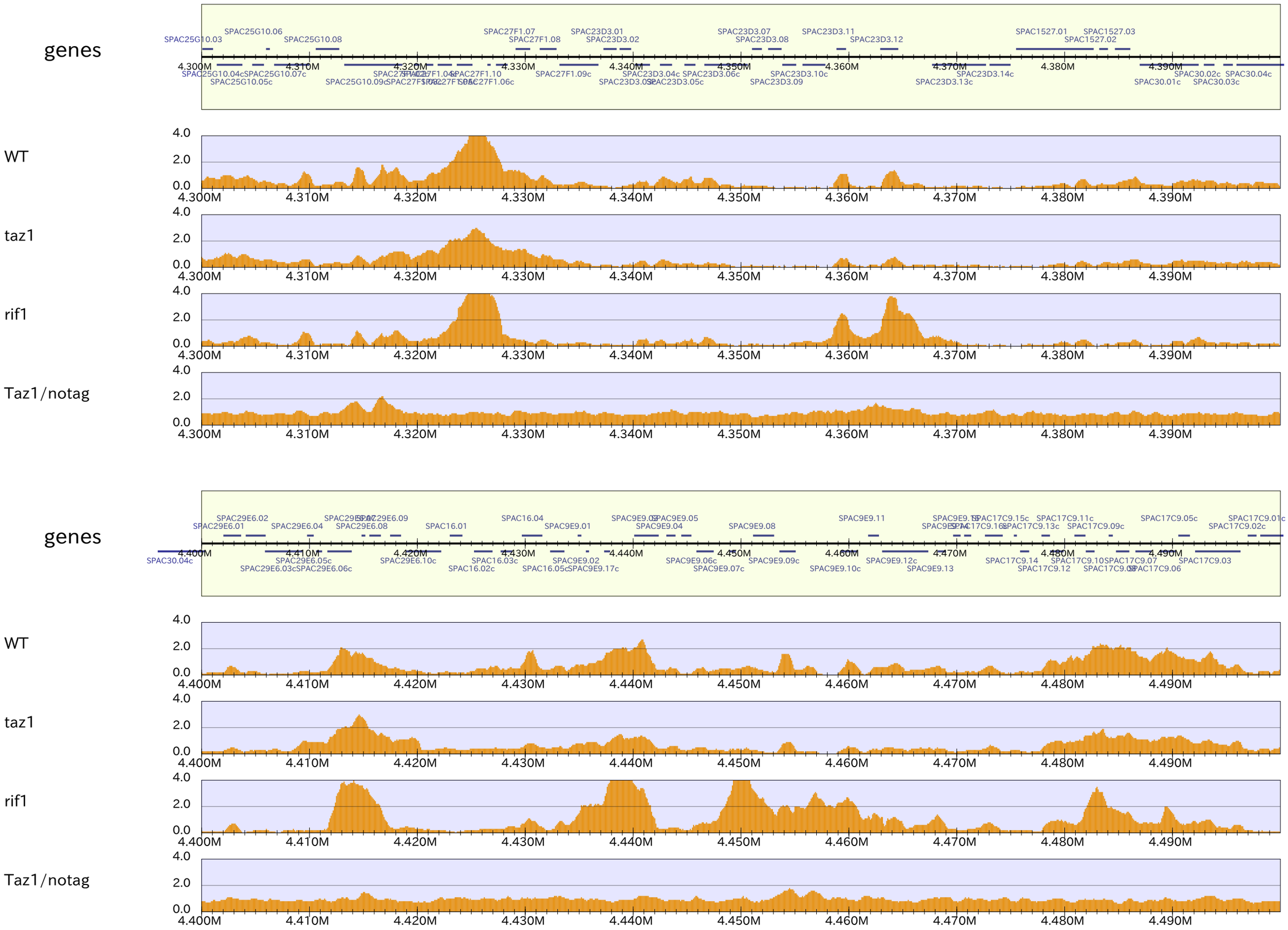
genes
WT
taz1
rif1
Taz1/notag
4.300M
4.310M
4.320M
4.330M
4.340M
4.350M
4.360M
4.370M
4.380M
4.390M
4.0
2.0
0.0

genes
WT
taz1
rif1
Taz1/notag
4.400M
4.410M
4.420M
4.430M
4.440M
4.450M
4.460M
4.470M
4.480M
4.490M
4.0
2.0
0.0

chrI_16

genes

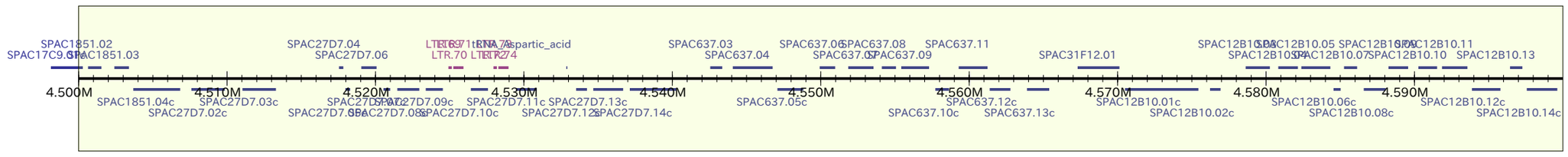

WT

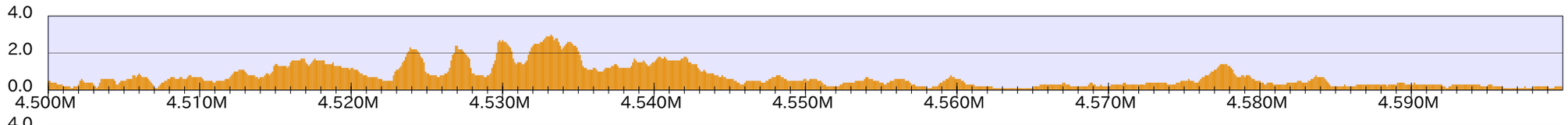

taz1

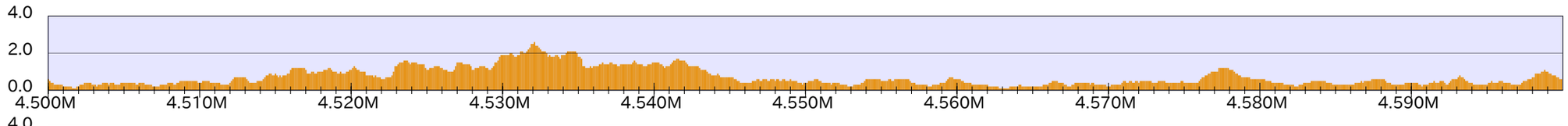

rif1

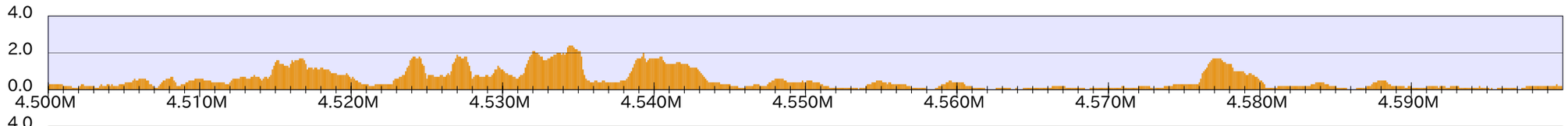

Taz1/notag

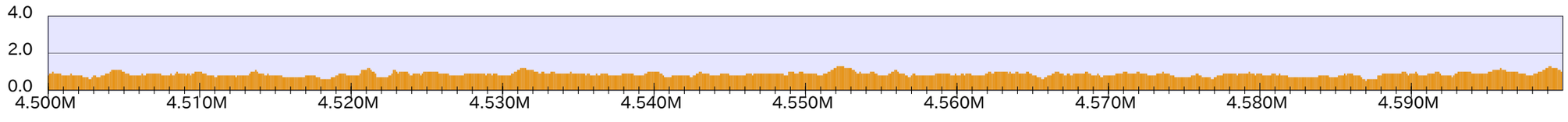

genes

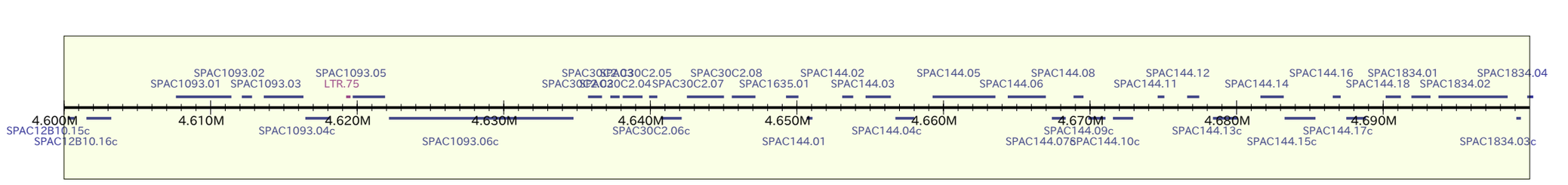

WT

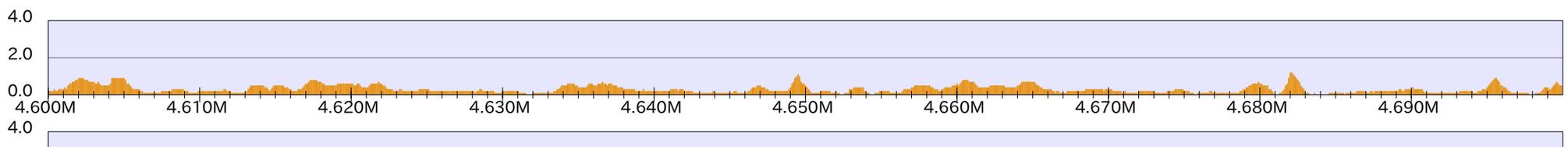

taz1

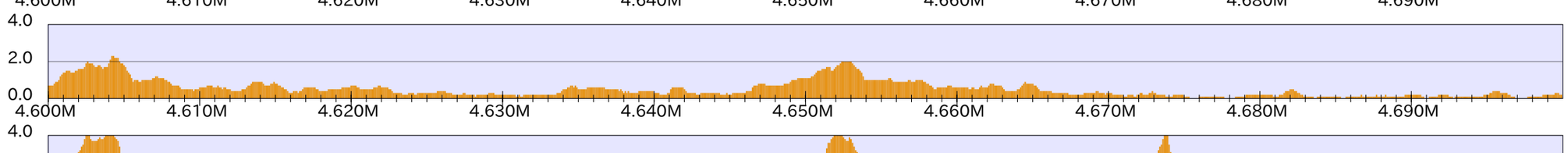

rif1

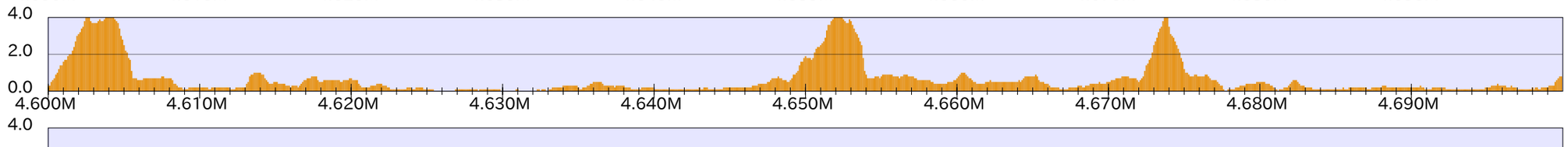

Taz1/notag

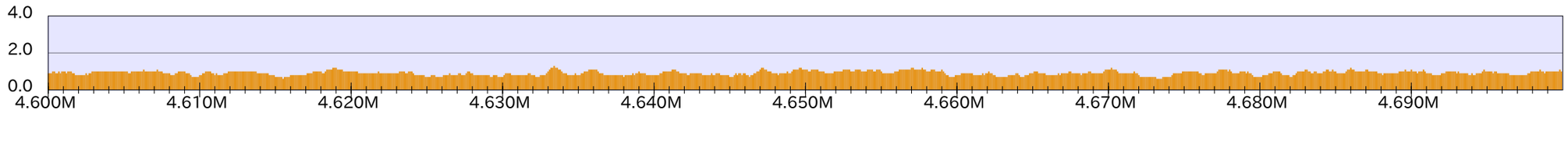

genes

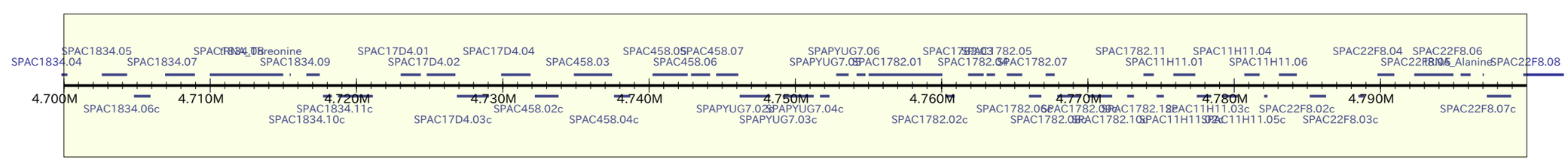

WT

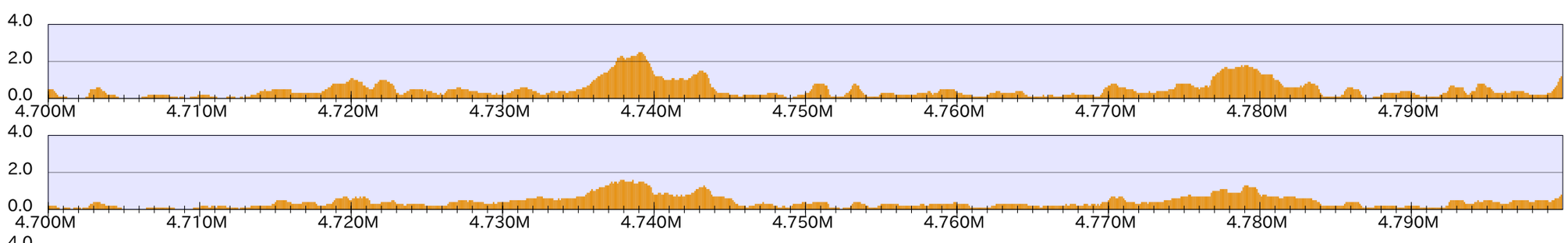

taz1

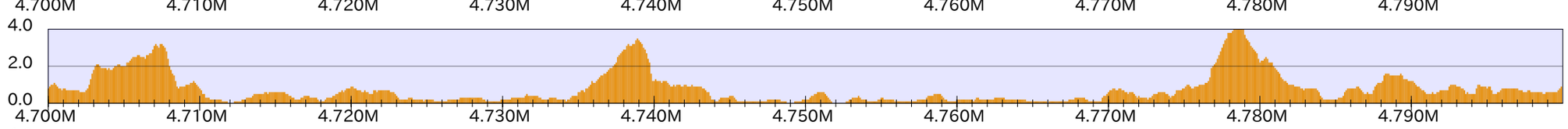

rif1

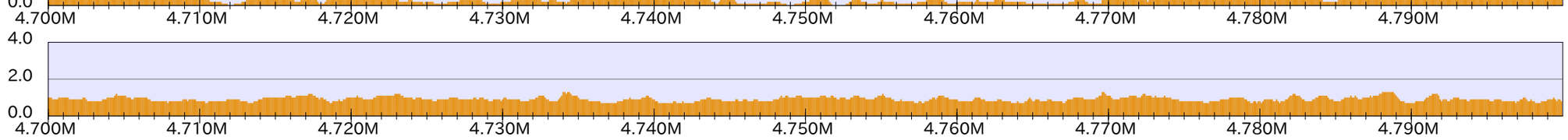

Taz1/notag

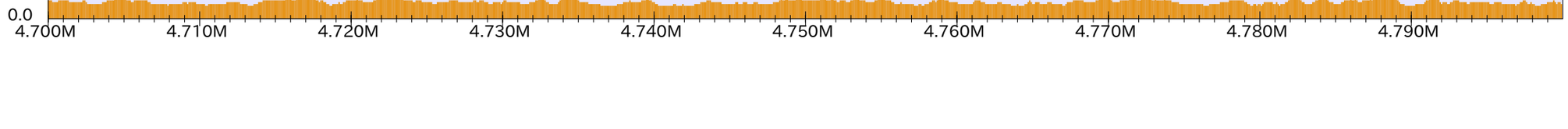

chrI_17

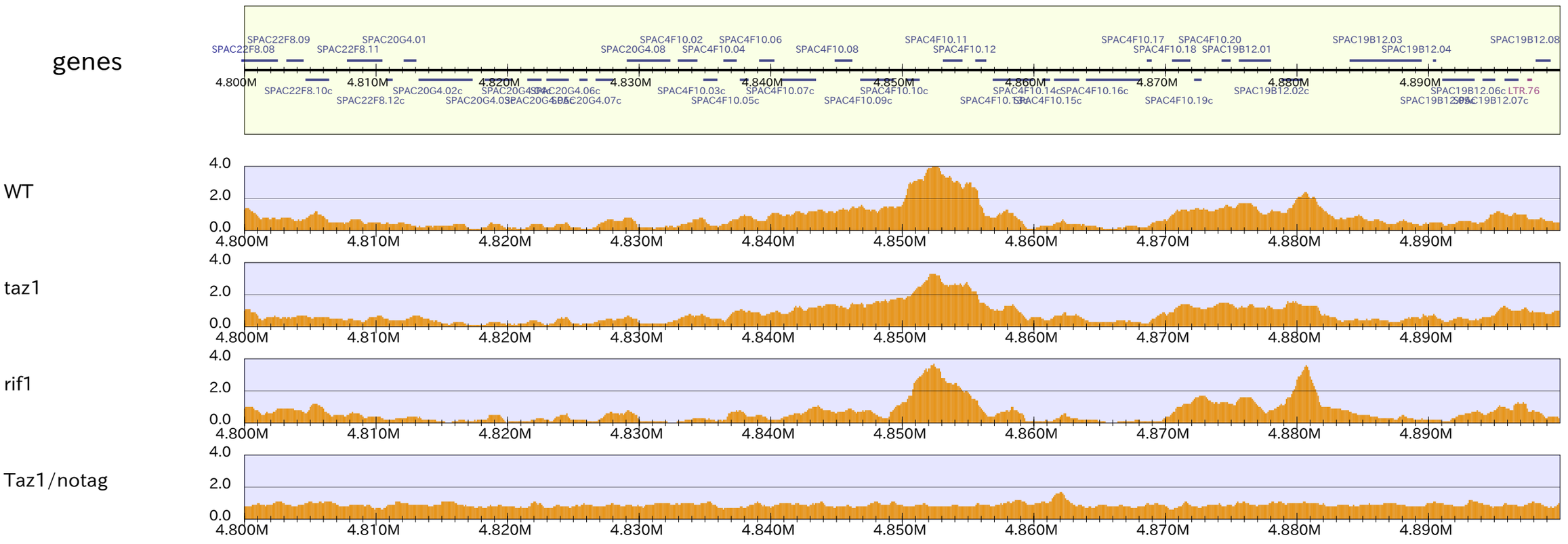
genes
WT
taz1
rif1
Taz1/notag
4.0
2.0
0.0
4.800M
4.810M
4.820M
4.830M
4.840M
4.850M
4.860M
4.870M
4.880M
4.890M

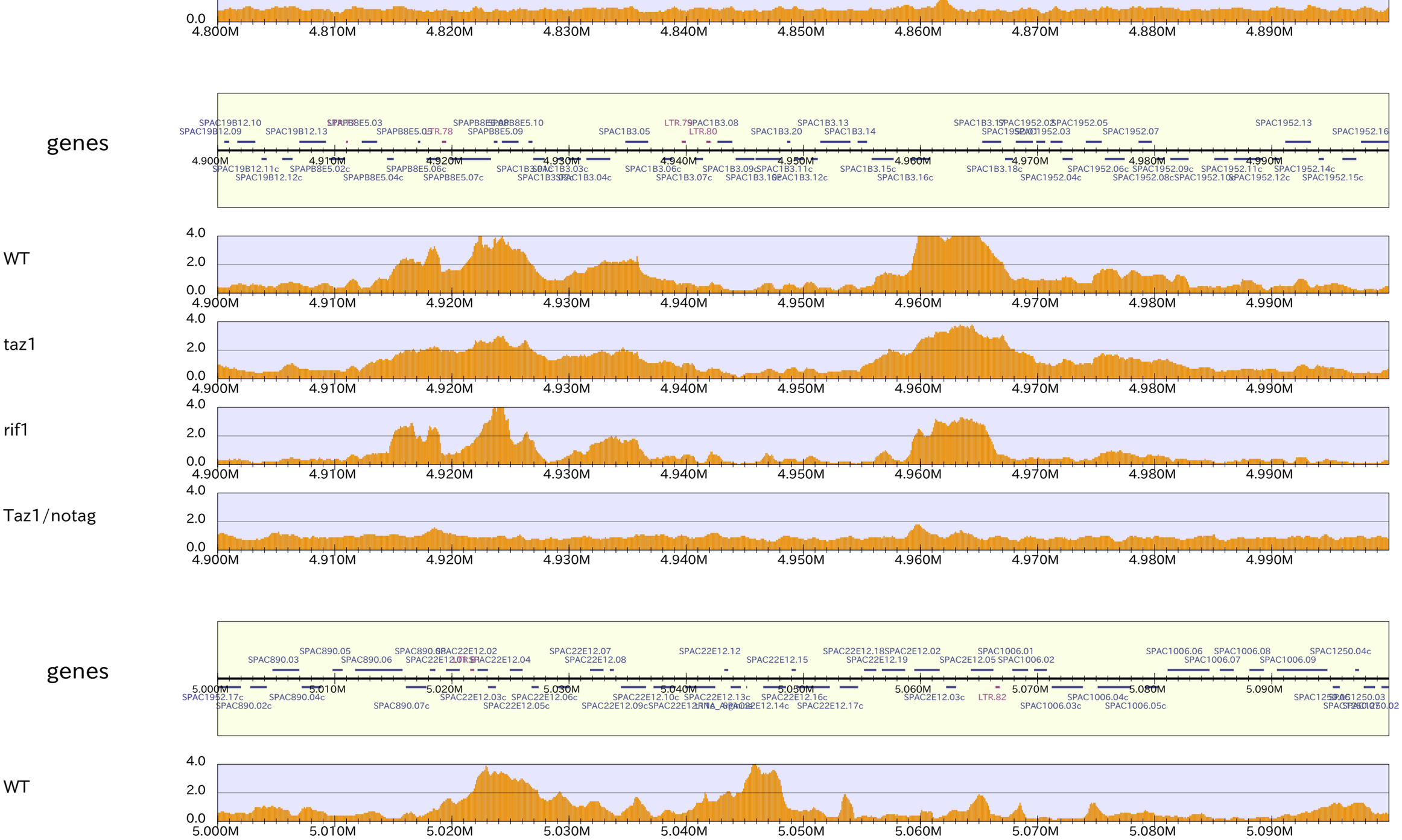
genes
WT
taz1
rif1
Taz1/notag
4.0
2.0
0.0
4.900M
4.910M
4.920M
4.930M
4.940M
4.950M
4.960M
4.970M
4.980M
4.990M

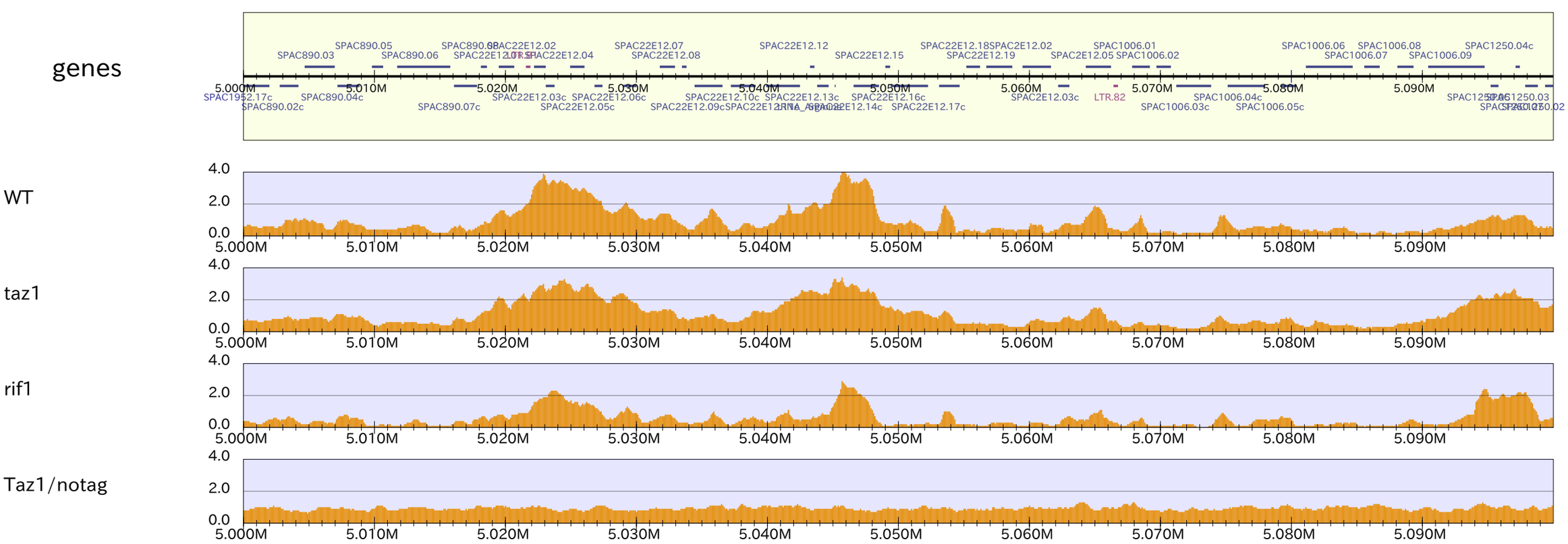
genes
WT
taz1
rif1
Taz1/notag
4.0
2.0
0.0
5.000M
5.010M
5.020M
5.030M
5.040M
5.050M
5.060M
5.070M
5.080M
5.090M

chrI_18

genes

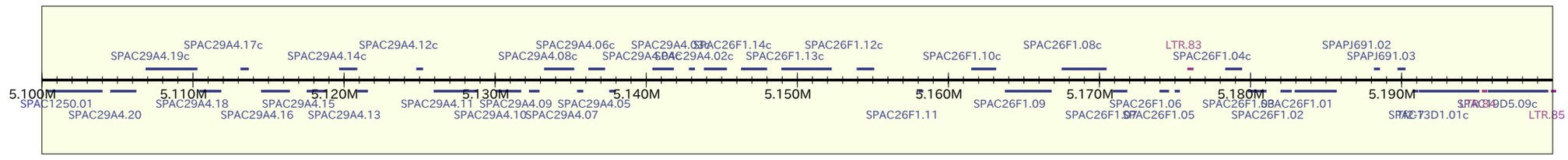

WT

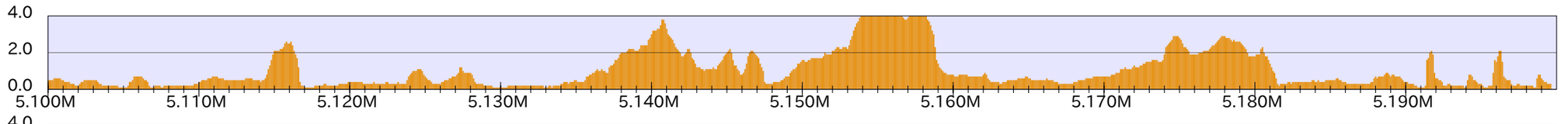

taz1

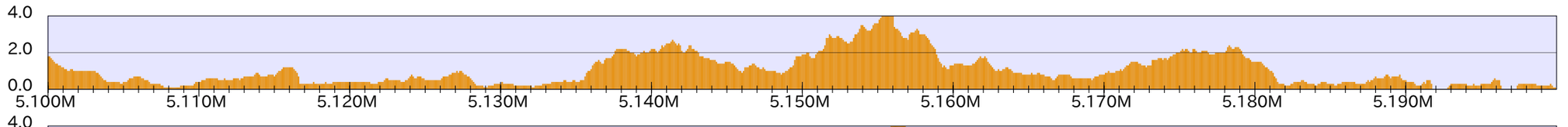

rif1

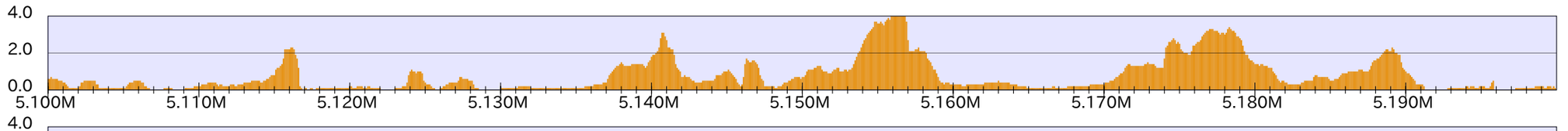

Taz1/notag

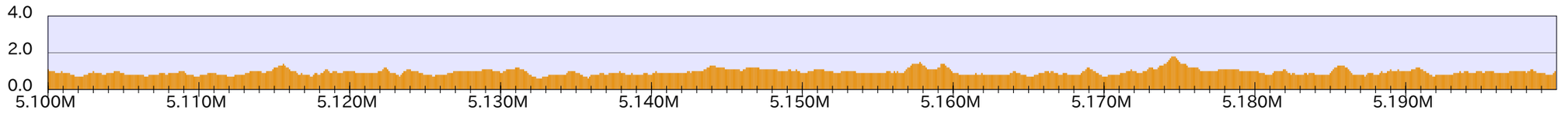

genes

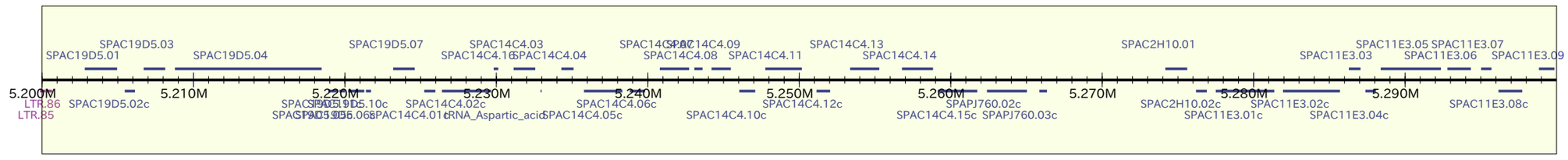

WT

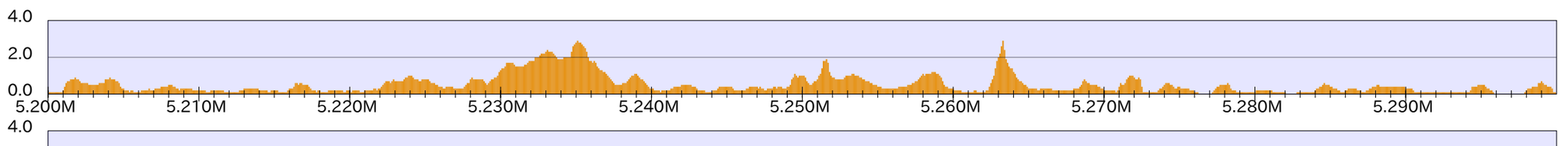

taz1

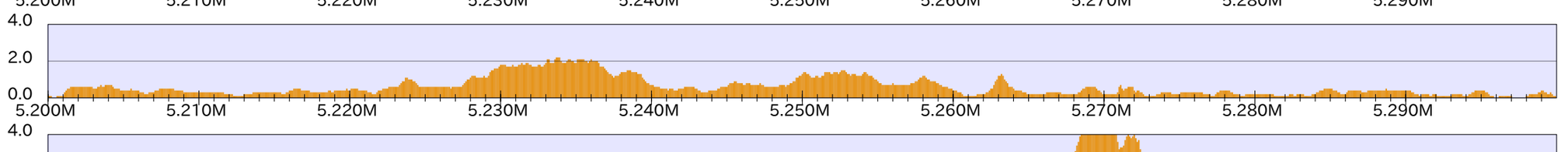

rif1

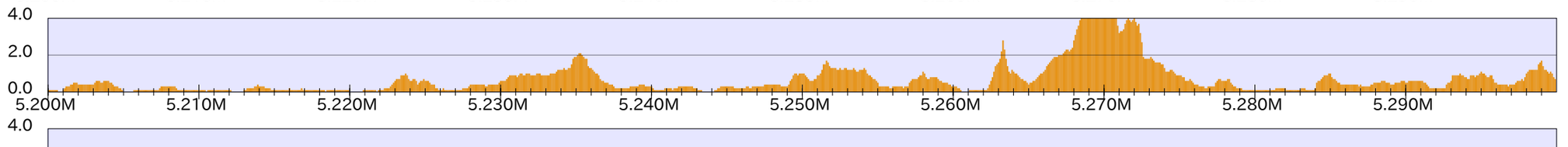

Taz1/notag

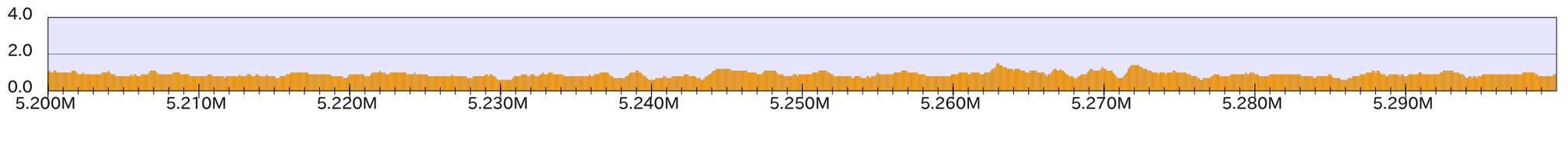

genes

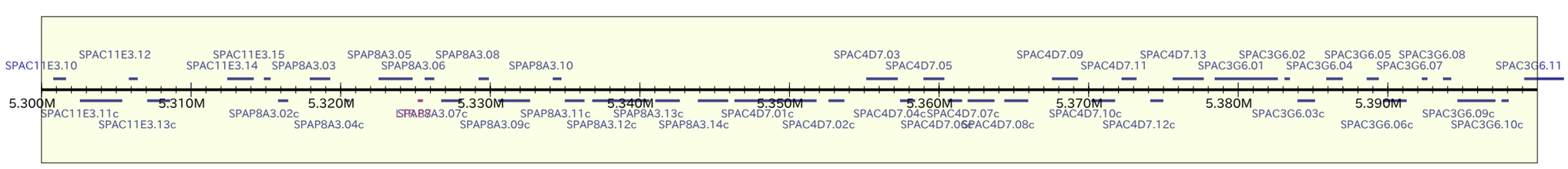

WT

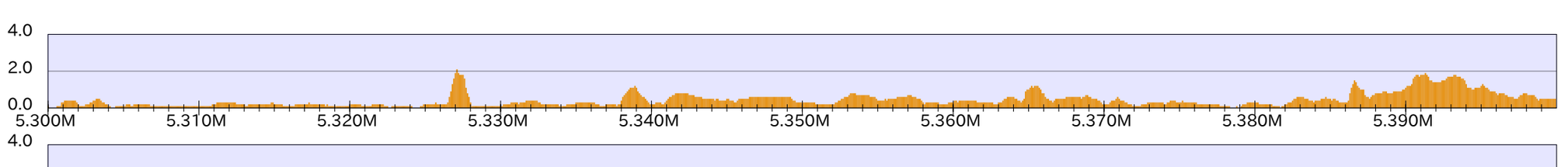

taz1

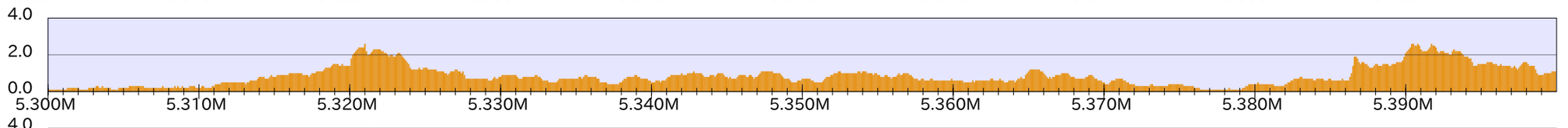

rif1

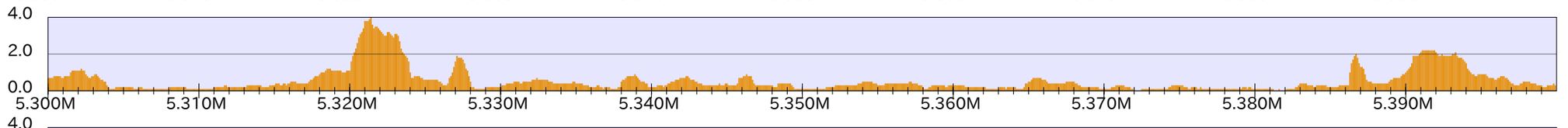

Taz1/notag

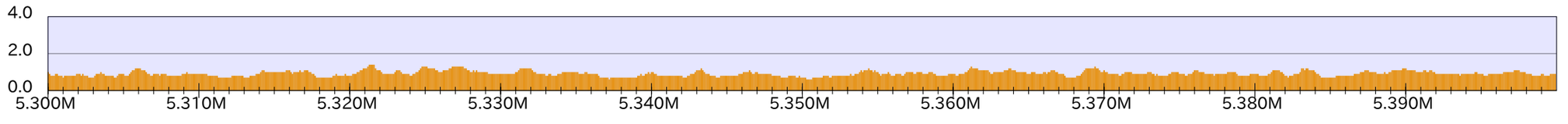

chrI_19

genes

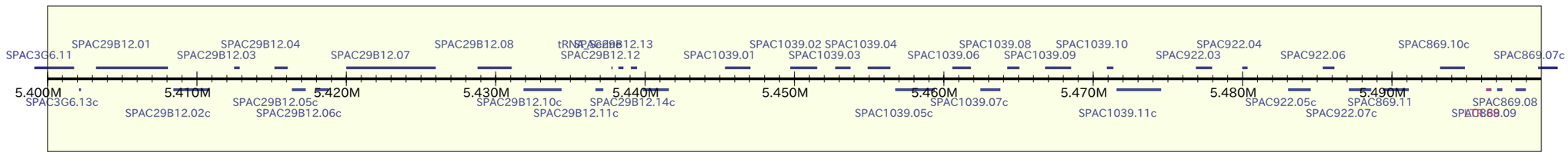

WT

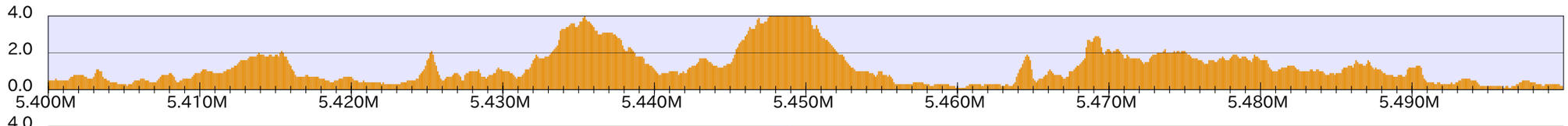

taz1

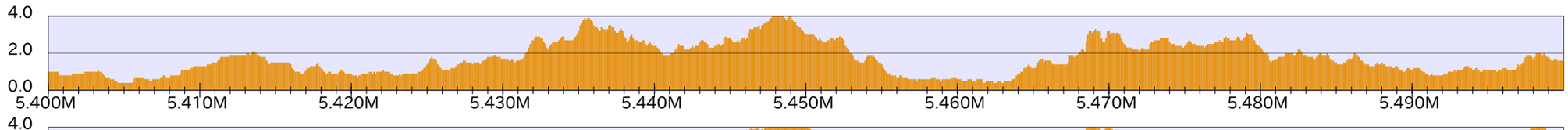

rif1

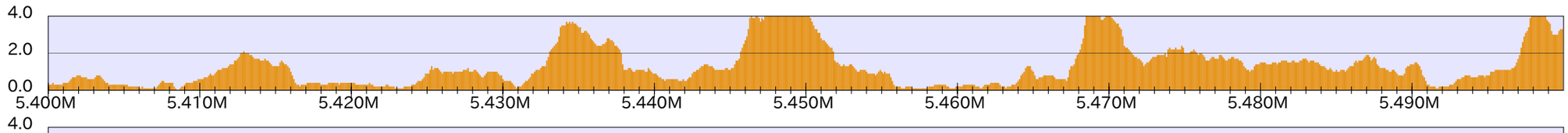

Taz1/notag

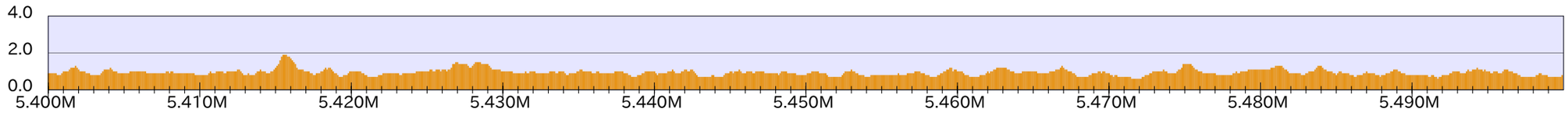

genes

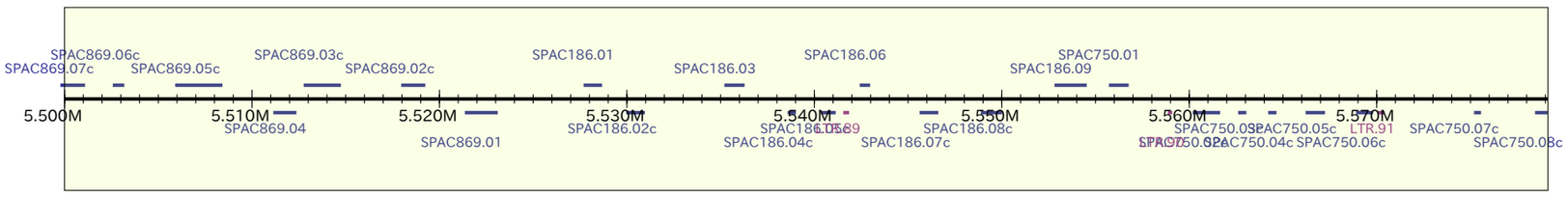

WT

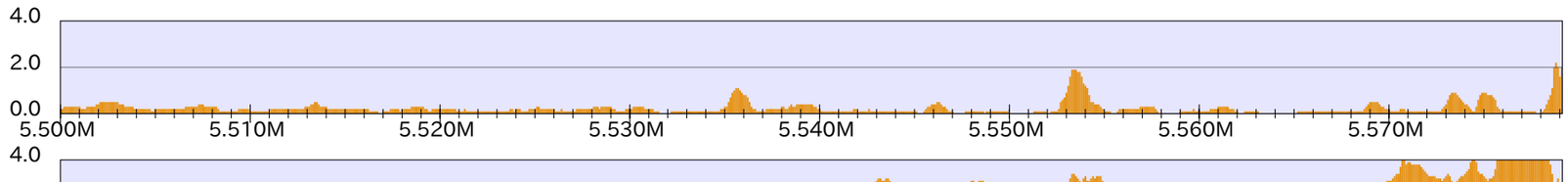

taz1

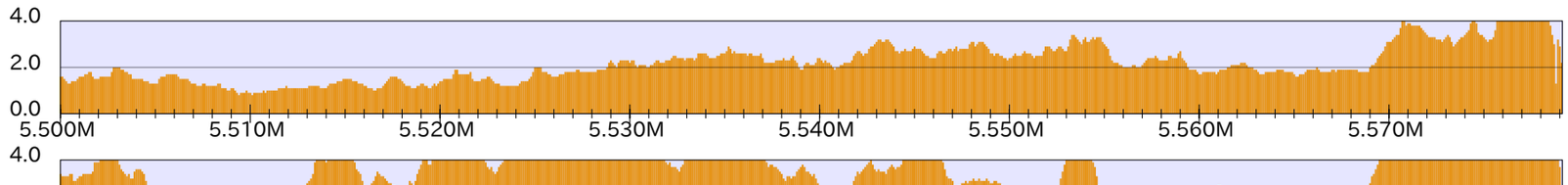

rif1

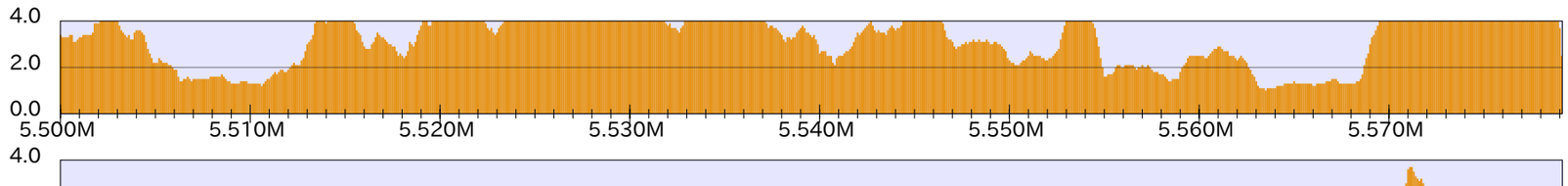

Taz1/notag

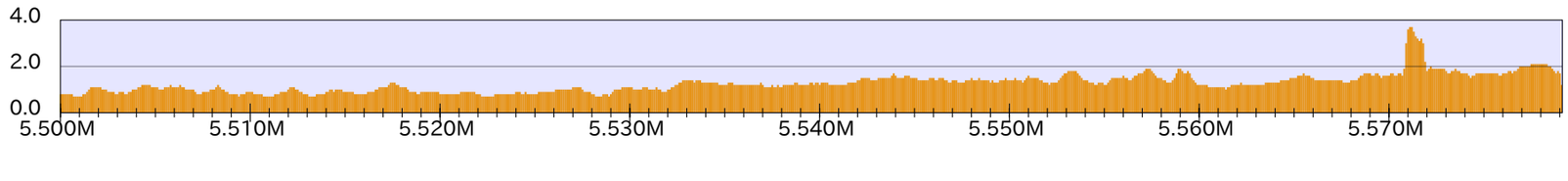

chrII_1

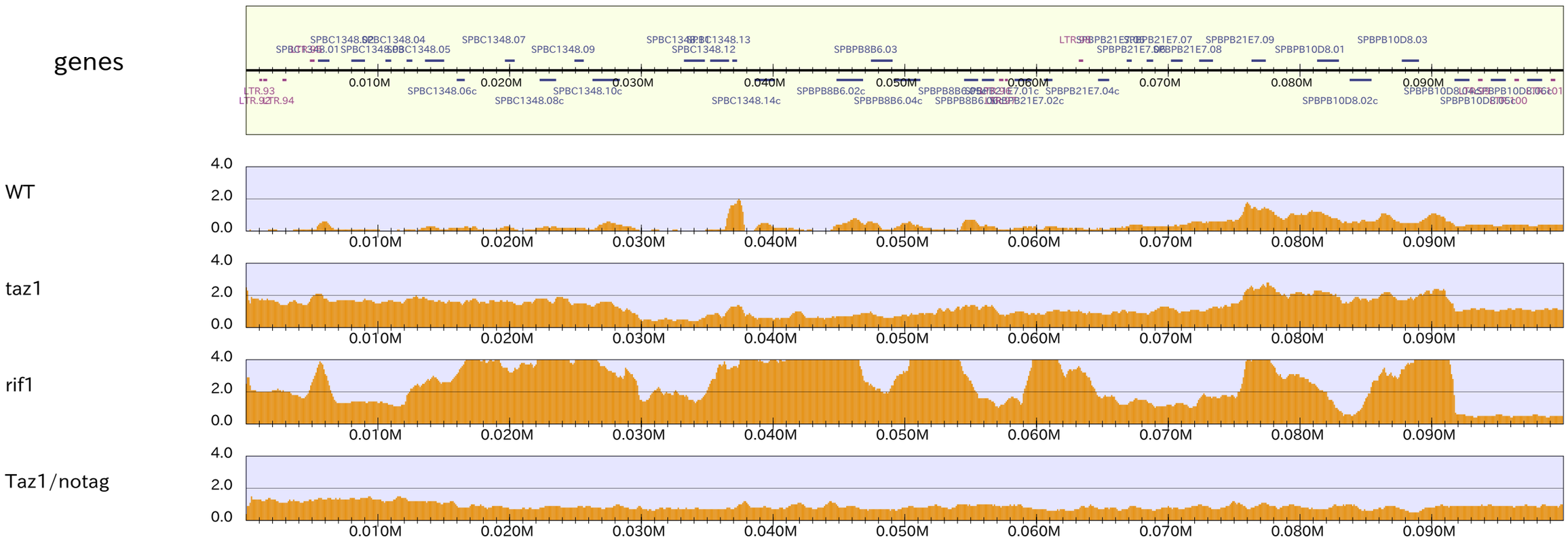
genes
SPBC1348.02
SPBC1348.04
SPBC1348.07
SPBC1348.09
SPBC1348.13
SPBC1348.12
SPBPB8B6.03
SPBPB21E7.07
SPBPB21E7.09
SPBPB10D8.03
SPBC1348.01
SPBC1348.05
SPBPB21E7.08
SPBPB10D8.01
LTR.93
LTR.94
SPBC1348.06c
SPBC1348.08c
SPBC1348.10c
SPBC1348.14c
SPBPB8B6.02c
SPBPB8B6.04c
SPBPB21E7.04c
SPBPB10D8.02c
0.010M
0.020M
0.030M
0.040M
0.050M
0.060M
0.070M
0.080M
0.090M
WT
taz1
rif1
Taz1/notag
4.0
2.0
0.0

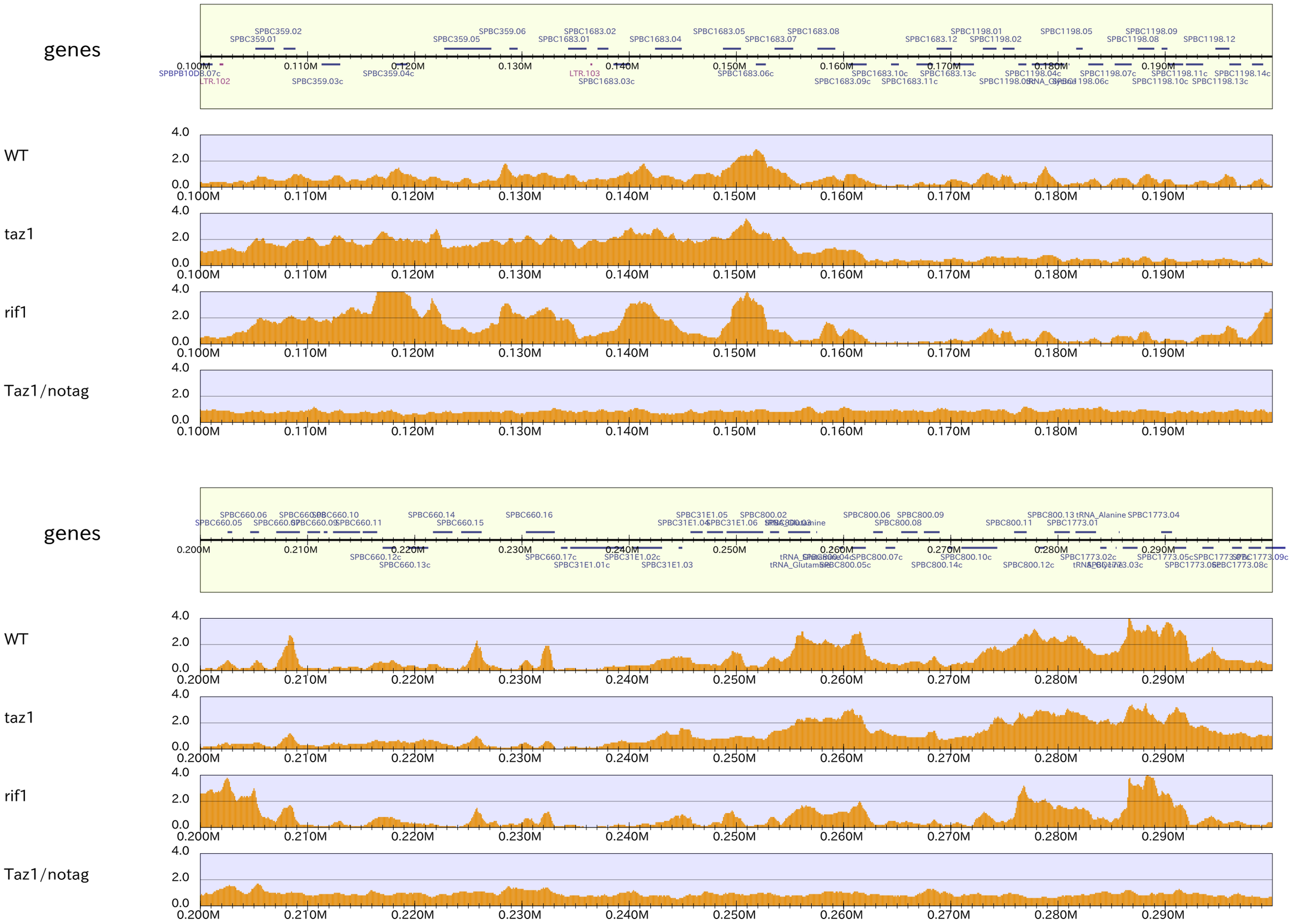
genes
SPBC359.02
SPBC359.01
SPBC359.06
SPBC359.05
SPBC1683.02
SPBC1683.01
SPBC1683.04
SPBC1683.05
SPBC1683.08
SPBC1683.07
SPBC1198.01
SPBC1198.05
SPBC1198.09
SPBC1198.12
SPBC1198.02
SPBC1198.08
SPBPB10D8.07c
LTR.102
SPBC359.03c
SPBC359.04c
LTR.103
SPBC1683.03c
SPBC1683.06c
SPBC1683.10c
SPBC1683.09c
SPBC1683.11c
SPBC1683.12
SPBC1683.13c
SPBC1198.04c
SPBC1198.07c
SPBC1198.11c
SPBC1198.14c
SPBC1198.10c
SPBC1198.13c
0.100M
0.110M
0.120M
0.130M
0.140M
0.150M
0.160M
0.170M
0.180M
0.190M
WT
taz1
rif1
Taz1/notag
4.0
2.0
0.0

genes
SPBC660.06
SPBC660.05
SPBC660.10
SPBC660.11
SPBC660.14
SPBC660.15
SPBC660.16
SPBC31E1.05
SPBC31E1.04
SPBC800.02
SPBC31E1.06
SPBC800.06
SPBC800.09
SPBC800.08
SPBC800.13
tRNA_Alanine
SPBC1773.04
SPBC800.11
SPBC1773.01
SPBC660.12c
SPBC660.13c
SPBC660.17c
SPBC31E1.01c
SPBC31E1.02c
SPBC31E1.03
tRNA_Glutamine
SPBC800.04c
SPBC800.07c
SPBC800.05c
SPBC800.10c
SPBC800.14c
SPBC800.12c
SPBC1773.02c
SPBC1773.03c
SPBC1773.05c
SPBC1773.06c
SPBC1773.09c
SPBC1773.08c
0.200M
0.210M
0.220M
0.230M
0.240M
0.250M
0.260M
0.270M
0.280M
0.290M
WT
taz1
rif1
Taz1/notag
4.0
2.0
0.0

chrII_2

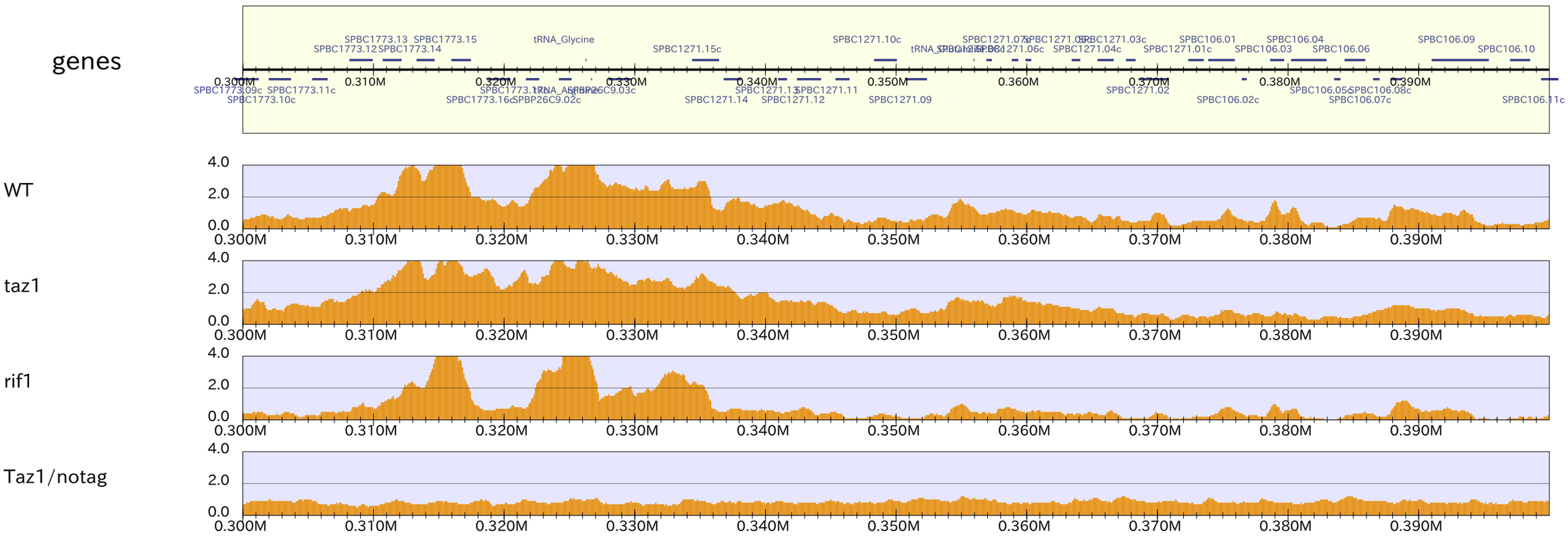
genes
SPBC1773.13 SPBC1773.15 tRNA_Glycine SPBC1271.10c SPBC1271.07c SPBC1271.05 SPBC1271.03c SPBC106.01 SPBC106.04 SPBC106.09
SPBC1773.12 SPBC1773.14 SPBC1271.15c SPBC1271.06c SPBC1271.04c SPBC1271.01c SPBC106.03 SPBC106.06 SPBC106.10
0.300M 0.310M 0.320M 0.330M 0.340M 0.350M 0.360M 0.370M 0.380M 0.390M
SPBC1773.09c SPBC1773.11c SPBC1773.10c SPBC1773.16c SPBP26C9.02c SPBC1271.14 SPBC1271.12 SPBC1271.09 SPBC1271.02 SPBC106.02c SPBC106.05c SPBC106.08c SPBC106.07c SPBC106.11c
WT
taz1
rif1
Taz1/notag
4.0
2.0
0.0

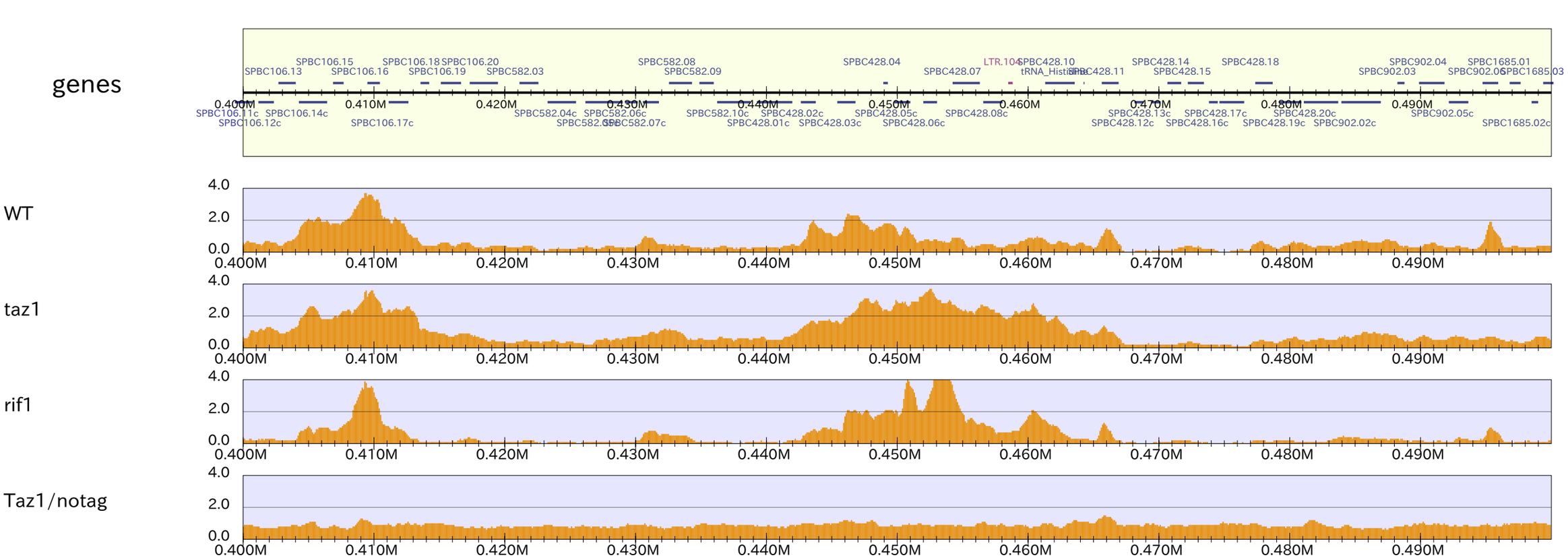
genes
SPBC106.15 SPBC106.18 SPBC106.20 SPBC582.08 SPBC428.04 LTR.104 SPBC428.10 SPBC428.14 SPBC428.18 SPBC902.04 SPBC1685.01
SPBC106.13 SPBC106.16 SPBC106.19 SPBC582.03 SPBC582.09 SPBC428.07 tRNA_His SPBC428.11 SPBC428.15 SPBC902.03 SPBC902.06 SPBC1685.03
0.400M 0.410M 0.420M 0.430M 0.440M 0.450M 0.460M 0.470M 0.480M 0.490M
SPBC106.11c SPBC106.14c SPBC106.12c SPBC106.17c SPBC582.04c SPBC582.06c SPBC582.10c SPBC428.02c SPBC428.05c SPBC428.08c SPBC428.13c SPBC428.17c SPBC428.20c SPBC902.05c
SPBC582.07c SPBC428.01c SPBC428.03c SPBC428.06c SPBC428.12c SPBC428.16c SPBC428.19c SPBC902.02c SPBC1685.02c
WT
taz1
rif1
Taz1/notag
4.0
2.0
0.0

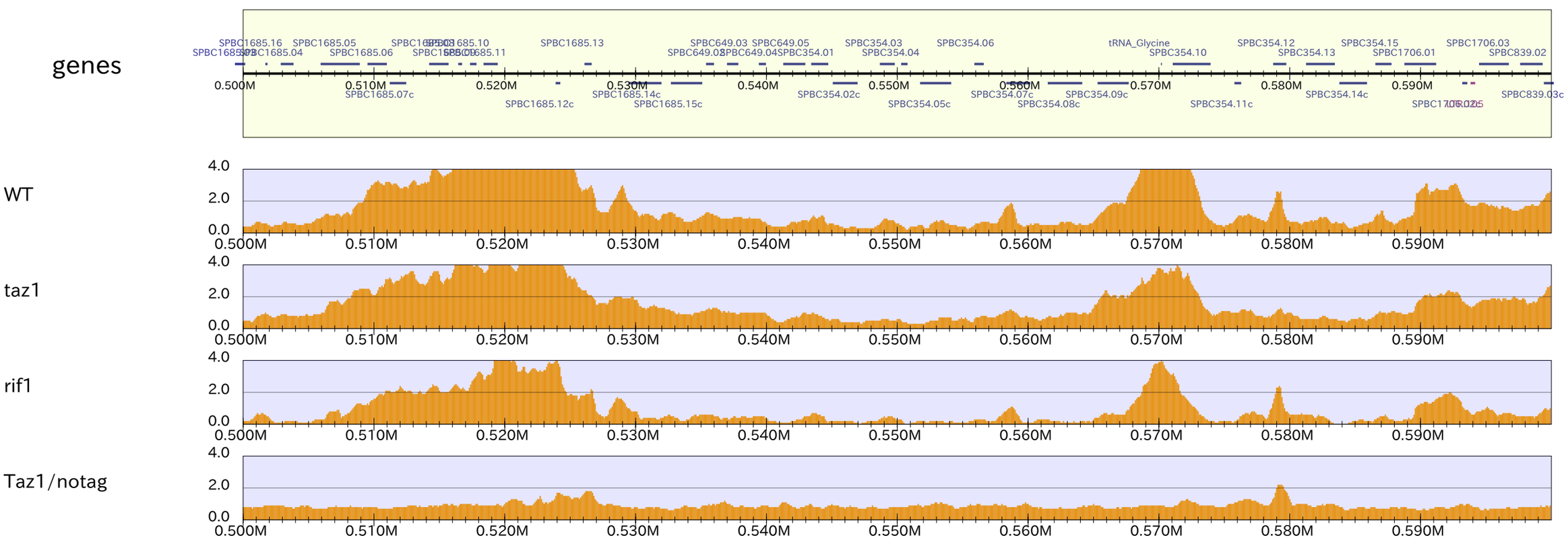
genes
SPBC1685.16 SPBC1685.05 SPBC1685.10 SPBC1685.13 SPBC649.03 SPBC649.05 SPBC354.03 SPBC354.06 tRNA_Gly SPBC354.12 SPBC354.15 SPBC1706.03
SPBC1685.03 SPBC1685.04 SPBC1685.06 SPBC1685.11 SPBC649.02 SPBC649.04 SPBC354.01 SPBC354.04 SPBC354.10 SPBC354.13 SPBC1706.01 SPBC839.02
0.500M 0.510M 0.520M 0.530M 0.540M 0.550M 0.560M 0.570M 0.580M 0.590M
SPBC1685.07c SPBC1685.14c SPBC1685.12c SPBC1685.15c SPBC354.02c SPBC354.07c SPBC354.09c SPBC354.14c SPBC839.03c
SPBC354.05c SPBC354.08c SPBC354.11c
WT
taz1
rif1
Taz1/notag
4.0
2.0
0.0

chrII_3

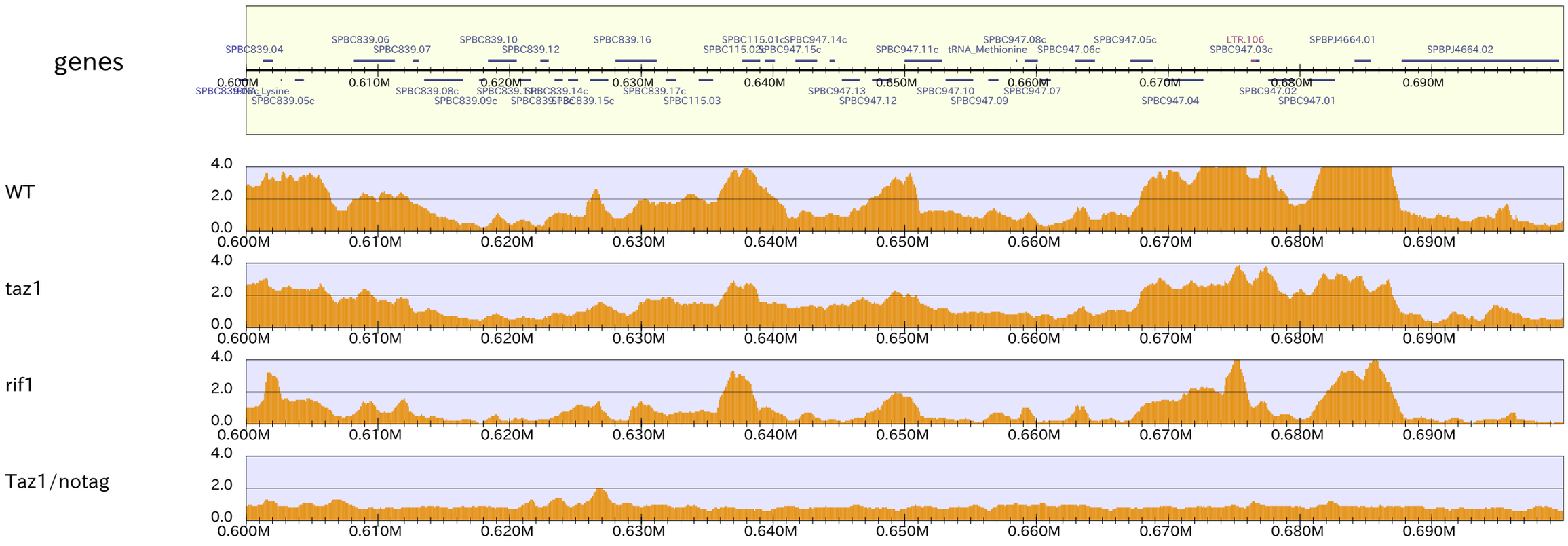
genes
SPBC839.04
SPBC839.06
SPBC839.07
SPBC839.10
SPBC839.12
SPBC839.16
SPBC115.01c
SPBC115.02c
SPBC947.14c
SPBC947.15c
SPBC947.11c
tRNA_Methionine
SPBC947.08c
SPBC947.06c
SPBC947.05c
LTR.106
SPBC947.03c
SPBPJ4664.01
SPBPJ4664.02
SPBC839.05c
SPBC839.08c
SPBC839.09c
SPBC839.14c
SPBC839.15c
SPBC839.17c
SPBC115.03
SPBC947.13
SPBC947.12
SPBC947.10
SPBC947.09
SPBC947.07
SPBC947.04
SPBC947.02
SPBC947.01
0.600M
0.610M
0.620M
0.630M
0.640M
0.650M
0.660M
0.670M
0.680M
0.690M
WT
taz1
rif1
Taz1/notag
4.0
2.0
0.0

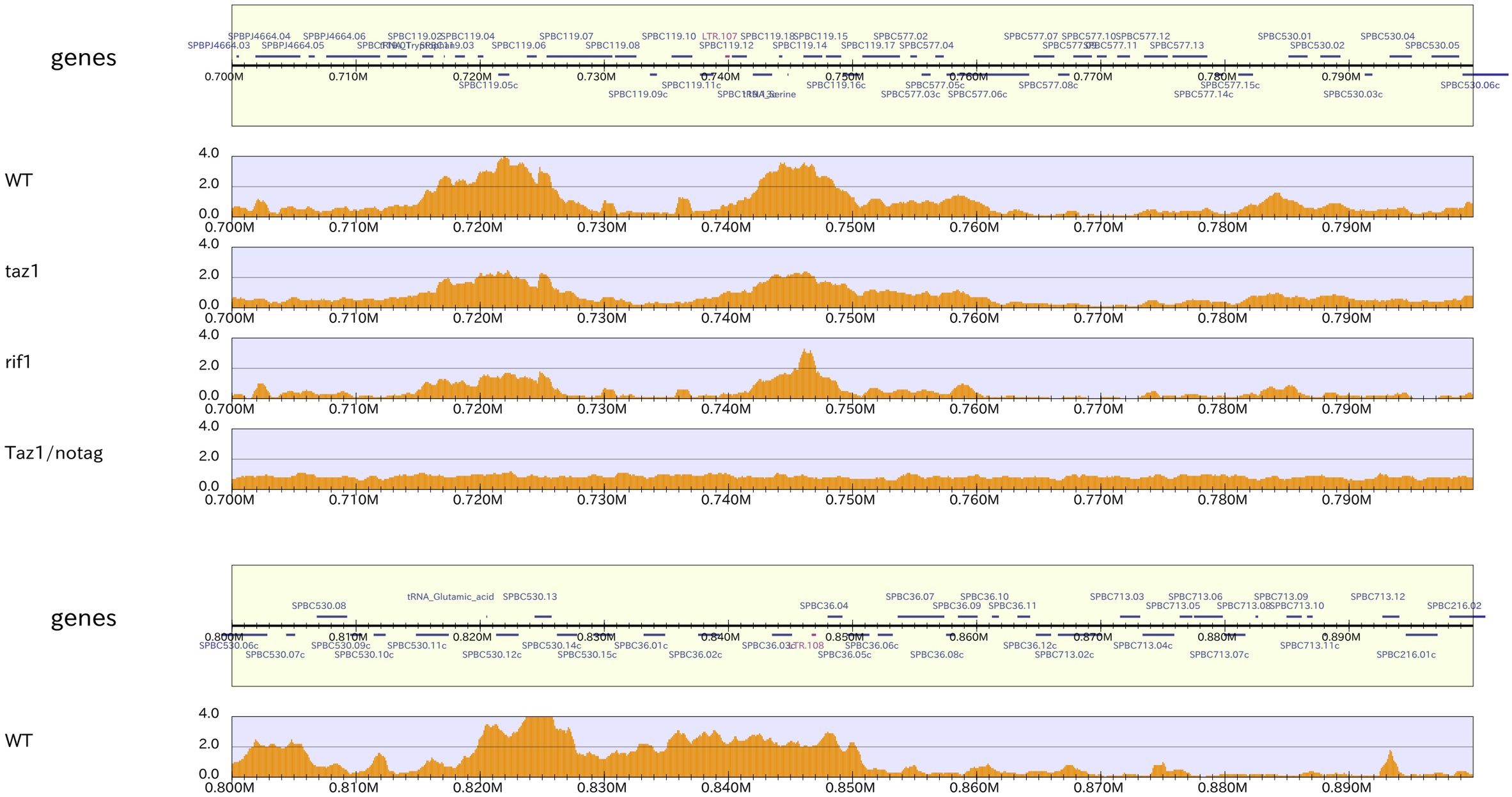
genes
SPBPJ4664.04
SPBPJ4664.03
SPBPJ4664.06
SPBPJ4664.05
SPBC119.02
SPBC119.04
SPBC119.03
SPBC119.06
SPBC119.07
SPBC119.08
SPBC119.10
LTR.107
SPBC119.12
SPBC119.18
SPBC119.14
SPBC119.15
SPBC119.17
SPBC577.02
SPBC577.04
SPBC577.07
SPBC577.10
SPBC577.12
SPBC577.11
SPBC577.13
SPBC530.01
SPBC530.02
SPBC530.04
SPBC530.05
SPBC530.06c
SPBC119.05c
SPBC119.09c
SPBC119.11c
SPBC119.16c
SPBC577.05c
SPBC577.03c
SPBC577.06c
SPBC577.08c
SPBC577.15c
SPBC577.14c
SPBC530.03c
0.700M
0.710M
0.720M
0.730M
0.740M
0.750M
0.760M
0.770M
0.780M
0.790M
WT
taz1
rif1
Taz1/notag
4.0
2.0
0.0

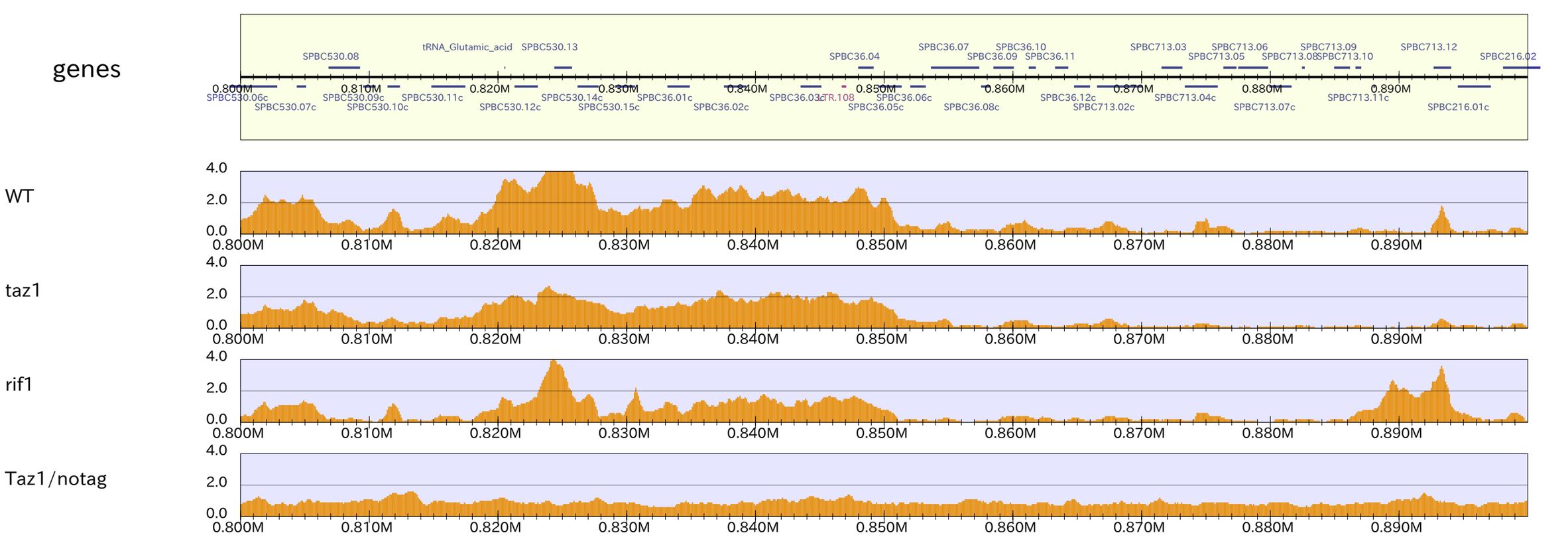
genes
SPBC530.08
tRNA_Glutamic_acid
SPBC530.13
SPBC36.04
SPBC36.07
SPBC36.10
SPBC36.09
SPBC36.11
SPBC713.03
SPBC713.06
SPBC713.09
SPBC713.12
SPBC713.05
SPBC713.08
SPBC713.10
SPBC216.02
SPBC530.06c
SPBC530.07c
SPBC530.09c
SPBC530.10c
SPBC530.11c
SPBC530.12c
SPBC530.14c
SPBC530.15c
SPBC36.01c
SPBC36.02c
SPBC36.03c
LTR.108
SPBC36.06c
SPBC36.05c
SPBC36.08c
SPBC36.12c
SPBC713.02c
SPBC713.04c
SPBC713.07c
SPBC713.11c
SPBC216.01c
0.800M
0.810M
0.820M
0.830M
0.840M
0.850M
0.860M
0.870M
0.880M
0.890M
WT
taz1
rif1
Taz1/notag
4.0
2.0
0.0

chrII_4

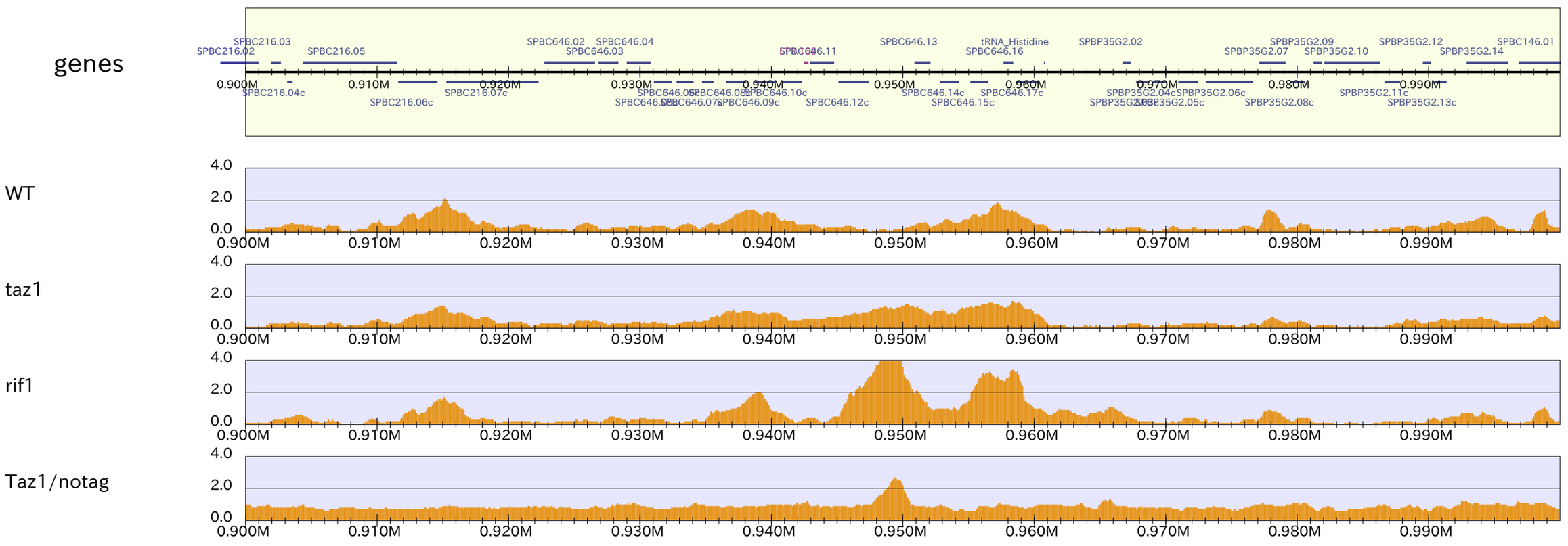
genes
SPBC216.03
SPBC216.02
SPBC216.05
SPBC646.02
SPBC646.04
SPBC646.03
SPBC646.13
tRNA_Histidine
SPBC646.16
SPBP35G2.02
SPBP35G2.09
SPBP35G2.12
SPBC146.01
SPBP35G2.07
SPBP35G2.10
SPBP35G2.14
0.900M
0.910M
0.920M
0.930M
0.940M
0.950M
0.960M
0.970M
0.980M
0.990M
SPBC216.04c
SPBC216.06c
SPBC216.07c
SPBC646.10c
SPBC646.09c
SPBC646.12c
SPBC646.14c
SPBC646.15c
SPBC646.17c
SPBP35G2.04c
SPBP35G2.06c
SPBP35G2.05c
SPBP35G2.08c
SPBP35G2.11c
SPBP35G2.13c
WT
taz1
rif1
Taz1/notag
4.0
2.0
0.0
genes
SPBC146.02
SPBC146.01
SPBC146.04
SPBC146.07
SPBC146.12
SPBC146.10
SPBC337.04
SPBC337.03
SPBC337.11
SPBC337.14
SPBC1734.03
SPBC1734.06
SPBC1734.13
SPBC1709.01
SPBC337.09
SPBC337.12
SPBC337.16
SPBC1734.04
SPBC1734.11
SPBC1734.15
1.000M
1.010M
1.020M
1.030M
1.040M
1.050M
1.060M
1.070M
1.080M
1.090M
SPBC146.03c
SPBC146.06c
SPBC146.09c
SPBC146.13c
SPBC337.02c
SPBC146.05c
SPBC146.08c
SPBC146.11c
SPBC146.14c
SPBC337.13c
SPBC1734.01c
SPBC1734.05c
SPBC1734.10c
SPBC1734.14c
SPBC1709.02c
SPBC337.10c
SPBC337.15c
SPBC1734.02c
SPBC1734.07c
SPBC1734.12c
SPBC1734.16c
WT
taz1
rif1
Taz1/notag
genes
SPBC1709.03
SPBC1709.08
SPBC1709.12
SPBC1709.17
SPBC409.03
SPBC409.06
SPBC409.10
SPBC409.13
SPBC409.18
SPBC1306.02
SPBC4.05
SPBC1709.20
SPBC1709.09
SPBC1709.14
SPBC1709.18
SPBC409.05
SPBC409.08
SPBC409.11
SPBC409.15
SPBC409.21
SPBC4.01
SPBC4.06
1.100M
1.110M
1.120M
1.130M
1.140M
1.150M
1.160M
1.170M
1.180M
1.190M
SPBC1709.02c
SPBC1709.04c
SPBC1709.10c
SPBC1709.13c
SPBC1709.16c
SPBC409.04c
SPBC409.09c
tRNA_Arginine
SPBC409.17c
SPBC409.20c
SPBC4.02c
SPBC4.04c
SPBC1709.11c
SPBC1709.15c
SPBC1709.19c
SPBC409.07c
SPBC409.12c
SPBC409.16c
SPBC409.19c
SPBC1306.01c
SPBC4.03c
SPBC4.07c
WT
taz1
rif1
Taz1/notag

chrII_5

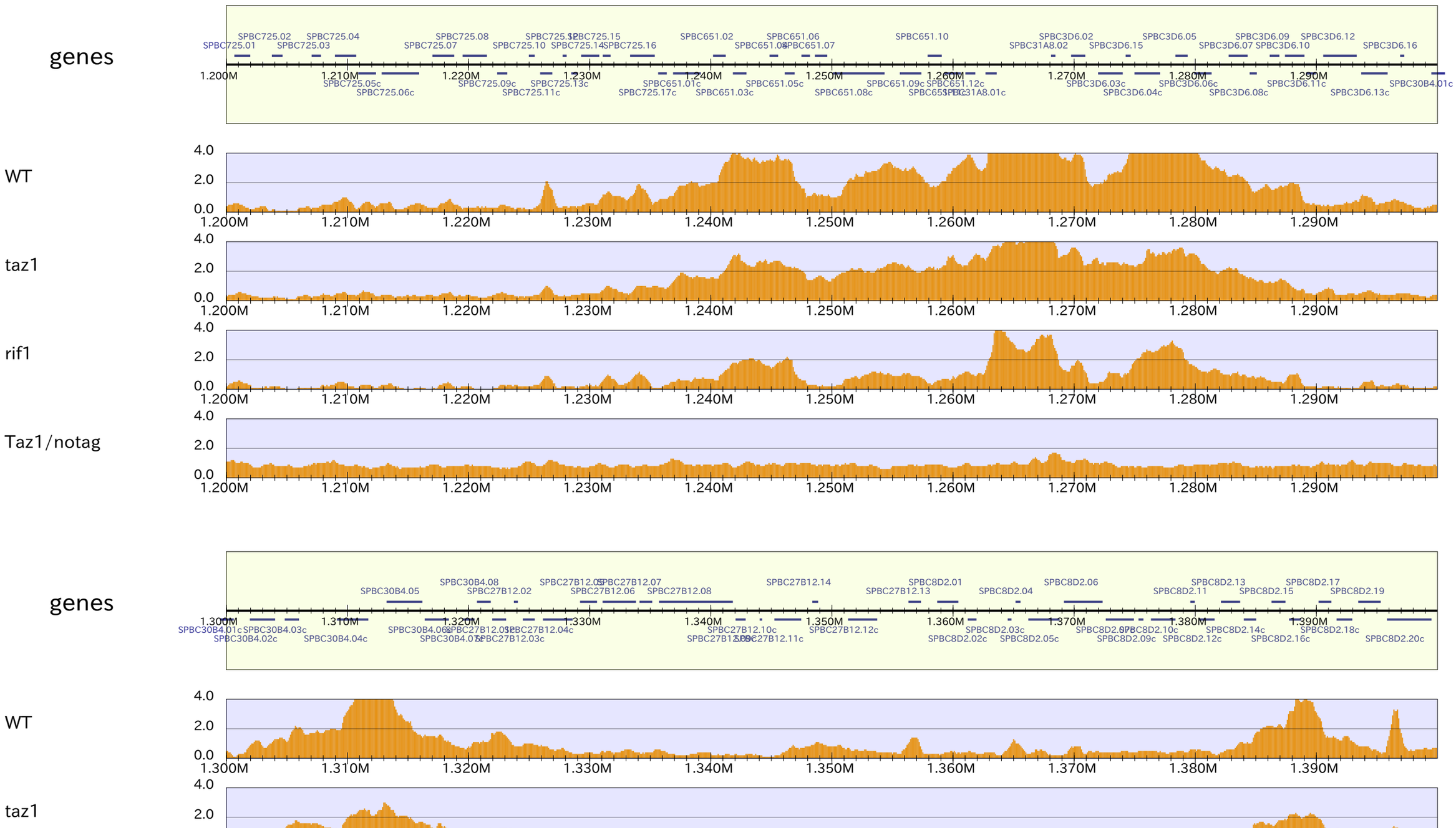
genes
WT
taz1
rif1
Taz1/notag
1.200M
1.210M
1.220M
1.230M
1.240M
1.250M
1.260M
1.270M
1.280M
1.290M
4.0
2.0
0.0

genes
WT
taz1
rif1
Taz1/notag
1.300M
1.310M
1.320M
1.330M
1.340M
1.350M
1.360M
1.370M
1.380M
1.390M
4.0
2.0
0.0

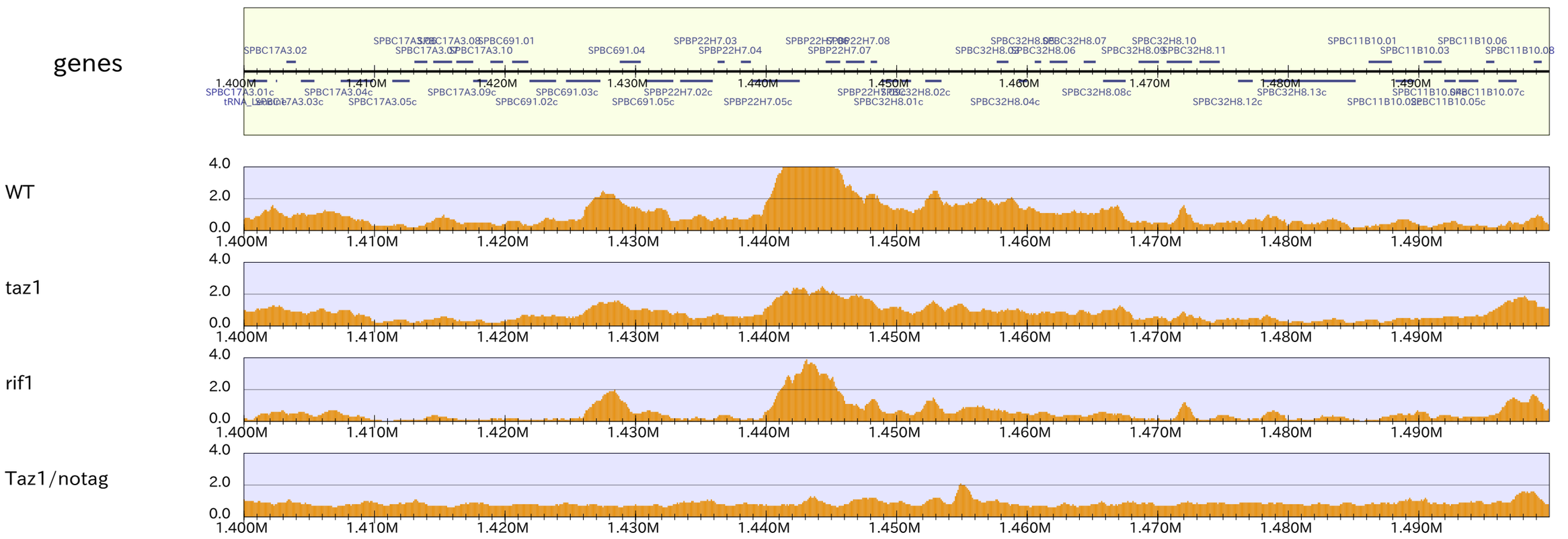
genes
WT
taz1
rif1
Taz1/notag
1.400M
1.410M
1.420M
1.430M
1.440M
1.450M
1.460M
1.470M
1.480M
1.490M
4.0
2.0
0.0

chrII_6

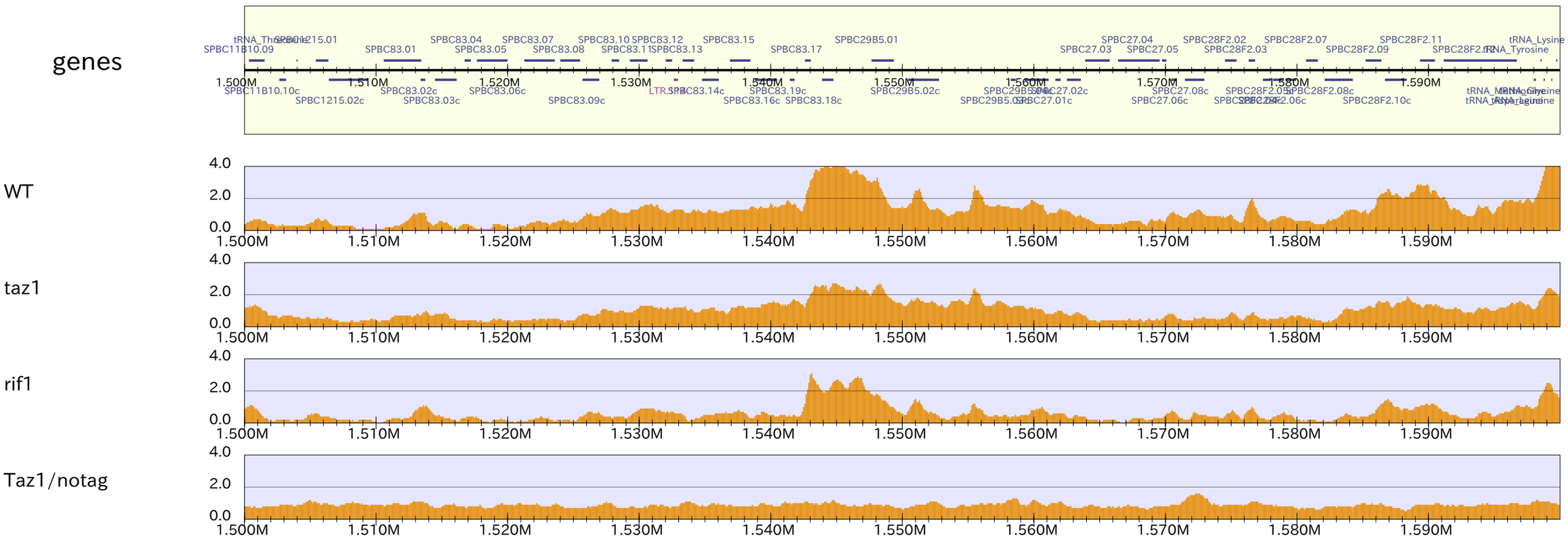
genes
WT
taz1
rif1
Taz1/notag
4.0
2.0
0.0
1.500M
1.510M
1.520M
1.530M
1.540M
1.550M
1.560M
1.570M
1.580M
1.590M

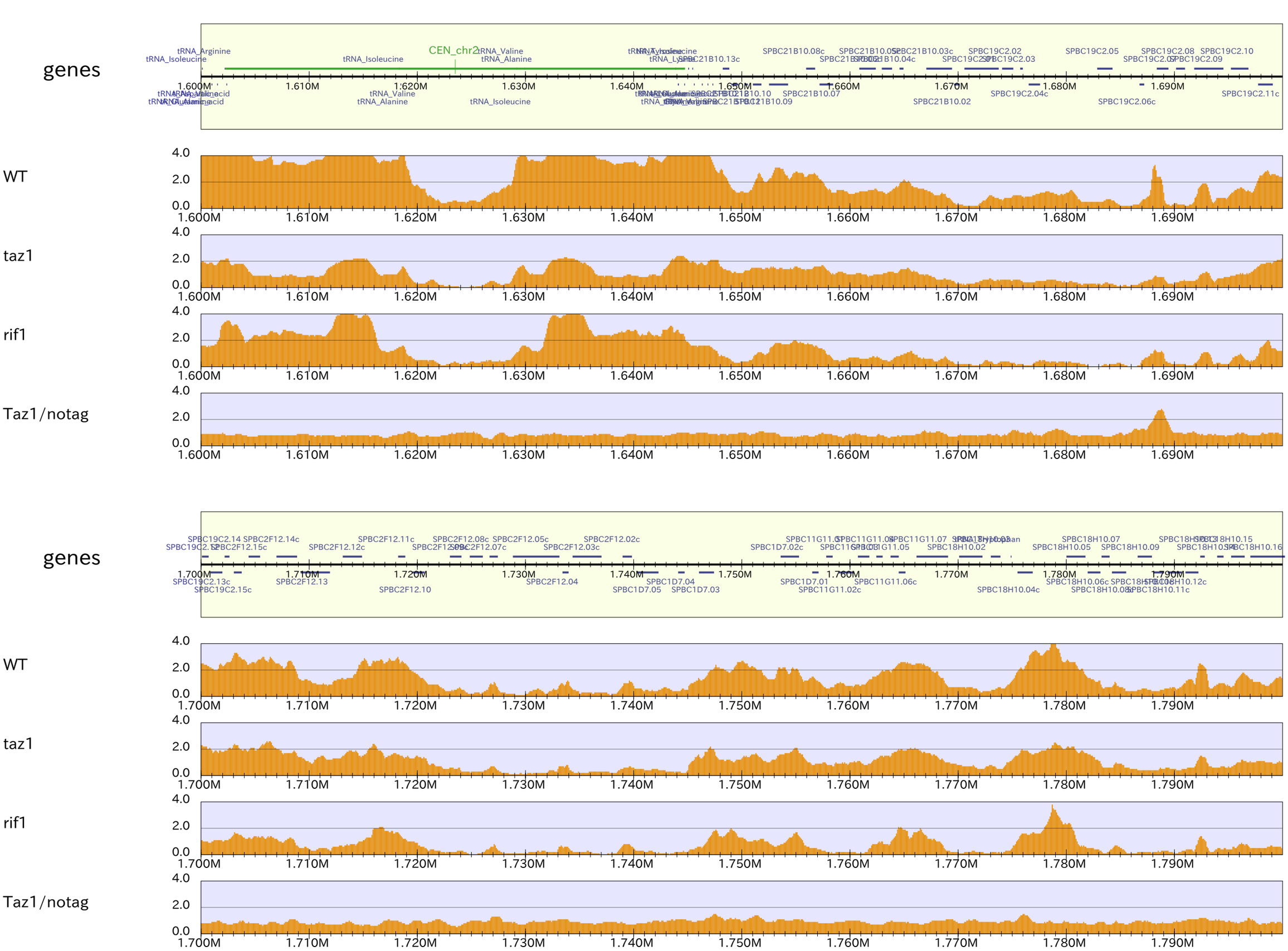
genes
CEN_chr2
WT
taz1
rif1
Taz1/notag
4.0
2.0
0.0
1.600M
1.610M
1.620M
1.630M
1.640M
1.650M
1.660M
1.670M
1.680M
1.690M

genes
WT
taz1
rif1
Taz1/notag
4.0
2.0
0.0
1.700M
1.710M
1.720M
1.730M
1.740M
1.750M
1.760M
1.770M
1.780M
1.790M

chrII_7

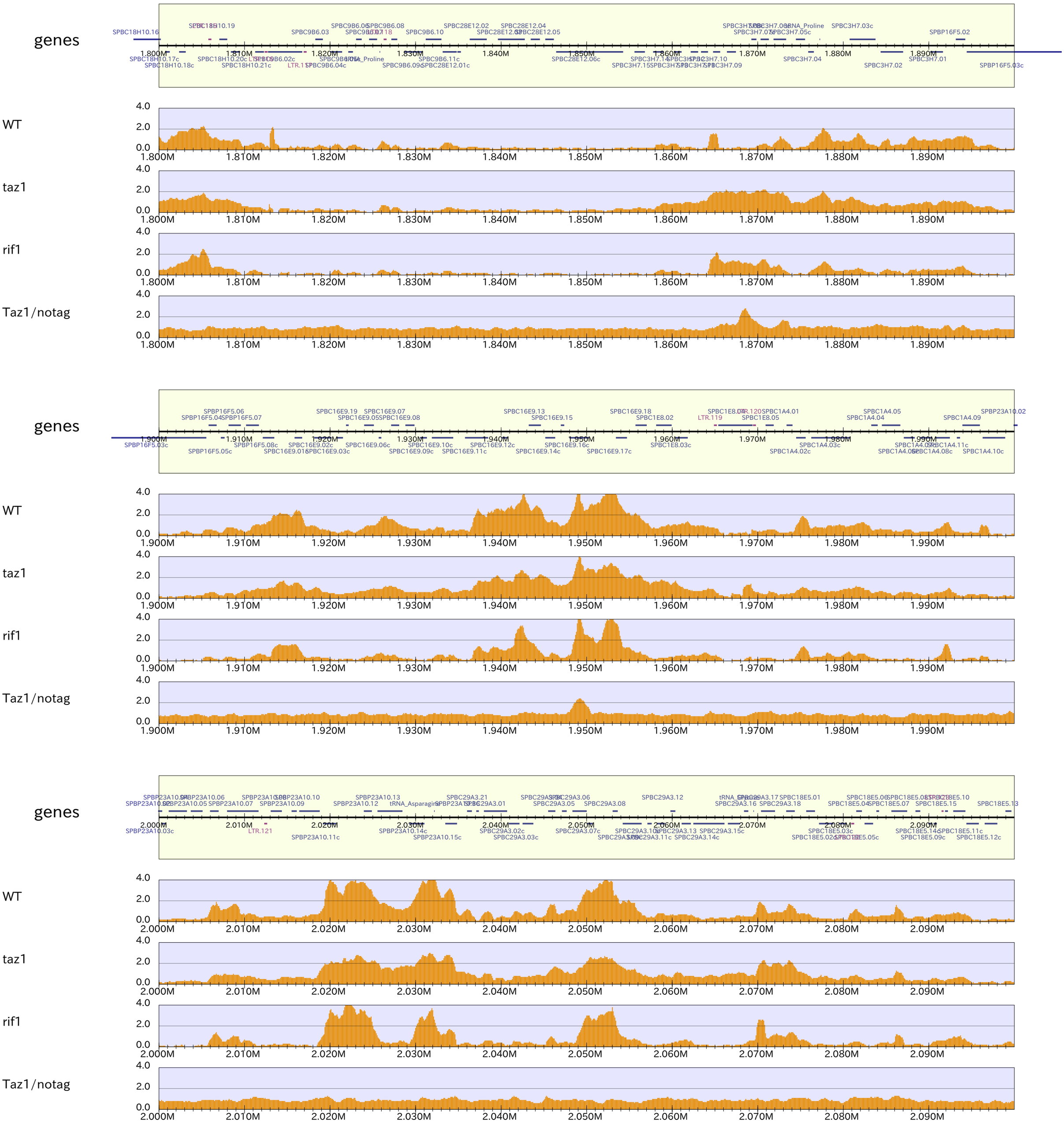
genes
WT
taz1
rif1
Taz1/notag
4.0
2.0
0.0
1.800M
1.810M
1.820M
1.830M
1.840M
1.850M
1.860M
1.870M
1.880M
1.890M
SPBC18H10.16
SPBC18H10.19
SPBC9B6.03
SPBC9B6.06
SPBC9B6.08
SPBC9B6.10
SPBC28E12.02
SPBC28E12.04
SPBC28E12.05
SPBC3H7.03c
SPBP16F5.02
SPBC18H10.17c
SPBC18H10.18c
SPBC18H10.20c
SPBC18H10.21c
SPBC9B6.02c
SPBC9B6.04c
SPBC9B6.09c
SPBC9B6.11c
SPBC28E12.01c
SPBC28E12.06c
SPBC3H7.15
SPBC3H7.09
SPBC3H7.04
SPBC3H7.02
SPBC3H7.01
SPBP16F5.03c
genes
WT
taz1
rif1
Taz1/notag
4.0
2.0
0.0
1.900M
1.910M
1.920M
1.930M
1.940M
1.950M
1.960M
1.970M
1.980M
1.990M
SPBP16F5.06
SPBP16F5.04
SPBP16F5.07
SPBC16E9.19
SPBC16E9.07
SPBC16E9.05
SPBC16E9.08
SPBC16E9.13
SPBC16E9.15
SPBC16E9.18
SPBC1E8.02
SPBC1E8.05
SPBC1A4.01
SPBC1A4.04
SPBC1A4.05
SPBC1A4.09
SPBP23A10.02
SPBP16F5.03c
SPBP16F5.05c
SPBP16F5.08c
SPBC16E9.02c
SPBC16E9.01c
SPBC16E9.03c
SPBC16E9.06c
SPBC16E9.10c
SPBC16E9.09c
SPBC16E9.11c
SPBC16E9.12c
SPBC16E9.14c
SPBC16E9.16c
SPBC16E9.17c
SPBC1E8.03c
SPBC1A4.02c
SPBC1A4.03c
SPBC1A4.11c
SPBC1A4.08c
SPBC1A4.10c
genes
WT
taz1
rif1
Taz1/notag
4.0
2.0
0.0
2.000M
2.010M
2.020M
2.030M
2.040M
2.050M
2.060M
2.070M
2.080M
2.090M
SPBP23A10.03c
SPBP23A10.06
SPBP23A10.05
SPBP23A10.07
SPBP23A10.09
SPBP23A10.10
SPBP23A10.11c
SPBP23A10.13
SPBP23A10.12
SPBP23A10.14c
SPBP23A10.15c
SPBC29A3.21
SPBC29A3.01
SPBC29A3.02c
SPBC29A3.03c
SPBC29A3.06
SPBC29A3.05
SPBC29A3.08
SPBC29A3.12
SPBC29A3.16
SPBC29A3.18
SPBC18E5.01
SPBC18E5.04
SPBC18E5.06
SPBC18E5.07
SPBC18E5.15
SPBC18E5.13
LTR.121
SPBC29A3.07c
SPBC29A3.11c
SPBC29A3.14c
SPBC29A3.15c
SPBC18E5.03c
SPBC18E5.09c
SPBC18E5.14c
SPBC18E5.11c
SPBC18E5.12c

chrII_8

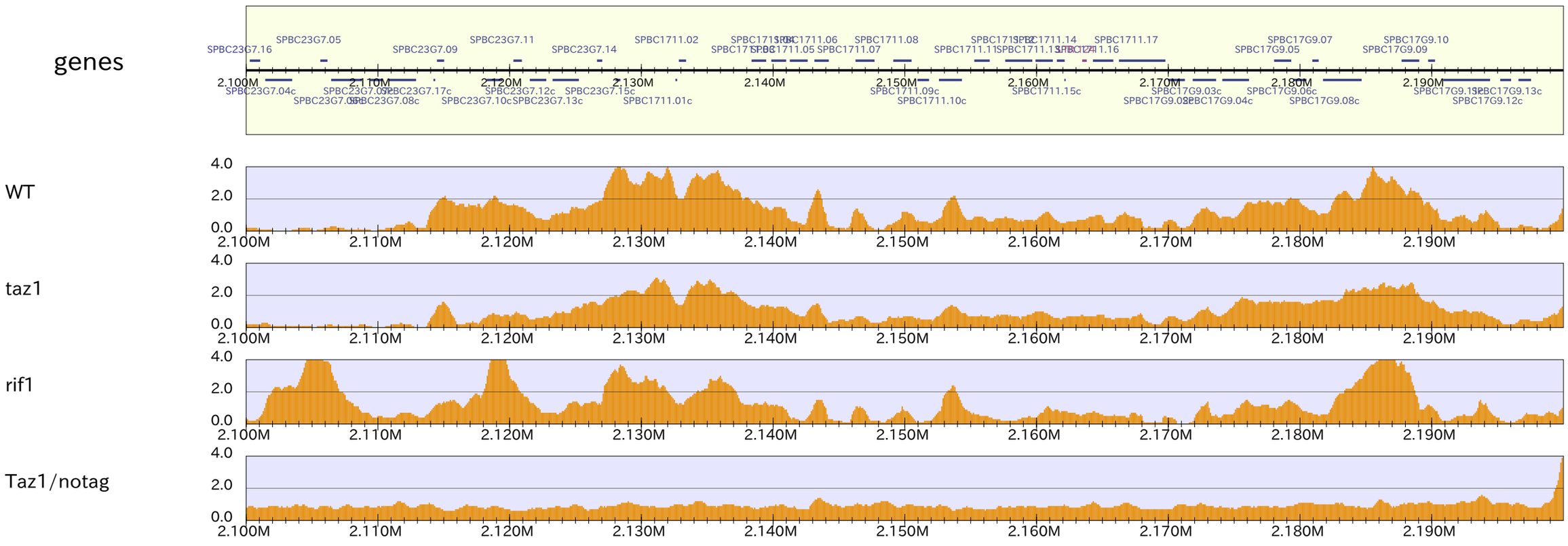
genes
WT
taz1
rif1
Taz1/notag
4.0
2.0
0.0
2.100M
2.110M
2.120M
2.130M
2.140M
2.150M
2.160M
2.170M
2.180M
2.190M

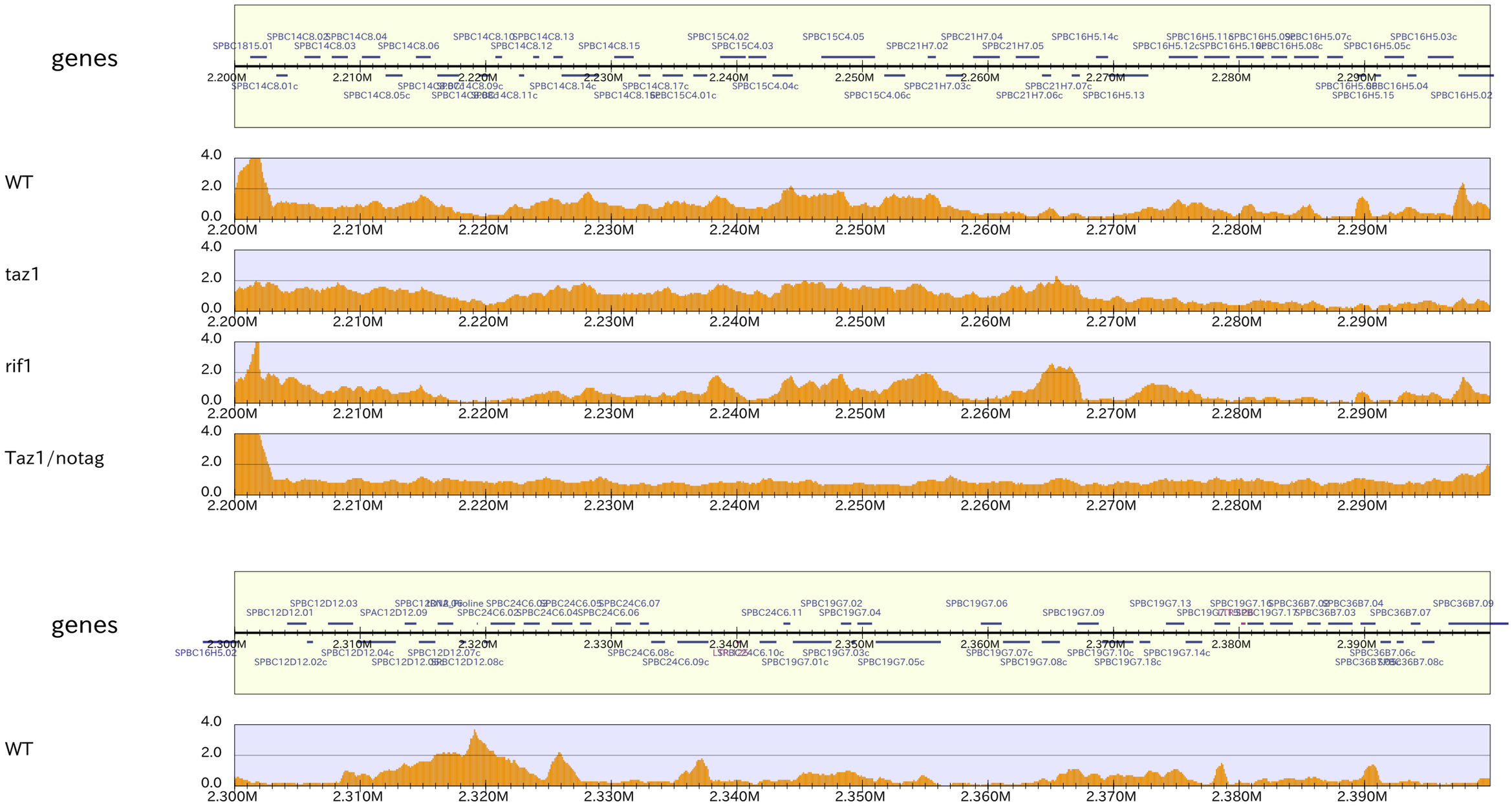
genes
WT
taz1
rif1
Taz1/notag
4.0
2.0
0.0
2.200M
2.210M
2.220M
2.230M
2.240M
2.250M
2.260M
2.270M
2.280M
2.290M

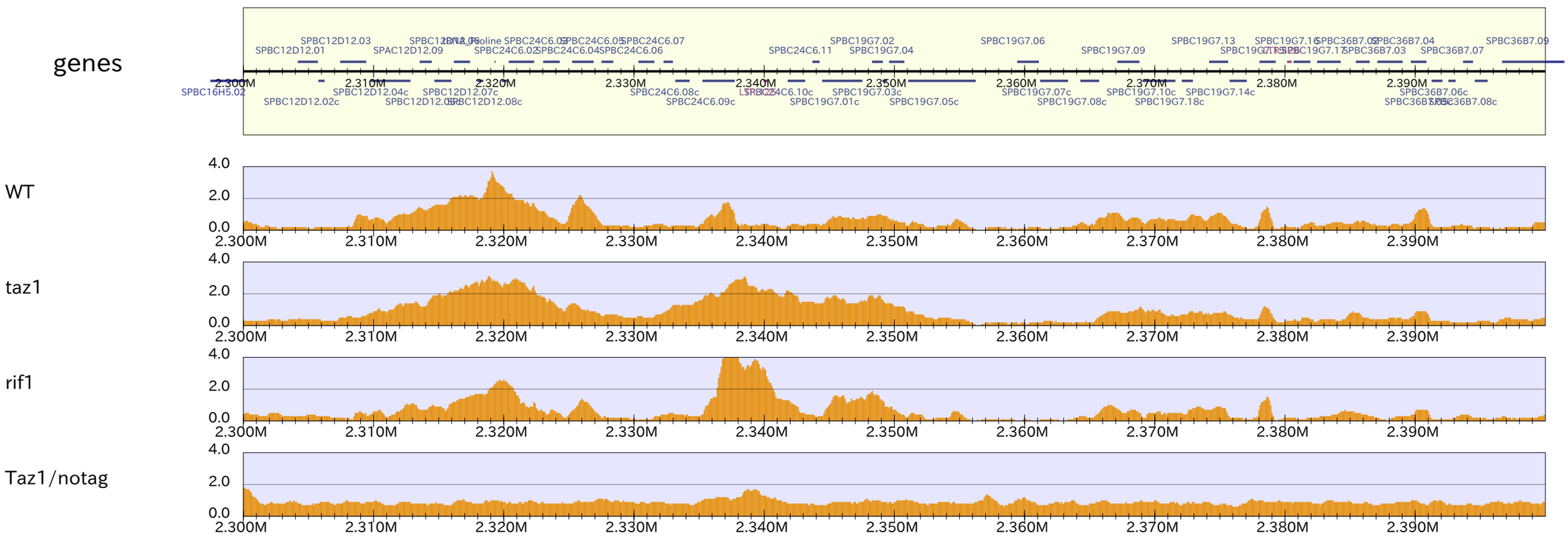
genes
WT
taz1
rif1
Taz1/notag
4.0
2.0
0.0
2.300M
2.310M
2.320M
2.330M
2.340M
2.350M
2.360M
2.370M
2.380M
2.390M

chrII_9

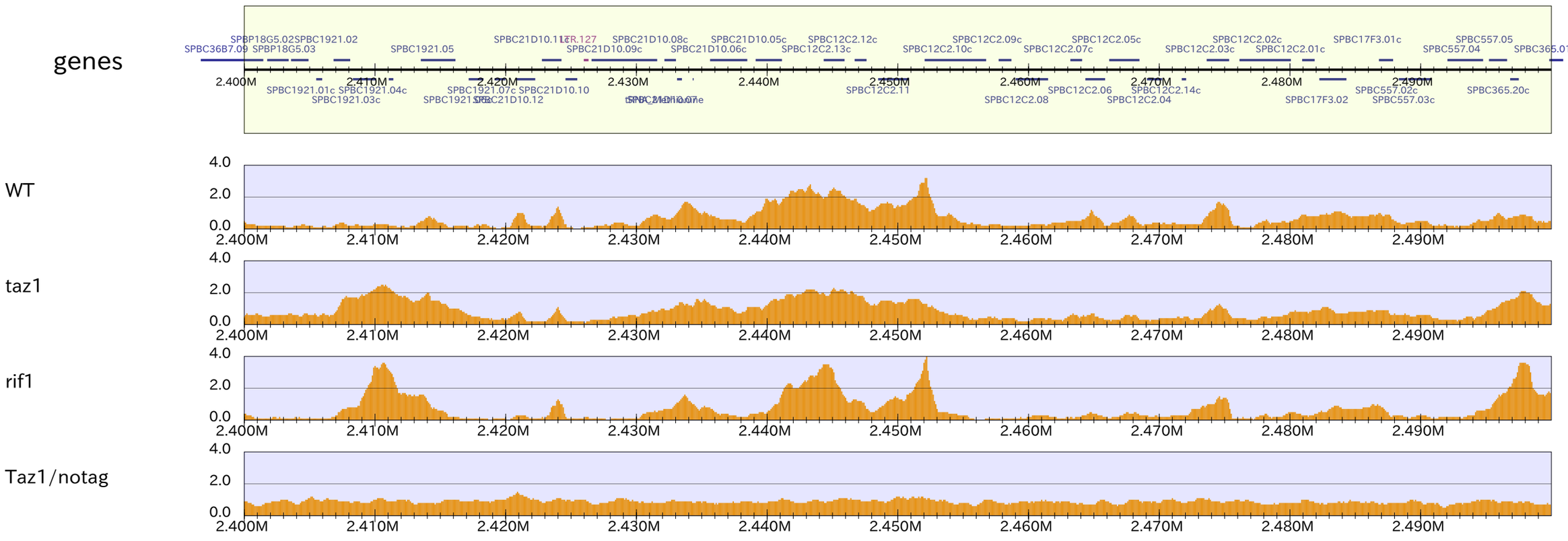
genes
WT
taz1
rif1
Taz1/notag
4.0
2.0
0.0
2.400M
2.410M
2.420M
2.430M
2.440M
2.450M
2.460M
2.470M
2.480M
2.490M

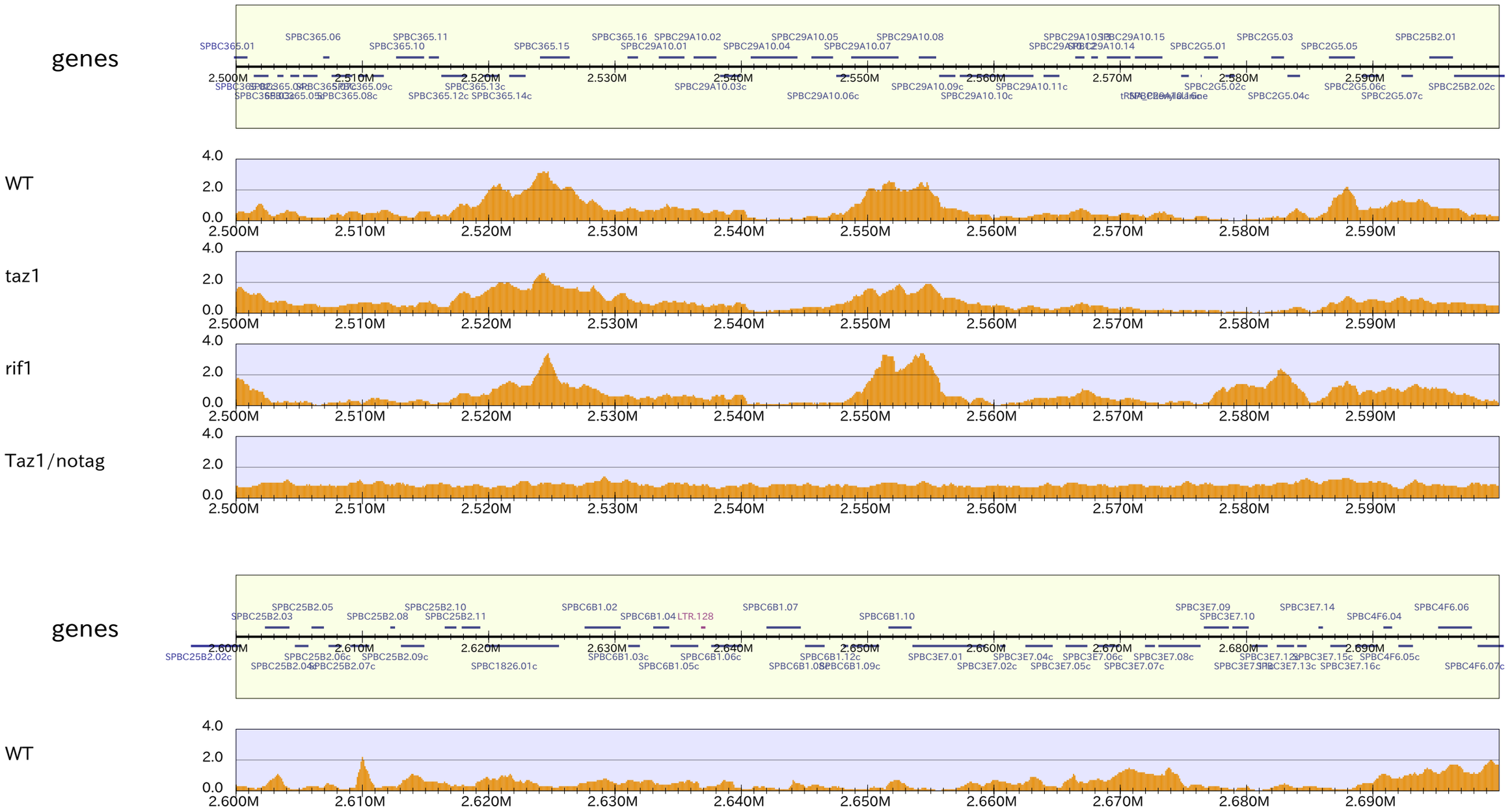
genes
WT
taz1
rif1
Taz1/notag
4.0
2.0
0.0
2.500M
2.510M
2.520M
2.530M
2.540M
2.550M
2.560M
2.570M
2.580M
2.590M

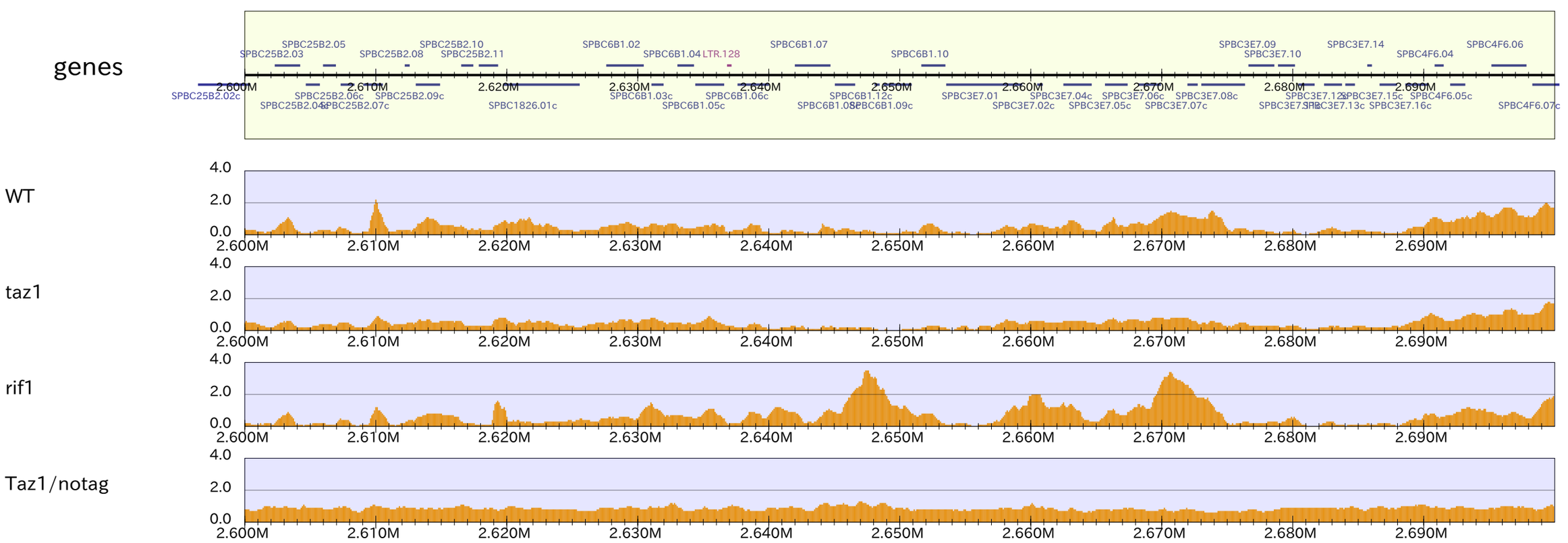
genes
WT
taz1
rif1
Taz1/notag
4.0
2.0
0.0
2.600M
2.610M
2.620M
2.630M
2.640M
2.650M
2.660M
2.670M
2.680M
2.690M

chrII_10

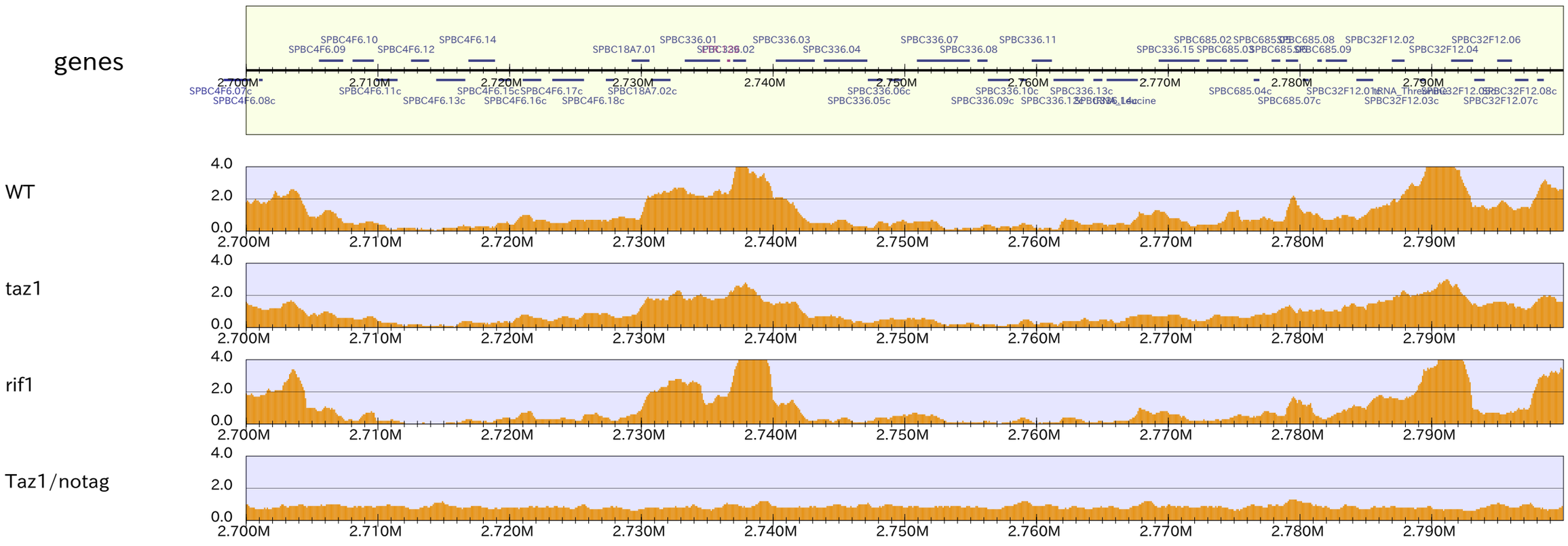
genes
WT
taz1
rif1
Taz1/notag
4.0
2.0
0.0
2.700M
2.710M
2.720M
2.730M
2.740M
2.750M
2.760M
2.770M
2.780M
2.790M
SPBC4F6.10
SPBC4F6.09
SPBC4F6.12
SPBC4F6.14
SPBC18A7.01
SPBC336.01
SPBC336.03
SPBC336.02
SPBC336.04
SPBC336.07
SPBC336.08
SPBC336.11
SPBC685.02
SPBC336.15
SPBC685.08
SPBC32F12.02
SPBC32F12.04
SPBC32F12.06
SPBC4F6.07c
SPBC4F6.08c
SPBC4F6.11c
SPBC4F6.13c
SPBC4F6.15c
SPBC4F6.16c
SPBC4F6.17c
SPBC4F6.18c
SPBC18A7.02c
SPBC336.05c
SPBC336.06c
SPBC336.09c
SPBC336.10c
SPBC336.13c
SPBC685.04c
SPBC685.07c
SPBC32F12.03c
SPBC32F12.07c
SPBC32F12.08c
genes
WT
taz1
rif1
Taz1/notag
4.0
2.0
0.0
2.800M
2.810M
2.820M
2.830M
2.840M
2.850M
2.860M
2.870M
2.880M
2.890M
SPBC32F12.10
SPBC32F12.09
SPBC32F12.15
SPBC32F12.11
SPBC19C7.02
SPBC19C7.03
SPBC19C7.06
SPBC19C7.05
SPBC19C7.11
SPBC19C7.10
SPBP19A11.01
SPBP19A11.06
SPBP4H10.04
SPBP4H10.03
SPBP4H10.08
SPBP4H10.07
SPBP4H10.10
SPBP4H10.09
SPBP4H10.13
SPBP4H10.12
SPBC32F12.12c
SPBC19C7.01
SPBC19C7.04c
SPBC19C7.08c
SPBC19C7.09c
SPBC19C7.12c
SPBP19A11.03c
SPBP19A11.02c
SPBP19A11.04c
SPAP19A11.05c
SPBP19A11.07c
SPBP4H10.05c
SPBP4H10.06c
SPBP4H10.11c
SPBP4H10.14c
genes
WT
taz1
rif1
Taz1/notag
4.0
2.0
0.0
2.900M
2.910M
2.920M
2.930M
2.940M
2.950M
2.960M
2.970M
2.980M
2.990M
SPBP4H10.15
SPBP4H10.20
SPBC1703.02
SPBC1703.04
SPBC1703.06
SPBC1703.05
SPBC1703.03
SPBC1703.12
SPBC2A9.02
SPBC2A9.03
SPBC2A9.10
SPBC2A9.09
SPBC2A9.12
SPBC2D10.04
SPBC2D10.06
SPBC2D10.05
SPBC2D10.09
SPBC2D10.12
SPBC2D10.13
SPBC2D10.16
SPBC2D10.17
SPBP4H10.21c
SPBC1703.03c
SPBC1703.01c
SPBC1703.08c
SPBC1703.13c
SPBC1703.15c
SPBC1703.14c
SPBC2A9.07c
SPBC2A9.11c
SPBC2D10.03c
SPBC2D10.08c
SPBC2D10.10c
SPBC2D10.11c
SPBC2D10.14c
SPBC2D10.15c

chrII_11

genes

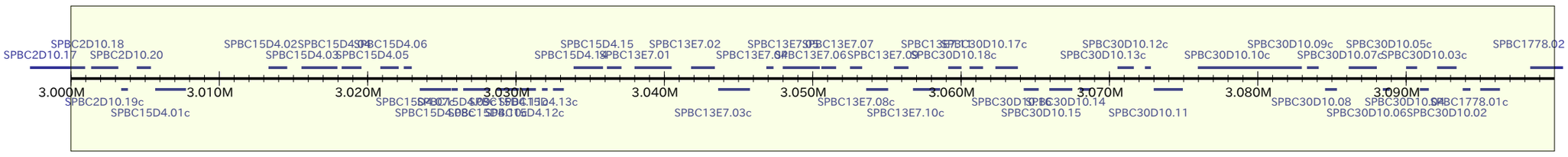

WT

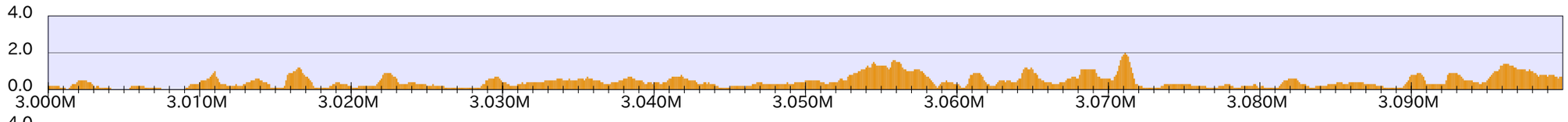

taz1

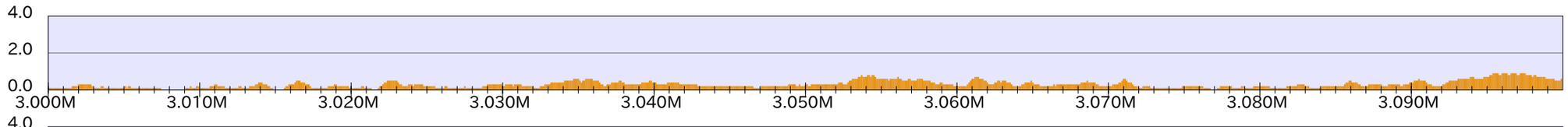

rif1

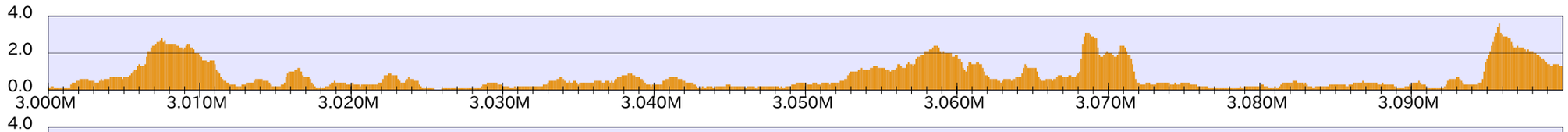

Taz1/notag

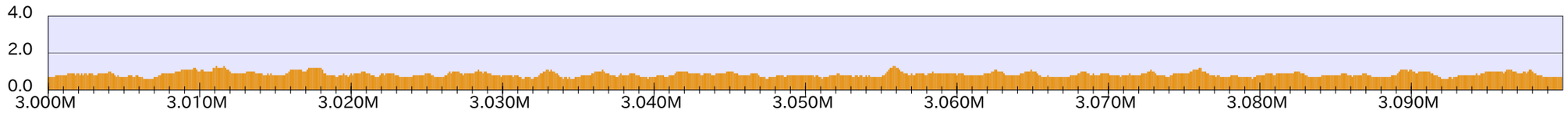

genes

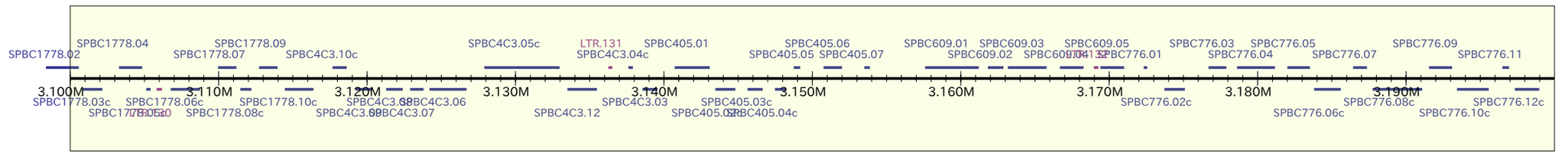

WT

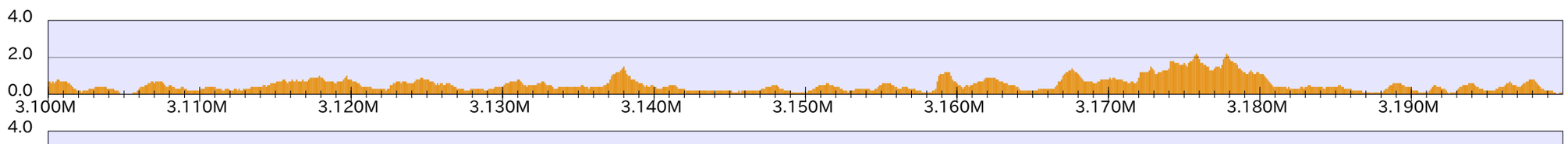

taz1

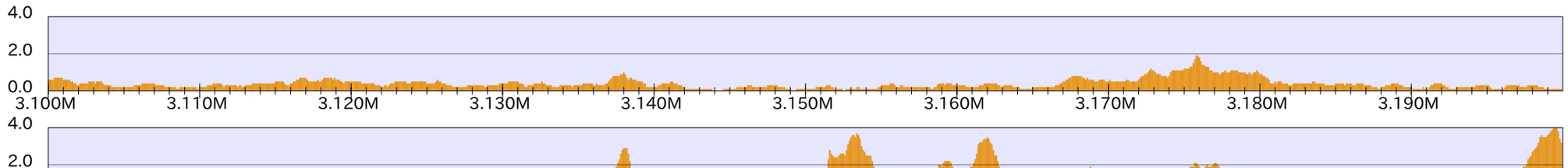

rif1

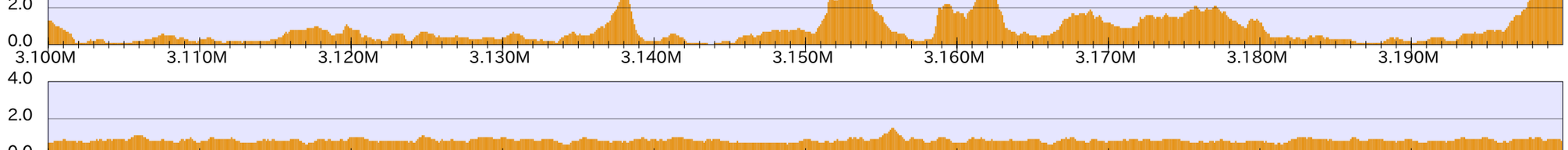

Taz1/notag

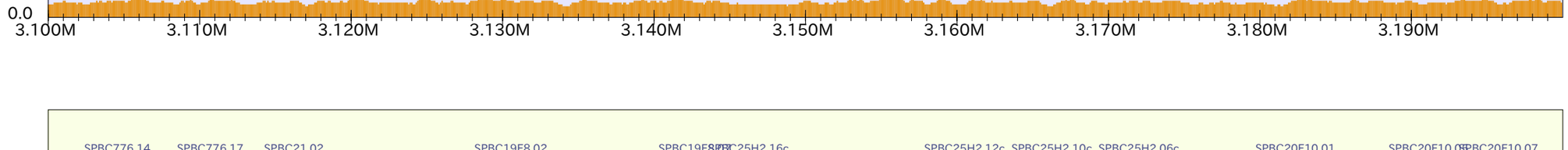

genes

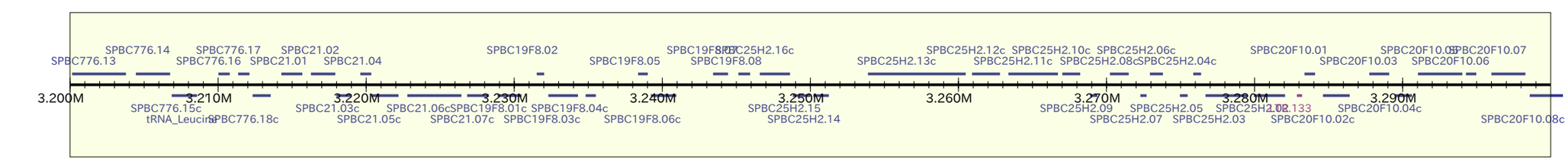

WT

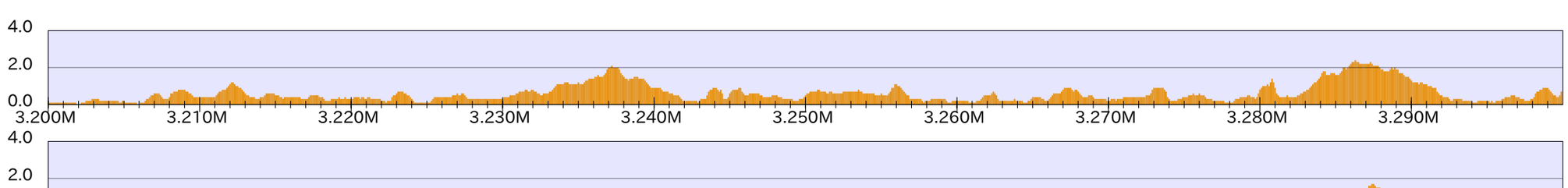

taz1

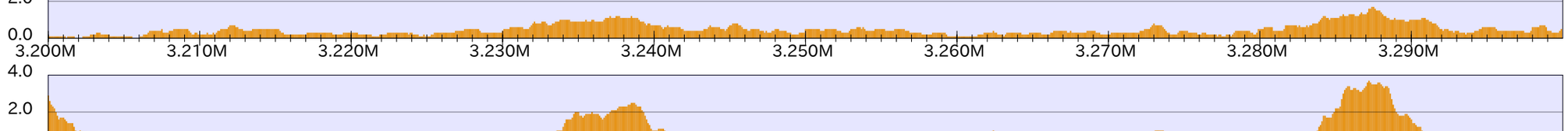

rif1

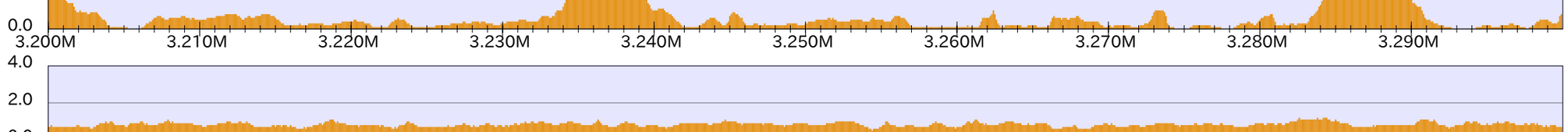

Taz1/notag

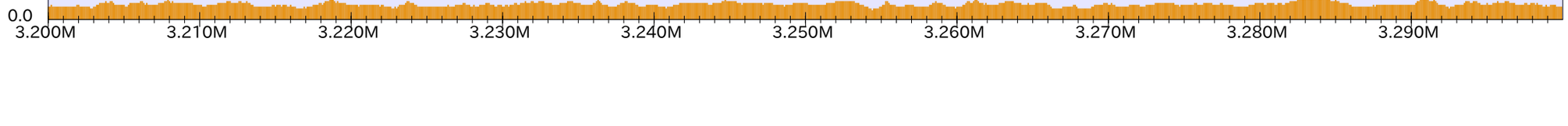

chrII_12

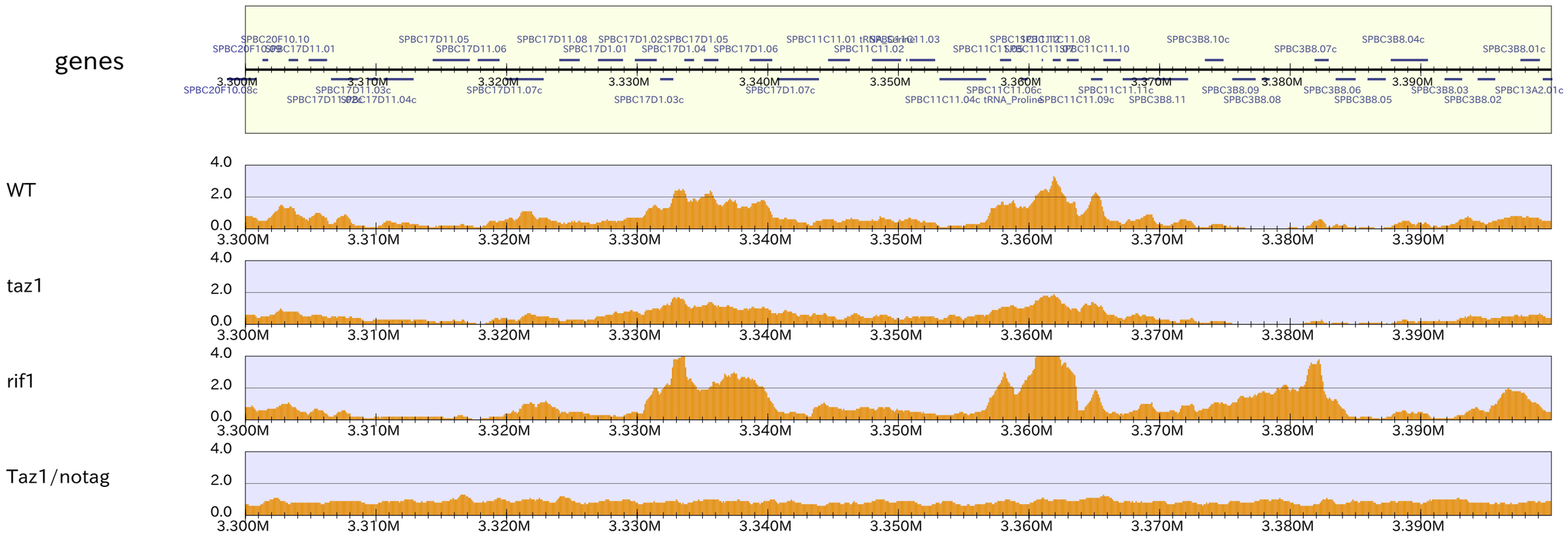
genes
WT
taz1
rif1
Taz1/notag
4.0
2.0
0.0
3.300M
3.310M
3.320M
3.330M
3.340M
3.350M
3.360M
3.370M
3.380M
3.390M

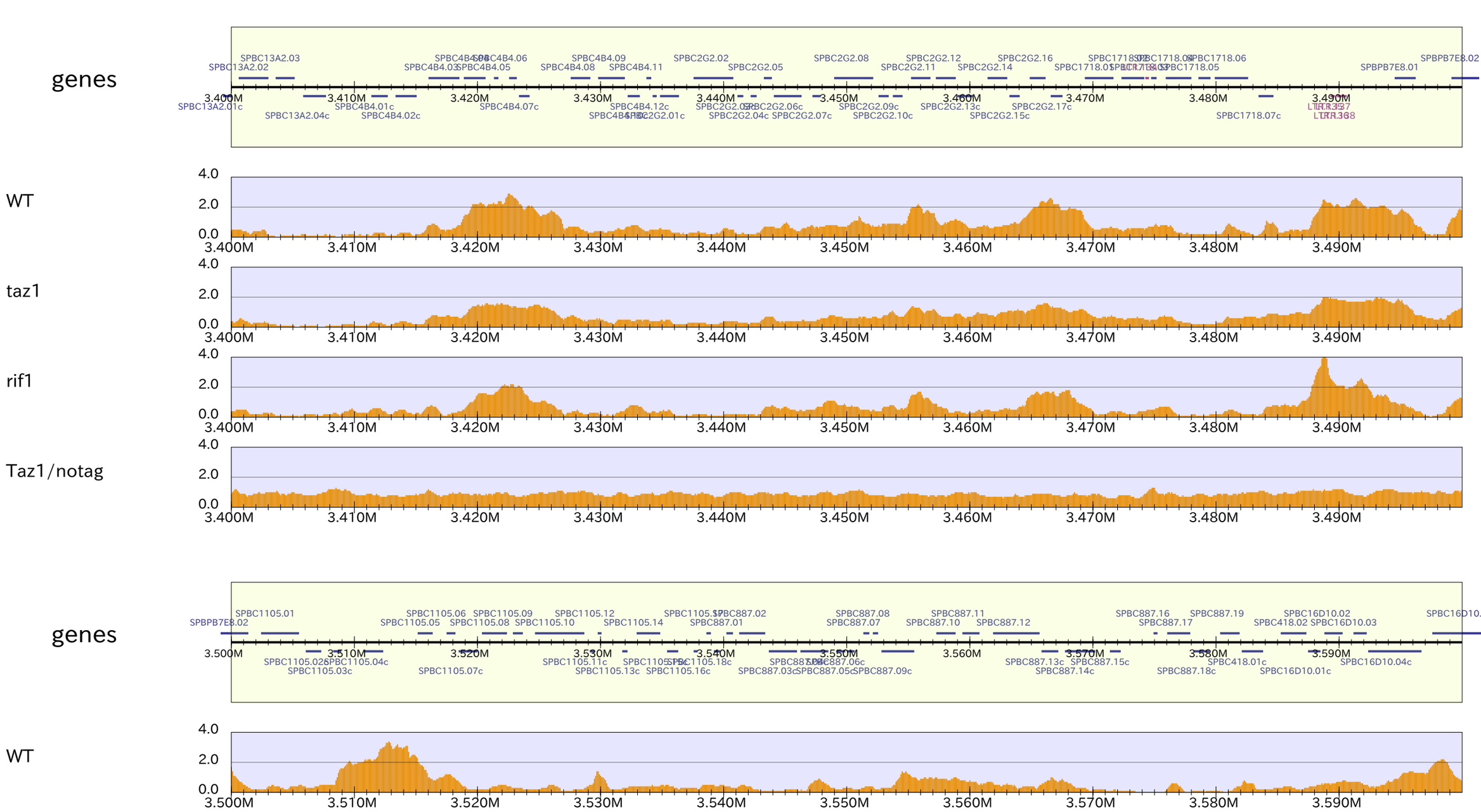
genes
WT
taz1
rif1
Taz1/notag
4.0
2.0
0.0
3.400M
3.410M
3.420M
3.430M
3.440M
3.450M
3.460M
3.470M
3.480M
3.490M

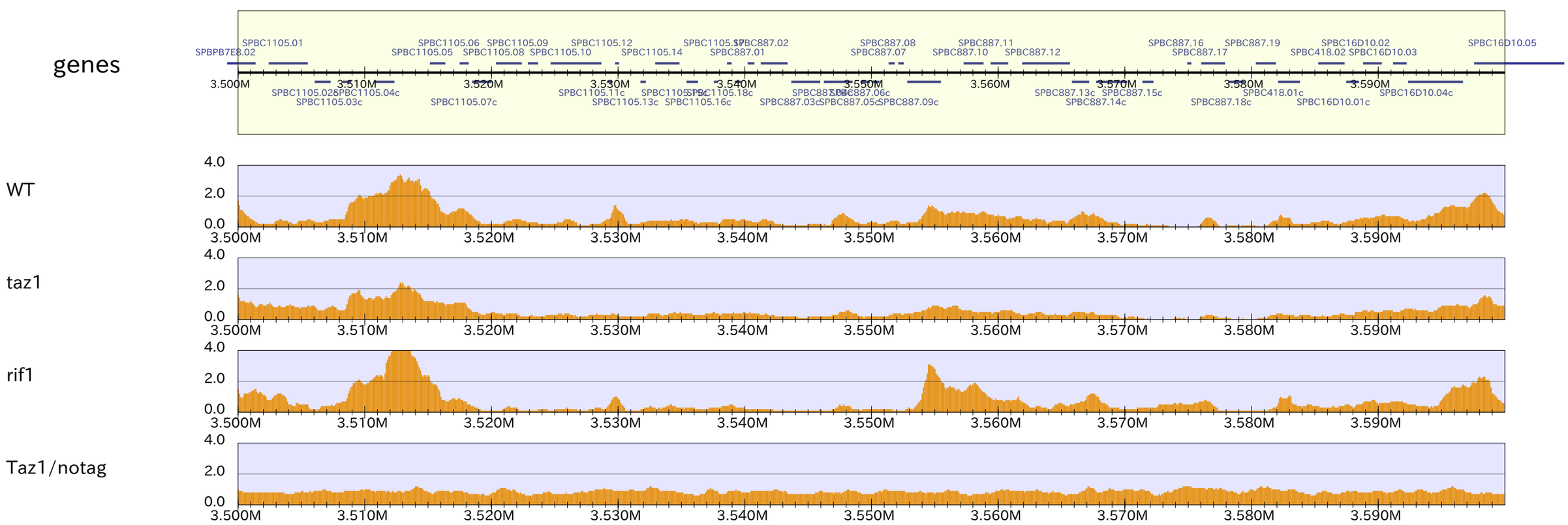
genes
WT
taz1
rif1
Taz1/notag
4.0
2.0
0.0
3.500M
3.510M
3.520M
3.530M
3.540M
3.550M
3.560M
3.570M
3.580M
3.590M

chrII_13

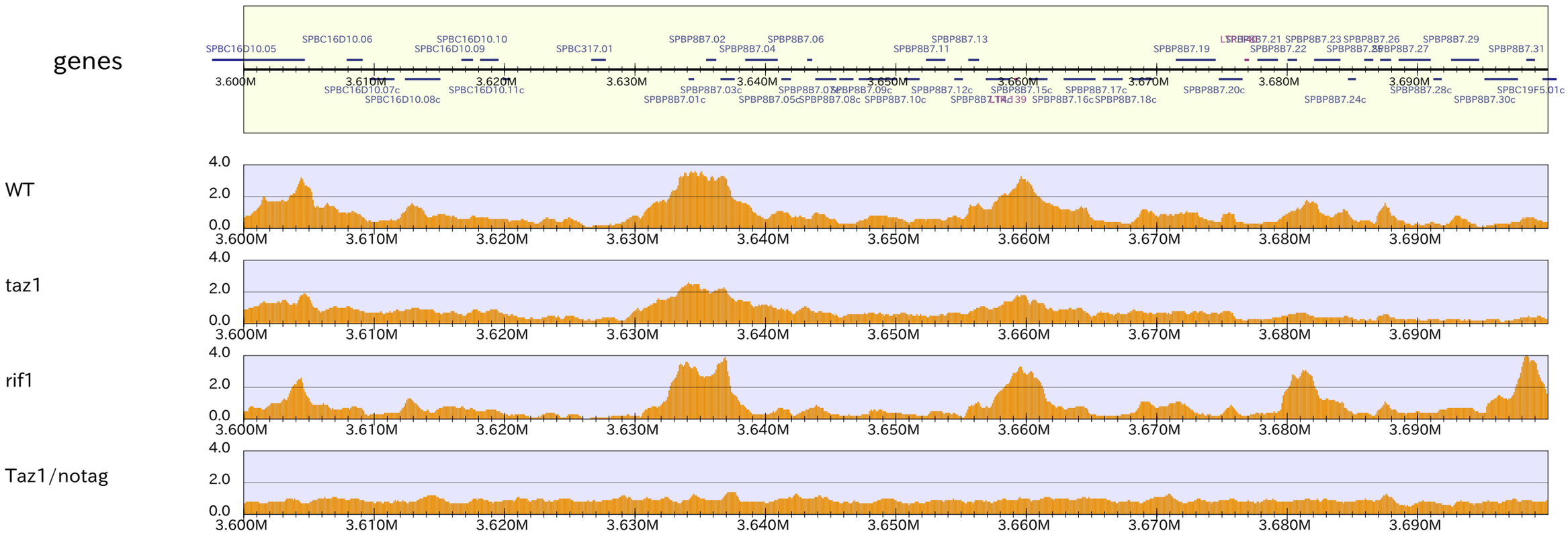
genes
WT
taz1
rif1
Taz1/notag
4.0
2.0
0.0
3.600M
3.610M
3.620M
3.630M
3.640M
3.650M
3.660M
3.670M
3.680M
3.690M

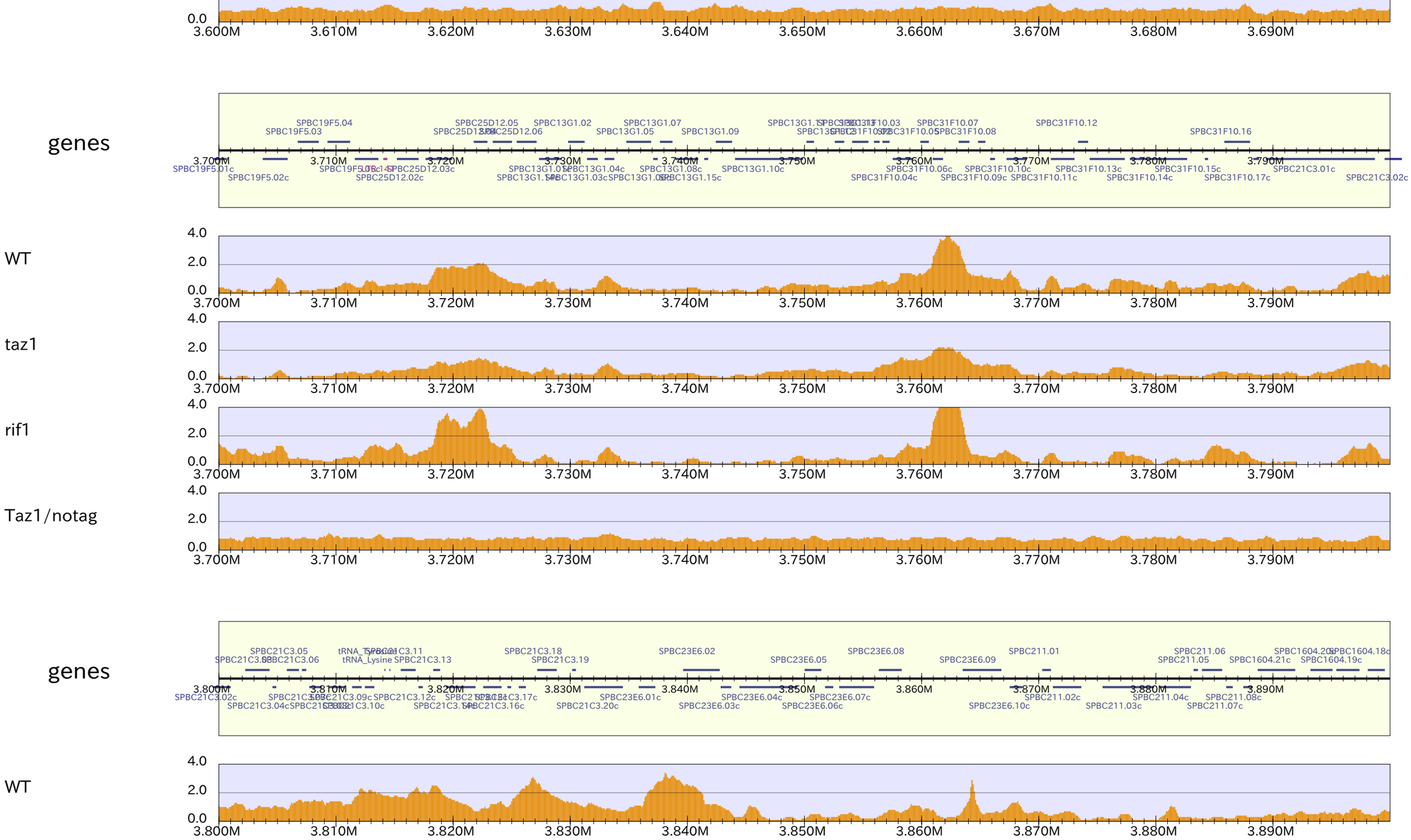
genes
WT
taz1
rif1
Taz1/notag
4.0
2.0
0.0
3.700M
3.710M
3.720M
3.730M
3.740M
3.750M
3.760M
3.770M
3.780M
3.790M

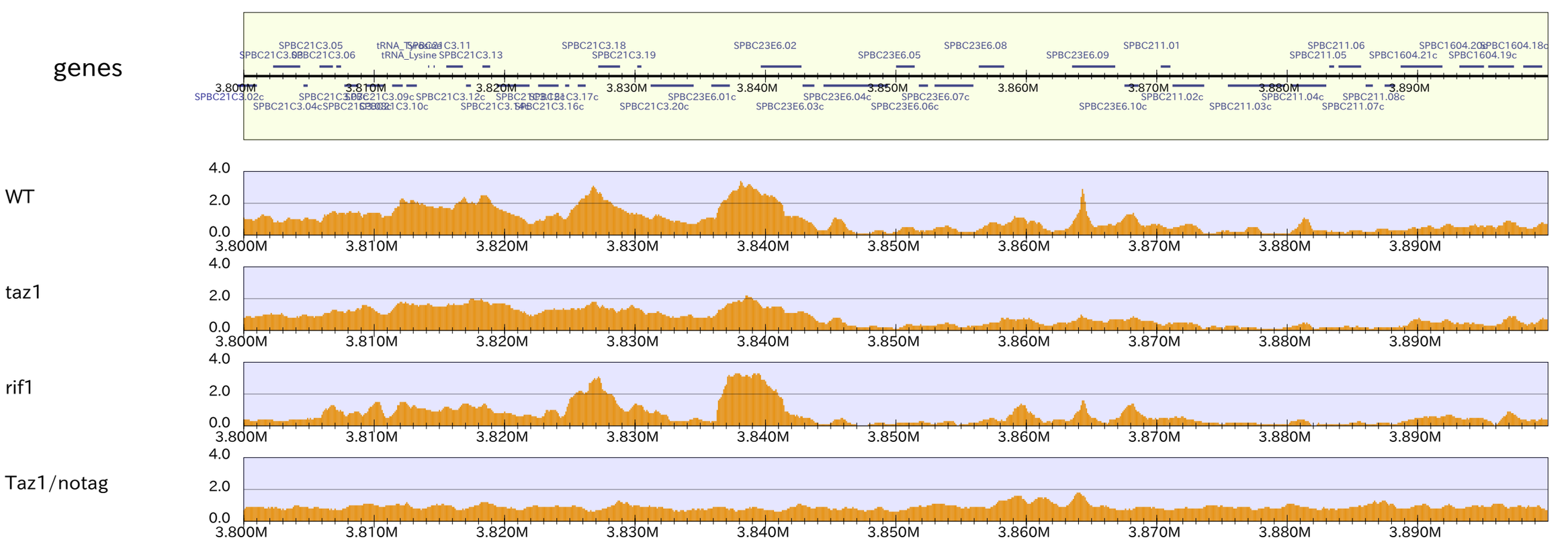
genes
WT
taz1
rif1
Taz1/notag
4.0
2.0
0.0
3.800M
3.810M
3.820M
3.830M
3.840M
3.850M
3.860M
3.870M
3.880M
3.890M

chrII_14

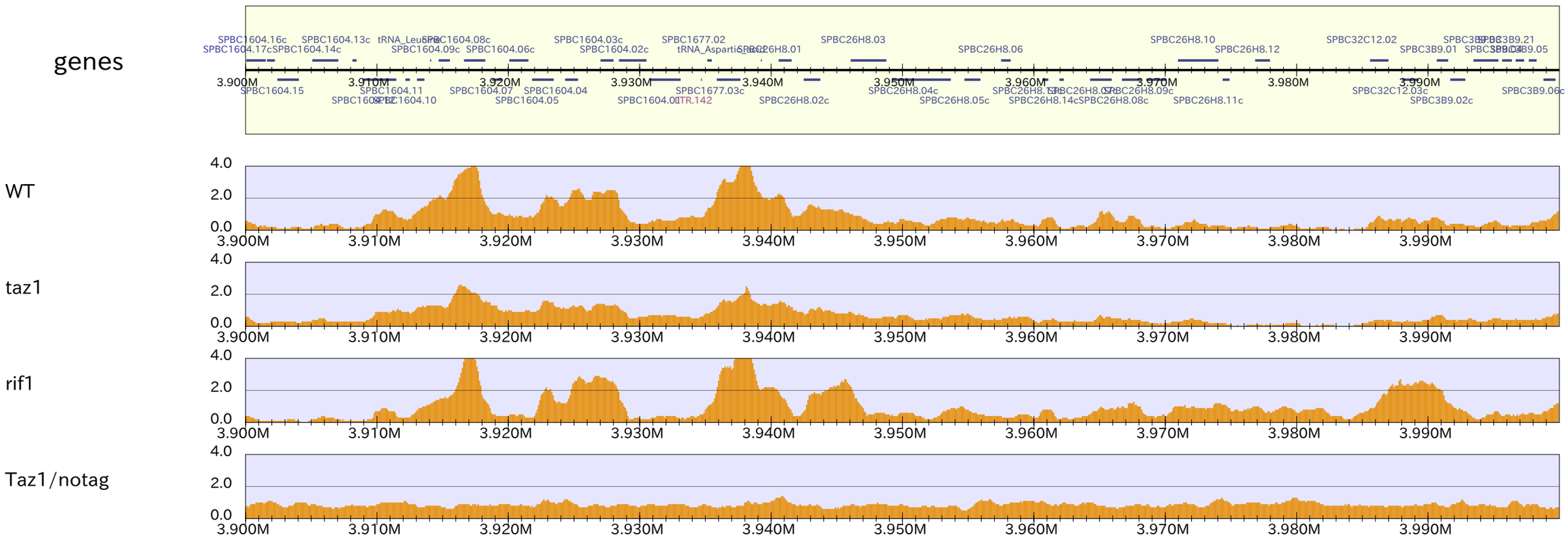
genes
WT
taz1
rif1
Taz1/notag
3.900M
3.910M
3.920M
3.930M
3.940M
3.950M
3.960M
3.970M
3.980M
3.990M
4.0
2.0
0.0

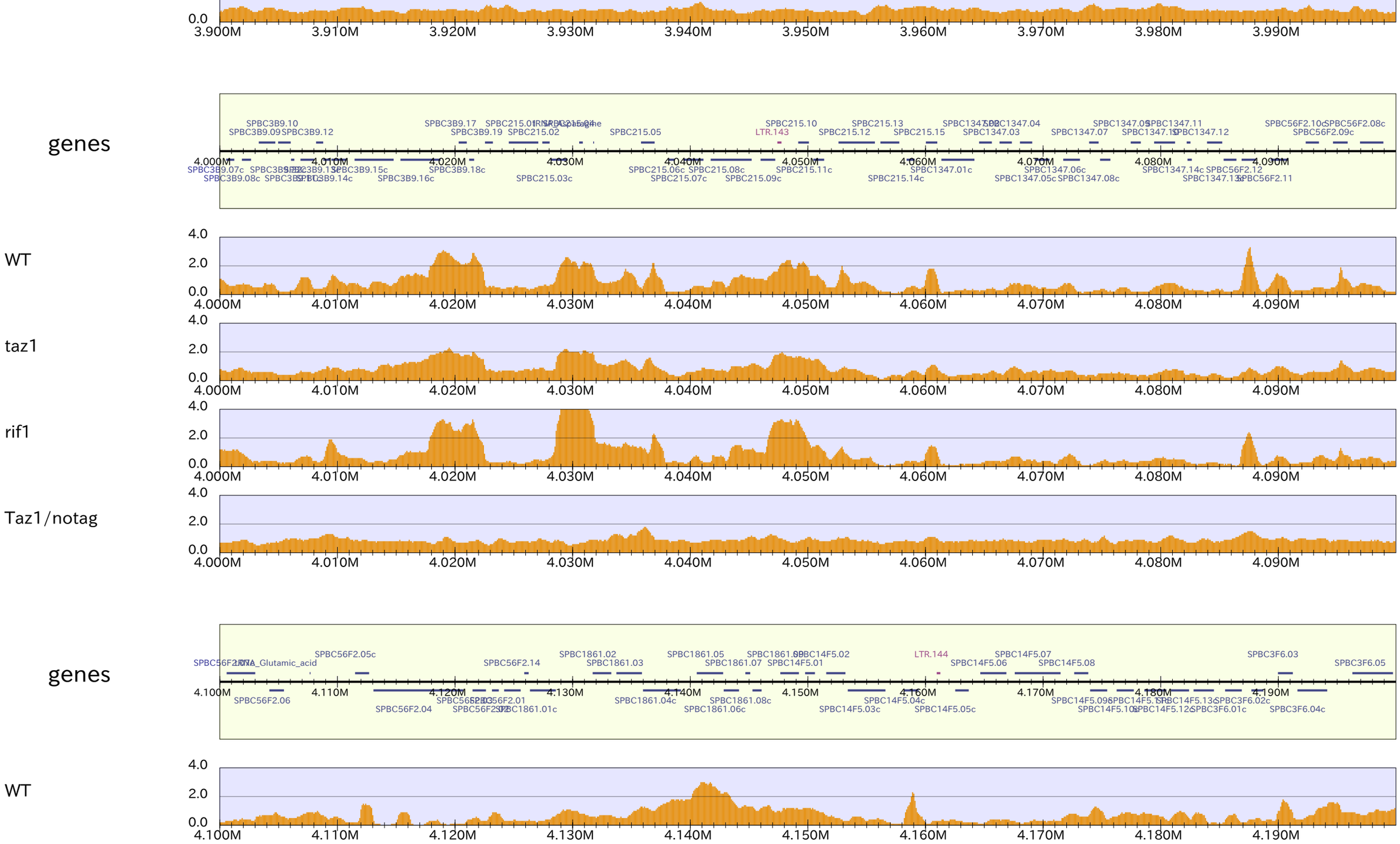
genes
WT
taz1
rif1
Taz1/notag
4.000M
4.010M
4.020M
4.030M
4.040M
4.050M
4.060M
4.070M
4.080M
4.090M
4.0
2.0
0.0

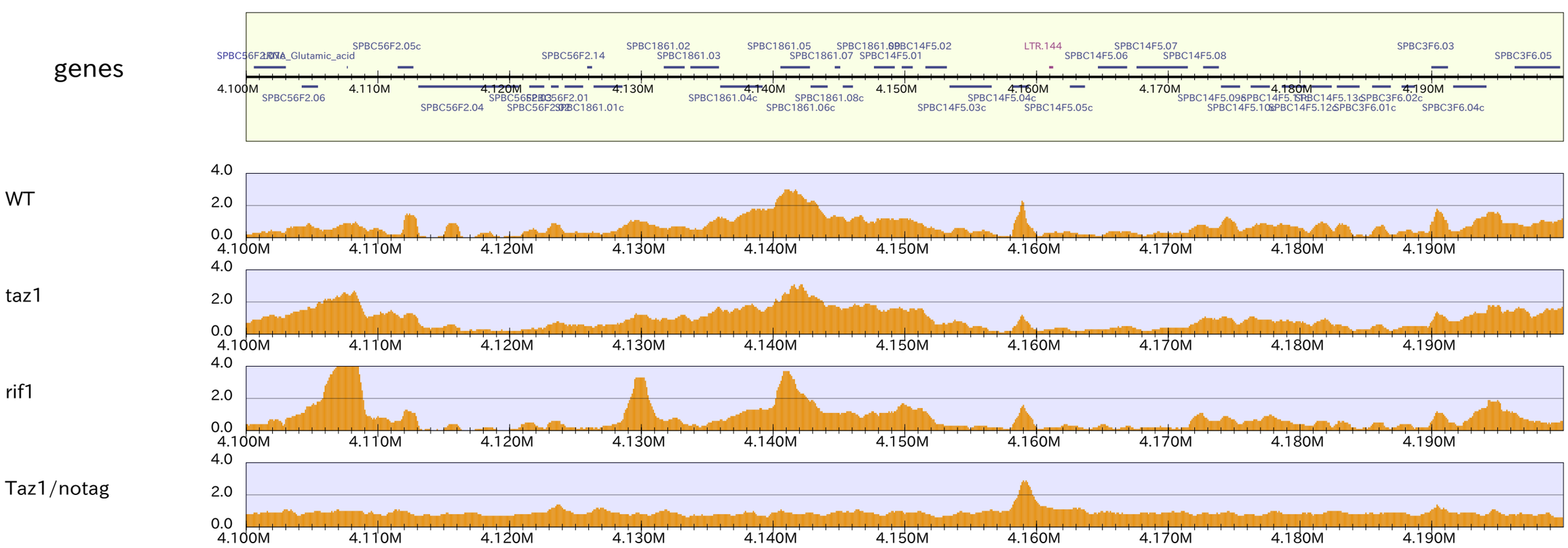
genes
WT
taz1
rif1
Taz1/notag
4.100M
4.110M
4.120M
4.130M
4.140M
4.150M
4.160M
4.170M
4.180M
4.190M
4.0
2.0
0.0

chrII_15

genes

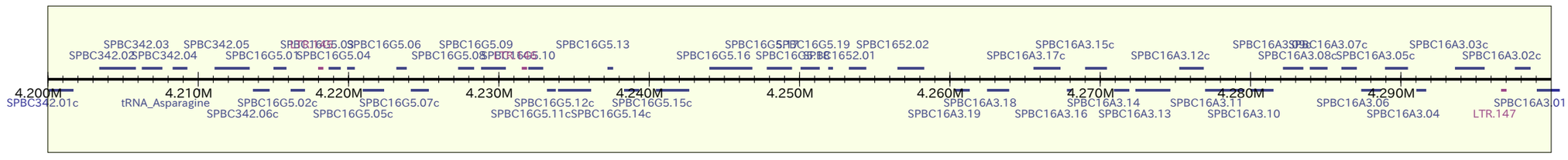

WT

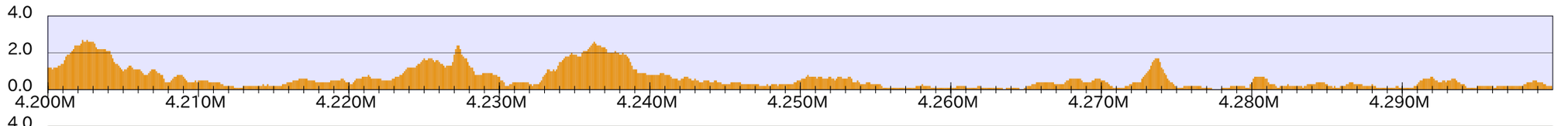

taz1

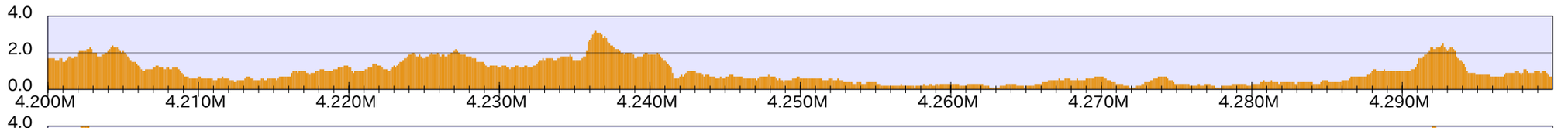

rif1

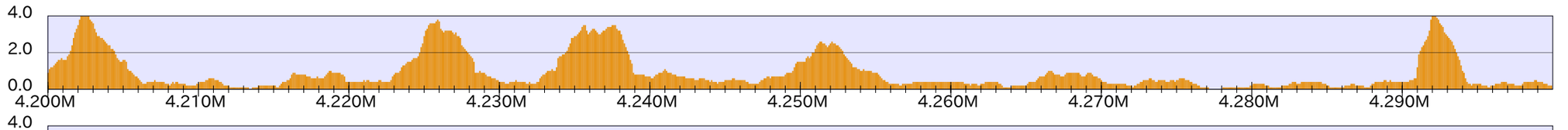

Taz1/notag

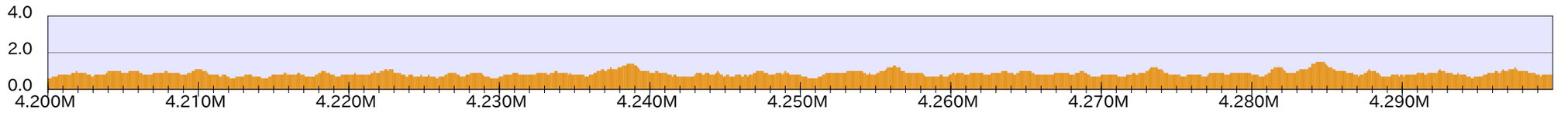

genes

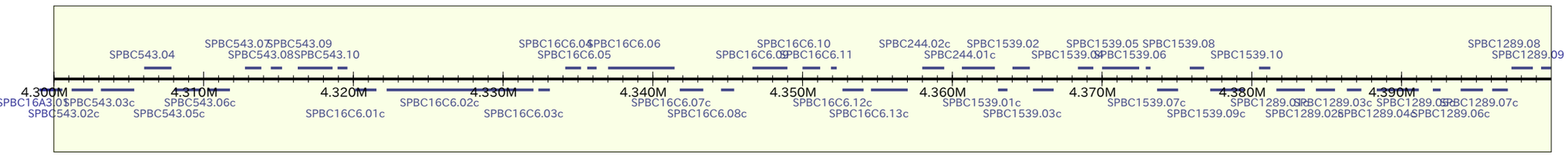

WT

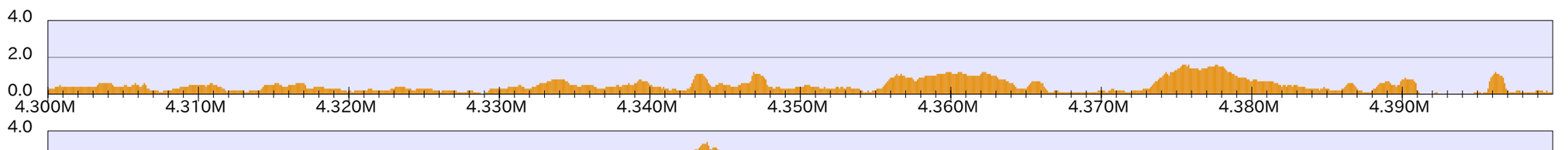

taz1

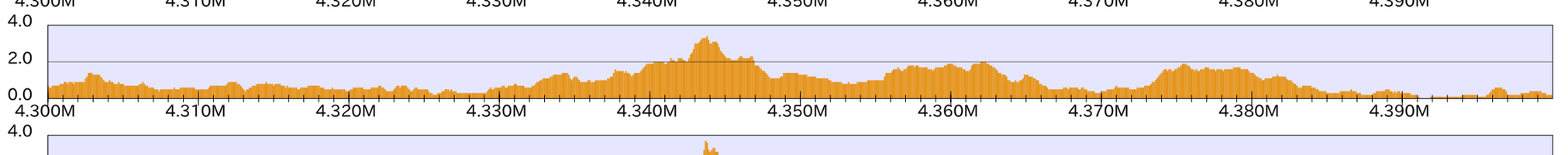

rif1

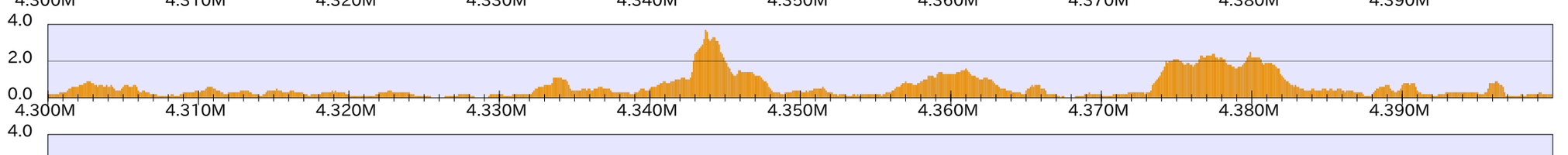

Taz1/notag

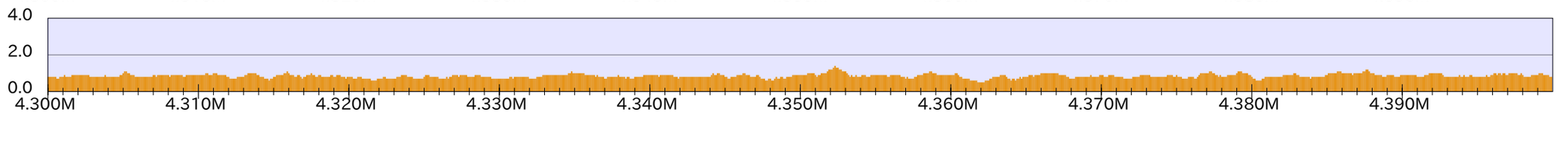

genes

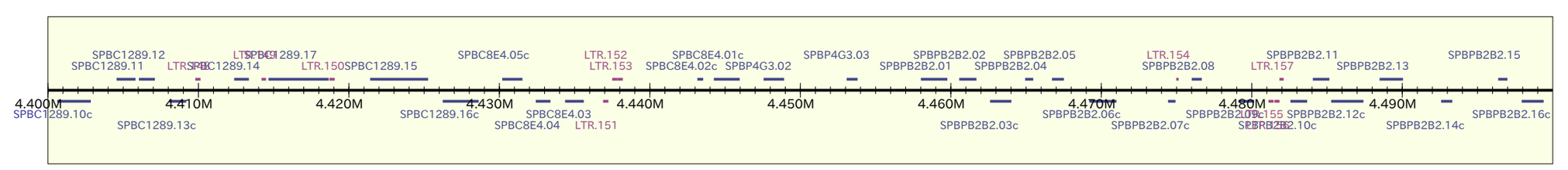

WT

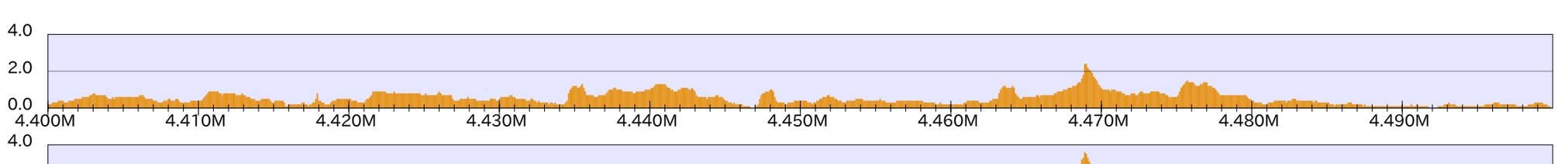

taz1

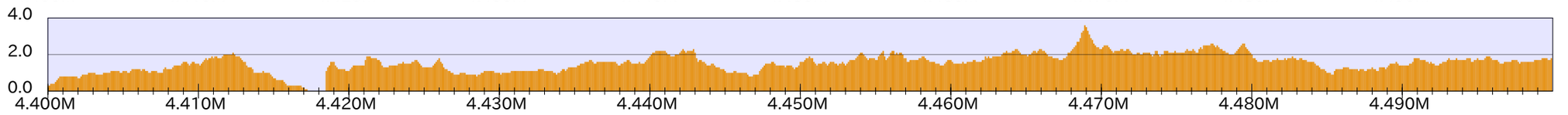

rif1

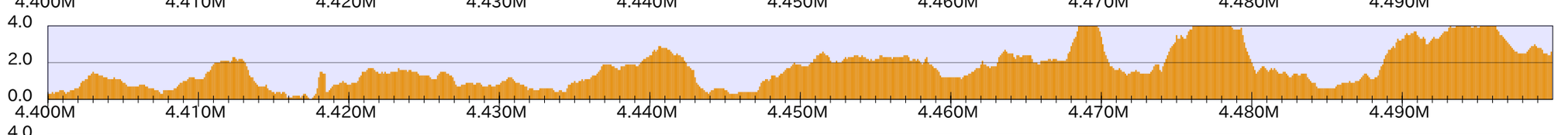

Taz1/notag

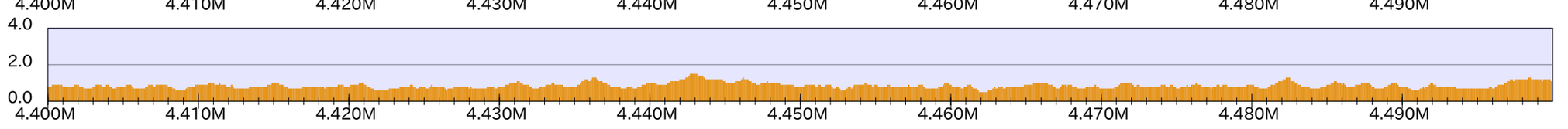

chrII_16

genes

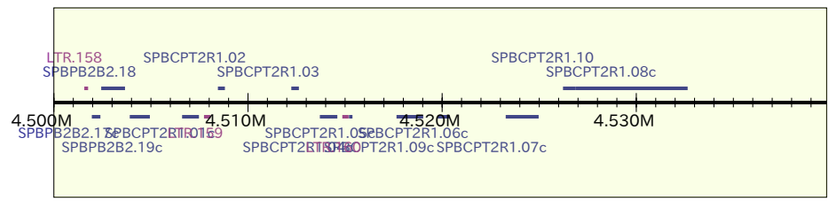

WT

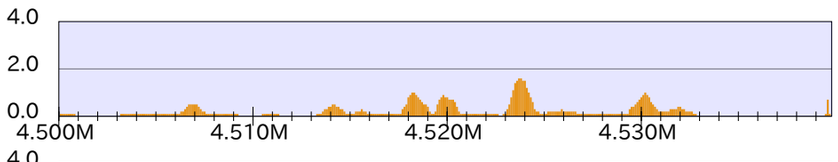

taz1

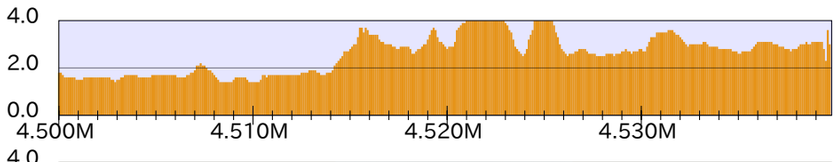

rif1

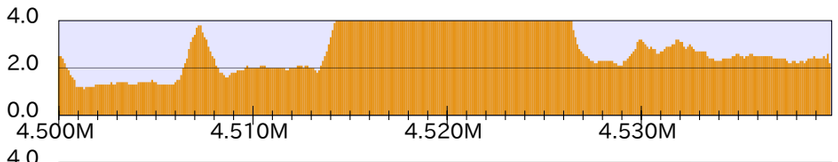

Taz1/notag

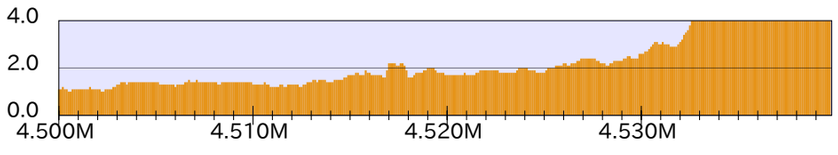

chrIII_1

genes

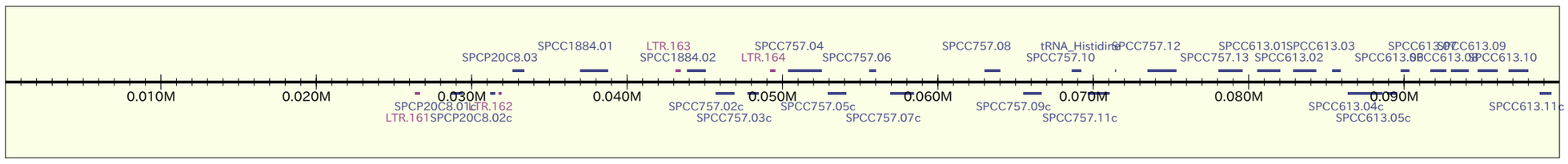

WT

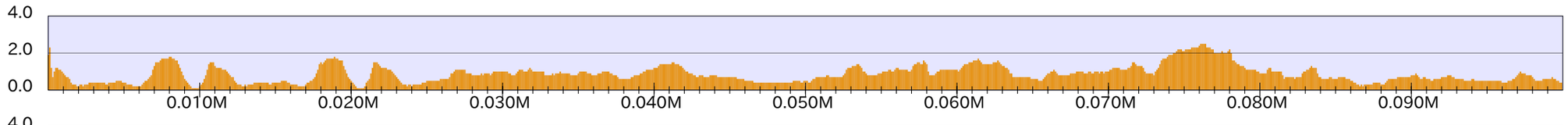

taz1

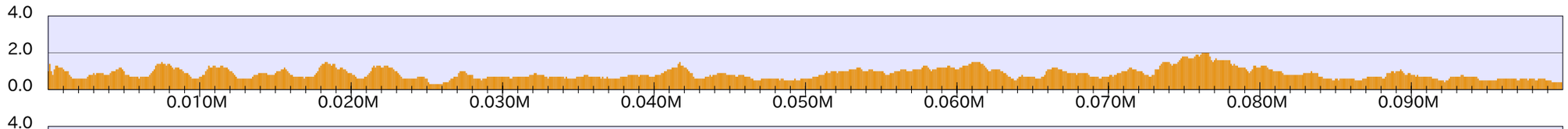

rif1

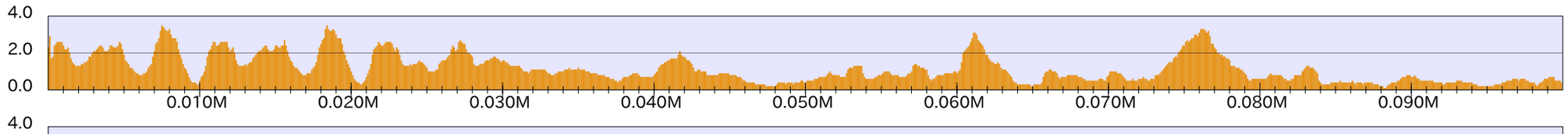

Taz1/notag

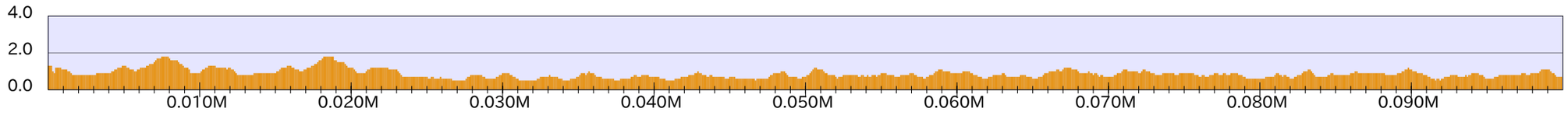

genes

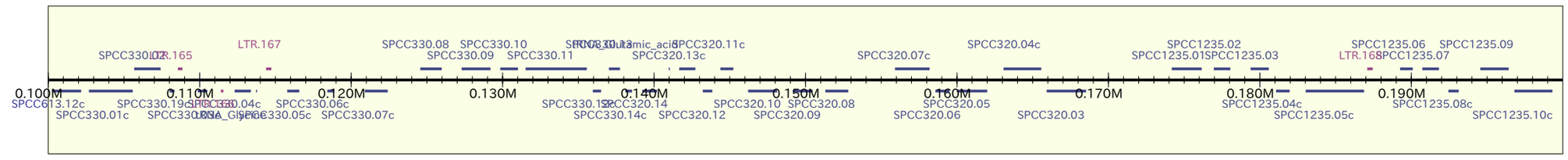

WT

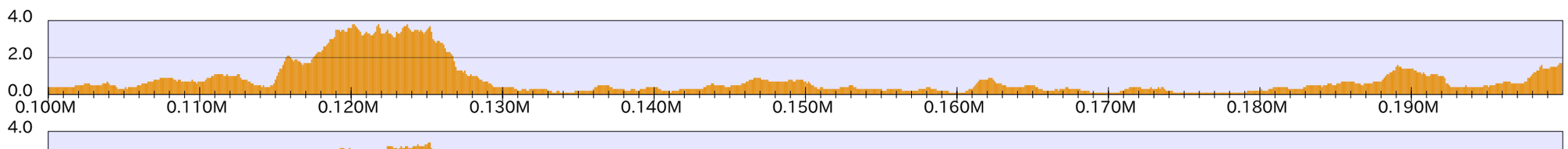

taz1

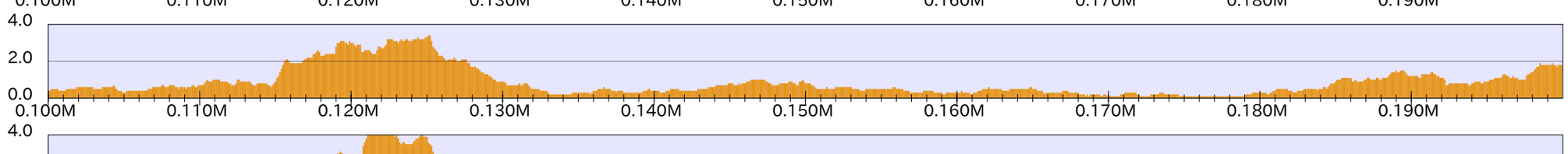

rif1

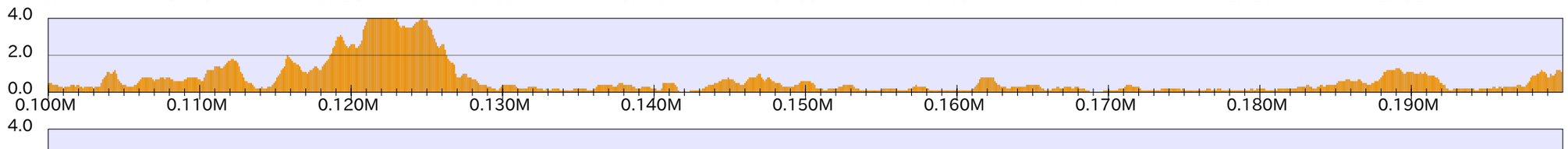

Taz1/notag

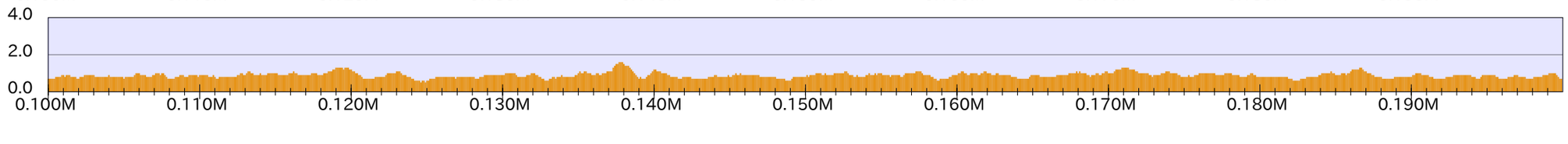

genes

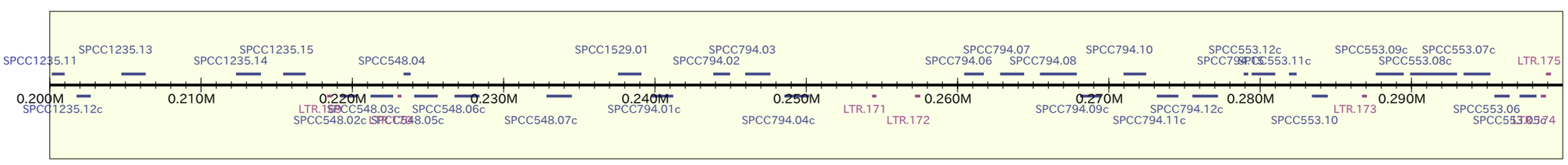

WT

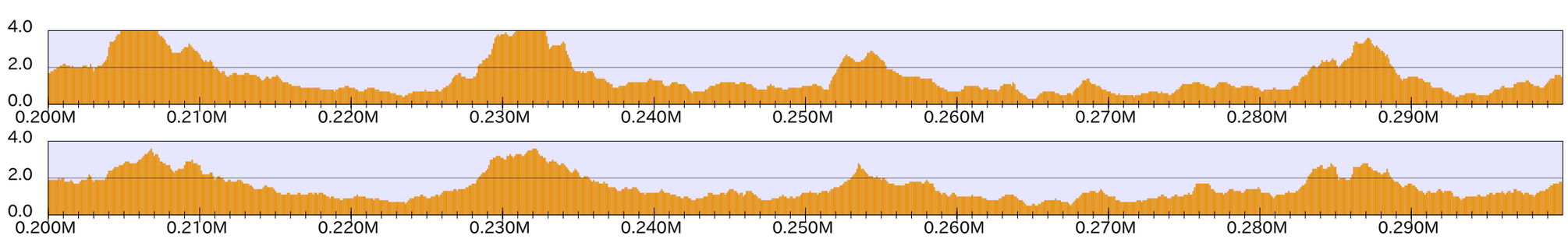

taz1

rif1

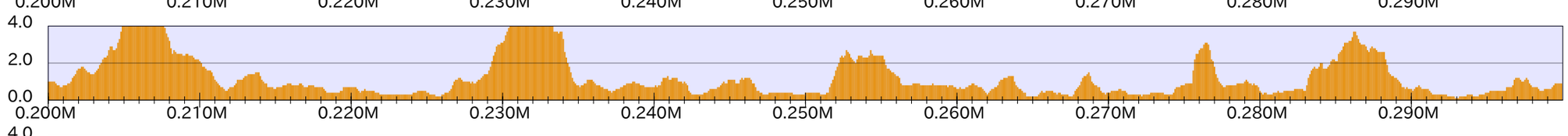

Taz1/notag

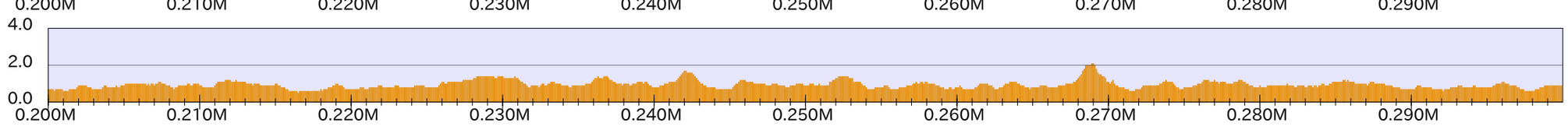

chrIII_2

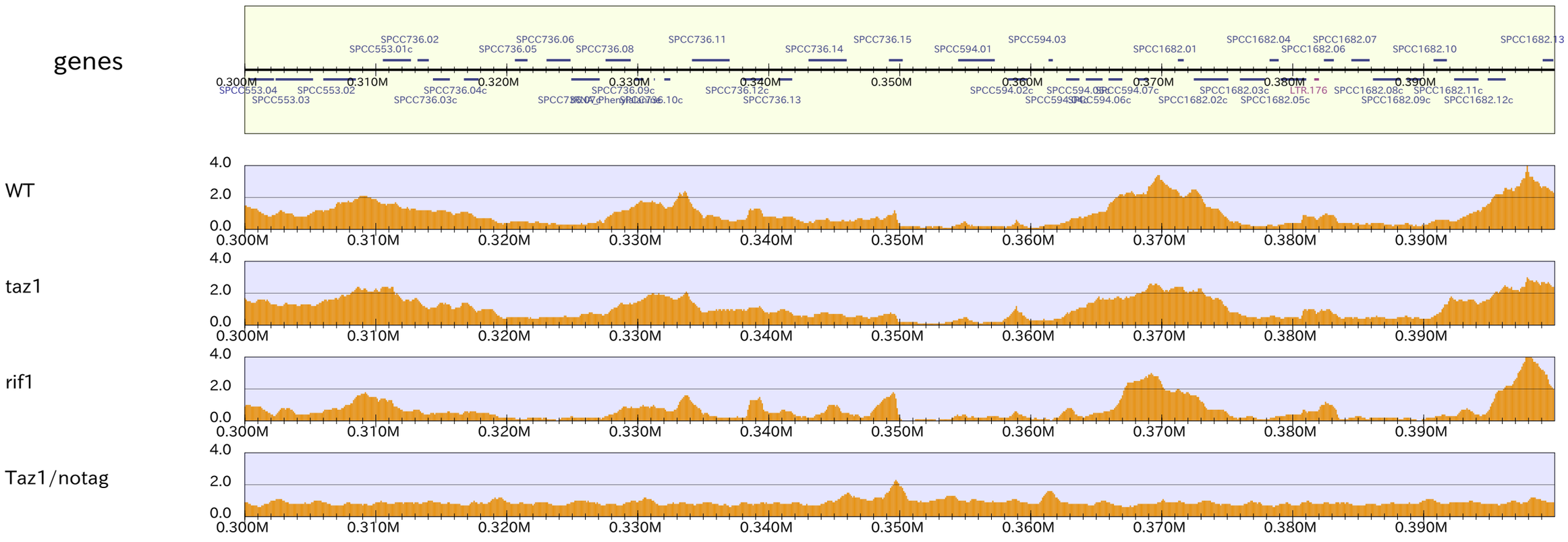
genes
WT
taz1
rif1
Taz1/notag
0.300M
0.310M
0.320M
0.330M
0.340M
0.350M
0.360M
0.370M
0.380M
0.390M
4.0
2.0
0.0

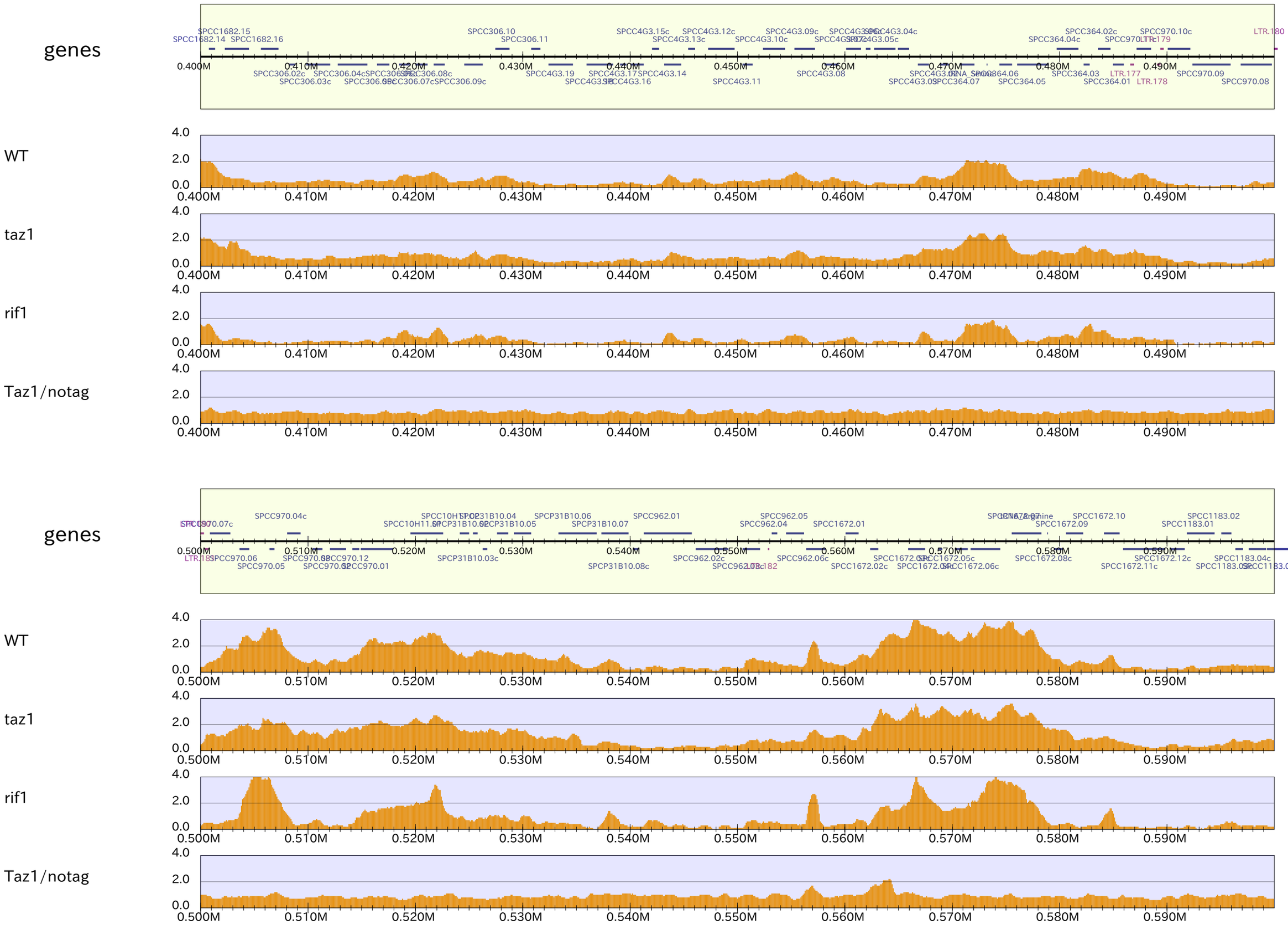
genes
WT
taz1
rif1
Taz1/notag
0.400M
0.410M
0.420M
0.430M
0.440M
0.450M
0.460M
0.470M
0.480M
0.490M
4.0
2.0
0.0

genes
WT
taz1
rif1
Taz1/notag
0.500M
0.510M
0.520M
0.530M
0.540M
0.550M
0.560M
0.570M
0.580M
0.590M
4.0
2.0
0.0

chrIII_3

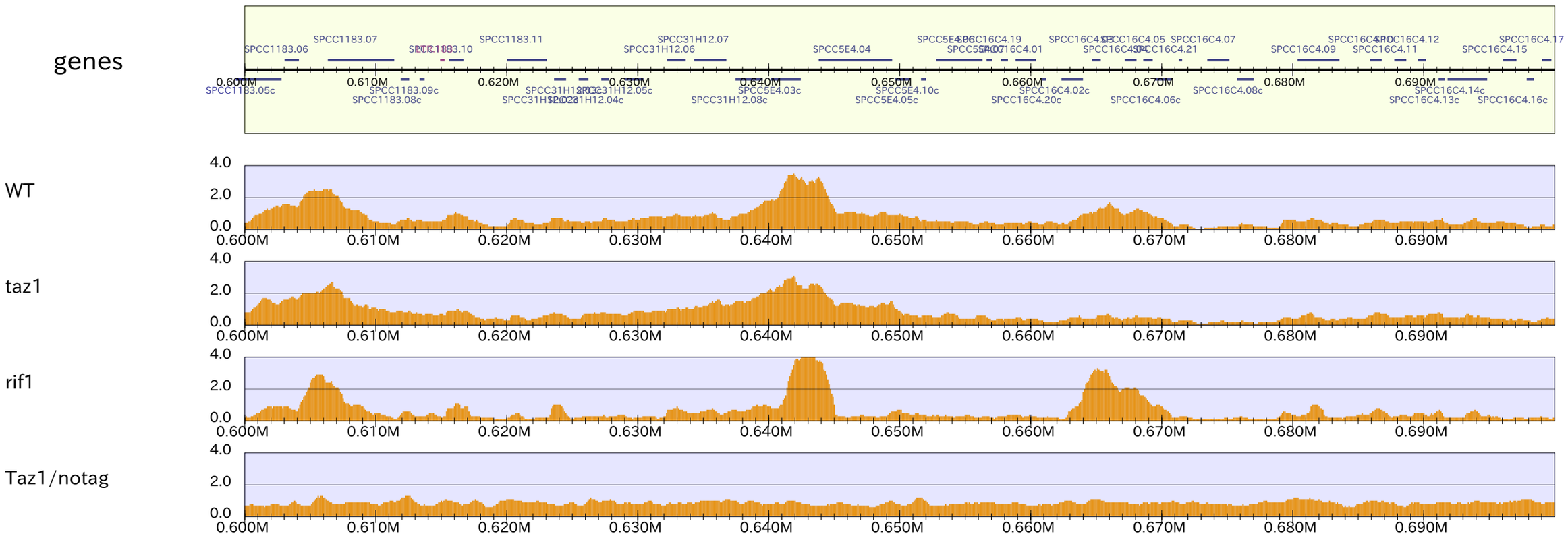
genes
SPCC1183.06
SPCC1183.07
SPCC1183.10
SPCC1183.11
SPCC31H12.06
SPCC31H12.07
SPCC5E4.04
SPCC16C4.19
SPCC16C4.01
SPCC16C4.21
SPCC16C4.09
SPCC16C4.11
SPCC16C4.12
SPCC16C4.15
SPCC16C4.17
SPCC1183.05c
SPCC1183.09c
SPCC1183.08c
SPCC31H12.05c
SPCC31H12.04c
SPCC31H12.08c
SPCC5E4.03c
SPCC5E4.10c
SPCC5E4.05c
SPCC16C4.20c
SPCC16C4.02c
SPCC16C4.06c
SPCC16C4.08c
SPCC16C4.14c
SPCC16C4.13c
SPCC16C4.16c
0.600M
0.610M
0.620M
0.630M
0.640M
0.650M
0.660M
0.670M
0.680M
0.690M
WT
taz1
rif1
Taz1/notag
4.0
2.0
0.0

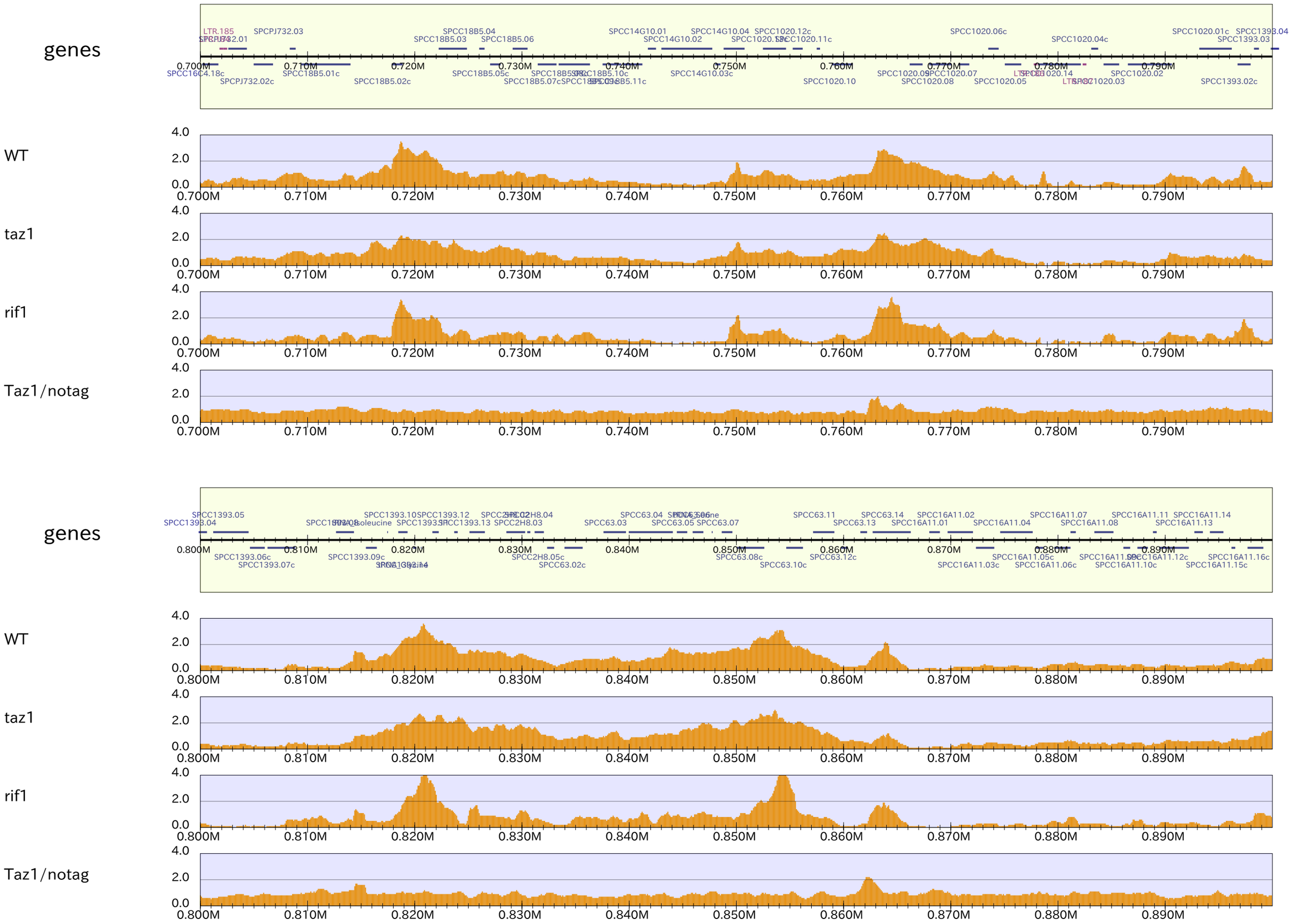
genes
LTR.185
SPCPJ732.03
SPCC18B5.04
SPCC18B5.03
SPCC18B5.06
SPCC14G10.01
SPCC14G10.04
SPCC1020.12c
SPCC14G10.02
SPCC1020.06c
SPCC1020.04c
SPCC1020.01c
SPCC1393.04
SPCC1393.03
SPCC16C4.18c
SPCPJ732.02c
SPCC18B5.01c
SPCC18B5.02c
SPCC18B5.05c
SPCC18B5.07c
SPCC14G10.03c
SPCC1020.10
SPCC1020.09
SPCC1020.07
SPCC1020.08
SPCC1020.05
SPCC1020.14
SPCC1020.03
SPCC1020.02
SPCC1393.02c
0.700M
0.710M
0.720M
0.730M
0.740M
0.750M
0.760M
0.770M
0.780M
0.790M
WT
taz1
rif1
Taz1/notag
4.0
2.0
0.0

genes
SPCC1393.05
SPCC1393.04
SPCC1393.10
SPCC1393.12
SPCC2H8.04
SPCC63.04
SPCC63.11
SPCC63.14
SPCC16A11.02
SPCC16A11.07
SPCC16A11.11
SPCC16A11.14
SPCC1393.13
SPCC2H8.03
SPCC63.03
SPCC63.05
SPCC63.07
SPCC63.13
SPCC16A11.01
SPCC16A11.04
SPCC16A11.08
SPCC16A11.13
SPCC1393.06c
SPCC1393.07c
SPCC1393.09c
SPCC2H8.05c
SPCC63.02c
SPCC63.08c
SPCC63.10c
SPCC63.12c
SPCC16A11.03c
SPCC16A11.05c
SPCC16A11.06c
SPCC16A11.09c
SPCC16A11.10c
SPCC16A11.12c
SPCC16A11.15c
SPCC16A11.16c
0.800M
0.810M
0.820M
0.830M
0.840M
0.850M
0.860M
0.870M
0.880M
0.890M
WT
taz1
rif1
Taz1/notag
4.0
2.0
0.0

chrIII_4

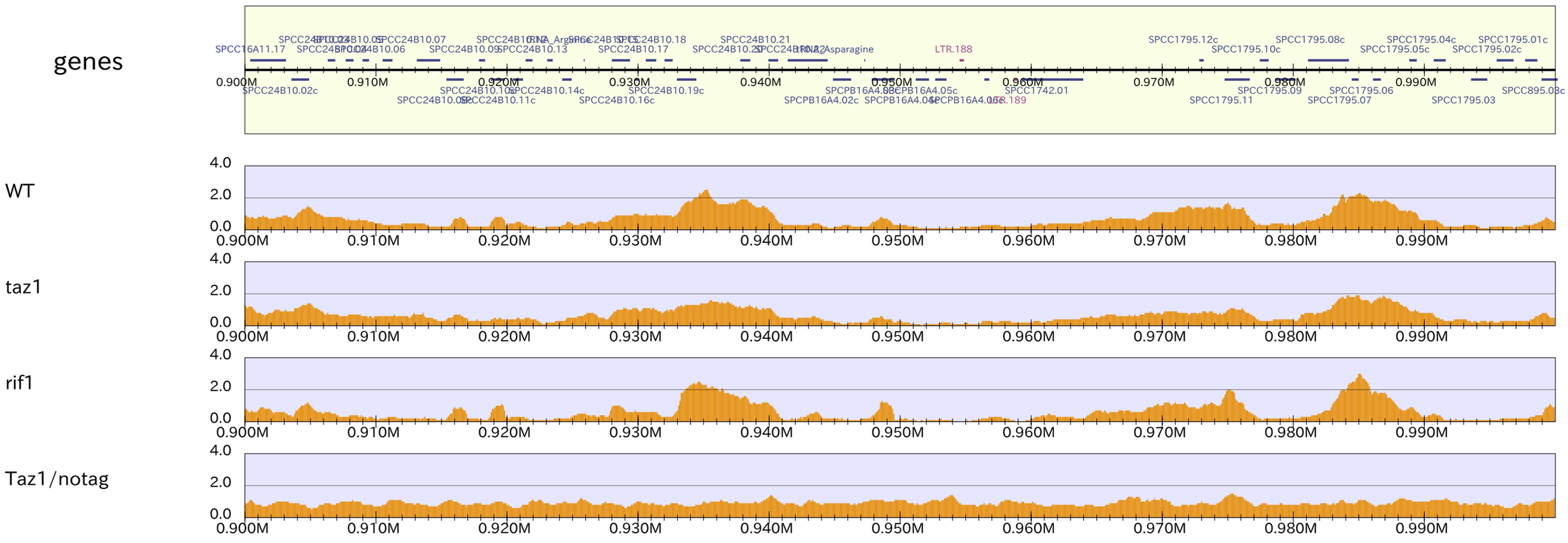
genes
WT
taz1
rif1
Taz1/notag
SPCC16A11.17
SPCC24B10.02c
SPCC24B10.05c
SPCC24B10.11c
SPCC24B10.14c
SPCC24B10.16c
SPCC24B10.19c
SPCPB16A4.02c
SPCPB16A4.05c
SPCC1742.01
LTR.189
SPCC1795.11
SPCC1795.09
SPCC1795.07
SPCC1795.06
SPCC1795.03
SPCC895.03c
0.900M
0.910M
0.920M
0.930M
0.940M
0.950M
0.960M
0.970M
0.980M
0.990M
4.0
2.0
0.0

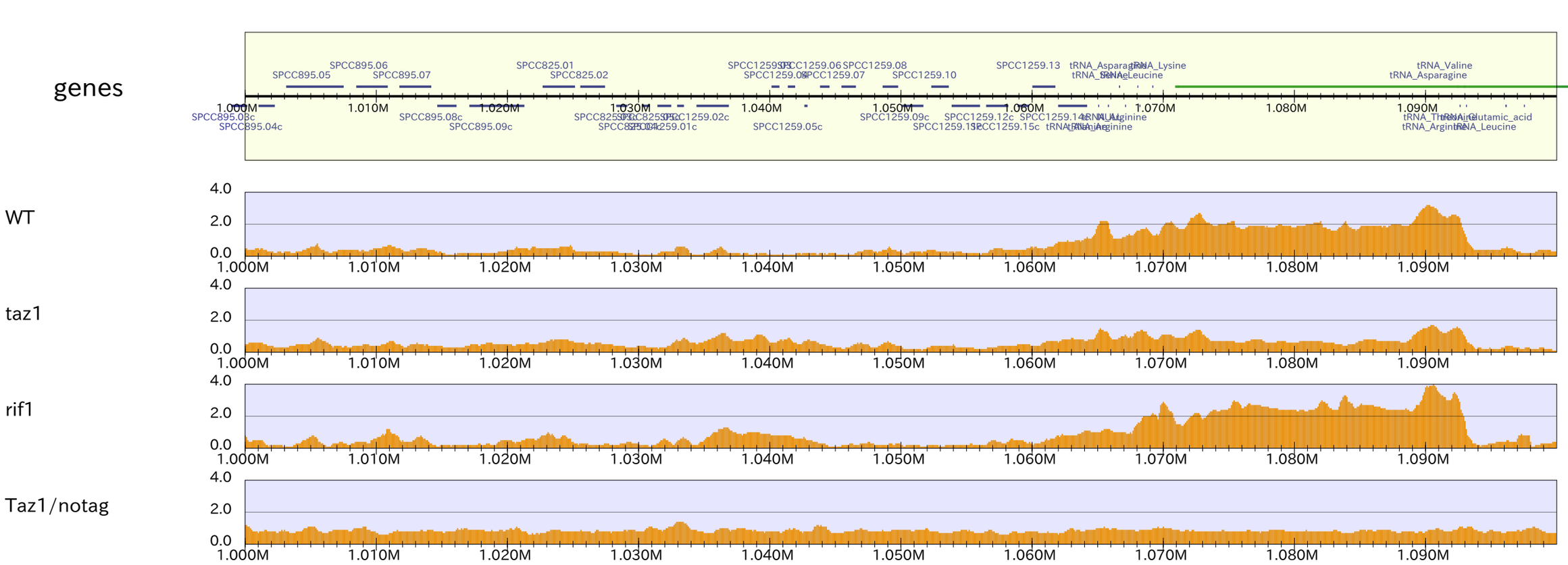
genes
WT
taz1
rif1
Taz1/notag
CEN_chr3
SPCC895.05
SPCC895.06
SPCC895.07
SPCC895.08c
SPCC895.09c
SPCC825.01
SPCC825.02
SPCC1259.01c
SPCC1259.02c
SPCC1259.05c
SPCC1259.06
SPCC1259.07
SPCC1259.08
SPCC1259.09c
SPCC1259.10
SPCC1259.12c
SPCC1259.13
tRNA_Asparagine
tRNA_Lysine
tRNA_Leucine
tRNA_Valine
tRNA_Glutamic_acid
tRNA_Arginine
1.000M
1.010M
1.020M
1.030M
1.040M
1.050M
1.060M
1.070M
1.080M
1.090M
4.0
2.0
0.0

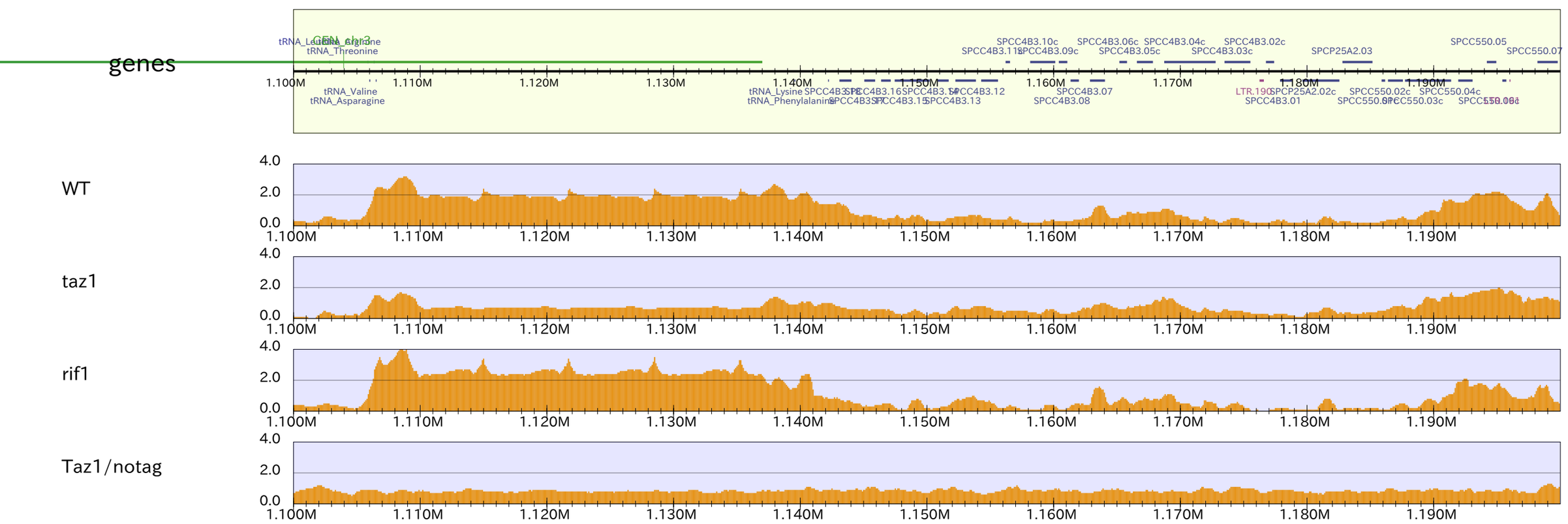
genes
WT
taz1
rif1
Taz1/notag
CEN_chr3
tRNA_Leucine
tRNA_Threonine
tRNA_Valine
tRNA_Asparagine
tRNA_Lysine
tRNA_Phenylalanine
SPCC4B3.10c
SPCC4B3.09c
SPCC4B3.06c
SPCC4B3.05c
SPCC4B3.04c
SPCC4B3.03c
SPCC4B3.02c
SPCC4B3.16
SPCC4B3.13
SPCC4B3.12
SPCC4B3.08
SPCC4B3.07
SPCC4B3.01
SPCP25A2.03
SPCP25A2.02c
SPCC550.05
SPCC550.07
SPCC550.02c
SPCC550.04c
SPCC550.03c
LTR.190
1.100M
1.110M
1.120M
1.130M
1.140M
1.150M
1.160M
1.170M
1.180M
1.190M
4.0
2.0
0.0

chrIII_5

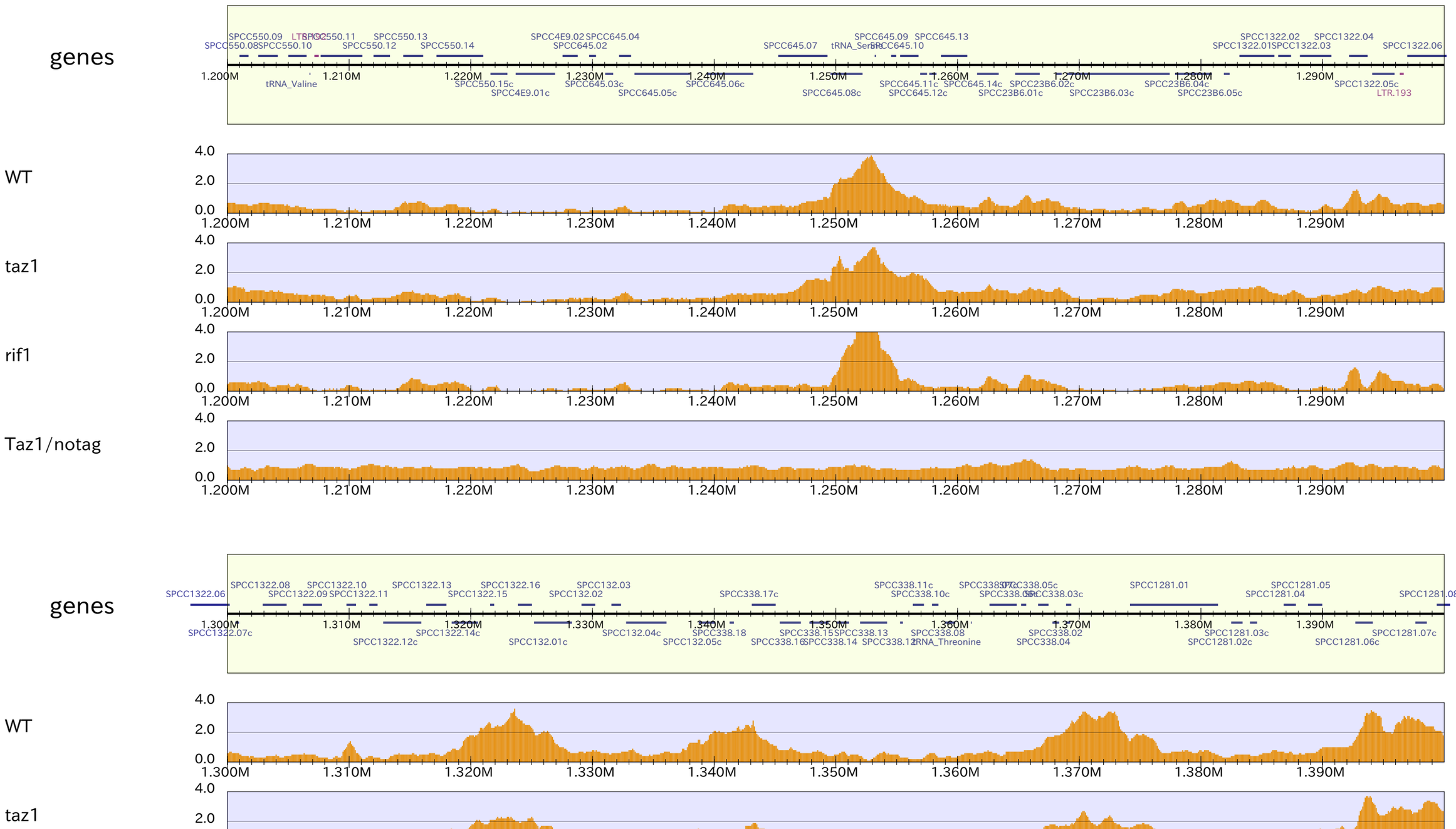
genes
SPCC550.09 SPCC550.11 SPCC550.13 SPCC4E9.02 SPCC645.04 SPCC645.09 SPCC645.13 SPCC1322.02 SPCC1322.04
SPCC550.08 SPCC550.10 SPCC550.12 SPCC550.14 SPCC645.02 SPCC645.07 SPCC645.10 SPCC1322.01 SPCC1322.03 SPCC1322.06
1.200M 1.210M 1.220M 1.230M 1.240M 1.250M 1.260M 1.270M 1.280M 1.290M
tRNA_Valine SPCC550.15c SPCC645.03c SPCC645.06c SPCC645.11c SPCC645.14c SPCC23B6.02c SPCC23B6.04c SPCC1322.05c
SPCC4E9.01c SPCC645.05c SPCC645.08c SPCC645.12c SPCC23B6.01c SPCC23B6.03c SPCC23B6.05c LTR.193
WT
taz1
rif1
Taz1/notag
4.0
2.0
0.0

genes
SPCC1322.06 SPCC1322.08 SPCC1322.10 SPCC1322.13 SPCC1322.16 SPCC132.03 SPCC338.11c SPCC338.05c SPCC1281.01 SPCC1281.05
SPCC1322.09 SPCC1322.11 SPCC1322.15 SPCC132.02 SPCC338.17c SPCC338.10c SPCC338.06c SPCC338.03c SPCC1281.04 SPCC1281.08
1.300M 1.310M 1.320M 1.330M 1.340M 1.350M 1.360M 1.370M 1.380M 1.390M
SPCC1322.07c SPCC1322.14c SPCC132.04c SPCC338.18 SPCC338.15 SPCC338.13 SPCC338.08 SPCC338.02 SPCC1281.03c SPCC1281.07c
SPCC1322.12c SPCC132.01c SPCC132.05c SPCC338.16 SPCC338.14 SPCC338.12 tRNA_Threonine SPCC338.04 SPCC1281.02c SPCC1281.06c
WT
taz1
rif1
Taz1/notag
4.0
2.0
0.0

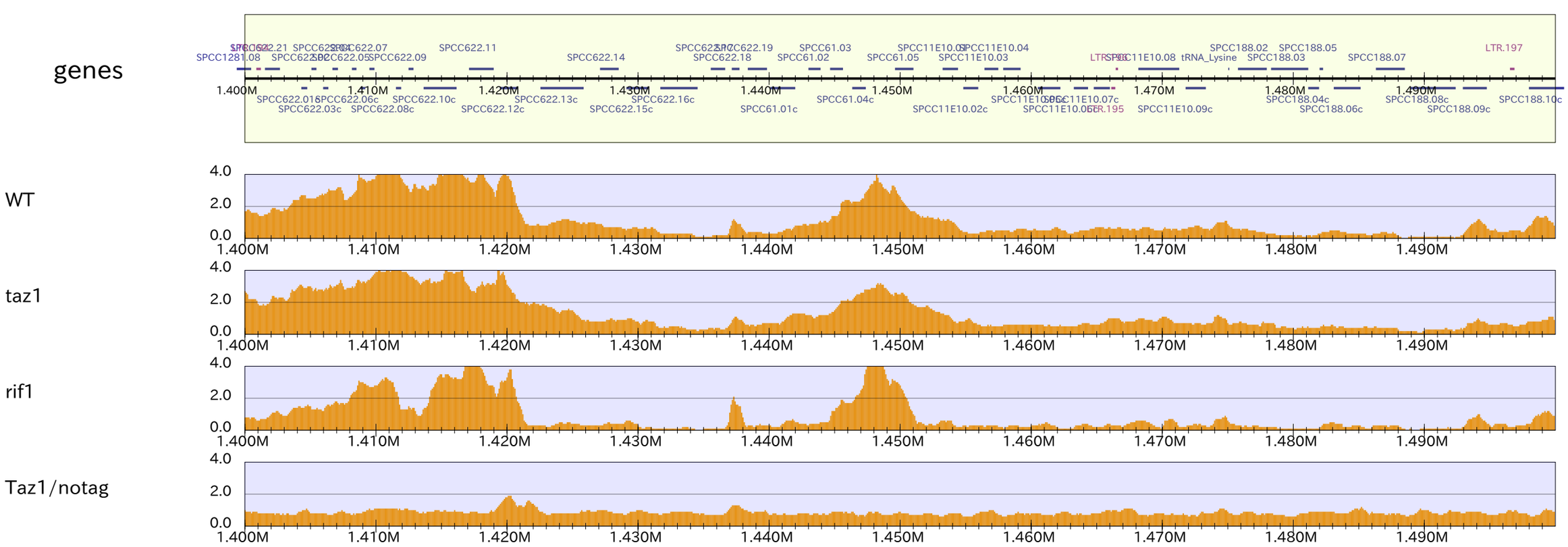
genes
SPCC1281.08 SPCC622.07 SPCC622.11 SPCC622.14 SPCC622.19 SPCC61.03 SPCC11E10.04 SPCC188.02 SPCC188.05 LTR.197
SPCC622.05 SPCC622.09 SPCC622.18 SPCC61.02 SPCC61.05 SPCC11E10.03 SPCC11E10.08 tRNA_Lysine SPCC188.03 SPCC188.07
1.400M 1.410M 1.420M 1.430M 1.440M 1.450M 1.460M 1.470M 1.480M 1.490M
SPCC622.016 SPCC622.06c SPCC622.10c SPCC622.13c SPCC622.16c SPCC61.04c SPCC11E10.07c SPCC188.04c SPCC188.08c SPCC188.10c
SPCC622.03c SPCC622.08c SPCC622.12c SPCC622.15c SPCC61.01c SPCC11E10.02c SPCC11E10.06c LTR.195 SPCC11E10.09c SPCC188.06c SPCC188.09c
WT
taz1
rif1
Taz1/notag
4.0
2.0
0.0

chrIII_6

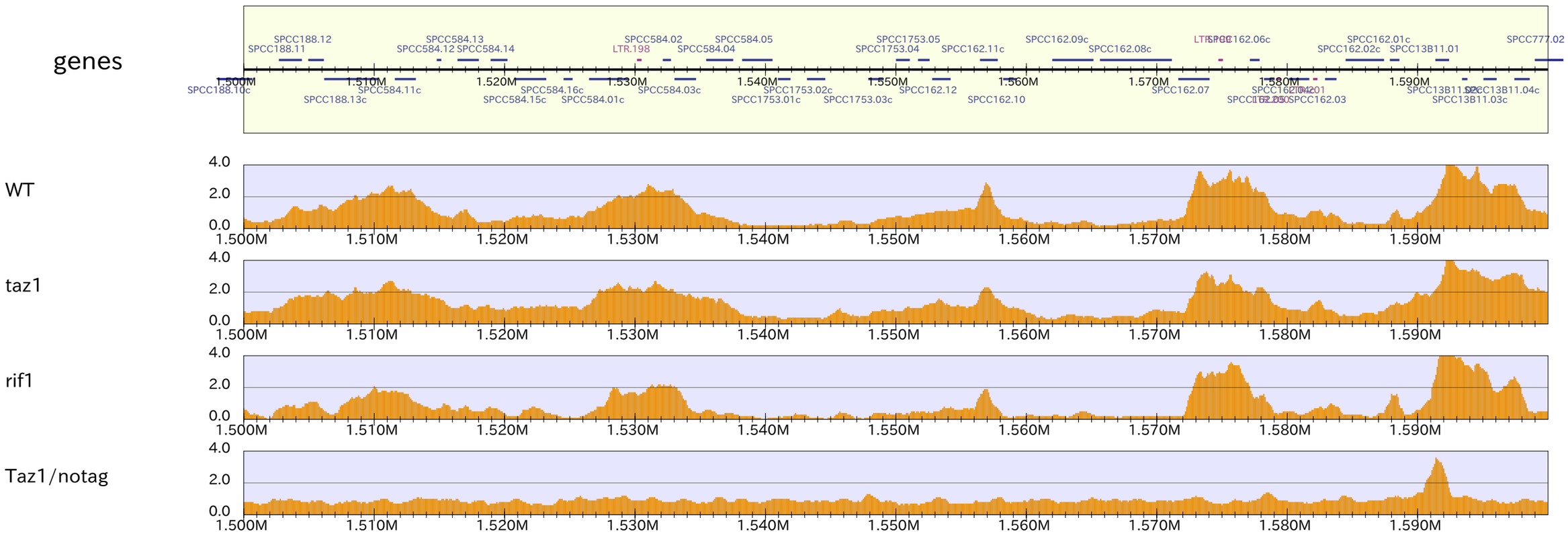
genes
SPCC188.12
SPCC188.11
SPCC584.13
SPCC584.12
SPCC584.14
SPCC584.02
LTR.198
SPCC584.05
SPCC584.04
SPCC1753.05
SPCC1753.04
SPCC162.11c
SPCC162.09c
SPCC162.08c
SPCC162.06c
SPCC162.01c
SPCC162.02c
SPCC13B11.01
SPCC777.02
1.500M
1.510M
1.520M
1.530M
1.540M
1.550M
1.560M
1.570M
1.580M
1.590M
SPCC188.10c
SPCC584.11c
SPCC188.13c
SPCC584.16c
SPCC584.15c
SPCC584.01c
SPCC584.03c
SPCC1753.02c
SPCC1753.01c
SPCC1753.03c
SPCC162.12
SPCC162.10
SPCC162.07
SPCC162.03
SPCC13B11.04c
SPCC13B11.03c
WT
taz1
rif1
Taz1/notag
4.0
2.0
0.0

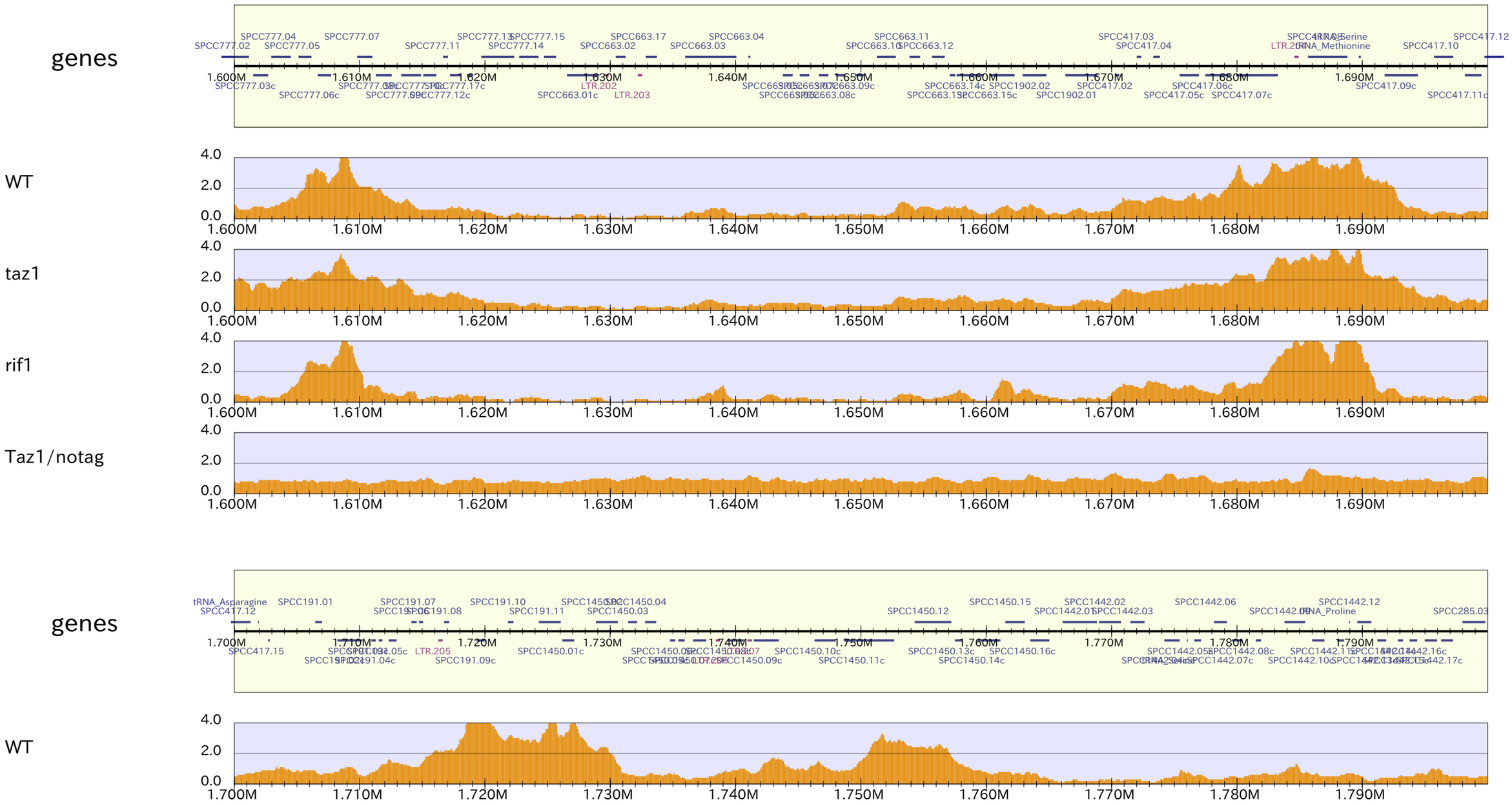
genes
SPCC777.04
SPCC777.07
SPCC777.02
SPCC777.05
SPCC777.11
SPCC777.13
SPCC777.14
SPCC777.15
SPCC663.02
SPCC663.17
SPCC663.03
SPCC663.04
SPCC663.11
SPCC663.10
SPCC663.12
SPCC417.03
SPCC417.04
tRNA_Serine
tRNA_Methionine
SPCC417.12
SPCC417.10
1.600M
1.610M
1.620M
1.630M
1.640M
1.650M
1.660M
1.670M
1.680M
1.690M
SPCC777.03c
SPCC777.06c
SPCC777.12c
SPCC777.17c
LTR.202
SPCC663.01c
LTR.203
SPCC663.14c
SPCC663.15c
SPCC1902.02
SPCC1902.01
SPCC417.02
SPCC417.06c
SPCC417.05c
SPCC417.07c
SPCC417.09c
SPCC417.11c
WT
taz1
rif1
Taz1/notag
4.0
2.0
0.0
genes
tRNA_Asparagine
SPCC417.12
SPCC191.01
SPCC191.07
SPCC191.10
SPCC1450.02
SPCC1450.04
SPCC1450.03
SPCC1450.12
SPCC1450.15
SPCC1442.02
SPCC1442.06
SPCC1442.12
tRNA_Proline
SPCC285.03
1.700M
1.710M
1.720M
1.730M
1.740M
1.750M
1.760M
1.770M
1.780M
1.790M
SPCC417.15
LTR.205
SPCC191.09c
SPCC1450.01c
SPCC1450.11c
SPCC1450.13c
SPCC1450.14c
SPCC1450.16c
SPCC1442.05c
SPCC1442.08c
SPCC1442.07c
SPCC1442.10c
SPCC1442.16c
SPCC1442.17c
WT
taz1
rif1
Taz1/notag
4.0
2.0
0.0

chrIII_7

genes

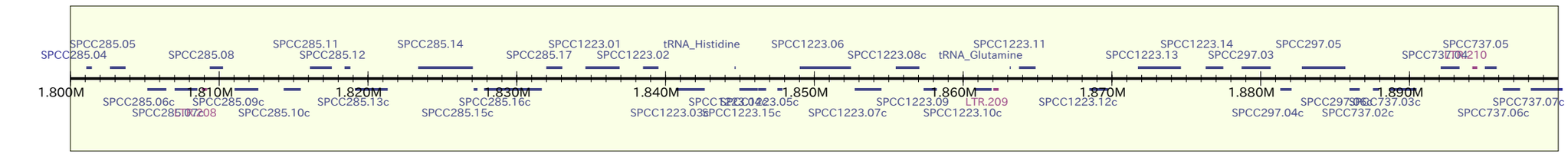

WT

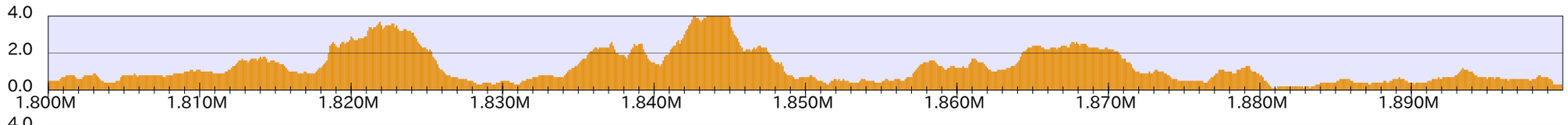

taz1

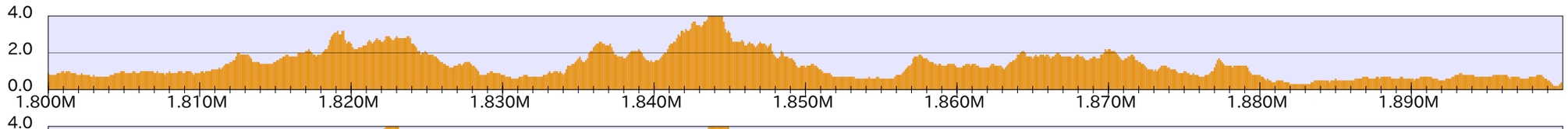

rif1

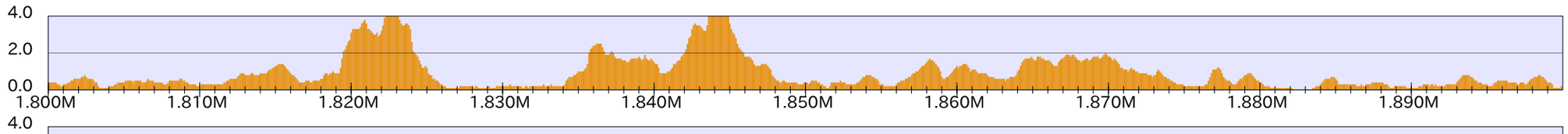

Taz1/notag

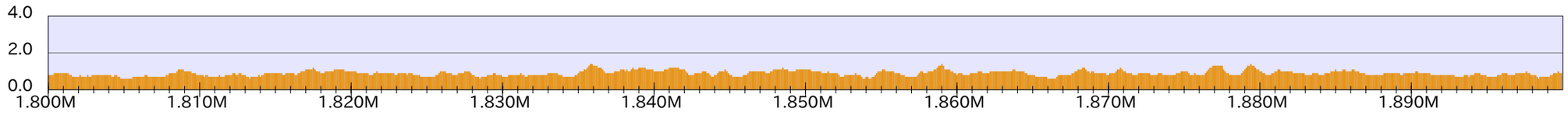

genes

WT

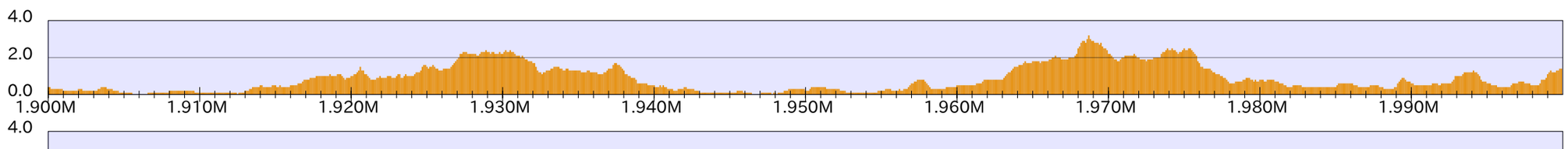

taz1

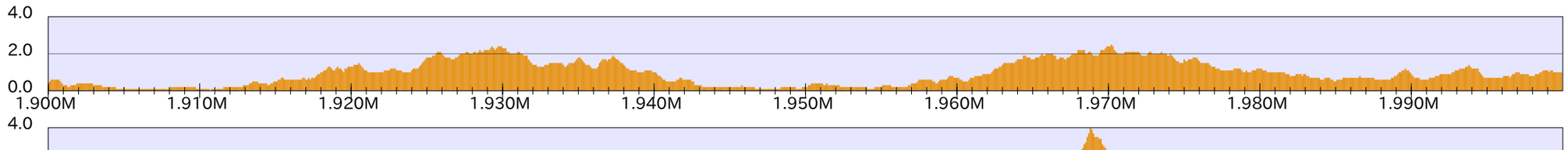

rif1

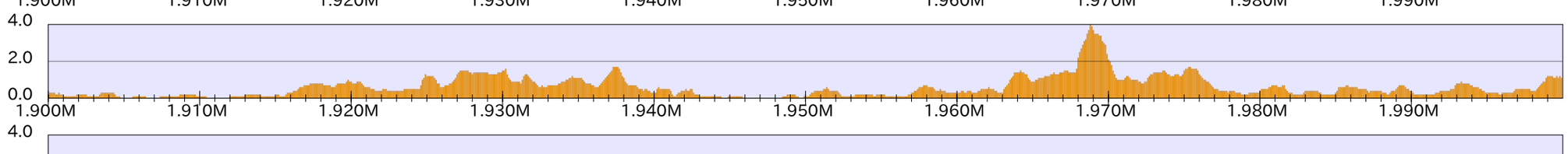

Taz1/notag

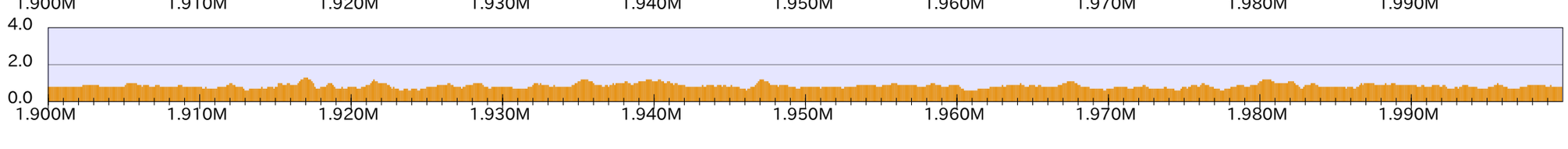

genes

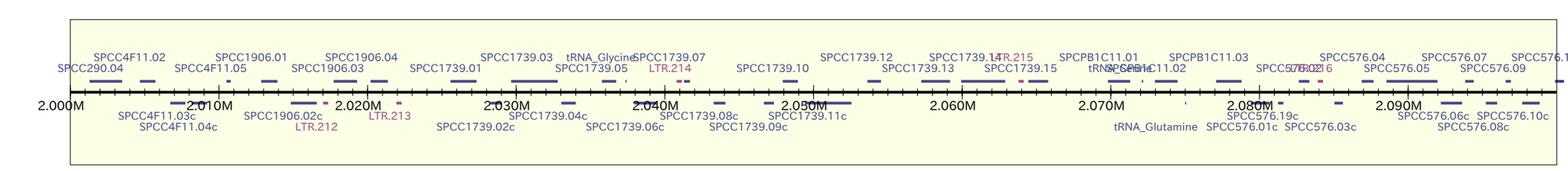

WT

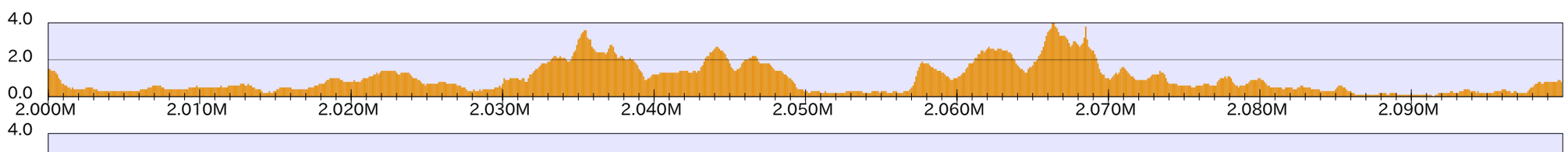

taz1

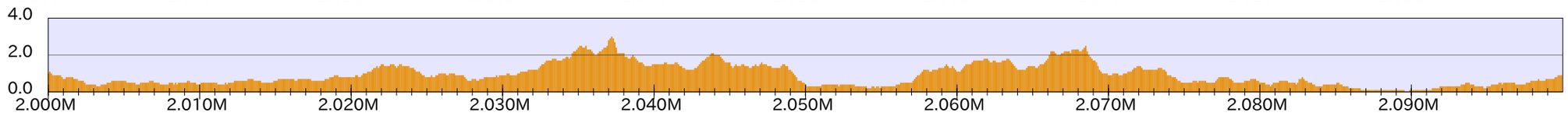

rif1

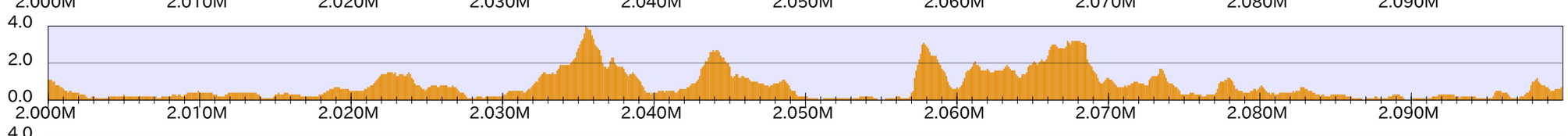

Taz1/notag

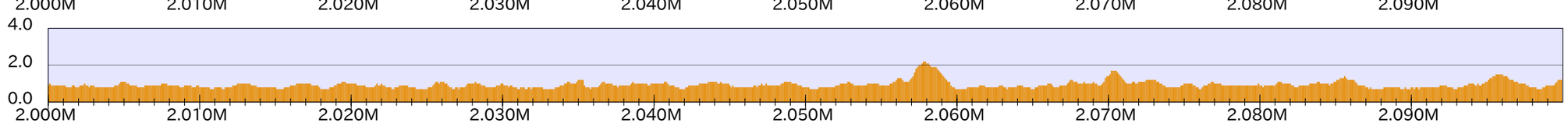

chrIII_8

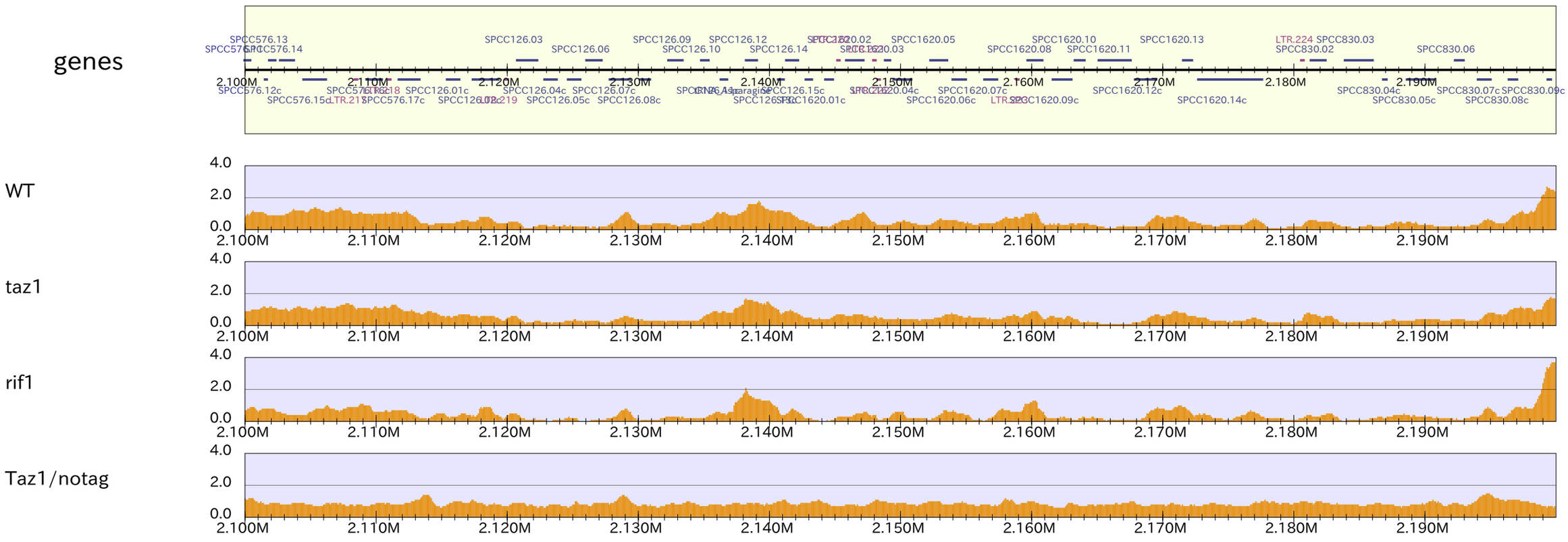
genes
WT
taz1
rif1
Taz1/notag
4.0
2.0
0.0
2.100M
2.110M
2.120M
2.130M
2.140M
2.150M
2.160M
2.170M
2.180M
2.190M

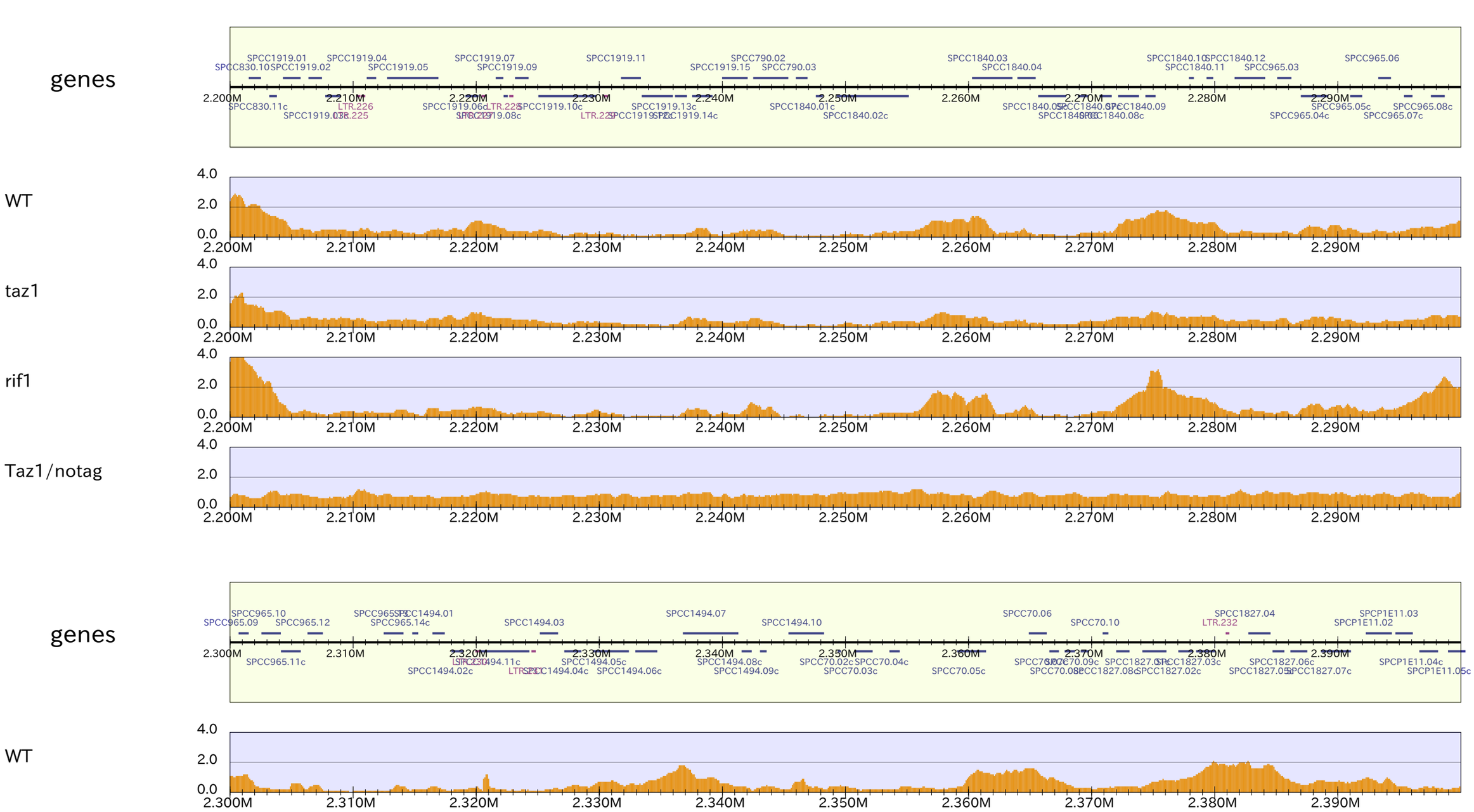
genes
WT
taz1
rif1
Taz1/notag
4.0
2.0
0.0
2.200M
2.210M
2.220M
2.230M
2.240M
2.250M
2.260M
2.270M
2.280M
2.290M

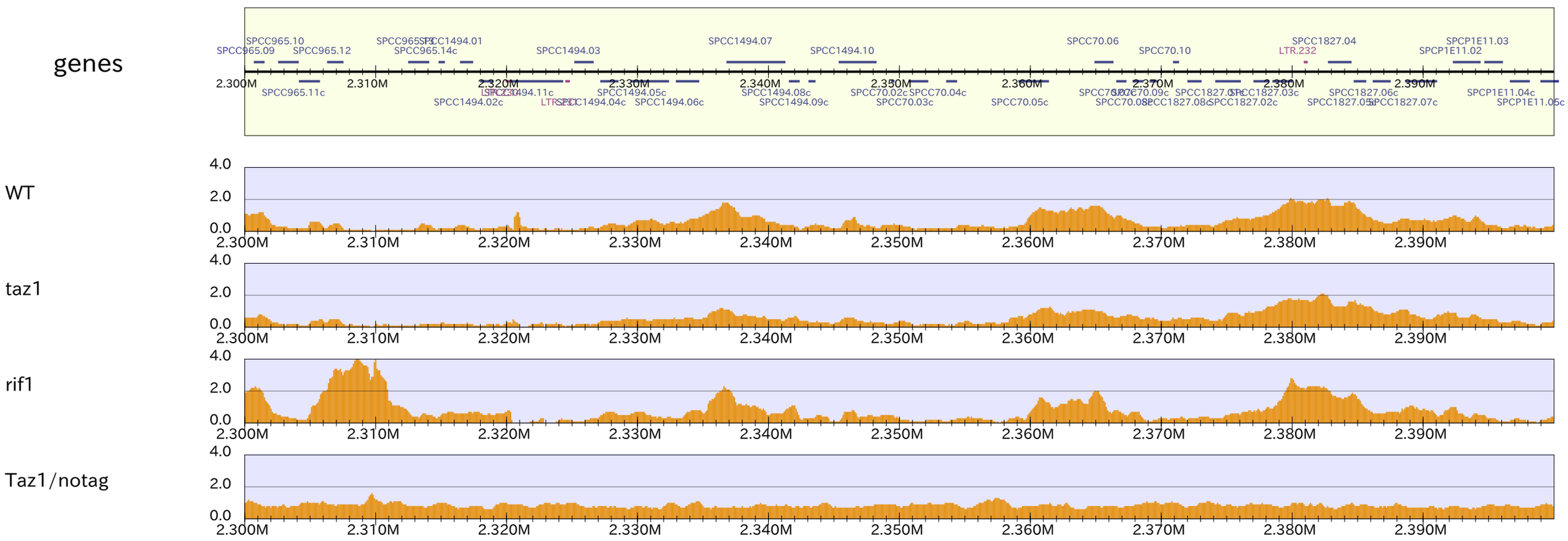
genes
WT
taz1
rif1
Taz1/notag
4.0
2.0
0.0
2.300M
2.310M
2.320M
2.330M
2.340M
2.350M
2.360M
2.370M
2.380M
2.390M

chrIII_9

genes

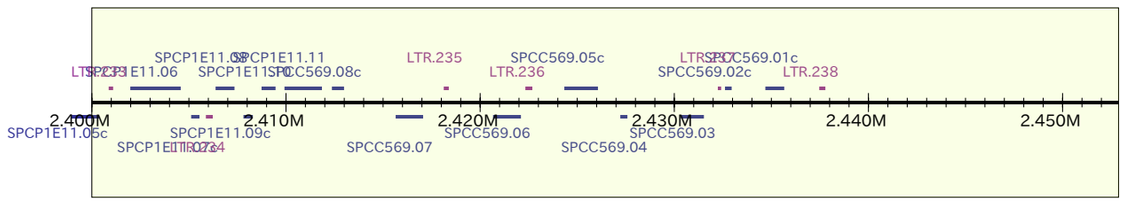

WT

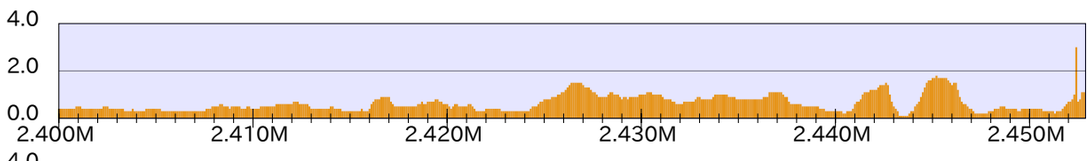

taz1

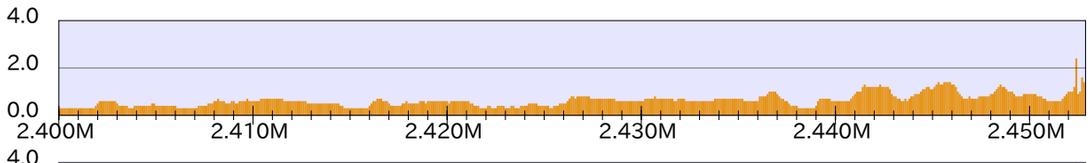

rif1

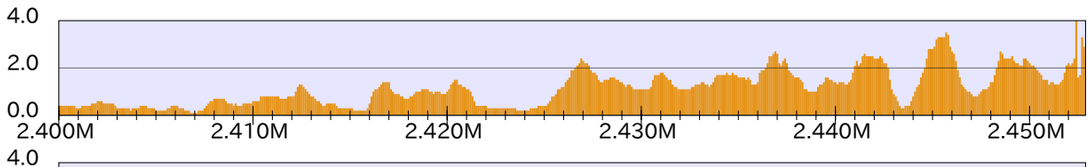

Taz1/notag

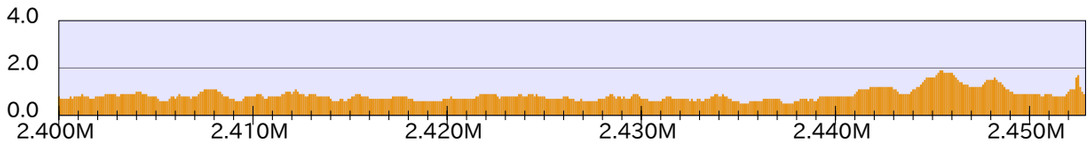

chrM

genes

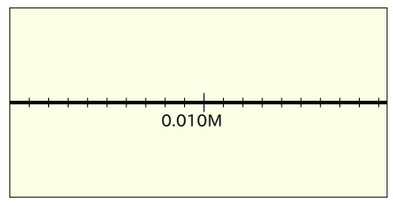

WT

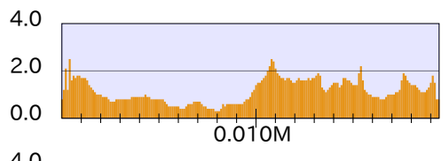

taz1

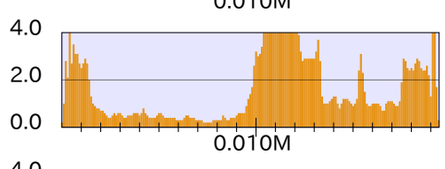

rif1

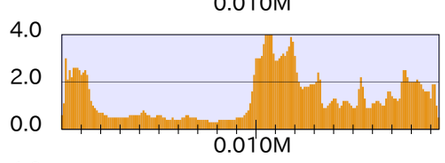

Taz1/notag